THE UNIVERSITY
of EDINBURGH

Infrared Divergences in Scattering Amplitudes from Correlators of Wilson Lines

Calum Milloy

Doctor of Philosophy
The University of Edinburgh
May 2020

Abstract

Scattering amplitudes in theories with massless particles feature infrared (IR) divergences. In QCD, gluons are massless and when their momenta tends to zero the amplitude diverges. We call this a *soft* divergence. For massless external particles there are further divergences called *collinear* divergences, when the invariant jet mass of the external and a radiated gluon tends to zero. Even in a UV finite theory such as $\mathcal{N} = 4$ super-Yang Mills there exists infrared divergences. In fact, in the planar theory there exists an all-order ansatz for the IR divergences called the BDS ansatz which amounts to the exponentiation of the one loop result with anomalous dimensions that can be computed to all orders. In this thesis we shall be considering the more complicated case of non-planar QCD with both massless and massive scattering particles.

First, we shall review the IR factorisation formula for massive scattering amplitudes. Here, soft divergences are described by the soft anomalous dimension matrix. It is defined to be a vacuum expectation value of non-lightlike Wilson lines. This object is calculable in perturbation theory. It exponentiates and the exponent is a sum over *webs*. We will then focus on how to calculate the individual integrals that appear in webs. The technique of differential equations is explained and applied to integrals up to two loops for webs. We then discuss a basis of functions for these specific integrals with the idea of creating an ansatz for the soft anomalous dimension and other related quantities.

The second half of the thesis concerns massless scattering amplitudes. By factorising not only the amplitude but also a parton distribution function we find that they share the same hard collinear behaviour. They differ in their pure soft poles which are governed by lightlike Wilson-line correlators that follow different contours dictated by the kinematics. It allows us to explain an observed relation between the subleading pole of the form factor, γ_G, and the coefficient of $\delta(1-x)$ in the DGLAP splitting kernels, B_δ. We then argue that divergences of lightlike Wilson-line correlators take a general form that only depend on local features, individual line lengths, and not on the global geometry.

Lay Summary

The best description of the fundamental theory describing elementary particles is the Standard Model. To test it, we collide particles and observe the outcome at colliders such as the Large Hadron Collider (LHC). Many different final states can appear and along with many intermediate states, a plethora of different collision processes can occur. One way to test the Standard Model is to search for new particles. If they are observed then one can easily conclude that the Standard Model is not a complete description and new physics describing the new particles needs to be included. However, as of present, no new particles have been discovered at the LHC.

Another way to test the validity of the theory is to perform precision tests. We do this by comparing highly accurate experimental data with similarly accurate theoretical predictions. If they match then the theory describes nature well, up to that precision. If they do not match then that hints at new physics.

As the LHC is one of the most advanced technological machines in the world, theorists need to provide ever more accurate predictions. The problem is that calculations become ever more difficult. In certain regions of particle momentum, conventional approaches break down and are wildly inaccurate as divergences arise. To fix this we *resum* these divergences to give a convergent result. Resummation can be performed on quantities that factorise, where there is a large separation of scales. For instance, when a heavy particle radiates a low energy particle.

In this thesis we apply novel techniques to the required calculations for the resummation. We also explore conceptual issues regarding the factorisation and relations between various quantities that emerge.

Acknowledgements

I am intensely grateful to my supervisor Einan Gardi for giving me his guidance and undivided attention during my studies. His continued enthusiasm has influenced my passion for the field. Special thanks also go to my collaborator Giulio Falcioni for various discussions, teaching me so much more about the subject and for comments on the thesis.

Thanks to my fellow students and colleagues: Ben, Saad, Leonardo, Christian, Ben, Sebastian and Andries early on for those late-night discussions and for making it all the more enjoyable. Thanks to everyone else in the PPT corridor for the coffee breaks and whisky sessions.

Thanks to friends met further afield during this work in London, Florence, California, Erice, Hamburg, Avignon... fun conferences are the best conferences.

I am grateful for the funding that I received from the Carnegie Trust for the Universities of Scotland.

Thanks to several friends and flatmates over the years: Glenn, Jake... and everyone else outwith physics. You have kept me sane in showing me there is more to life than Wilson lines. For keeping me healthy, thanks to everyone that took part in the running club and the wider running community in Edinburgh.

Thanks to my Gran, and thanks to my Grandpa, who instilled a natural curiosity but sadly passed away during my PhD. Lastly, I am eternally indebted to my Mum, Dad and my brother, without their love, support and encouragement this would not have been possible.

Contents

List of Figures

List of Tables

Chapter 1

Introduction and Background

In perturbative quantum field theories, one can calculate loop corrections to scattering amplitudes. These are fundamental building blocks to perturbative cross sections for scattering events which, in turn, can be compared or used as input to experimental observations or measurements. As experimental machines are becoming ever more accurate we need to increase the predictive power of our theories.

The most complete description of the fundamental particles that constitute matter is the Standard Model. One of its sectors is quantum chromodynamics (QCD) which describes quark and gluon interactions,

$$\mathcal{L}_{\text{QCD}} = -\frac{1}{4}F^{a\mu\nu}F^{a}_{\mu\nu} + i\sum_{q}\bar{\psi}_q(\not{D} - m_q)\psi_q \tag{1.1}$$

where the sum is over quark flavours. It is an SU(3) gauge theory where quarks are in the fundamental representation and gluons are in the adjoint representation. The field strength in eq. (1.1) is defined as

$$F^{a}_{\mu\nu} = \partial_\mu A^a_\nu - \partial_\nu A^a_\mu + g_s f^{abc} A^b_\mu A^c_\nu \tag{1.2}$$

where A_μ is the gluon field and g_s is the strong coupling. We compute amplitudes perturbatively assuming small values in the coupling. For quark masses lower than the scale at which perturbation theory breaks down, Λ_{QCD}, we can consider them massless. However, the top-quark mass is roughly three orders of magnitude greater than Λ_{QCD}. As such, in QCD, we require amplitudes that have external

particles that are massless or massive, or both.

It is well known that perturbative QCD at fixed order in the coupling, which is highly successful in describing hard processes at colliders, loses its predictive power in kinematic regions and starts to diverge where there is a large hierarchy of scales. Familiar examples are Drell-Yan or Higgs production near threshold, see e.g. [2–7], or at small transverse momentum, which are dominated by soft-gluon radiation. Another example is the high-energy limit of QCD scattering, where the centre-of-mass energy is much larger than the momentum transfer [8–15]. In each of these cases, and many others, the presence of scale hierarchies allows us to factorise the contributions of the most relevant regions. In turn, we can derive all-order resummation formulae, which extend the predictive power of QCD, leading to highly successful phenomenology in many cases.

The theory underlying factorisation relies on identifying the origin of any parametrically-enhanced corrections through operators, which capture the relevant divergences. Independently of whether one uses QCD fields [16, 17], or Soft-Collinear Effective Theory [18] ones, the relevant operators involve Wilson lines, which follow the trajectory of fast-moving partons, and capture their interactions with soft gluons. These operators obey evolution equations, governed by corresponding anomalous dimensions, which are computable order by order in QCD perturbation theory. Resummation formulae are obtained upon solving the aforementioned evolution equations, leading to exponentiation. The anomalous dimensions therefore have a central role in the predictive power of QCD, and in certain cases their computation has been recently pushed to three-loop order, e.g. [19–25], with very recent progress towards four loops [26–36] (even more is known in maximally supersymmetric $\mathcal{N}=4$ Yang-Mills theory, see e.g. [37–42]).

To quantify the above let us look at Drell-Yan near threshold. This process involves the production of a colour-singlet state from two hadrons $A(p_1)+B(p_2)\to \mathrm{DY}(Q)+X$ with $s=(p_1+p_2)^2$ and X is an unobserved QCD final state. Schematically the differential cross section factorisation takes the form [2, 3]

$$\frac{d\sigma}{dQ^2}=\sum_{i,j}\int_0^1 dx_1dx_2 f_{iA}(x_1)f_{jB}(x_2)\left[\mathcal{S}^{ij}_{\mathrm{DY}}\mathcal{H}_{ij}+\mathcal{O}(\alpha_s^n\log^m(1-z))\right]+\mathcal{O}\left(\frac{\Lambda^2_{\mathrm{QCD}}}{Q^4}\right) \tag{1.3}$$

where Q^2 is the centre of mass energy of the outgoing state DY state, $z=\frac{Q^2}{\hat{s}}$ and $\hat{s}=x_1x_2s$. The function $\mathcal{S}_{\mathrm{DY}}$ is calculable in perturbation theory and resums the distributions $\frac{\log^n(1-z)}{(1-z)_+}$ and $\delta(1-z)$ of the partonic cross section. Currently $\mathcal{S}_{\mathrm{DY}}$ is

known to three loops [19,20], which means that the cross section is known to next-to-next-to-next-to-leading logarithmic accuracy [7,43]. After convolution with the parton distribution functions, $f_{ij}(x)$, we would yield higher precision in the region $Q^2 \to s$. There have been recent advances in understanding factorisation beyond these distribution terms, namely the $\alpha_s^n \log^m(1-z)$ where $n \geq m$. Factorisation of the leading logarithms, where $n = m$, has been demonstrated from either using SCET [44, 45] or a diagrammatic approach [46]. The corrections of $\mathcal{O}(\Lambda^2_{\rm QCD}/Q^4)$ are known as *higher-twist* corrections and given explicitly in [47, 48] for this process.

In this chapter we will review the factorisation of scattering amplitudes, considering massive and massless particles separately and derive the framework that allows the computation of the anomalous dimensions.

1.1 Factorisation of Massive Gauge Theory Amplitudes

We consider a generic n-particle massive scattering amplitude which we shall denote as $\mathcal{M}_n$. This object has two kinds of divergences: ultraviolet (UV) and infrared (IR). The UV singularities occur because we approximate particles to be point-like. We are unable to probe short distances or, correspondingly, high energies. These divergences are well understood and we can absorb them into the parameters of the theory through a process called renormalisation (eg. the fields and masses in eq. (1.1)). From now on we consider that this has been performed on $\mathcal{M}_n$, i.e. it is a renormalised quantity.

The IR singularities are less well understood. In comparison to the UV they occur because of states interacting at long distances. In the limit of vanishing momenta, the so-called *soft* limit, a virtual exchange and unresolved radiation, shown in Figures 1.1a and 1.1b respectively, are degenerate. Both quantities are individually singular in this limit. The divergences are realised in the integration over off-shell (Figure 1.1a) or on-shell (Figure 1.1b) degrees of freedom. Quantum mechanics tells us to sum over all possibilities and, if properly regularised, we will arrive at a meaningful result. This cancellation of infrared divergences was first realised by Bloch and Nordsieck in 1937 [49] when applied to quantum electrodynamics. The generalisation to non-Abelian gauge theories such as QCD

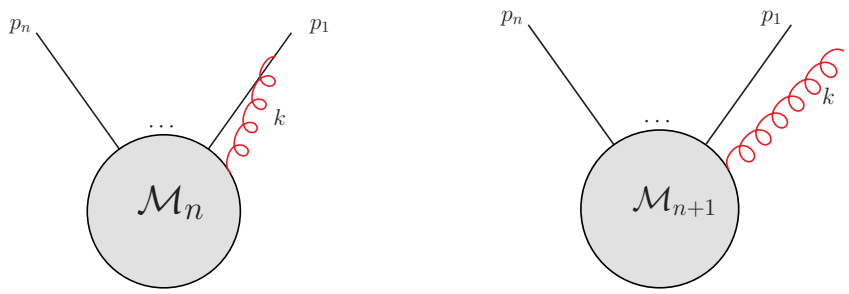

(a) Virtual correction to $\mathcal{M}_n$ **(b)** Radiative $\mathcal{M}_{n+1}$ amplitude

Figure 1.1: Degenerate states in the limit $k \to 0$

is the so-called KLN theorem, which states that for a properly defined observable it is infrared finite once all possible states are included [50, 51].

A perturbative factorisation theorem states the n-legged amplitude $\mathcal{M}_n$ can be written as

$$\mathcal{M}_n = \mathcal{S}_n \cdot \mathcal{H}_n, \tag{1.4}$$

where $\mathcal{H}_n$ is the hard function and captures all the process dependent information about the scattering amplitude $\mathcal{M}_n$ and is infrared finite. The function $\mathcal{S}_n$ is the universal n-particle soft function and captures all the divergence of $\mathcal{M}_n$, regulated by a suitable regulator ϵ. For the present thesis, we shall solely use dimensional regularisation, where spacetime is continued to $d = 4 - 2\epsilon$ dimensions and the divergences manifest themselves as poles of ϵ. Equation (1.4) separates the scales between the energies of the external momenta, which are non-zero because of their mass, and the internal soft gluons. For phenomenological uses, $\mathcal{S}_n$ gives the virtual corrections to soft functions for massive external states in factorisation formula such as eq. (1.3). As an example, resummation for heavy quark production given in [52].

The soft function $\mathcal{S}_n$ is given by the vacuum expectation value of n semi-infinite Wilson lines

$$\mathcal{S}_n \equiv \langle 0|\mathrm{T}[W_{\beta_1}(\infty, 0) \otimes \ldots \otimes W_{\beta_n}(\infty, 0)]|0\rangle\,, \tag{1.5}$$

where the β_i are the velocities of particle i. A Wilson line is defined as the *path-ordered exponential of the gauge field*,

$$W_\beta(y, x) \equiv \mathbf{P} \exp\left(ig_s \int_x^y dz\, \beta_\mu A^\mu(z\beta)\right), \tag{1.6}$$

where β is the direction of the line and x and y are its endpoints. In the limit of soft gluon radiation, radiative particles will follow their classical trajectory as

there is zero recoil momentum. Such an object that transports gauge information, gluon radiation, along classical velocities is the Wilson line. The vector β can be either lightlike $\beta^2 = 0$ or non-lightlike $\beta^2 \neq 0$. For massless particles it is lightlike and for massive particles it is non-lightlike. It is path ordered because the gauge field is for a general SU(N) colour group and hence non-Abelian. We have to be careful about the ordering of emissions of gluons. Notice that in an axial gauge, $\beta \cdot A = 0$, the Wilson line in the direction of β is trivial $W_\beta(y, x) = \mathbf{I}$.

The representation of the gauge field $A_\mu = A^a_\mu \mathbf{T}^a$ in eq. (1.6) is prescribed by the corresponding particle. For final-state quarks it is $(\mathbf{T}^a)_{ij} = t^a_{ij}$, initial-state quarks it is $(\mathbf{T}^a)_{ij} = -t^a_{ji}$ and for gluons $(\mathbf{T}^a)_{bc} = -if_{abc}$. The usefulness of this so-called Catani-Seymour colour charge operator notation [53, 54] is to produce representation-independent factorisation formula and only specialise when required. The infrared-singular soft function $\mathcal{S}_n$ in eq. (1.4) is seen as an operator in colour space acting on the finite hard function $\mathcal{H}_n$ to produce the full scattering amplitude $\mathcal{M}_n$. Importantly, $W_\beta(y, x)$ and consequently $\mathcal{S}_n$ does not depend on the spin of the underlying particles, only on their colour representation. Under an infinitesimal local gauge transformation $A^\mu \to A^\mu - \frac{1}{g_s}\partial^\mu \alpha$, eq. (1.4) transforms as

$$\mathcal{M}_n \to \mathcal{M}_n + \alpha^a(0)\mathcal{S}_n \left(\sum_{i=1}^{n} \mathbf{T}^a_i \right) \mathcal{H}_n. \tag{1.7}$$

Gauge invariance or, equivalently, colour charge conservation in this formalism is the statement

$$\left(\sum_{i=1}^{n} \mathbf{T}^a_i \right) \mathcal{H}_n = 0. \tag{1.8}$$

The function $\mathcal{S}_n$ is invariant under the rescaling $\beta_i \to \lambda\beta_i$ which can be readily checked using the definition of the Wilson line in eq. (1.6). As a consequence of this and Lorentz invariance we know that $\mathcal{S}_n$ can only depend on the so-called cusp angles

$$\gamma_{ij} = \frac{2\beta_i \cdot \beta_j}{\sqrt{\beta_i^2}\sqrt{\beta_j^2}} \tag{1.9}$$

and our factorisation theorem now reads

$$\mathcal{M}_n(\{p_i \cdot p_j\}, \{m_i^2\}, \alpha(\mu^2), \epsilon) = \mathcal{S}_n(\{\gamma_{ij}\}, \alpha(\mu^2), \epsilon) \cdot \mathcal{H}_n(\{p_i \cdot p_j\}, \{m_i^2\}, \alpha(\mu^2)), \tag{1.10}$$

with $\mathcal{S}_n$ depending on the scale μ only through the running coupling $\alpha_s(\mu^2)$. As a result of being scaleless the bare $\mathcal{S}_n$ is the identity in dimensional regularisation.

It does not mean that $\mathcal{S}_n$ has no infrared divergence, instead it means that, in perturbation theory, the infrared exactly cancels the ultraviolet behaviour. The renormalised $\mathcal{S}_n$ which appears in eq. (1.10) is obtained through the multiplicative renormalisation [55, 56]

$$\mathcal{S}_n(\gamma_{ij}, \epsilon_{\rm IR}) = \mathcal{S}_n^{\rm bare}(\gamma_{ij}, \epsilon_{\rm IR}, \epsilon_{\rm UV}) Z_n(\gamma_{ij}, \epsilon_{\rm UV}) = Z_n(\gamma_{ij}, \epsilon_{\rm UV}). \tag{1.11}$$

Instead of calculating the infrared we shall calculate the ultraviolet. We can do this by regulating the infrared which gives a well-defined function in perturbation theory. We shall implement this by adding an exponential damping term to the definition of the Wilson line in eq. (1.6),

$$W_\beta^{(m)}(y, x) \equiv \mathbf{P} \exp\left(i g_s \int_x^y dz\, \beta_\mu A^\mu(z\beta) e^{-imz\sqrt{\beta^2}} \right) \tag{1.12}$$

and define an infrared finite soft function given by

$$\mathcal{S}_n^{(m)}(\{\gamma_{ij}\}, \alpha(\mu^2), \epsilon, m) \equiv \langle 0 | \mathrm{T}[W_{\beta_1}^{(m)}(\infty, 0) \otimes \ldots \otimes W_{\beta_n}^{(m)}(\infty, 0)] | 0 \rangle \,. \tag{1.13}$$

The argument of the exponential is chosen specifically to keep rescaling invariance. The UV divergence of this object also renormalises multiplicatively with the same factor as in eq. (1.11)

$$\mathcal{S}_n^{\rm ren}(\{\gamma_{ij}\}, \alpha_s(\mu^2), \epsilon, m) = Z_n(\gamma_{ij}, \alpha_s(\mu^2), \epsilon) \mathcal{S}_n^{(m)}(\{\gamma_{ij}\}, \alpha_s(\mu^2), \epsilon, m) \tag{1.14}$$

where we have made explicit the dependence on α_s and ϵ is the ultraviolet poles. Using eq. (1.14) we can calculate the pure counterterm Z_n from the poles of the well defined function $\mathcal{S}_n^{(m)}$ which, in turn, allows us to find $\mathcal{S}_n = Z_n$ from eq. (1.11). The anomalous dimension from the renormalisation group (RG) evolution of $\mathcal{S}_n$ in eq. (1.11) is called the *soft anomalous dimension* Γ_n which is found from Z_n by

$$\mu \frac{dZ_n(\gamma_{ij}, \alpha_s(\mu^2), \epsilon)}{d\mu} = -Z_n(\gamma_{ij}, \alpha_s(\mu^2), \epsilon) \Gamma_n(\gamma_{ij}, \alpha_s(\mu^2)). \tag{1.15}$$

An important property of soft functions is that they exponentiate. The Abelian soft exponentiation was hinted at in Bloch and Nordsieck's original paper [49] and then reformulated in later papers by Yennie et al. [57] and Weinberg [58]. The extension relevant for QCD, the non-Abelian exponentiation theorem was found in [59–62]. In order to compute Z_n in eq. (1.15) we use this property as

it allows to determine directly $\log \mathcal{S}_n^{(m)}$ by computing only the *webs* that capture the maximally non-Abelian colour factors of each Feynman diagram, as defined in [62],

$$\mathcal{S}_n^{(m)} = \exp\left(\sum_{n,k} w^{(n,k)} \left(\frac{\alpha_s}{4\pi}\right)^n \epsilon^k\right). \tag{1.16}$$

In the exponent there is an overall single pole, higher order poles are generated by expanding the exponential in a power series. This allows the calculation of the soft anomalous dimension directly using eq. (1.15) and ensuring that the product on the right hand side of eq. (1.14) is finite. Expanding Γ_n as $\Gamma_n = \sum_{i=1}^{\infty} \Gamma_n^{(i)} \left(\frac{\alpha_s}{4\pi}\right)^i$ we can solve for the coefficients $\Gamma_n^{(i)}$ in terms of the web coefficients $w^{(n,k)}$ [63]

$$\Gamma_n^{(1)} = -2w^{(1,-1)} \tag{1.17a}$$

$$\Gamma_n^{(2)} = -4w^{(2,-1)} - 2[w^{(1,-1)}, w^{(1,0)}] \tag{1.17b}$$

$$\begin{aligned}\Gamma_n^{(3)} = &-6w^{(3,-1)} + 6\hat{b}_0 \left[w^{(1,-1)}, w^{(1,1)}\right] + 3\left[w^{(1,0)}, w^{(2,-1)}\right] + 3\left[w^{(2,0)}, w^{(1,-1)}\right] \\ &+ \left[w^{(1,0)}, \left[w^{(1,-1)}, w^{(1,0)}\right]\right] - \left[w^{(1,-1)}, \left[w^{(1,-1)}, w^{(1,1)}\right]\right].\end{aligned} \tag{1.17c}$$

The soft anomalous dimension is given by single poles of webs plus counterterms of lower order commutators. The one-loop beta function $\hat{b}_0$ is given in eq. (4.7a) and appears from the renormalisation of the coupling, see eq. (4.6). The factorisation in eq. (1.10) and the exponentiation of $\mathcal{S}_n$ in eq. (1.16) is shown schematically in Figure 1.2.

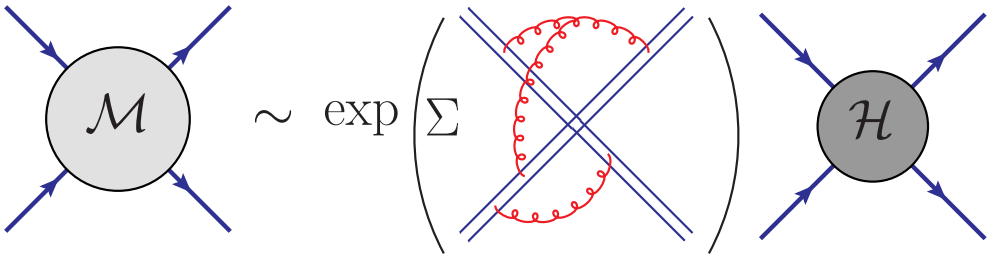

Figure 1.2: A schematic picture of the amplitude factorisation and exponentiation of the soft function

It is useful to define *subtracted webs*. These are webs with the subtraction of the relevant commutator counterterms from subdivergences of the original web [64]. For instance, we shall study the so-called $[1,2,1]$-web in Section 2.3, w_{121} which has the one-loop web, $w^{(1,n)}$ as a subdiagram. The subtracted $[1,2,1]$-web, using eq. (1.17b), is then given by

$$\bar{w}_{121}^{(2,-1)} = w_{121}^{(2,-1)} + \frac{1}{2}[w^{(1,-1)}, w^{(1,0)}]. \tag{1.18}$$

Subtracted webs have a simpler functional form [64, 65] than unsubtracted webs. We shall review this and extend this function space in Chapter 3. There are also further constraints from the renormalisation between higher order poles of webs, which ensures the overall single pole of the exponent. For instance, at three loops the double pole of the sum over webs is equal to the commutator of the lower webs

$$w^{(3,-2)} = \frac{1}{6}\left[w^{(2,-1)}, w^{(1,-1)}\right]. \tag{1.19}$$

We will use this as a check in the study of the three loop $[1,1,2,1]$-web in Section 3.4.

1.2 Factorisation of Massless Gauge Theory Amplitudes

In the previous section we discussed the infrared factorisation properties of massive scattering amplitudes. We shall now discuss the case when massless external particles are present. When this is the case there are additional, so-called *collinear*, singularities which occur. These arise when the radiated gluon in Figure 1.1b becomes collinear with an external massless particle. For example when $k \to p_1$, the total mass of the state vanishes $(p_1 + k)^2 \to 0$.

For outgoing states the KLN theorem tells us that we have to sum over all possible final states, including any number of radiated gluons, in the cross section. This is reasonable since, experimentally, given a certain detector resolution, we cannot distinguish between a single particle and a sufficiently narrow jet consisting of many radiative gluons.

Incoming states are more tricky. The KLN theorem still holds but we would need to sum over all possible initial states. That is, run an experiment an infinite number of times each with different initial states. What comes to the rescue is that we cannot prepare a quark or gluon initial state, we can only do so with bound states, e.g. hadrons. Factorisation, in eq. (1.3), allows us to absorb the long distance singularities into non-perturbative parameters, the so-called *parton distribution functions* (PDFs) which describe, in essence, the probability of finding a parton in a hadron with a given momentum fraction. The scale evolution of the PDFs are discussed, in detail, in Section 4.3.

At the perturbative level, the factorisation of the infrared divergences (soft and collinear) in on-shell massless partonic scattering amplitudes takes the form [66–73]

$$\mathcal{M}_n(\{p_i\cdot p_j\},\epsilon) = \left[\prod_{i=1}^{n} J_i\left(\frac{(2p_i\cdot n_i)^2}{n_i^2\mu^2},\alpha_s(\mu^2),\epsilon\right)\right]\left[\frac{\mathcal{S}_n\left(\{\beta_i\cdot\beta_j\},\alpha_s(\mu^2),\epsilon\right)}{\prod_{i=1}^{n}\mathcal{J}_i\left(\frac{2(\beta_i\cdot n_i)^2}{n_i^2},\alpha_s(\mu^2),\epsilon\right)}\right] \times H\left(\left\{\frac{(p_i\cdot p_j)^2}{\mu^2}\right\},\left\{\frac{(2p_i\cdot n_i)^2}{n_i^2\mu^2}\right\},\alpha_s(\mu^2)\right), \tag{1.20}$$

where the jet function J_i, one for each massless external leg, captures the collinear singularities, the soft function $\mathcal{S}_n$ contains the contribution of any long-wavelength gluons exchanged between the external particles and the eikonal jet function $\mathcal{J}_i$ captures all the singularities that are present both in $\mathcal{S}_n$ and in the jet function J_i, which are associated with exchanges that are both soft and collinear to the massless external particles. Therefore, the ratio $\frac{\mathcal{S}_n}{\prod\mathcal{J}_i}$ in eq. (1.20) includes only the divergences associated with soft wide-angle emissions. H is the hard function, found from matching to the amplitude. Each other factor in eq. (1.20) has an operator definition which dictates their functional dependencies in eq. (1.20), involving the momenta p_i of the external particles and their lightlike velocities β_i, defined by

$$p_i^\mu = Q_0\beta_i^\mu, \tag{1.21}$$

where Q_0 is an arbitrary normalisation and would typically be of the order of the hard scale of the process, Q. The operator definitions of $\mathcal{S}_n$, J_i and $\mathcal{J}_i$ are written in terms of the expectation values of Wilson lines, defined in eq. (1.6). In the context of on-shell massless scattering amplitudes, we use lightlike kinematics for the external legs[1], $\beta_i^2 = 0$, and along with the definition of $\mathcal{S}_n$ in eq. (1.5) we define the functions entering the factorisation formula (1.20) by:

$$u(p)\,J_i\left(\frac{(2p_i\cdot n_i)^2}{n_i^2\mu^2},\alpha_s(\mu^2),\epsilon\right) = \langle 0|\mathrm{T}\Big[W_{n_i}(\infty,0)\psi(0)\Big]|p\rangle\,, \tag{1.22}$$

$$\mathcal{J}_i\left(\frac{2(\beta_i\cdot n_i)^2}{n_i^2},\alpha_s(\mu^2),\epsilon\right) = \langle 0|\mathrm{T}\Big[W_{n_i}(\infty,0)W_{\beta_i}(0,\infty)\Big]|0\rangle\,, \tag{1.23}$$

where n_i is an auxiliary non-lightlike vector and the dependence on its choice must cancel in eq. (1.20). In eq. (1.22) we presented the jet function J_i for fermion fields; for a definition of the gluon jet function see refs. [74–76]. Any function

[1]Note that the dependence of $\mathcal{S}_n$ is no longer on γ_{ij} in eq. (1.9) but rather on $\beta_i\cdot\beta_j$

built solely from Wilson lines, such as $\mathcal{S}_n$ and $\mathcal{J}_i$, is called eikonal.

We shall consider an anomalous dimension for the infrared divergent terms of eq. (1.20)

$$\mu\frac{d}{d\mu}\left(\mathcal{S}_n\prod_{i=1}^{n}\frac{J_i}{\mathcal{J}_i}\right)=-\Gamma_n^{\text{ll}}\left(\mathcal{S}_n\prod_{i=1}^{n}\frac{J_i}{\mathcal{J}_i}\right) \tag{1.24}$$

where ll symbolises that it describes lightlike behaviour. The factorisation functions in eq. (1.24) are heavily constrained and satisfy equations which are explained in Section 4.2. By direct calculation [69] it was shown that the tripole colour structure $f^{abc}\mathbf{T}_i^a\mathbf{T}_j^b\mathbf{T}_k^c$ vanishes at two loops in lightlike kinematics. As such, Γ_n^{ll} obeys the *sum-over-dipole* formula to two loops

$$\Gamma_n^{\text{ll}}=-\frac{1}{2}\gamma_{\text{cusp}}(\alpha_s)\sum_{(i,j)}^{n}\log(\beta_i\cdot\beta_j)\mathbf{T}_i^a\mathbf{T}_j^a+\sum_{i=1}^{n}\gamma_G^i+\mathcal{O}(\alpha_s^3). \tag{1.25}$$

General arguments were then made as to why it had to vanish based on Bose symmetry and scaling invariance [70, 72]. It has been claimed recently that there are no colour structures with an odd number of generators at any loop order [77].

Higher order corrections to eq. (1.25) depend on conformally-invariant cross ratios (CICRs) defined as

$$\rho_{ijkl}=\frac{(\beta_i\cdot\beta_j)(\beta_k\cdot\beta_l)}{(\beta_i\cdot\beta_k)(\beta_j\cdot\beta_l)}. \tag{1.26}$$

The three-loop correction to eq. (1.25) was completed in the highly ambitious calculation of ref. [24] and depends on one simple function

$$\mathcal{F}(z)=\mathcal{L}_{10101}(z)+2\zeta_2\left[\mathcal{L}_{001}(z)+\mathcal{L}_{100}(z)\right] \tag{1.27}$$

where it is written in terms of single valued harmonic polylogarithms (SVHPLs), which we shall define in Section 1.3, with argument z which is a function of a combination of ρ's. The exact expression for the correction can be found in other publications [24, 25, 78].

The lightlike cusp anomalous dimension [79], γ_{cusp}, in eq. (1.25) describes double poles in massless amplitudes, originating in overlapping soft and collinear singularities. This is related to the non-lightlike angle-dependent cusp anomalous dimension $\Gamma_{\text{cusp}}\equiv\Gamma_2$, from the two-leg soft function $\mathcal{S}_2$ in eq. (1.5), by the large angle limit [79]

$$\lim_{\gamma_{ij}\to\infty}\Gamma_{\text{cusp}}(\gamma_{ij},\alpha_s)=\gamma_{\text{cusp}}(\alpha_s)\log(\gamma_{ij}). \tag{1.28}$$

The large angle limit is from taking the lightlike limit $\beta_i^2 \to 0$ in the definition of γ_{ij} eq. (1.9). The function Γ_{cusp} itself is a widely researched quantity [79], known to three loops [22], and we study it in detail in Section 3.3.

While the lightlike cusp anomalous dimension occurs universally, governing the leading singularities in any kinematic limit, single-logarithmic contributions (γ_G in eq. (1.25)) characterising separately large-angle soft or hard-collinear or rapidity divergences, are somewhat less universal, and yet recur in a variety of physical quantities that are not a priori related.

In Chapter 4 we study two fundamental physical quantities, which are recurrent ingredients in the factorisation of amplitudes and cross sections [17, 80]. The first is the massless on-shell form factor, associated e.g. with an electromagnetic vector current in the case of quarks, or effective Higgs production vertex, $gg \to H$ (in the limit where the top mass is much larger than m_H), in the case of gluons. It is essentially a two-leg scattering amplitude. The second is parton distribution functions (PDFs), or more precisely, the large-x limit of diagonal qq and gg Altarelli-Parisi splitting functions, governing the scale dependence of PDFs according to the Dokshitzer-Gribov-Lipatov-Altarelli-Parisi (DGLAP) evolution equation [81–83]. Each of these physical quantities is important in its own sake, and their infrared factorisation will be discussed in some detail in Sections 4.2 and 4.3, respectively. The main motivation to our study comes from the relation between the two, namely a particular combination of single-pole anomalous dimensions, which respectively capture collinear singularities in these two quantities. The relation holds separately for quarks and for gluons:

$$\gamma_G^q - 2\,B_\delta^q \equiv f_{\text{eik}}^q\,, \qquad\qquad \gamma_G^g - 2\,B_\delta^g \equiv f_{\text{eik}}^g, \tag{1.29}$$

where γ_G^q (γ_G^g) is defined by the function G (see eq. (4.9)), which along with the cusp anomalous dimension, governs the infrared structure of the quark (gluon) form factor in eq. (1.25); and B_δ^q (B_δ^g) is the coefficient of the $\delta(1-x)$ term, in the large-x limit of the quark-quark (gluon-gluon) splitting function, see eq. (4.31) below. It was observed long ago [84, 85] that while the separate perturbative results for γ_G and B_δ are very different between quarks and gluons (this is expected: collinear singularities are known to depend on the parton's spin), the combination (1.29) vanishes at one loop in both cases, and admits a Casimir-

scaling relation[2] at two loops, namely

$$\frac{f^q_{\rm eik}}{C_F} = \frac{f^g_{\rm eik}}{C_A} = \left(\frac{\alpha_s}{\pi}\right)^2 \left[C_A \left(\frac{101}{54} - \frac{11}{24}\zeta_2 - \frac{7}{4}\zeta_3\right) + T_f n_f \left(-\frac{14}{27} + \frac{1}{6}\zeta_2\right)\right] + \mathcal{O}\left(\alpha_s^3\right) \tag{1.30}$$

The same Casimir-scaling property persists at three loops [85]. This is a clear indication that $f_{\rm eik}$ has an interpretation purely in terms of Wilson lines – hence the name, an *eikonal* function. A Wilson-line-based definition would explain why the result does not depend on the parton's spin, while it depends on its colour representation in proportion to the relevant quadratic Casimir through three loops. The question we address in Chapter 4 is what is the Wilson-loop correlator corresponding to $f_{\rm eik}$.

1.3 Iterated Integrals

We now present a brief overview of functions that appear in scattering amplitudes and, hence, the webs that we will compute in Chapters 2 and 3.

It is well-known that many Feynman integrals evaluate to functions that are essentially generalisations of the logarithm. The first immediate generalisation are the classical polylogarithms

$$\mathrm{Li}_n(z) = \sum_{k=1}^{\infty} \frac{z^k}{k^n}. \tag{1.31}$$

The generalisation that we will work with are called multiple polylogarithms (MPLs) [87]. These are defined through the iterated integration

$$G(a_1, \cdots, a_n; z) = \int_0^z \frac{dt}{t - a_1} G(a_2, \ldots, a_n; t) \tag{1.32}$$

with

$$G(\underbrace{0, \ldots, 0}_{\text{n times}}; z) = \frac{1}{n!} \log^n z. \tag{1.33}$$

Each a_i are called letters and for a given Feynman integral are drawn from a finite set called an alphabet. The tuple of letters $(a_1, \ldots, a_n)$ in eq. (1.32) is called a

[2] A Casimir-scaling relation similar to (1.29) and (1.30) was deduced from factorisation already in [86]; in this analysis single-pole collinear singularities are controlled by the anomalous dimension of the quark or gluon fields in axial gauge.

word which we shall denote $\mathbf{a}$. Each MPL has a number associated with it, known as its weight which is the length of $\mathbf{a}$, the number of iterated integrals. MPLs satisfy the mathematical structure known as a Hopf algebra. We will not deal with the subtleties in its construction but rather state results that we will use in Chapters 2 and 3. One of these is the fact that MPLs satisfy the so-called shuffle algebra

$$G(\mathbf{a};z)G(\mathbf{b};z) = \sum_{w\in\mathbf{a}\sqcup\sqcup\mathbf{b}} G(w;z) \tag{1.34}$$

where the symbol $\sqcup\sqcup$ is the shuffle product which mixes $\mathbf{a}$ and $\mathbf{b}$ in such a way that it preserves their internal order. The sum is then over all possible words obtained via this procedure. As an example we have

$$\begin{aligned} G(a_1,a_2;z)G(b_1,b_2;z) = {} & G(a_1,a_2,b_1,b_2;z) + G(a_1,b_1,a_2,b_2;z) + G(a_1,b_1,b_2,a_2;z) \\ & + G(b_1,a_1,a_2,b_2;z) + G(b_1,a_1,b_2,a_2;z) + G(b_1,b_2,a_1,a_2;z) \end{aligned} \tag{1.35}$$

Note that the shuffle algebra preserves the weight. A given MPL of weight n is an element of the algebra $\mathcal{H}_n$, orthogonal to other spaces. Essentially saying that there are no functional relations between MPLs of different weight. The algebra of MPLs is known as a *graded algebra*, with the full algebra being sum over spaces with different weight $\mathcal{H} \cong \bigoplus_{n=1}^{\infty} \mathcal{H}_n$.

The Hopf algebra $\mathcal{H}$ structure includes a decomposition-type operation called the coproduct $\Delta : \mathcal{H} \to \mathcal{H}\otimes\mathcal{H}$.

$$\Delta\left(G(a_1,\ldots,a_n;z)\right) = \sum G(b_1,\ldots,b_i;z)\otimes G(c_{i+1},\ldots,c_n;z) \tag{1.36}$$

which is coassociative

$$\begin{aligned} \Delta\left(\Delta\left(G(a_1,\ldots,a_n;z)\right)\right) &= \sum \Delta G(b_1,\ldots,b_i;z)\otimes G(c_{i+1},\ldots,c_n;z) && \text{(1.37a)} \\ &= \sum G(b_1,\ldots,b_i;z)\otimes \Delta G(c_{i+1},\ldots,c_n;z) && \text{(1.37b)} \\ &= \sum G(b_1,\ldots,b_i;z)\otimes G(c_{i+1},\ldots,c_j;z) \\ &\qquad \otimes G(d_{j+1},\ldots,d_n;z). && \text{(1.37c)} \end{aligned}$$

Each summand of eq. (1.37c) is known as an entry of the coproduct, labelled according to the distribution of weights in each component $\Delta_{i,j-i,n-j}$, of $G(a_1,\ldots,a_n;z)$. One very useful property of the coproduct, that we will use several times, is known as the *symbol*. This is formally the maximal iteration of

the coproduct $\Delta_{1,\ldots,1}$. For practical purposes, for functions of one variable, the definition of ref. [88] is more intuitive. This arises from the kernel in the definition of the MPLs in eq. (1.32)

$$\mathcal{S}\left[G(a_1,\ldots,a_n;z)\right] = \log(z-a_n)\otimes\ldots\otimes\log(z-a_1) \tag{1.38a}$$

$$\equiv (z-a_n)\otimes\ldots\otimes(z-a_1). \tag{1.38b}$$

Between eqs. (1.38a) and (1.38b) we used the convenient shorthand notation that drops the "log". The symbol encodes the iterative branch cut behaviour of the function. It is useful in finding functional relations between MPLs which, in turn, helps find a minimal basis which spans the possible function space. As an example consider $G(1,0;\frac{1}{z})$. Its symbol is readily computed to be

$$\mathcal{S}\left[G\left(1,0;\frac{1}{z}\right)\right] = -z\otimes(1-z)+z\otimes z. \tag{1.39}$$

Another function with this symbol is

$$\mathcal{S}\left[-G\left(1,0;z\right)+G(0,0;z)\right] = -z\otimes(1-z)+z\otimes z. \tag{1.40}$$

Hence, at symbol level, they are equal. The only difference between the two at function level are quantities that vanish under the symbol map. At weight two, these are constants. A boundary condition is all that is needed to derive

$$G\left(1,0;\frac{1}{z}\right) = -G\left(1,0;z\right)+G(0,0;z)+2\zeta_2. \tag{1.41}$$

We will often use the shorthand notation $G(\mathbf{a};z)=G_{\mathbf{a}}(z)$.

An efficient numerical evaluation algorithm exists giving arbitrary precision for MPLs [89]. The work in this thesis made extensive use of the public package `PolyLogTools` [90] for the algebraic manipulations of the MPLs. In the above, we have been nonchalant with mathematical subtleties of the algebra, these are deferred to the review by Duhr [91] and references therein.

A restricted set of MPLs with letters from the set $\{0,\pm1\}$ are called harmonic polylogarithms (HPLs) [92]. There are a subset of webs defined in eq. (1.16) which are known to evaluate to HPLs [64, 65]. These are called multiple gluon exchange webs (MGEWs) which are those without internal gluon vertices and a conjectured functional basis exists for them.

We wrote the three-loop correction to the lightlike soft anomalous dimension in eq. (1.27) in terms of SVHPLs [93]. These are combinations of HPLs such that there are no branch cuts. The simplest SVHPL is the log plus its complex conjugate

$$\mathcal{L}_0(z) = G(0; |z|^2) = G(0; z) + G(0; \bar{z}). \tag{1.42}$$

This gives a function space which is restrictive enough for finding the full functional form in eq. (1.27) by a process known as *bootstrapping* [25], where an ansatz of SVHPLs is created and then constrained using a few known limits. In Chapter 3 we extend this idea and construct a similar function space for functions, not only of MGEW-type, appearing in the non-lightlike angle-dependent soft anomalous dimension defined in eq. (1.15).

The MPLs are instances of an even wider class of functions called Chen iterated integrals [94, 95]. The definition of which proceeds as follows. Let us first define a curve γ on a manifold $\mathcal{M}$, $\gamma : [0, 1] \to \mathcal{M}$ and a set of smooth one forms on $\mathcal{M}$, $w_i \in \Omega^1(\mathcal{M})$. If $f_i(t)$ is defined through the pullback $\gamma^\star(w_i) = f_i(t)\mathrm{d}t$ then the following is the iterated integral of $w_1 \dots w_n$ along γ

$$\int_\gamma w_1 \dots w_n = \int_{0 \leq t_1 \leq \dots \leq t_n \leq 1} f_1(t_1) dt_1 \dots f_n(t_n) dt_n. \tag{1.43}$$

The above does not depend on the choice of parameterisation γ, only on the endpoints. MPLs are a subset of the above with w_i being dlog forms $w_i = \mathrm{d}\log(x - a_i)$.

One property of iterated integrals that we will use is that of path decomposition. If we decompose the contour γ into two piecewise components where we first traverse γ_A then γ_B such that $\gamma(0) = \gamma_A(0)$, $\gamma_A(1) = \gamma_B(0)$ and $\gamma_B(1) = \gamma(1)$ then the following path decomposition formula holds

$$\int_\gamma w_1 \dots w_n = \sum_{i=0}^{n} \int_{\gamma_A} w_1 \dots w_i \int_{\gamma_B} w_{i+1} \dots w_n. \tag{1.44}$$

1.4 Thesis Overview

We conclude this introduction with a summary of the contents of the remaining chapters.

In Chapter 2 we concern ourselves with the explicit computation of webs that are present in the non-lightlike soft function. We use the technique of differential equations. In Section 2.1 we explain the technique. The one-loop computation in Section 2.2 serves as a pedagogical example. In Section 2.3 we compute a two-loop web depending on more than one variable using the method. The remaining two-loop web is computed in Section 2.4 using a modified approach. The results are then consolidated in Section 2.5.

In Chapter 3 we discuss an extension to the MGEW functional basis. We review the basis in Section 3.1. In Section 3.2 we explain and construct the extension. We perform speculative research into bootstrapping the non-lightlike cusp anomalous dimension in Section 3.3 and a three-loop non-MGEW web in Section 3.4. We then conclude with future prospects of the technique in Section 3.5.

In Chapter 4 we switch to discussing massless scattering amplitudes and discuss as follows. Section 4.1 provides further motivation to the study of understanding f_{eik} in eq. (1.29). In Section 4.2 we review the factorisation of long-distance singularities of the massless QCD form factor and identify the process-independent spin-dependent hard-collinear component of γ_G in eq. (1.25). In Section 4.3 we discuss the factorisation of PDFs in the limit $x \to 1$. To this end we perform an explicit two-loop calculation of the splitting functions at large x (the details are presented in Appendix C.1). Next we identify the eikonal component of B_δ as the anomalous dimension associated with a $\sqcap$-shaped Wilson-line geometry, see Figure 4.1b. By using the known value of B_δ along with the hard-collinear anomalous dimension extracted from the form factor, we then predict the subleading anomalous dimension of the $\sqcap$ shaped contour $\Gamma_\sqcap$ at two loops. Then, in Section 4.4 we compute $\Gamma_\sqcap$ directly to this order, finding agreement with the extracted result of Section 4.3. In Section 4.5 we put together our results for the factorisation of the form factor and the PDF, and establish the relation of eq. (1.29) to all orders identifying f_{eik} with the anomalous dimension associated with a parallelogram shaped contour, see Figure 4.1c.

Chapter 2

Webs by Differential Equations

In this chapter we give an introduction to solving Feynman integrals by differential equations. We then use this technique to compute the one-loop correction to the soft function defined in eq. (1.5) and the two-loop corrections that connect multiple external legs (more than two). We will see that we need to modify the technique for the most complicated contribution.

2.1 Solving Feynman Integrals by Differential Equations

As mentioned in Chapter 1, we need to compute integrals corresponding to Feynman diagrams in perturbative quantum field theories to increase precision in our theoretical predictions. Not only does the quantity of integrals increase but also the complexity of the integrals and the functions they evaluate to. The technique of evaluating integrals by differential equations is a powerful and efficient technique [96–99]. Rather than solving integrals individually by Feynman parameters and variations thereof, the technique allows one to construct a *system* of differential equations that can then be solved as a whole. The observation by Henn in 2013 [100] that the dependence on the dimensional regularisation parameter ϵ is trivial when selecting a convenient basis of integrals helped spark renewed interest in this computational technique. Once a transformation is achieved, integrals can then be solved order-by-order in ϵ. We now proceed to explain the method step-by-step with a pedagogical example.

2.1.1 Differentiation

We shall consider a scalar Feynman integral $\tilde{I}(\{s_i\},\epsilon)$ that can depend on several kinematic invariants s_i and the dimensional regularisation parameter ϵ. The integral will have a known mass dimension λ_d which can be extracted to define a dimensionless integral

$$\tilde{I}\left(\{s_i\},\epsilon\right) = s_1^{\lambda_d} I\left(\left\{\frac{s_{i\neq 1}}{s_1}\right\},\epsilon\right) = s_1^{\lambda_d} I\left(\{x_i\},\epsilon\right), \tag{2.1}$$

where we have chosen s_1 to scale out but this choice is arbitrary. We now want to find $I\left(\{x_i\},\epsilon\right)$. To find the dependence on x_j we take a derivative w.r.t. x_j. To do so we need to write these derivatives as derivatives with respect to the external momenta present in the propagators. According to the chain rule we have

$$p_k^\mu \frac{\partial}{\partial p_j^\mu} = \sum_i p_k^\mu \frac{\partial x_i}{\partial p_j^\mu} \frac{\partial}{\partial x_i}. \tag{2.2}$$

As there will often be more p_i than x_i the equations in (2.2) are linearly dependent. After removal of these eq. (2.2) can be inverted to find $\frac{\partial}{\partial x_i}$ in terms of $\frac{\partial}{\partial p_j^\mu}$.

As a simple example, let us consider the bubble integral with one mass on one propagator

$$I^{\text{bub}}(x,\epsilon) = (m^2)^\epsilon \int \frac{d^dk}{(2\pi)^d} \frac{1}{(k^2-m^2)(p-k)^2}, \tag{2.3}$$

where the factor $(m^2)^\epsilon$ ensures that the integral is dimensionless and depends only on the ratio $x \equiv \frac{p^2}{m^2}$. Using $x\partial_x = \frac{1}{2}p^\mu \frac{\partial}{\partial p^\mu}$ and

$$\begin{aligned} p^\mu \frac{\partial}{\partial p^\mu} \frac{1}{(k^2-m^2)(p-k)^2} &= -\frac{2(p^2-k\cdot p)}{(k^2-m^2)((p-k)^2)^2} \\ &= -\frac{1}{(k^2-m^2)(p-k)^2} - \frac{p^2-m^2}{(k^2-m^2)((p-k)^2)^2} \\ &\quad + \frac{1}{((p-k)^2)^2} \end{aligned} \tag{2.4}$$

we find

$$\partial_x I^{\text{bub}}(x,\epsilon) = -\frac{1}{2x} I^{\text{bub}}(x,\epsilon) + \frac{1-x}{2x} \int \frac{d^dk}{(2\pi)^d} \frac{m^2}{(k^2-m^2)((p-k)^2)^2} \tag{2.5}$$

where we have used the fact that scaleless integrals vanish in dimensional regularisation. In the differential equation eq. (2.5) we have now a new unknown

integral. It seems that we have just replaced our original unknown integral $I^{\text{bub}}(x,\epsilon)$ with a new integral with a new power on the propagator. It turns out that there are relations between Feynman integrals that will allow us to deal with the remaining integral.

2.1.2 Integration-by-parts (IBP) identities

Feynman integrals are related to one another by certain relations called IBP identities [101]. They arise from the following identity in dimensional regularisation

$$\int \frac{d^dk}{(2\pi)^d}\frac{\partial}{\partial k^\mu}v^\mu f(k^2,\{k\cdot p_i\},\epsilon)=0, \tag{2.6}$$

where p_i are external or subsequent loop momenta and v can be chosen to be either k or one of the p_i. After explicitly performing the derivative on the integrand, f, and then partial fractioning and reducing the numerator, such as in eq. (2.4), we find relations among integrals for each possible v.

One of the concepts in IBP relations is that of an integral family, where we let propagators have arbitrary integer powers and the propagators span all possible scalar products that can be made from momenta present in the integrand. We can define the family corresponding to the bubble integral in eq. (2.3) as simply

$$I^{\text{bub}}_{ab}(x,\epsilon)=(m^2)^{a+b-d/2}\int\frac{d^dk}{(2\pi)^d}\frac{1}{(k^2-m^2)^a((p-k)^2)^b}, \tag{2.7}$$

where a and b are integers. Our differential equation eq. (2.5) is then

$$\partial_x I^{\text{bub}}_{11}=-\frac{1}{2x}I^{\text{bub}}_{11}+\frac{1-x}{2x}I^{\text{bub}}_{12}. \tag{2.8}$$

At two loops and beyond it may not be possible to simply generalise propagator powers to define a family from specific integrals. One may have to add new propagators to span all possible scalar products. These are known as irreducible scalar products (ISPs) in the literature. However, it is always possible to take a Feynman integral and define a family.

There are two choices of v in this example of eq. (2.7) that give two IBP relations,

$v = k$ or $v = p$,

$$(-2a - b + d)I^{\text{bub}}_{ab} + b(x-1)I^{\text{bub}}_{a,b+1} - bI^{\text{bub}}_{a-1,b+1} - 2aI^{\text{bub}}_{a+1,b} = 0 \quad (2.9a)$$

$$b(x-1)I^{\text{bub}}_{a,b+1} - a(x+1)I^{\text{bub}}_{a+1,b} - bI^{\text{bub}}_{a-1,b+1} + (b-a)I^{\text{bub}}_{ab} + aI^{\text{bub}}_{a+1,b-1} = 0 \quad (2.9b)$$

By setting $a = 1$ and $b = 1$ in eqs. (2.9a) and (2.9b) and $a = 1$ and $b = 0$ in eq. (2.9a) we can solve the equations for I^{bub}_{12}

$$I^{\text{bub}}_{12} = \frac{(d-2)}{2(x-1)} I^{\text{bub}}_{10} - \frac{(d-3)}{x-1} I^{\text{bub}}_{11} \quad (2.10)$$

In fact, we can write any integral in this family in terms of the integrals I^{bub}_{10} and I^{bub}_{11}. These are known as *master* or *basis* integrals because it spans the vector space of the integral family. Notice that we have *chosen* these integrals, we could also change basis, for instance, to $(I^{\text{bub}}_{20}, I^{\text{bub}}_{12})$.

In general, the decomposition of a generic integral belonging to a family into basis integrals takes the following form

$$I(\{x_i\}, \epsilon) = \sum_{\mathbf{b} \in B} p_{\mathbf{b}}(\{x_i\}, \epsilon) I_{\mathbf{b}}(\{x_i\}, \epsilon) \quad (2.11)$$

where $\mathbf{b}$ is a vector of integers specifying the powers of the propagators in a given basis integral and B is a set of vectors identifying a basis. The size of this set and the coefficients $p_{\mathbf{b}}$ depend on the IBP system. The idea of IBP reduction is to take a large expression with many numerators and different powers of propagators and reduce it down to a sum over a smaller set of integrals. The unknowns now are the basis integrals, for which we will use the differential equations technique to evaluate in the next section.

A way to organise the resultant basis vectors is to define sectors. Two integrals are in the same sector if they share the same set of positive indices i.e. $I_{1,5,0,3}$ and $I_{2,1,-3,7}$ are in the same sector but $I_{1,5,0,3}$ and $I_{3,2,4,1}$ are not. We will denote the set of positive indices of sector S_i as ν_i. The sector of $I_{1,5,0,3}$ and $I_{2,1,-3,7}$ has $\nu = \{1, 2, 4\}$.

A sector S_1 is said to be *higher* than sector S_2 if ν_2, is contained in ν_1, i.e. $\nu_2 \subset \nu_1$. Notice that this will not fully order sectors. A convenient way to impose

full sector ordering is to give a number, known as the sector id, to each sector,

$$\mathrm{ID}[S_i] = \sum_{r \in \nu_i} 2^{r-1}. \tag{2.12}$$

The main reason to organise by sector is that the act of differentiating an integral will not create a new positive power propagator but may remove some and/or induce numerators, negative powers. It means that through differentiation an integral will never become a member of a higher sector.

Another concept is that of cuts. For the present thesis *cutting an integral* will involve specifying a set of propagators and finding the residue at the poles of those propagators in complex momenta space. If the propagator is not present then

$$\mathrm{Cut}_{\mathbf{b}}\, I_{\mathbf{a}} = 0 \text{ if any } b_i \notin \nu(\mathbf{a}). \tag{2.13}$$

Taking a cut on an integral is synonymous with selecting a specific sector and all higher sectors. A *maximal cut* is cutting all propagators present

$$\mathrm{MaximalCut}\,[I_{\mathbf{a}}] = \mathrm{Cut}_{\mathbf{b}}\, I_{\mathbf{a}} \text{ when } \nu(\mathbf{b}) = \nu(\mathbf{a}) \tag{2.14}$$

The IBP reduction process readies itself for automation. Using Laporta's algorithm [102] many publicly available codes exist [103–105]. Recent developments in multivariate rational reconstruction [106, 107], implemented in `Kira` [108] and `FIRE6` [109], have helped push the efficiency for reduction at high loop orders.

2.1.3 Solving the differential equation system

We have reduced our generic integral down to a set of basis integrals in eq. (2.11). We first order the basis integrals by sector id, and call the vector of basis integrals $\mathbf{f}$. To find these integrals we take a derivative,

$$\mathrm{d} = \sum_i \mathrm{d}x_i \frac{\partial}{\partial x_i}. \tag{2.15}$$

We then reduce the resultant integrals back to the basis using the IBP system. We obtain a system of first-order differential equations:

$$\mathrm{d}\mathbf{f}(\{x_i\}, \epsilon) = A(\{x_i\}, \epsilon)\mathbf{f}(\{x_i\}, \epsilon), \tag{2.16}$$

where A is a matrix-valued one-form. The system satisfies the consistency condition

$$\mathrm{d}A \wedge A - A \wedge A = 0, \tag{2.17}$$

which says that partial derivatives commute and serves as a good check for complex systems. For the two-dimensional bubble integral example we have

$$\partial_x \begin{pmatrix} I_{10}^{\text{bub}} \\ I_{11}^{\text{bub}} \end{pmatrix} = \begin{pmatrix} 0 & 0 \\ \frac{\epsilon-1}{(x-1)x} & \frac{1-\epsilon(x+1)}{(x-1)x} \end{pmatrix} \begin{pmatrix} I_{10}^{\text{bub}} \\ I_{11}^{\text{bub}} \end{pmatrix} \tag{2.18}$$

We have now derived a system of differential equations. Equation (2.18) can be solved to all orders in ϵ and I_{11}^{bub} evaluates to a ${}_2F_1$ hypergeometric function. The general system in eq. (2.16) is not so simple. One approach to proceed is to find a transformation of the basis $\mathbf{f} = T\mathbf{g}$ such that the differential equation for $\mathbf{g}$ has trivial ϵ dependence

$$\mathrm{d}\mathbf{g}(\{x_i\}, \epsilon) = \epsilon \tilde{A}(\{x_k\})\mathbf{g}(\{x_i\}, \epsilon), \tag{2.19}$$

we will call this form ϵ-form. The matrix $\tilde{A}$ can be found from the original by

$$\tilde{A} = T^{-1}AT - T^{-1}\mathrm{d}T. \tag{2.20}$$

As an example if we were instead to choose the basis

$$\mathbf{g}^{\text{bub}}(x, \epsilon) = \left((1-\epsilon)I_{10}^{\text{bub}}, \frac{\epsilon\, x}{1-x} I_{11}^{\text{bub}}\right) \tag{2.21}$$

in eq. (2.18) we would have the ϵ-form

$$\partial_x\, \mathbf{g}^{\text{bub}}(x, \epsilon) = \epsilon \begin{pmatrix} 0 & 0 \\ \frac{1}{(x-1)^2} & \frac{1+x}{x-x^2} \end{pmatrix} \mathbf{g}^{\text{bub}}(x, \epsilon). \tag{2.22}$$

We can rescale $\mathbf{g}$ by any function of ϵ and leave eq. (2.19) unchanged. It is useful to do so to render $\mathbf{g}$ finite. Then the system can then be solved order by order in ϵ by writing $\mathbf{g}(\{x_i\}, \epsilon) = \sum_{i=0}^{\infty} \epsilon^i \mathbf{g}^{(i)}(\{x_i\})$, with the solution in term of iterated integrals over $\tilde{A}$. Often $\tilde{A}$ is also in the so-called *dlog form*,

$$\tilde{A} = \sum_{i=1}^{|\mathcal{A}|} c_i\, \mathrm{d}\log \mathcal{A}_i, \tag{2.23}$$

where the $\mathcal{A}_i$ are called letters, the set of all letters $\mathcal{A}$ is called the alphabet and c_i are constant matrices. The iterated integrals can often be cast in terms of the Goncharov polylogarithms defined in eq. (1.32). Note that eq. (2.22) is not in dlog form. For a differential system that is both in ϵ-form and in dlog form we shall call this *canonical form*.

The main challenge is finding the transformation T. Methods of doing so are scattered throughout the literature. The methods we will use in this thesis are what we shall call the *leading singularity method* and the *algorithmic approach*.

Leading singularities

This method involves choosing integrals whose integrands (in four dimensions) have what are called unit leading singularities. They are integrands whose (multivariate-)residues are all equal to ± 1. As an example let us take the integrand

$$\Omega = \frac{\mathrm{d}\alpha \wedge \mathrm{d}\beta}{(\alpha\gamma - \beta)\beta}. \tag{2.24}$$

The integral $\int \Omega$ would be a member of our original basis $\mathbf{f}$. One can take a residue at $\alpha = \beta/\gamma$ and then $\beta = 0$ giving $\mathrm{Res}_{\beta=0}\mathrm{Res}_{\alpha=\beta/\gamma}\,\Omega = 1/\gamma$. Or the other possible orders $\mathrm{Res}_{\alpha=0}\mathrm{Res}_{\beta=\alpha\gamma}\,\Omega = -1/\gamma$ and $\mathrm{Res}_{\alpha=0}\mathrm{Res}_{\beta=0}\,\Omega = 1/\gamma$. This tells us that $\gamma\int\Omega$ is a good candidate for $\mathbf{g}$. Alternatively, we can write $\gamma\,\Omega$ in a dlog form,

$$\gamma\,\Omega = \mathrm{d}\log(\alpha\gamma - \beta) \wedge \mathrm{d}\log\beta. \tag{2.25}$$

Equivalently we can compute these by replacing all denominators with delta functions

$$\frac{1}{(\alpha\gamma - \beta)\beta} \to \delta(\beta)\delta(\alpha\gamma - \beta) \tag{2.26}$$

these are then solved in four dimensions to find leading singularities or in d dimensions for the maximal cut in eq. (2.14).

The main difficulty when applying to Feynman integrals is finding the best way to parameterise loop momenta such that square roots do not appear when calculating residues. Once a convenient parameterisation is chosen, to find candidate integrals in a given sector an ansatz for the numerator is established and repeated residues are taken to fix the ansatz such that integrals give unit leading singularities. A recent algorithm and computer implementation is given in [110].

Algorithmic approach

Another method is to create a rational ansatz for the transformation T. An algorithm to construct and fit such an ansatz was given by Meyer in [111]. It requires the condition that a rational transformation exists and that the alphabet is rational. Other than that the only limitation is computer memory. Meyer also provided a public implementation of the algorithm in the form of `CANONICA` [112].

We shall now use the technique of differential equations to evaluate integrals arising from the soft function defined in Section 1.1.

2.2 The One-loop Soft Function

We will now explicitly calculate the soft function eq. (1.5) to first order in perturbation theory. It captures all the infrared singularities of massive scattering amplitudes to one-loop. We will also use it as a pedagogical example of the technique of differential equations. We first expand the Wilson line eq. (1.12) to first order in g_s,

$$W_{\beta_i}^{(m)}(\infty,0) = 1 + ig_s\mathbf{T}_i^a \int_0^\infty d\lambda\, \beta_i \cdot A^a(\lambda\beta_i) e^{-im\lambda\sqrt{\beta_i^2}} + \mathcal{O}(g_s^2). \tag{2.27}$$

The n-leg soft function $\mathcal{S}_n^{(m)}$ eq. (1.13) to this order is

$$\begin{aligned}
\mathcal{S}_n^{(m)} &= \langle 0|\mathrm{T}\left\{\prod_{i=1}^n W_\beta^{(m)}(\infty,0)\right\}|0\rangle && \text{(2.28a)}\\
&= \langle 0|1 + ig_s\sum_{i=1}^n \mathbf{T}_i^a \int_0^\infty d\lambda\, \beta_i \cdot A^a(\lambda\beta_i) e^{-im\lambda\sqrt{\beta_i^2}}|0\rangle && \text{(2.28b)}\\
&= \langle 0|0\rangle + ig_s\sum_{i=1}^n \mathbf{T}_i^a \int_0^\infty d\lambda\, \beta_i \cdot \langle 0|A^a(\lambda\beta_i)|0\rangle\, e^{-im\lambda\sqrt{\beta_i^2}} && \text{(2.28c)}\\
&= 1, && \text{(2.28d)}
\end{aligned}$$

where we used $\langle 0|0\rangle = 1$ and $\langle 0|A^\mu(x)|0\rangle = 0$. The former holds because we normalise our states to the vacuum, the latter is a standard result in QFT

textbooks (e.g. [113]). Since $\mathcal{S}_n^{(m)}$ vanishes at $\mathcal{O}(g_s)$ we go to the next order,

$$\begin{aligned}\mathcal{S}_n^{(m)} =& 1 + (ig_s)^2 \sum_{\substack{i,j=1\\ i<j}}^{n} \mathbf{T}_i^a \mathbf{T}_j^b \int_0^\infty d\lambda d\sigma \beta_i^\mu \beta_j^\nu \langle 0|\mathrm{T}\left\{A_\mu^a(\lambda\beta_i) A_\nu^b(\sigma\beta_j)\right\}|0\rangle f_i(\lambda) f_j(\sigma) \\ &+ (ig_s)^2 \sum_{i=1}^{n} \mathbf{T}_i^a \mathbf{T}_i^b \int_0^\infty d\lambda \int_0^\lambda d\sigma \beta_i^\mu \beta_i^\nu \langle 0|\mathrm{T}\left\{A_\mu^a(\lambda\beta_i) A_\nu^b(\sigma\beta_i)\right\}|0\rangle f_i(\lambda) f_i(\sigma) \\ =& 1 + (ig_s)^2 \sum_{\substack{i,j=1\\ i<j}}^{n} \mathbf{T}_i^a \mathbf{T}_j^a \int \frac{d^dk}{(2\pi)^d} \frac{i\beta_i\cdot\beta_j}{k^2(k\cdot\beta_i - m + i\varepsilon)(-k\cdot\beta_j - m + i\varepsilon)} \\ &+ \frac{(ig_s)^2}{2m} \sum_{i=1}^{n} C_i \int \frac{d^dk}{(2\pi)^d} \frac{i}{k^2(k\cdot\beta_i - m + i\varepsilon)} \end{aligned} \tag{2.29}$$

where $f_i(\lambda) = e^{-im\lambda\sqrt{\beta_i^2}}$ is the exponential damping term. We have inserted the gluon propagator in Feynman gauge [113],

$$\langle 0|\mathrm{T}\left\{A_\mu^a(\lambda\beta_i) A_\nu^b(\sigma\beta_j)\right\}|0\rangle = -\frac{\Gamma(1-\epsilon)}{4\pi^{2-\epsilon}} \frac{\delta^{ab}\eta_{\mu\nu}}{(-(\lambda\beta_i - \sigma\beta_j)^2 + i\varepsilon)^{1-\epsilon}}, \tag{2.30}$$

Fourier transformed to momentum space and performed the simple integrals over λ and σ. In the third term of the first line we integrate σ from 0 to λ because of the path ordering on the Wilson line. We have also explicitly broken the rescaling invariance by setting $\beta_i^2 = 1$. This is just for simplicity and the full dependence can always be reinstated knowing that the result depends on the scale invariant quantity in eq. (1.9). Also, $\mathbf{T}_i^2 = C_i$ is the Casimir in the representation of Wilson line i. The $+i\varepsilon$ prescription on the momentum space quadratic propagators is implicit.

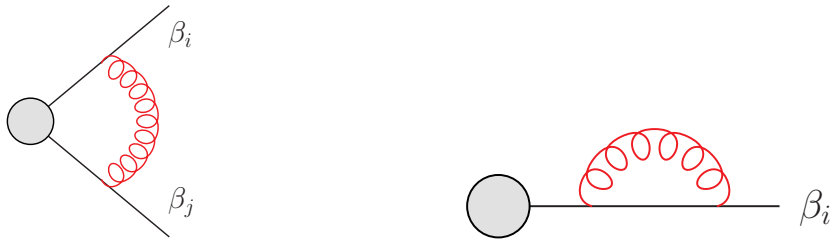

(a) Diagram connecting two lines **(b)** Self energy on one line

Figure 2.1: Diagrams contributing to the one loop soft function

We can represent the two non-trivial terms in eq. (2.29) diagrammatically as shown in Figure 2.1. The first term connects both Wilson lines (β_i and β_j) whereas the second term is of a self energy type. The Feynman rules for the diagrams are the standard QCD rules plus rules for the emission of a gluon with

momentum k and spin index μ from the Wilson line β

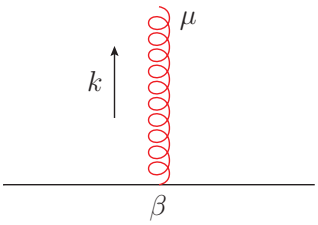

$$= \frac{i\,\beta^\mu}{k\cdot\beta + i\varepsilon} \tag{2.31}$$

and the absorption is also eq. (2.31) but with $k \to -k$.

We calculate the integrals in eq. (2.29) by differential equations. We shall follow the procedure outlined in Section 2.1. Let us first define the following family of integrals

$$I^{[1,1]}_{a_1,a_2,a_3}(\beta_i\cdot\beta_j,\epsilon) = e^{\epsilon\gamma_E} m^{2a_1+a_2+a_3-d} \int \frac{d^dk}{i\pi^{d/2}} \frac{1}{(k^2)^{a_1}(k\cdot\beta_i - m)^{a_2}(-k\cdot\beta_j - m)^{a_3}}. \tag{2.32}$$

The factor of $e^{\epsilon\gamma_E}/i\pi^{d/2}$ is a convenient normalisation choice because it eliminates γ_E terms and π factors, readying the computation for $\overline{\text{MS}}$ coupling renormalisation. We now write the soft function in eq. (2.29) as

$$\mathcal{S}^{(m)}_n = 1 - (ig_s)^2 \left(\frac{\mu}{m}\right)^{2\epsilon} \frac{e^{-\epsilon\gamma_E}}{2^d\pi^{d/2}} \left(\sum_{\substack{i,j=1\\ i<j}}^{n} \mathbf{T}^a_i \mathbf{T}^a_j \beta_i\cdot\beta_j I^{[1,1]}_{111} + \frac{1}{2}\sum_{i=1}^{n} C_i I^{[1,1]}_{110} \right). \tag{2.33}$$

Using eqs. (1.14) and (1.15), the one-loop coefficient of the corresponding soft anomalous dimension is given by

$$\Gamma^{(i)}_n = -2 \left(\sum_{\substack{i,j=1\\ i<j}}^{n} \mathbf{T}^a_i \mathbf{T}^a_j \beta_i\cdot\beta_j I^{[1,1],(-1)}_{111} + \frac{1}{2}\sum_{i=1}^{n} C_i I^{[1,1],(-1)}_{110} \right) \tag{2.34}$$

In the above we define the strong coupling constant

$$\alpha_s = \frac{g_s^2}{4\pi}, \tag{2.35}$$

and the superscript (-1) means the $\frac{1}{\epsilon}$ pole of the integral. In the following section we compute $I^{[1,1]}_{111}$ using differential equations.

2.2.1 Integration-by-parts relations

The IBP relations for the family in eq. (2.32) are,

$$-(2a_1+a_2+a_3-d)I^{[1,1]}_{a_1,a_2,a_3}-(a_3I^{[1,1]}_{a_1,a_2,a_3+1}+a_2I^{[1,1]}_{a_1,a_2+1,a_3})=0 \tag{2.36a}$$

$$a_3\beta_i\cdot\beta_jI^{[1,1]}_{a_1,a_2,a_3+1}-a_2I^{[1,1]}_{a_1,a_2+1,a_3}-2a_1(I^{[1,1]}_{a_1,a_2-1,a_3}+I^{[1,1]}_{a_1+1,a_2,a_3})=0 \tag{2.36b}$$

$$a_3I^{[1,1]}_{a_1,a_2,a_3+1}-a_2\beta_i\cdot\beta_jI^{[1,1]}_{a_1,a_2+1,a_3}+2a_1(I^{[1,1]}_{a_1,a_2,a_3-1}+I^{[1,1]}_{a_1+1,a_2,a_3})=0. \tag{2.36c}$$

Using these relations we can find the set of basis integrals to be

$$\mathbf{f}^{[1,1]}=\left(I^{[1,1]}_{110},I^{[1,1]}_{101},I^{[1,1]}_{111}\right), \tag{2.37}$$

where the integrals are ordered by sector ID as defined in eq. (2.12). In the kinematics of $\beta_i^2=1\,\forall i$, $I^{[1,1]}_{110}=I^{[1,1]}_{101}$ but we shall continue as if they are different and have only solved the system in eqs. (2.36a) to (2.36c).

2.2.2 Differential system

The convenient variables to use for these integrals are not the natural (dimensionless) scalar products $\beta_i\cdot\beta_j$ but rather the α_{ij} variables which are defined through [64],

$$\beta_i\cdot\beta_j=-\frac{1}{2}\left(\alpha_{ij}+\frac{1}{\alpha_{ij}}\right). \tag{2.38}$$

These remove the presence of square roots in the differential equations. In Chapter 3 we will explore why these are a good choice of variables. For now, we take a derivative with respect to α_{ij} of the vector of integrals $\mathbf{f}$,

$$\partial_{\alpha_{ij}}\mathbf{f}^{[1,1]}=\begin{pmatrix}0&0&0\\0&0&0\\\frac{2\epsilon-1}{1-\alpha_{ij}^2}&\frac{2\epsilon-1}{1-\alpha_{ij}^2}&\frac{1+\alpha_{ij}^2-(1-\alpha_{ij})^2\epsilon}{\alpha_{ij}(1-\alpha_{ij}^2)}\end{pmatrix}\mathbf{f}^{[1,1]}. \tag{2.39}$$

The first two rows are 0 because $I^{[1,1]}_{110}$ and $I^{[1,1]}_{101}$ do not depend on α_{ij}. We can actually solve this system for general ϵ but for more complicated systems at higher loops it is often impossible. As a pedagogical example we shall now take the opportunity to find the transformation to canonical form (2.19) by integrand analysis. To achieve this, we consider the integrals in turn.

We can compute the (eikonal) bubble integrals $I^{[1,1]}_{110}$ and $I^{[1,1]}_{101}$ by simple Feynman

integral techniques. We find,

$$I^{[1,1]}_{a_1,0,a_2} = I^{[1,1]}_{a_1,a_2,0} = \frac{2^{4-2\epsilon-2a_1}(-1)^{a_1+a_2}\Gamma(2a_1+a_2-4+2\epsilon)\Gamma(2-\epsilon-a_1)}{\Gamma(a_1)\Gamma(a_2)}. \quad (2.40)$$

By expanding in ϵ we find that $\epsilon(1-2\epsilon)I^{[1,1]}_{110}$ is an integral of uniform weight,

$$\begin{aligned}\epsilon(1-2\epsilon)I^{[1,1]}_{110} =& -2 + 4\epsilon\log(2) + \epsilon^2\left(-5\zeta_2 - 4\log^2(2)\right) \\ &+ \epsilon^3\left(10\zeta_2\log(2) + \frac{14\zeta_3}{3} + \frac{8\log^3(2)}{3}\right) + \mathcal{O}(\epsilon^4) \end{aligned} \quad (2.41)$$

and the same is true for $\epsilon(1-2\epsilon)I^{[1,1]}_{101}$. It means that $\epsilon(1-2\epsilon)I^{[1,1]}_{110}$ is a good choice of basis integral. The $\log 2$ terms appear because of the regulator m that is used. If we were to rescale m by 2 then the $\log 2$ terms would disappear.

To test the uniform weight potential of $I^{[1,1]}_{111}$ we shall compute its leading singularity

$$\text{LeadingSingularity}[I^{[1,1]}_{111}] \sim \int d^4k \;\; \delta(k^2)\,\delta(k\cdot\beta_i - m)\,\delta(-k\cdot\beta_j - m). \quad (2.42)$$

We have removed overall numerical prefactors as they are irrelevant. We can evaluate eq. (2.42) by using Sudakov decomposition by setting $k = \gamma_1\beta_i + \gamma_2\beta_j + k_\perp$. The Jacobian of this change of variables is given by,

$$J = \sqrt{\left|\det \frac{\partial k^\mu}{\partial(\gamma_1,\gamma_2,k_\perp)}\frac{\partial k_\mu}{\partial(\gamma_1,\gamma_2,k_\perp)}\right|} = \sqrt{1-(\beta_i\cdot\beta_j)^2}. \quad (2.43)$$

After performing the delta function integrals we find that the leading singularity is

$$\text{LeadingSingularity}[I^{[1,1]}_{111}] \sim \frac{\alpha_{ij}}{1-\alpha_{ij}^2} \equiv s(\alpha_{ij}). \quad (2.44)$$

The rational function $s(\alpha)$ often appears for these types of integrals and we shall discuss it further in Chapter 3. If we normalise the integral by this factor, defining $\frac{1}{s(\alpha_{ij})}I^{[1,1]}_{111}$, then we know it is a good candidate for a uniform weight integral because it has unit leading singularity. We then define our new basis and

find for the system in eq. (2.19)

$$\mathbf{g}^{[1,1]} = \left(\epsilon(1-2\epsilon) f_1^{[1,1]}\,,\, \epsilon(1-2\epsilon) f_2^{[1,1]}\,,\, \frac{\epsilon^2}{s(\alpha_{ij})} f_3^{[1,1]}\right) \tag{2.45a}$$

$$\mathrm{d}\mathbf{g}^{[1,1]}(\alpha_{ij},\epsilon) = \epsilon \tilde{A}^{[1,1]}(\alpha_{ij})\mathbf{g}^{[1,1]}(\alpha_{ij},\epsilon) \tag{2.45b}$$

$$\tilde{A}^{[1,1]} = \begin{pmatrix} 0 & 0 & 0 \\ 0 & 0 & 0 \\ -\frac{1}{\alpha_{ij}} & -\frac{1}{\alpha_{ij}} & \frac{\alpha_{ij}-1}{\alpha_{ij}(\alpha_{ij}+1)} \end{pmatrix} \mathrm{d}\alpha_{ij} \tag{2.45c}$$

$$= c_1^{[1,1]}\,\mathrm{d}\log\alpha_{ij} + c_2^{[1,1]}\,\mathrm{d}\log(1+\alpha_{ij})\,, \tag{2.45d}$$

where $c_i^{[1,1]}$ are constant matrices. Since we can write the system in $\mathrm{d}\log$ form and can factor ϵ out it proves that the elements of $\mathbf{g}^{[1,1]}$ are uniform weight. We can always choose the overall ϵ normalisation such that $\mathbf{g}^{[1,1]}$ admits an expansion in ϵ starting at ϵ^0. The alphabet for the $[1,1]$-web is $\mathcal{A}^{[1,1]} = \{\alpha_{ij}, 1+\alpha_{ij}\}$.

2.2.3 Boundary conditions

In order to solve the differential equation system in eq. (2.45) we need boundary conditions. For this we choose the special configuration where the Wilson lines are such that $\beta_i = -\beta_j$. It is easy to see that this corresponds to $\alpha_{ij} = 1$ in eq. (2.38). We shall explore the physical meaning of this limit in Section 3.3 when we use it as a constraint for bootstrapping functions. At this boundary point, $g_3^{[1,1]}(1,\epsilon) = 0$ due to the rational prefactor. Whereas for $g_1^{[1,1]}$ and $g_2^{[1,1]}$ we already know their result from eq. (2.40).

2.2.4 Solution

We can solve the system in eq. (2.45) order by order in ϵ by first expanding the integrals in ϵ

$$\mathbf{g}^{[1,1]}(\alpha_{ij},\epsilon) = \sum_{n=0}^{\infty} \mathbf{g}^{[1,1],(n)}(\alpha_{ij})\,\epsilon^n. \tag{2.46}$$

Plugging this into eq. (2.45b) and integrating along the contour from the boundary $\alpha_{ij} = 1$ to an arbitrary value of α_{ij} we find

$$\mathbf{g}^{[1,1],(0)}(\alpha_{ij}) = \mathbf{g}^{[1,1],(0)}(1) \tag{2.47a}$$

$$\mathbf{g}^{[1,1],(1)}(\alpha_{ij}) = \int_1^{\alpha_{ij}} \tilde{A}^{[1,1]}(\alpha'_{ij}).\mathbf{g}^{[1,1],(0)}(1) + \mathbf{g}^{[1,1],(1)}(1) \tag{2.47b}$$

$$\mathbf{g}^{[1,1],(2)}(\alpha_{ij}) = \int_1^{\alpha_{ij}} \tilde{A}^{[1,1]}(\alpha'_{ij}).\mathbf{g}^{[1,1],(1)}(\alpha'_{ij}) + \mathbf{g}^{[1,1],(2)}(1) \tag{2.47c}$$

and so on. Explicitly performing the integrals we have

$$\mathbf{g}^{[1,1],(0)}(\alpha_{ij}) = (-2, -2, 0) \tag{2.48a}$$

$$\mathbf{g}^{[1,1],(1)}(\alpha_{ij}) = (4\log 2, 4\log 2, 4\log(\alpha_{ij})) \tag{2.48b}$$

$$\begin{aligned}\mathbf{g}^{[1,1],(2)}(\alpha_{ij}) = \Big(&-5\zeta_2 - 4\log(2)^2, -5\zeta_2 - 4\log(2)^2, \\ &4\zeta_2 - 8G_0(2)G_0(\alpha_{ij}) + 8G_{-1,0}(\alpha_{ij}) - 4G_{00}(\alpha_{ij})\Big)\end{aligned} \tag{2.48c}$$

where we have written the result of $\mathbf{g}^{(2)}(\alpha_{ij})$ in terms of the multiple polylogarithms defined in eq. (1.32). To go back to the original $\mathbf{f}$ basis of integrals we simply invert eq. (2.45a). Using eqs. (2.48b) and (2.48c) we have for $I^{[1,1]}_{111}$,

$$I^{[1,1]}_{111} = 4s_{ij}\left[\frac{G_0(\alpha_{ij})}{\epsilon} + \Big(\zeta_2 - 2G_0(2)G_0(\alpha_{ij}) + 2G_{-1,0}(\alpha_{ij}) - G_{00}(\alpha_{ij})\Big) + \mathcal{O}(\epsilon)\right] \tag{2.49}$$

with $s_{ij} \equiv s(\alpha_{ij})$. We now have all the ingredients for the one-loop soft anomalous dimension. Inserting eqs. (2.41) and (2.49) into eq. (2.34) we arrive at,

$$\Gamma^{(1)}_n = \underbrace{4\sum_{i,j=1,i<j}^{n} \mathbf{T}^a_i \mathbf{T}^a_j \frac{1+\alpha_{ij}^2}{1-\alpha_{ij}^2}\log(\alpha_{ij})}_{\sum_{\text{pairs}} \Gamma^{(1)}_{\text{dipole}}} + \underbrace{2\sum_{i=1}^{n} C_i}_{\sum_{I=1}^{n}\gamma^{(1)}_I} \tag{2.50a}$$

$$= \sum_{\text{pairs}} \Gamma^{(1)}_{\text{dipole}} + \sum_{I=1}^{n} \gamma^{(1)}_I \tag{2.50b}$$

Equation (2.50a) captures all infrared divergences of massive scattering amplitudes at one-loop. In eq. (2.50b) we have decomposed $\Gamma^{(1)}_n$ into $\Gamma^{(1)}_{\text{dipole}}$, which captures correlations between two particles, and $\gamma^{(1)}_I$ which captures self energies and solely depends on the colour representation of line I. Both of these functions extend to all loop orders with Γ_{dipole} calculated at two loops in [79] and three loops in [22] and γ_I can be found from Γ_{dipole} via Ward identities [79]. The technique of

differential equations was used in the three-loop two-line case of $\Gamma^{(3)}_{\text{dipole}}$ [22]. We have written eq. (2.50b) in that way to be clear where contributions are coming from.

The constituent one-loop web functions defined in eq. (1.16) are,

$$w^{(1,-1)} = -2\mathbf{T}_i^a\mathbf{T}_j^a r(\alpha_{ij})\log(\alpha_{ij}) \tag{2.51a}$$

$$w^{(1,0)} = -2\mathbf{T}_i^a\mathbf{T}_j^a r(\alpha_{ij})\Big(\zeta_2 - 2G_0(2)G_0(\alpha_{ij}) + 2G_{-1,0}(\alpha_{ij}) - G_{00}(\alpha_{ij})\Big) \tag{2.51b}$$

where we have defined the common rational function

$$r(\alpha) = \frac{1+\alpha^2}{1-\alpha^2}. \tag{2.52}$$

At two loops there are also corrections to eq. (2.50b) that connect three legs which we shall call $\Gamma^{(2)}_{\text{tripole}}$. In the following two sections we shall compute these using differential equations.

2.3 $[1,2,1]$-web

There are two two-loop corrections to the soft function that connect three lines, contributing to $\Gamma^{(2)}_{\text{tripole}}$. The first that we shall consider is the so-called $[1,2,1]$-web, $w^{(2)}_{121}$. There are two diagrams that contribute to such a web which are shown in Figure 2.2. Letting the colour and kinematic factor of each diagram be $\mathcal{C}$ and $\mathcal{F}$ respectively,

$$w^{(2)}_{121}\left(\frac{\alpha_s}{4\pi}\right)^2 = \frac{1}{2}(\mathcal{C}_A - \mathcal{C}_B)(\mathcal{F}_A - \mathcal{F}_B) \tag{2.53a}$$

$$= -\frac{1}{2}\mathrm{i}f^{abc}\mathbf{T}_1^a\mathbf{T}_2^b\mathbf{T}_3^c(\mathcal{F}_A - \mathcal{F}_B) \tag{2.53b}$$

The two kinematic factors $\mathcal{F}_A$ and $\mathcal{F}_B$ are related by exchanging lines 1 and 3. We proceed as before by defining the family of integrals,

$$I^{[1,2,1]}{}_{a_1a_2a_3a_4a_5a_6a_7a_8a_9}(\beta_1\cdot\beta_2, \beta_1\cdot\beta_3, \beta_2\cdot\beta_3, \epsilon) = m^{M_d}e^{2\epsilon\gamma}\int\frac{d^dk_1}{i\pi^{d/2}}\int\frac{d^dk_2}{i\pi^{d/2}}\frac{1}{D_1^{a_1}D_2^{a_2}D_3^{a_3}D_4^{a_4}D_5^{a_5}D_6^{a_6}D_7^{a_7}D_8^{a_8}D_9^{a_9}} \tag{2.54}$$

$$D_1 = k_1^2 \qquad D_2 = k_2^2 \qquad D_3 = -k_1 \cdot \beta_1 - m$$
$$D_4 = k_2 \cdot \beta_2 - m \qquad D_5 = (k_1 + k_2) \cdot \beta_2 - m \qquad D_6 = -k_2 \cdot \beta_3 - m$$
$$D_7 = k_1 \cdot \beta_3 \qquad D_8 = k_2 \cdot \beta_1 \qquad D_9 = k_1 \cdot k_2$$

with M_d fixed such that $I^{[1,2,1]}_{\mathbf{a}}$ is dimensionless. The integral that appears in the web in eq. (2.53) is $I^{[1,2,1]}_{111111000}$. Note we are using a different regularisation scheme than that in eq. (1.12). Only the gluon emitted last has an exponential damping term. If it was attached to all gluons then D_5 would have $2m$ instead of just m. This would complicate the differential equations and, in momentum space, it is simpler to add a single m to each eikonal propagator. It does not change the final result.

A priori $I^{[1,2,1]}_{111111000}$ depends on three variables, the scalar products between the Wilson lines or the α variables $\{\alpha_{12}, \alpha_{13}, \alpha_{23}\}$ but as no gluon spans the angle between β_1 and β_3 it does not depend on α_{13}. We shall use shorthand notation that drops trailing zeroes from the definition of the family $I^{[1,2,1]}$ i.e. $I^{[1,2,1]}_{111111} \equiv I^{[1,2,1]}_{111111000}$. We can then write the web in terms of this family

$$w^{(2)}_{(121)}(\alpha_{12}, \alpha_{23}, m, \epsilon) = \mathrm{i}m^{-4\epsilon}\frac{1}{2} f^{abc}\mathbf{T}_1^a\mathbf{T}_2^b\mathbf{T}_3^c \beta_1 \cdot \beta_2 \beta_2 \cdot \beta_3 \left(I^{[1,2,1]}_{111111} - 1 \leftrightarrow 3\right) \quad (2.55)$$

where $1 \leftrightarrow 3$ represents the exchange $\{\alpha_{12}, \alpha_{23}\} \to \{\alpha_{23}, \alpha_{12}\}$. We now proceed to compute $I^{[1,2,1]}_{111111}$ by differential equations.

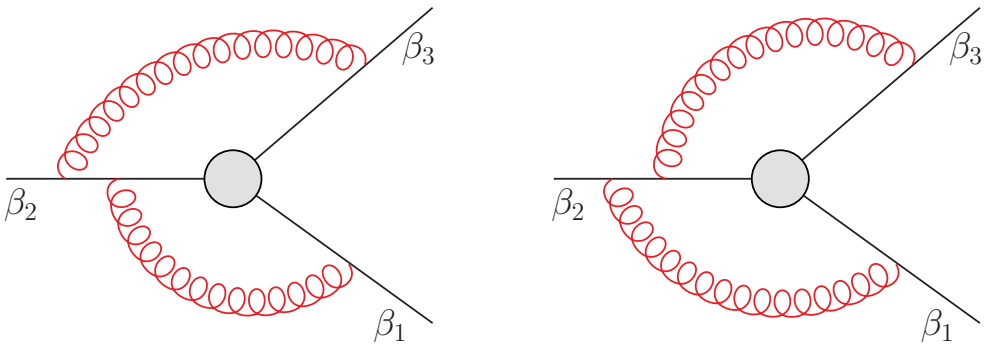

(a) Diagram A **(b)** Diagram B

Figure 2.2: Diagrams contributing to the $[1, 2, 1]$-web

2.3.1 Differential equation

We go through the now standard procedure of taking a derivative with respect to the two variables and reduce the resultant integrals down to a set of 12 basis

integrals. We write the differential equation as

$$\mathrm{d}\,\mathbf{f}^{[1,2,1]} \;=\; A^{[1,2,1]}\,\mathbf{f}^{[1,2,1]}, \tag{2.56}$$

where d is the exterior derivative with respect to the variables $\{\alpha_{12}, \alpha_{23}\}$ such that A has the form $A^{[1,2,1]} = A_{12}^{[1,2,1]}\,\mathrm{d}\alpha_{12} + A_{23}^{[1,2,1]}\,\mathrm{d}\alpha_{23}$. The matrix A also respects the consistency condition in eq. (2.17). The basis integrals we have are

$$\begin{aligned}\mathbf{f}^{[1,2,1]} = (&I_{1111}^{[1,2,1]}, I_{11001}^{[1,2,1]}, I_{11101}^{[1,2,1]}, I_{11102}^{[1,2,1]}, I_{11111}^{[1,2,1]}, I_{111101}^{[1,2,1]},\\ &I_{110011}^{[1,2,1]}, I_{110012}^{[1,2,1]}, I_{111011}^{[1,2,1]}, I_{111012}^{[1,2,1]}, I_{111021}^{[1,2,1]}, I_{111111}^{[1,2,1]}\,)\end{aligned} \tag{2.57}$$

2.3.2 Solving the equation

Transformation to canonical form

In order to find the transformation we use Meyer's algorithm [111] implemented in the computer package `CANONICA` [112]. The algorithm gives the transformation $T^{[1,2,1]}$ where $\mathbf{f}^{[1,2,1]} = T^{[1,2,1]}\mathbf{g}^{[1,2,1]}$ and

$$\mathrm{d}\,\mathbf{g}^{[1,2,1]} = \epsilon\,\tilde{A}^{[1,2,1]}\,\mathbf{g}^{[1,2,1]}. \tag{2.58}$$

Furthermore, $\tilde{A}^{[1,2,1]}$ is in the d log form

$$\tilde{A}^{[1,2,1]} = \sum_{i=1}^{|\mathcal{A}^{[1,2,1]}|} c_i^{[1,2,1]}\mathrm{d}\log\mathcal{A}_i^{[1,2,1]}, \tag{2.59}$$

where the alphabet for the $[1,2,1]$-web is $\mathcal{A}^{[1,2,1]} = \{\alpha_{12}-1, \alpha_{12}, \alpha_{12}+1, \alpha_{23}-1, \alpha_{23}, \alpha_{23}+1, \alpha_{12}+\alpha_{23}-1, 1+\alpha_{12}\alpha_{23}-\alpha_{12}, 1+\alpha_{12}\alpha_{23}-\alpha_{23}, \alpha_{12}\alpha_{23}-\alpha_{12}-\alpha_{23}\}$. The matrices $c_i^{[1,2,1]}$ and the specific integrals $\mathbf{g}^{[1,2,1]}$ are given in Appendix A.1. The transformation $T^{[1,2,1]}$ can also be found by analysing the integrands of $\mathbf{f}^{[1,2,1]}$.

Boundary

We will choose as our boundary $\alpha_{12} = \alpha_{23} = 1$ which corresponds to the Wilson line configuration $\beta_1 = -\beta_2 = \beta_3$. We shall define the boundary vector $\mathbf{b}^{[1,2,1]} = \mathbf{g}^{[1,2,1]}(\alpha_{12}=1, \alpha_{23}=1)$.

We use as a building block for the boundary calculations, the eikonal bubble

result in eq. (2.40)

$$\int \frac{d^dk}{i\pi^{d/2}} \frac{1}{(k_1^2)^{a_1}(k_1\cdot\beta_1 - M)^{a_2}} = L(a_1,a_2)M^{d-2a_1-a_2},$$
$$L(a_1,a_2) = \frac{2^{d-2a_1}(-1)^a\Gamma(2a_1+a_2-d)\Gamma(\frac{d}{2}-a_1)}{\Gamma(a_1)\Gamma(a_2)}, \tag{2.60}$$

here M could depend on scalar products of external momenta and loop momenta yet to be performed. Evaluating the integrals at the boundary we find

$$\begin{aligned} b_1^{[1,2,1]} &= -2^{4-4\epsilon}(1-2\epsilon)^2\epsilon^2 e^{2\epsilon\gamma}\Gamma(1-\epsilon)^2\Gamma(2\epsilon-1)^2 \\ &= -4 + 16\epsilon\log(2) - \frac{2}{3}\epsilon^2\left(5\pi^2 + 48\log(2)^2\right) + \mathcal{O}(\epsilon^3) \qquad (2.61a) \\ b_2^{[1,2,1]} &= \frac{1}{3}2^{4-4\epsilon}\epsilon(1-2\epsilon)(3-4\epsilon)(-1+4\epsilon)e^{2\epsilon\gamma}\Gamma(1-\epsilon)^2\Gamma(-3+4\epsilon) \\ &= \frac{2}{3} - \frac{8}{3}\epsilon\log(2) + \frac{1}{3}\epsilon^2(3\pi^2 + 16\log(2)^2) + \mathcal{O}(\epsilon^3) \qquad (2.61b) \end{aligned}$$

and all the other g_i vanish on the boundary. In eqs. (2.61a) and (2.61b) we clearly see the uniform weight nature of the integrals.

Integrating dlog forms

We now have what we need to explicitly integrate eq. (2.58). We focus on the twelfth component of $\mathbf{g}^{[1,2,1]}$,

$$g_{12}^{[1,2,1]} = \epsilon^4 \frac{1-\alpha_{12}^2}{\alpha_{12}} \frac{1-\alpha_{23}^2}{\alpha_{23}} I_{111111}^{[1,2,1]}, \tag{2.62}$$

since we require the integral $I_{111111}^{[1,2,1]}$. The first non-zero terms of this are

$$g_{12}^{[1,2,1],(2)} = 8\int_\gamma (\,\mathrm{d}\log\alpha_{12}\,\mathrm{d}\log\alpha_{23} + \mathrm{d}\log\alpha_{23}\mathrm{d}\log\alpha_{12}) \tag{2.63a}$$

$$\begin{aligned} g_{12}^{[1,2,1],(3)} = 16\int_\gamma \Big(&\mathrm{d}\log(y_{23})\mathrm{d}\log(\alpha_{23})\mathrm{d}\log(\alpha_{12}) - \mathrm{d}\log(\eta_{12})\mathrm{d}\log(\alpha_{23})\mathrm{d}\log(\alpha_{12}) \\ &+ \mathrm{d}\log(\alpha_{23})\mathrm{d}\log(\eta_{12})\mathrm{d}\log(\alpha_{12}) + \mathrm{d}\log(\eta_{12})\mathrm{d}\log(\alpha_{12})\mathrm{d}\log(\alpha_{23}) \\ &- \mathrm{d}\log(y_{23})\mathrm{d}\log(\alpha_{12})\mathrm{d}\log(\alpha_{23}) - \mathrm{d}\log(\alpha_{12})\mathrm{d}\log(y_{23})\mathrm{d}\log(\alpha_{23})\Big) \end{aligned} \tag{2.63b}$$

where $y_{ij} = \frac{1+\alpha_{ij}}{1-\alpha_{ij}}$ and $\eta_{ij} = \frac{\alpha_{ij}}{1-\alpha_{ij}^2}$. It is now worthwhile to explain how to integrate the $\mathrm{d}\log$ integrals of multiple variables given in eqs. (2.63a) and (2.63b).

Individual terms are not "integrable" in the sense that the contours are not parameterisation invariant, only the sum does not depend on the choice of contour.

To illustrate this we integrate the first term of eq. (2.63a) on a straight line contour from $(1,1) \to (\alpha_{12}, \alpha_{23})$. The contour is then parameterised as $\gamma_1(t) = ((\alpha_{12}-1)t+1, (\alpha_{23}-1)t+1)$. Then applying the formula for iterated integrals eq. (1.43) we have,

$$\int_{\gamma_1} \mathrm{d}\log\alpha_{12}\,\mathrm{d}\log\alpha_{23} = \int_0^1 dt_1 \int_0^{t_1} dt_2 \frac{(\alpha_{12}-1)}{(\alpha_{12}-1)t_1+1}\frac{(\alpha_{23}-1)}{(\alpha_{23}-1)t_2+1} \tag{2.64a}$$

$$= G_0(\alpha_{12})G_0(\alpha_{23}) - G_0(\alpha_{23})G_{\alpha_{23}}(\alpha_{12}) + G_{\alpha_{23},0}(\alpha_{12}) - G_{1,0}(\alpha_{12}) - G_{0,0}(\alpha_{23}) + G_{1,0}(\alpha_{23}) - \frac{\pi^2}{6} \tag{2.64b}$$

If we were to instead choose a contour γ_2 that first traverses α_{23} then α_{12} i.e. $\gamma_A = (1, (\alpha_{23}-1)t+1)$, $\gamma_B = ((\alpha_{12}-1)t+1, \alpha_{23})$ with $\gamma_2 = \gamma_B \circ \gamma_A$. Both contours γ_1 and γ_2 are illustrated in Figure 2.3. Using the path decomposition formula of Chen's iterated integrals given in eq. (1.44) we have

$$\int_{\gamma_2} \mathrm{d}\log\alpha_{12}\,\mathrm{d}\log\alpha_{23} = \int_{\gamma_B} \mathrm{d}\log\alpha_{12} \int_{\gamma_A} \mathrm{d}\log\alpha_{23} = \log\alpha_{12}\log\alpha_{23} \tag{2.65}$$

It is clear that eqs. (2.64b) and (2.65) are different. It is only when combined with the other term in eq. (2.63a) will they be the same. Integrating the other term over γ_2 we find

$$\int_{\gamma_2} \mathrm{d}\log\alpha_{23}\,\mathrm{d}\log\alpha_{12} = \int_{\gamma_B} \mathrm{d}\log\alpha_{23} \int_{\gamma_A} \mathrm{d}\log\alpha_{12} = 0. \tag{2.66}$$

We then find that

$$g_{12}^{[1,2,1],(2)} = 8\log(\alpha_{12})\log(\alpha_{23}). \tag{2.67}$$

If we were to integrate the other term over γ_1 then we result in a similar unwieldy expression to eq. (2.67). Only in the total do we achieve the straightforward result in eq. (2.67) which suggests that γ_2 is the simple contour to choose.

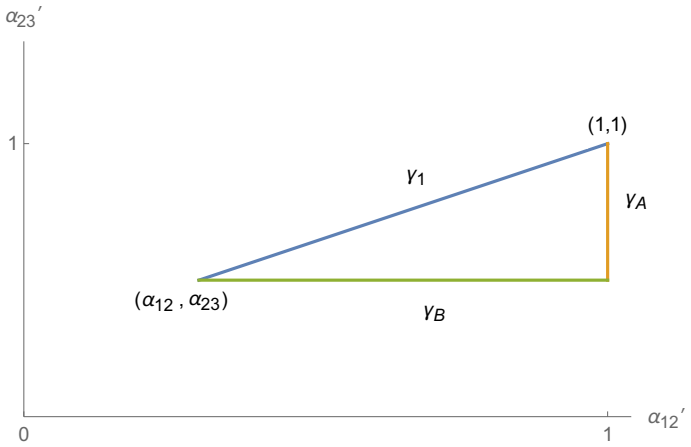

Figure 2.3: Plot showing the contours γ_1 and $\gamma_2 = \gamma_B \circ \gamma_A$ which originate at point $(1,1)$ to some arbitrary point $(\alpha_{12}, \alpha_{23})$

At the subsequent order in ϵ we integrate eq. (2.63b) and obtain

$$g_{12}^{[1,2,1],(3)} = 16\Big(G_0(\alpha_{12})\Big(G_{-1,0}(\alpha_{23}) - G_{1,0}(\alpha_{23}) + \frac{\pi^2}{4}\Big) + G_0(\alpha_{23})\Big(G_{-1,0}(\alpha_{12}) - G_{0,0}(\alpha_{12}) + G_{1,0}(\alpha_{12}) - 2\log(2)G_0(\alpha_{12}) - \frac{\pi^2}{12}\Big)\Big) \tag{2.68}$$

The next order in ϵ for $g_{12}^{[1,2,1]}$ is given in the Appendix A.1.3. Given that we know the boundary integrals to all orders in ϵ and that the differential equation matrices are in canonical form we can find $\mathbf{g}^{[1,2,1]}$ in terms of MPLs to any order in ϵ.

2.3.3 Calculating the web

To find the web in eq. (2.55) we first need to invert from the uniform weight basis $\mathbf{g}^{[1,2,1]}$ back to the original basis $\mathbf{f}^{[1,2,1]}$. In the antisymmetric sum over α_{12}, α_{23} the leading double pole eq. (2.67) vanishes. The single pole of the web is then proportional to

$$I_{111111}^{[1,2,1],(-1)}(\alpha_{12},\alpha_{23}) - I_{111111}^{[1,2,1],(-1)}(\alpha_{23},\alpha_{12}) = \frac{8\alpha_{12}\alpha_{23}}{(\alpha_{12}^2-1)(\alpha_{23}^2-1)}(\log(\alpha_{23})S_1(\alpha_{12}) - \log(\alpha_{12})S_1(\alpha_{23})), \tag{2.69}$$

where we have defined

$$S_1(\alpha_{12}) = -2G_{0,0}(\alpha_{12}) + 4G_{1,0}(\alpha_{12}) - \frac{2\pi^2}{3}. \tag{2.70}$$

Plugging eq. (2.69) into eq. (2.55) we get the following result for the web,

$$w_{121}^{(2,-1)} = if^{abc}\mathbf{T}_1^a\mathbf{T}_2^b\mathbf{T}_3^c\, r(\alpha_{12})r(\alpha_{23})\left(\log(\alpha_{23})S_1(\alpha_{12}) - \log(\alpha_{12})S_1(\alpha_{23})\right),$$

with $r(a_{ij}) = \frac{1+a_{ij}^2}{1-a_{ij}^2}$. The web agrees precisely with previous calculations [64, 114, 115]. We can calculate the subtracted web which is defined in eq. (1.18)

$$\bar{w}_{121}^{(2,-1)} = w_{121}^{(2,-1)} + \frac{1}{2}\left[w^{(1,-1)}, w^{(1,0)}\right], \tag{2.71}$$

where the web functions $w^{(1,-1)}$ and $w^{(1,0)}$ were found in eqs. (2.51a) and (2.51b). Using these we find

$$\begin{aligned}\bar{w}_{121}^{(2,-1)} =& if^{abc}\mathbf{T}_1^a\mathbf{T}_2^b\mathbf{T}_3^c\, r(\alpha_{12})r(\alpha_{23})\frac{1}{2} \\ &\times \left(M_{000}(\alpha_{23})M_{100}(\alpha_{12}) - M_{000}(\alpha_{12})M_{100}(\alpha_{23})\right),\end{aligned} \tag{2.72}$$

where M_{000} and M_{100} are members of the basis of MGEW functions mentioned in Section 1.3. Their explicit forms are

$$M_{000}(\alpha) = 2G_0(\alpha) \tag{2.73}$$

$$M_{100}(\alpha) = -2\zeta_2 + 4G_{-1,0}(\alpha) - 4G_{00}(\alpha) + 4G_{10}(\alpha) \tag{2.74}$$

These functions and their generalisations will be explored in greater detail in Chapter 3.

2.4 $[3gv]$-web

The most difficult two-loop web is the three-gluon-vertex web which is shown diagramatically in Figure 2.4. As opposed to the two-loop MGEW web calculated previously in Section 2.3 this is the first instance of a maximally-connected web with full dependence on all three cusp angles. It was explicitly calculated in [115] and again in [78] using Mellin-Barnes techniques. In [116] the novel unitarity cut method was employed to evaluate the integral. Here we shall employ the technique of differential equations.

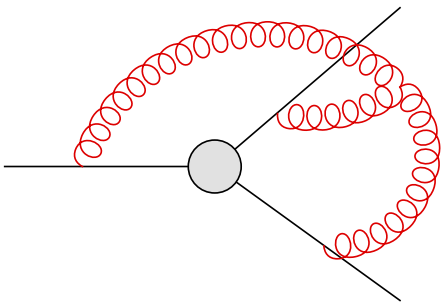

Figure 2.4: Diagram corresponding to the three gluon vertex web w_{3gv}

2.4.1 Integral family

The expression for the three-gluon-vertex web is,

$$w_{3gv}\left(\frac{\alpha_s}{4\pi}\right)^2 = -ig_s^4 f^{abc}\mathbf{T}_1^a\mathbf{T}_2^b\mathbf{T}_3^c \int \frac{d^dk_1}{(2\pi)^d}\int \frac{d^dk_2}{(2\pi)^d}\int \frac{d^dk_3}{(2\pi)^d}(2\pi)^d\delta^{(d)}(k_1+k_2+k_3) \frac{\epsilon_{ijk}\beta_i\cdot\beta_j k_i\cdot\beta_k}{k_1^2k_2^2k_3^2(k_1\cdot\beta_1-m)(k_2\cdot\beta_2-m)(k_3\cdot\beta_3-m)}. \tag{2.75}$$

Writing the numerator out fully, we can write the web as

$$w_{3gv} = if^{abc}\mathbf{T}_1^a\mathbf{T}_2^b\mathbf{T}_3^c\left(\frac{\mu}{m}\right)^{4\epsilon}\Big(\beta_1\cdot\beta_2 I^{[3gv]}(\alpha_{12},\alpha_{13},\alpha_{23}) - \beta_1\cdot\beta_3 I^{[3gv]}(\alpha_{13},\alpha_{12},\alpha_{23}) - \beta_2\cdot\beta_3 I^{[3gv]}(\alpha_{23},\alpha_{13},\alpha_{12})\Big), \tag{2.76}$$

where we have defined the term proportional to $\beta_1\cdot\beta_2$ to be the integral

$$I^{[3gv]}(\alpha_{12},\alpha_{13},\alpha_{23}) = m^{4\epsilon}e^{2\epsilon\gamma_E} \int\frac{d^dk_1}{i\pi^{d/2}}\int\frac{d^dk_2}{i\pi^{d/2}}\frac{(k_1-k_2)\cdot\beta_3}{k_1^2k_2^2(k_1+k_2)^2(k_1\cdot\beta_1-m)(k_2\cdot\beta_2-m)(-(k_1+k_2)\cdot\beta_3-m)} \tag{2.77}$$

and the other terms can be found from cyclic permutations of the α variables. From the definition in eq. (2.77), we define the integral family

$$I^{[3gv]}_{a_1a_2a_3a_4a_5a_6a_7a_8a_9} = m^{M_d}e^{2\epsilon\gamma}\int\frac{d^dk_1}{i\pi^{d/2}}\int\frac{d^dk_2}{i\pi^{d/2}}\frac{1}{P_1^{a_1}P_2^{a_2}P_3^{a_3}P_4^{a_4}P_5^{a_5}P_6^{a_6}P_7^{a_7}P_8^{a_8}P_9^{a_9}}, \tag{2.78}$$

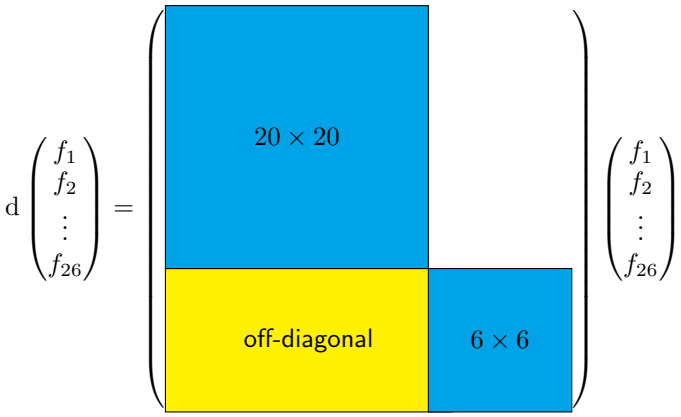

Figure 2.5: Schematic representation of the lower block-diagonal matrix $A^{[3gv]}$. The 20×20 block is itself lower block-diagonal, with the largest sub-block being 3×3. The 6×6 is the coupled system of the 6-dimensional top sector.

$$
\begin{aligned}
P_1 &= k_1^2 & P_2 &= k_2^2 & P_3 &= (k_1 + k_2)^2 \\
P_4 &= k_1 \cdot \beta_1 - m & P_5 &= k_2 \cdot \beta_2 - m & P_6 &= -(k_1 + k_2) \cdot \beta_3 - m \\
P_7 &= k_1 \cdot \beta_2 & P_8 &= k_2 \cdot \beta_3 & P_9 &= k_2 \cdot \beta_1
\end{aligned}
$$

with $\beta_i^2 = 1$ and M_d chosen such that $I_{\mathbf{a}}^{[3gv]}$ is dimensionless. Expressing the numerator of eq. (2.77) as $(k_1 - k_2) \cdot \beta_3 = -2P_8 - P_6 - m$, we can write the integral $I^{[3gv]}(\alpha_{12}, \alpha_{13}, \alpha_{23})$ in terms of this family,

$$
I^{[3gv]}(\alpha_{12}, \alpha_{13}, \alpha_{23}) = -2I^{[3gv]}_{1111110-10} - I^{[3gv]}_{111110000} - I^{[3gv]}_{111111000}. \tag{2.79}
$$

2.4.2 Differential equation

There are three variables that the family depends on: $\{\alpha_{12}, \alpha_{13}, \alpha_{23}\}$. We find for the whole system 26 basis integrals where 6 form the top sector. We then build our system of differential equations,

$$
\mathrm{d}\mathbf{f}^{[3gv]}(\epsilon, \alpha_{12}, \alpha_{13}, \alpha_{23}) = A^{[3gv]}(\epsilon, \alpha_{12}, \alpha_{13}, \alpha_{23})\mathbf{f}^{[3gv]}(\epsilon, \alpha_{12}, \alpha_{13}, \alpha_{23}), \tag{2.80}
$$

where $A^{[3gv]}$ satisfies the integrability condition eq. (2.17). It provides a non-trivial check on the derived differential system. The differential equation is shown schematically in Figure 2.5. To extract the ϵ dependence from A we seek a transformation $\mathbf{f}^{[3gv]} \to T\mathbf{g}^{[3gv]}$ to canonical form such that,

$$
\mathrm{d}\mathbf{g}^{[3gv]}(\epsilon, \alpha_{12}, \alpha_{13}, \alpha_{23}) = \epsilon\, \tilde{A}^{[3gv]}(\alpha_{12}, \alpha_{13}, \alpha_{23})\mathbf{g}^{[3gv]}(\epsilon, \alpha_{12}, \alpha_{13}, \alpha_{23}). \tag{2.81}
$$

Leading singularity

To find such a transformation we will compute the leading singularity of the three-gluon vertex web in an attempt to identify uniform weight integrals. The integrand in four dimensions without numerators is given as

$$I^{[3gv]} = \frac{d^4k_1 d^4k_2}{k_1^2 k_2^2 (k_1+k_2)^2 (k_1\cdot\beta_1 - m)(k_2\cdot\beta_2 - m)(-(k_1+k_2)\cdot\beta_3 - m)} \tag{2.82}$$

We decompose β_1 in terms of two lightlike vectors p_1 and p_2. Then we parameterise[1] the other Wilson lines in the following way,

$$\beta_1 = p_1 + p_2 \tag{2.83a}$$
$$\beta_2 = -\frac{p_1}{\alpha_{12}} - \alpha_{12} p_2 \tag{2.83b}$$
$$\beta_3 = a_1 p_1 + a_2 p_2 + a_3 \frac{\langle 23\rangle}{\langle 13\rangle}\lambda_1\tilde{\lambda}_2 + a_4 \frac{\langle 13\rangle}{\langle 23\rangle}\lambda_2\tilde{\lambda}_1. \tag{2.83c}$$

We have decomposed β_3 into p_1 and p_2 but also into vectors that are in the orthogonal space, $p_i = \lambda_i\tilde{\lambda}_i$ and have used the notation $\lambda_i \to |i\rangle$. The detailed explanation for the parameterisation is deferred to Appendix A.3. The kinematics of the vectors are $p_i^2 = 0$ and $2p_1\cdot p_2 = 1$. We can then solve for the coefficients in eq. (2.83c)

$$a_1 = \frac{-\alpha_{12}\alpha_{13}\alpha_{23}^2 - \alpha_{12}\alpha_{13} + \alpha_{13}^2(-\alpha_{23}) - \alpha_{23}}{(1-\alpha_{12}^2)\,\alpha_{13}\alpha_{23}} \tag{2.84a}$$
$$a_2 = \frac{\alpha_{12}^2\alpha_{13}^2\alpha_{23} + \alpha_{12}^2\alpha_{23} + \alpha_{12}\alpha_{13}\alpha_{23}^2 + \alpha_{12}\alpha_{13}}{(1-\alpha_{12}^2)\,\alpha_{13}\alpha_{23}}. \tag{2.84b}$$

The integrand in eq. (2.82) will only depend on $\{\alpha_{12}, \alpha_{13}, \alpha_{23}\}$ or, equivalently, $\{\alpha_{12}, a_1, a_2\}$. The dependence on a_3 and a_4 is only on the product $a_3 a_4$ which, in turn, is equal to $1 - a_1 a_2$ coming from $\beta_3^2 = 1$. We then parameterise the loop momenta in terms of p_1, p_2 and the momenta in the orthogonal space

$$k_i = b_{1i}p_1 + b_{2i}p_2 + b_{3i}\frac{\langle 23\rangle}{\langle 13\rangle}\lambda_1\tilde{\lambda}_2 + b_{4i}\frac{\langle 13\rangle}{\langle 23\rangle}\lambda_2\tilde{\lambda}_1. \tag{2.85}$$

[1] We would like to thank Johannes Henn for suggesting this parameterisation

The scalar products appearing in eq. (2.82) are then

$$\begin{aligned} k_i^2 &= b_{1i}b_{2i} - b_{3i}b_{4i} & 2k_i\cdot\beta_3 &= a_1 b_{2i} + a_2 b_{1i} - a_3 b_{4i} - a_4 b_{3i} \\ 2k_i\cdot\beta_1 &= b_{2i} + b_{1i} & 2k_i\cdot\beta_2 &= -\frac{b_{2i}}{\alpha_{12}} - \alpha_{12}\, b_{1i} \\ (k_1+k_2)^2 &= (b_{11}+b_{12})(b_{21}+b_{22}) & -(b_{31}+b_{32})&(b_{41}+b_{42}) \end{aligned}$$

The Jacobian of the transformation is simply a numerical factor

$$d^4k_1 d^4k_2 = \frac{1}{4}\prod_{j=1}^{2}\prod_{i=1}^{4} db_{ij}. \tag{2.86}$$

Now we have everything we need to take successive residues at the poles of the denominators in eq. (2.82) in the variables b_{ij}. In doing so we arrive at

$$\text{LeadingSingularity}\left[I^{[3gv]}\right] \sim \oint \frac{db}{\sqrt{(b-r_1)(b-r_2)(b-r_3)(b-r_4)}}, \tag{2.87}$$

where b is one of the original b_{ij}. The r_i are functions of α_{12}, α_{13} and α_{23}. The appearance of the square root of a quartic polynomial in the denominator of eq. (2.87) heavily signifies an *elliptic* integral, one that does not evaluate to MPLs. It then implies that there is *no* rational transformation to canonical form of the six-dimensional differential equation. In order to solve the integral in eq. (2.77) we need to change our approach.

2.4.3 New strategy

Our new approach will be, rather than solving the system as a whole, we will only look at functions that have *physical* relevance. In the three-gluon-vertex web it is the single pole in ϵ of the integral $I^{[3gv]}$ defined in eq. (2.77) which constitutes the $[1,1,1]$-web. We shall define the following function

$$\varphi \equiv \frac{1-\alpha_{12}^2}{\alpha_{12}} I^{[3gv]} = \frac{1-\alpha_{12}^2}{\alpha_{12}}\left(-2I^{[3gv]}_{1111110-1} - I^{[3gv]}_{11111} - I^{[3gv]}_{111111}\right). \tag{2.88}$$

Now we observe that $I^{[3gv]}_{111111}$ is finite. If k_1 and k_2 scale in the same way then its integrand (see eq. (2.82)) in the UV scales as $\frac{k^{2d}}{k^9}$ which vanishes as $k\to\infty$. Similarly in the IR the integrand scales as $\frac{k^{2d}}{k^6}\to 0$ which vanishes as $k\to 0$. Hence, there are no overall divergences. If, instead, k_2 is fixed then in the UV

the k_1 integrand scales as $\frac{k_1^d}{k_1^6} \to 0$ and in the IR as $\frac{k_1^d}{k_1^2} \to 0$. This shows that there are no subdivergences present in $I^{[3gv]}_{111111}$. We can then write

$$\varphi = \frac{1-\alpha_{12}^2}{\alpha_{12}} \left(-2I^{[3gv]}_{1111110-1} - I^{[3gv]}_{11111} \right) + \mathcal{O}(\epsilon^0). \tag{2.89}$$

As we seek the pole of φ we do not require its evaluation and to this end we define

$$\tilde{\varphi} \equiv \frac{1-\alpha_{12}^2}{\alpha_{12}} \left(-2I^{[3gv]}_{1111110-1} - I^{[3gv]}_{11111} \right). \tag{2.90}$$

In order to calculate $\tilde{\varphi}$ we will still use differential equations and IBP reduction but only on $\tilde{\varphi}$. We find $\mathrm{d}\tilde{\varphi}$

$$\mathrm{d}\tilde{\varphi} = \frac{\partial\tilde{\varphi}}{\partial\alpha_{12}}\mathrm{d}\alpha_{12} + \frac{\partial\tilde{\varphi}}{\partial\alpha_{13}}\mathrm{d}\alpha_{13} + \frac{\partial\tilde{\varphi}}{\partial\alpha_{23}}\mathrm{d}\alpha_{23} \tag{2.91}$$

and reduce the right hand side down to a basis of integrals. We choose basis integrals that are finite in the top sector because, as we will see, they do not contribute to the leading pole of $\tilde{\varphi}$. A similar observation was made in [36]. As we have shown that $I^{[3gv]}_{111111}$ is finite only integrals with additional numerators are UV divergent. Hence we choose integrals without any numerators. Integrals with a double propagator on the first three indices are not chosen because they have unregulated infrared divergences. Only multiple powers on the last three indices are finite because the infrared is being regulated by m. A basis that satisfies this and one that we choose is

$$\begin{aligned} &I^{[3gv]}_{0111}, I^{[3gv]}_{11011}, I^{[3gv]}_{10111}, I^{[3gv]}_{10112}, I^{[3gv]}_{11111}, I^{[3gv]}_{110101}, I^{[3gv]}_{110102}, I^{[3gv]}_{111101}, I^{[3gv]}_{110011}, I^{[3gv]}_{110012}, \\ &I^{[3gv]}_{111011}, I^{[3gv]}_{110111}, I^{[3gv]}_{110112}, I^{[3gv]}_{110121}, I^{[3gv]}_{101111}, I^{[3gv]}_{101121}, I^{[3gv]}_{101211}, I^{[3gv]}_{011111}, I^{[3gv]}_{011112}, I^{[3gv]}_{011211}, \\ &I^{[3gv]}_{111111}, I^{[3gv]}_{111112}, I^{[3gv]}_{111113}, I^{[3gv]}_{111121}, I^{[3gv]}_{111122}, I^{[3gv]}_{111131}. \end{aligned} \tag{2.92}$$

We can solve the first 20 integrals by differential equations, the first two lines of eq. (2.92). Their evaluation is given in Appendix A.2. To extract the poles in ϵ we write the integrals as a series expansion in ϵ,

$$I^{[3gv]}_{\mathbf{a}} = \sum_{i=-2}^{\infty} I^{[1,1,1],(i)}_{\mathbf{a}} \epsilon^i. \tag{2.93}$$

The sum starts at $i = -2$ since some of the integrals in eq. (2.92) have a term of order $\frac{1}{\epsilon^2}$. Expanding the differential equation for $\tilde{\varphi}$ we find that it starts at ϵ^{-3}

$$\mathrm{d}\tilde{\varphi} = \sum_{i=-3}^{\infty} \phi^{(i)}\epsilon^i = \sum_{i=-3}^{\infty} \left(\phi_{12}^{(i)}\mathrm{d}\alpha_{12} + \phi_{13}^{(i)}\mathrm{d}\alpha_{13} + \phi_{23}^{(i)}\mathrm{d}\alpha_{23}\right)\epsilon^i. \tag{2.94}$$

Written in terms of the basis we find that one of the terms evaluates to

$$\begin{aligned}\phi_{12}^{(-3)}(\alpha_{12},\alpha_{13},\alpha_{23}) \propto \Bigg[&\alpha_{23}\left(\left(\alpha_{13}^2+1\right) I^{[1,1,1],(-2)}_{110102}(\alpha_{13}) + 2\alpha_{13} I^{[1,1,1],(-2)}_{110101}(\alpha_{13})\right)\\ &-\alpha_{13}\left(\left(\alpha_{23}^2+1\right) I^{[1,1,1],(-2)}_{110012}(\alpha_{23}) + 2\alpha_{23} I^{[1,1,1],(-2)}_{110011}(\alpha_{23})\right)\Bigg].\end{aligned} \tag{2.95}$$

Seemingly it is non-zero but the term vanishes upon the replacement of the values of the integrals. The vanishing is due to the $\alpha_{23} \leftrightarrow \alpha_{13}$ anti-symmetry of the term in square brackets.

The same also happens for the full $\phi^{(-3)}$ expression and for $\phi^{(-2)}$ as expected. This serves as a good check of the evaluation of the lower sector integrals. If non-finite integrals were chosen for the top sector then there may have been dependence on them for these terms which is why finite integrals were selected.

For $\mathrm{d}\tilde{\varphi}^{(-1)}$ we find the first non-zero result

$$\begin{aligned}\mathrm{d}\tilde{\varphi}^{(-1)} = 8\,(&\mathrm{d}\log\alpha_{12}\mathrm{d}\log\alpha_{23}\mathrm{d}\log\alpha_{23} + \text{perm.}\\ &- \mathrm{d}\log\alpha_{12}\mathrm{d}\log\alpha_{13}\mathrm{d}\log\alpha_{13} + \text{perm.}).\end{aligned} \tag{2.96}$$

The additional terms ensure that eq. (2.96) is integrable. We also see no dependence on the top sector because the rational prefactor in the definition of φ in eq. (2.90) removes homogeneous terms. The integration is on a contour from the boundary $(1,1,1) \to (\alpha_{12},\alpha_{13},\alpha_{23})$. Conveniently, $\tilde{\varphi}$ vanishes at the boundary due to the rational factor. This gives the immediate result,

$$\tilde{\varphi}^{(-1)} = 4\log(\alpha_{12})\Big(\log^2(\alpha_{23}) - \log^2(\alpha_{13})\Big) \tag{2.97}$$

Using this result in eq. (2.76) we find for the single pole of the $[3gv]$-web

$$w_{3gv}^{(-1)} = 2if^{abc}\mathbf{T}_1^a\mathbf{T}_2^b\mathbf{T}_3^c\left(r(\alpha_{12})\log(\alpha_{12})\left(\log^2(\alpha_{13})-\log^2(\alpha_{23})\right)+\text{perm.}\right) \tag{2.98a}$$

$$= 2if^{abc}\mathbf{T}_1^a\mathbf{T}_2^b\mathbf{T}_3^c\sum\epsilon_{ijk}r(\alpha_{ij})\log(\alpha_{ij})\log^2(\alpha_{ik}), \tag{2.98b}$$

which agrees with previous calculations [78,115,116]. At the next order in ϵ, $\mathrm{d}\tilde{\varphi}^{(0)}$ depend on the top sector which would need to be evaluated to find $w_{3gv}^{(0)}$, which contributes to the three-loop soft anomalous dimension.

2.5 Conclusion

The complete two-loop coefficient of the tripole contribution to the soft anomalous dimension Γ_{tripole} is eq. (1.17b) which is the combination of eqs. (2.72) and (2.98b) and evaluates to

$$\Gamma_{\text{tripole}}^{(2)} = if^{abc}\mathbf{T}_1^a\mathbf{T}_2^b\mathbf{T}_3^c\sum_{i,j,k}\epsilon_{ijk}r(\alpha_{ij})M_{000}(\alpha_{jk})\times \\ \left[M_{000}(\alpha_{ij})M_{000}(\alpha_{jk})-2r(\alpha_{jk})M_{100}(\alpha_{ij})\right]. \tag{2.99}$$

The technique of differential equations is certainly a powerful one as it is now almost trivial to find the $[1,2,1]$-web to any order in ϵ. However, there are clear limitations. The computation of the $[3gv]$-web by the standard technique of finding a transformation to canonical form fails due to the appearance of the elliptic integral eq. (2.87). Currently there is a major research focus in understanding elliptic integrals and their application to Feynman integrals. An interesting avenue to take would be to study the elliptic curve of eq. (2.87). By computing the periods associated to an elliptic curve, Adams and Weinzierl in [117] were able to transform the differential equation of an elliptically-valued Feynman integral into ϵ-form. The transformation was non-algebraic.

Another avenue to continue is the idea that *subtracted webs*, webs with relevant lower loop order counterterms, have a simpler structure. One would construct a differential equation for these and use a basis of finite integrals for the harder sectors such that one can extract the required poles. The method does not involve

solving individual integrals where complicated symbol letters can appear, such as the y symbol found in eq. (2.63b). These cancelled in the full expression for the $[1, 2, 1]$-web. Other letters appear in the subsectors that depend on multiple angles such as $\alpha_{12} + \alpha_{23} - 1$. Although the appearance of such are expected, we are complicating matters by calculating unnecessary integrals rather than focus on physically relevant functions. The next chapter will explore this further by constructing ansatze for functions arising from correlators of Wilson lines which are based solely on their physical properties and then constraining them using known limits.

Chapter 3

Bootstrapping

Although the technique of differential equations is very powerful it tends to overcomplicate matters. We are often not seeking the solution to *all* the integrals in a certain sector but rather specific integrals that arise in the perturbative expansion. One way to bypass integral evaluation entirely and to go straight to the function is to *bootstrap* the integral. The methodology behind bootstrapping quantities is to first write a general ansatz constructed from first principle arguments and then constrain it using known limits.

The concept of bootstrapping first appeared in the context of planar $\mathcal{N} = 4$ super-Yang-Mills amplitudes. By now immense progress has been made on the amplitudes and currently four-loop seven point symbols [118] or seven-loop six-point symbols [119, 120] are the state-of-the-art. The idea was then extended to lightlike Wilson-line correlators [25], namely the three loop QCD soft anomalous dimension, in eq. (1.27). In this chapter we review what is known about the function space for non-lightlike lines. We then explore an extension to the basis using the analytical properties of the functions. Finally, we consider two different types of applications. The first type is one that is a physical gauge-invariant quantity, the angle-dependent non-lightlike (two-line) cusp anomalous dimension, see the discussion around eq. (1.28). The second is an individual web comprising of four lines.

3.1 Multiple-Gluon-Exchange-Web Basis Functions

In order to construct a basis let us first define the kinematic variables. Diagrams contributing to semi-infinite non-lightlike Wilson-line correlators depend only on the angles where a gluon exchange occurs. Defining a Wilson line in direction β_i, the most convenient variables are the α's,

$$-\left(\frac{1}{\alpha_{ij}}+\alpha_{ij}\right)\equiv\frac{2\beta_i\cdot\beta_j}{\sqrt{\beta_i^2}\sqrt{\beta_j^2}},\qquad|\alpha_{ij}|<1. \tag{3.1}$$

c.f. eq. (2.38) where $\beta_i^2=1$. Due to the $\alpha\leftrightarrow\frac{1}{\alpha}$ symmetry in the definition we have chosen α to lie in the unit circle.

The first step towards constructing a basis for non-lightlike Wilson-line correlators was achieved in ref. [64]. Analysis was performed on multiple gluon exchange webs (MGEWs) which are diagrams arising from correlators of Wilson lines that have no three-gluon or four-gluon vertex. In [64] it was observed that subtracted webs of this type have a highly constrained structure.

One constraint is that they are only sums of products of polylogarithms that depend only on one α. Another is that the subtracted web is invariant under $\alpha\to-\alpha$ up to terms arising from analytic continuation ($i\pi$). It follows from the fact that there should not be branch points from square roots of masses and means that the symbol should be invariant since it is blind to these $i\pi$ terms. Note that webs without subtraction terms, in general, will not obey this symmetry. These we will call *unsubtracted* webs.

Subsequently, in [65] it was conjectured that all subtracted webs in this family can be written in terms of the following functions

$$M_{kln}(\alpha)=\frac{1}{r(\alpha)}\int_0^1 dx\,p_0(x,\alpha)\log^k\left(\frac{q(x,\alpha)}{x^2}\right)\log^l\left(\frac{x}{1-x}\right)\log^n\tilde{q}\,(x,\alpha)\,, \tag{3.2}$$

where the constituent functions p_0, q and $\tilde{q}$ are defined as

$$\log\frac{q(x,\alpha)}{x^2}=\log\left(\frac{1}{x}+\alpha-1\right)+\log\left(\frac{1}{x}+\frac{1}{\alpha}-1\right) \tag{3.3a}$$

$$p_0(x,\alpha)=-\left(\alpha+\frac{1}{\alpha}\right)\frac{1}{q(x,\alpha)} \tag{3.3b}$$

$$\log \tilde{q}\,(x,\alpha) = \frac{1}{r(\alpha)} \int_0^1 dy\, p_0(y,\alpha)\theta(x-y) \tag{3.3c}$$

$$= \log\left(\frac{1}{x}+\alpha-1\right) - \log\left(\frac{1}{x}+\frac{1}{\alpha}-1\right). \tag{3.3d}$$

Some explicit examples, M_{000} and M_{100}, written in terms of MPLs, are given in eqs. (2.73) and (2.74). The $M_{kln}(\alpha)$ are pure transcendental functions that have weight $k+l+n+1$. They have the alphabet $\{\alpha, \eta \equiv \frac{\alpha}{1-\alpha^2}\}$ and can be multiplied by the rational function $r(\alpha)$ defined in eq. (2.52). They also have the inversion property,

$$M_{kln}(1/\alpha) = (-1)^{(n+1)} M_{kln}(\alpha) \tag{3.4}$$

and vanish at $\alpha = 1$, $M_{kln}(1) = 0$. Taking into account dependencies between the functions such as $M_{001} = \frac{1}{2}M_{000}^2$, the basis functions suitable to three loops (up to weight five) are given in Table 3.1. As opposed to [65] we remove $M_{00n} \propto M_{000}^n$ from the basis to allow for any powers or products of the M_{kln} to appear.

Weight	M_{kln}	$\mathcal{S}[M_{kln}]$
one	M_{000}	$2 \otimes \alpha$
two	M_{100}	$-4\alpha \otimes \eta$
three	M_{011}	$-4\alpha \otimes \eta \otimes \alpha$
	M_{020}	$4\alpha \otimes \alpha \otimes \alpha$
	M_{200}	$16\alpha \otimes \eta \otimes \eta$
four	M_{102}	$-32\alpha \otimes \alpha \otimes \alpha \otimes \eta$
	M_{111}	$8\alpha \otimes \eta \otimes \alpha \otimes \eta + 8\alpha \otimes \eta \otimes \eta \otimes \alpha - 16\alpha \otimes \alpha \otimes \alpha \otimes \alpha$
	M_{120}	$-8\alpha \otimes \alpha \otimes \alpha \otimes \eta - 8\alpha \otimes \eta \otimes \alpha \otimes \alpha$
	M_{300}	$-96\alpha \otimes \eta \otimes \eta \otimes \eta$
five	M_{013}	$-96\alpha \otimes \alpha \otimes \alpha \otimes \eta \otimes \alpha - 96\alpha \otimes \alpha \otimes \eta \otimes \alpha \otimes \alpha$ $-96\alpha \otimes \eta \otimes \alpha \otimes \alpha \otimes \alpha$
	M_{022}	$32\alpha \otimes \eta \otimes \alpha \otimes \eta \otimes \alpha + 96\alpha \otimes \alpha \otimes \alpha \otimes \alpha \otimes \alpha$
	M_{031}	$-24\alpha \otimes \alpha \otimes \alpha \otimes \eta \otimes \alpha - 24\alpha \otimes \eta \otimes \alpha \otimes \alpha \otimes \alpha$
	M_{040}	$48\alpha \otimes \alpha \otimes \alpha \otimes \alpha \otimes \alpha$
	M_{202}	$128\alpha \otimes \alpha \otimes \alpha \otimes \eta \otimes \eta$
	M_{211}	$64\alpha \otimes \alpha \otimes \alpha \otimes \alpha \otimes \eta + 32\alpha \otimes \alpha \otimes \eta \otimes \alpha \otimes \alpha$ $+32\alpha \otimes \eta \otimes \alpha \otimes \alpha \otimes \alpha - 32\alpha \otimes \eta \otimes \alpha \otimes \eta \otimes \eta$ $-32\alpha \otimes \eta \otimes \eta \otimes \alpha \otimes \eta - 32\alpha \otimes \eta \otimes \eta \otimes \eta \otimes \alpha$
	M_{220}	$32\alpha \otimes \alpha \otimes \alpha \otimes \eta \otimes \eta + 32\alpha \otimes \eta \otimes \alpha \otimes \alpha \otimes \eta$ $+32\alpha \otimes \eta \otimes \eta \otimes \alpha \otimes \alpha + 32\alpha \otimes \alpha \otimes \alpha \otimes \alpha \otimes \alpha$
	M_{400}	$768\alpha \otimes \eta \otimes \eta \otimes \eta \otimes \eta$

Table 3.1: The M_{kln} basis and the respective symbols

As we can write the non-MGEW, $[1,1,1]$-web in the M_{kln} basis eq. (2.98b) it seems natural to consider an immediate generalisation of the conjecture, that all

webs that do not depend on CICRs, defined in eq. (1.26), evaluate to MGEW basis functions. We know from the three-loop correction to the lightlike soft function eq. (1.27), there is dependence that does not factorise into polylogarithms of individual angles.

One source of information about functions that appear in Wilson-line correlators is the explicit calculation of the three-loop cusp anomalous dimension [22, 23]. All the coefficient functions, that are given in eq. (5.2) of ref. [23] (the A_i and B_i) can be written in terms of MGEW basis functions apart from A_4 and B_5. We quote the functions that can in terms of the basis in Table 3.1

$$A_1(\alpha) = \frac{1}{2} r(\alpha) M_{000}(\alpha) \tag{3.5}$$

$$A_2(\alpha) = \frac{M_{000}(\alpha)^2}{4} + \frac{1}{2} M_{100}(\alpha) r(\alpha) \tag{3.6}$$

$$A_3(\alpha) = \frac{1}{2} M_{011}(\alpha) r(\alpha)^2 + \frac{1}{2} M_{020}(\alpha) r(\alpha) \tag{3.7}$$

$$B_3(\alpha) = \frac{1}{8} M_{000}(\alpha) M_{100}(\alpha) + r(\alpha) \left(\frac{M_{000}(\alpha)^3}{24} - \frac{M_{200}(\alpha)}{4} \right) - \frac{5}{4} M_{011}(\alpha) \tag{3.8}$$

$$\begin{aligned} A_5(\alpha) = r(\alpha)^3 \Bigg(& \frac{1}{32} M_{000}(\alpha) M_{100}(\alpha)^2 - \frac{1}{8} M_{000}(\alpha) M_{111}(\alpha) - \frac{1}{32} M_{000}(\alpha)^2 M_{200}(\alpha) \\ & - \frac{M_{000}(\alpha)^5}{384} + \frac{1}{8} M_{011}(\alpha) M_{100}(\alpha) - \frac{3 M_{022}(\alpha)}{16} \Bigg) \\ & + r(\alpha)^2 \Bigg(\frac{7}{16} M_{000}(\alpha)^2 M_{011}(\alpha) - \frac{3}{16} M_{000}(\alpha) M_{120}(\alpha) - \frac{M_{013}(\alpha)}{2} \\ & - \frac{1}{16} M_{020}(\alpha) M_{100}(\alpha) \Bigg) + r(\alpha) \left(-\frac{1}{28} M_{000}(\alpha)^2 M_{020}(\alpha) - \frac{5 M_{040}(\alpha)}{28} \right) \end{aligned} \tag{3.9}$$

The function A_4 cannot be written solely in terms of the M_{kln} basis

$$\begin{aligned} A_4(\alpha) = & r(\alpha) \Bigg(- \zeta_3 M_{000}(\alpha) - \frac{11 M_{102}(\alpha)}{8} - \frac{1}{2} M_{120}(\alpha) + \frac{3}{8} M_{000}(\alpha)^2 M_{100}(\alpha) \\ & - \frac{3}{2} M_{000}(\alpha) M_{011}(\alpha) \Bigg) + \frac{M_{000}(\alpha)^4}{96} - \frac{M_{000}(\alpha) M_{020}(\alpha)}{4} \\ & + r(\alpha)^2 \left(-\frac{1}{2} M_{000}(\alpha) M_{020}(\alpha) - \frac{1}{48} M_{000}(\alpha)^4 - M_{111}(\alpha) \right). \end{aligned} \tag{3.10}$$

Notice that there is a term $r(\alpha)\zeta_3 M_{000}(\alpha)$. Already here we see that we should extend our basis by including ζ values. It was also observed in an explicit calculation by Waelkens [116] that along with the MGEW functions, ζ_3 is present in a connected web. By including ζ values there are additional dependencies that

need to be taken into account such as

$$M_{020}(\alpha) = 2\zeta_2 M_{000}(\alpha) + \frac{1}{12} M_{000}(\alpha)^3. \tag{3.11}$$

After removing all such redundant products of M_{000} there are still dependencies which, to weight five, are

$$4M_{000}M_{011} - M_{000}^2 M_{100} + 16\zeta_3 M_{000} + 8\zeta_2 M_{100} + 4M_{102} - 4M_{120} = 0 \tag{3.12a}$$

$$24\zeta_2 M_{000}M_{100} - 3M_{000}^3 M_{100} + 12M_{000}M_{102} - 12M_{000}M_{120} + 48\zeta_3 M_{000}^2 + 96\zeta_2 M_{011} + 16M_{013} - 16M_{031} = 0 \tag{3.12b}$$

$$120M_{000}M_{111} - 15M_{000}^2 M_{200} + 200\zeta_2 M_{000}^3 + 2640\zeta_4 M_{000} + 7M_{000}^5 - 60M_{022} + 480\zeta_3 M_{100} + 120\zeta_2 M_{200} + 60M_{202} - 60M_{220} = 0. \tag{3.12c}$$

These can be derived by finding the relations between the symbols of the functions. The individual M_{kln} symbols can be found in Table 3.1 and the shuffle relation in eq. (1.34) can be used for products. The symbol matching is not all that is required to find the functional relations. The symbol is not sensitive to lower weight functions multiplied by ζ values.

Taking into account the relations, we choose to eliminate M_{120}, M_{220} and M_{031}. The M_{kln} functions present in this basis are then given in Table 3.2. Products between any functions and any ζ numbers are allowed. We call this basis the $(M + \zeta)$ basis. Taking these into account we are able to write all the coefficient functions in eqs. (3.5) to (3.10) in a unique way. The A_1, A_2 and B_3 do not change but the others do

$$A_3(\alpha) = r(\alpha)\left(\zeta_2 M_{000}(\alpha) + \frac{M_{000}(\alpha)^3}{24}\right) + \frac{1}{2} M_{011}(\alpha) r(\alpha)^2 \tag{3.13}$$

$$\begin{aligned} A_4(\alpha) = {} & r(\alpha)\Bigg(- 2M_{000}(\alpha)M_{011}(\alpha) + \frac{1}{2} M_{000}(\alpha)^2 M_{100}(\alpha) - 3\zeta_3 M_{000}(\alpha) \\ & - \zeta_2 M_{100}(\alpha) - \frac{15M_{102}(\alpha)}{8}\Bigg) - \frac{1}{96} M_{000}(\alpha)^4 - \frac{1}{2}\zeta_2 M_{000}(\alpha)^2 \\ & + r(\alpha)^2\left(-\zeta_2 M_{000}(\alpha)^2 - \frac{1}{16} M_{000}(\alpha)^4 - M_{111}(\alpha)\right) \end{aligned} \tag{3.14}$$

$$\begin{aligned} A_5(\alpha) = {} & r(\alpha)^2\Bigg(\frac{1}{4} M_{000}(\alpha)^2 M_{011}(\alpha) - \frac{1}{2}\zeta_2 M_{000}(\alpha) M_{100}(\alpha) \\ & + \frac{1}{24} M_{000}(\alpha)^3 M_{100}(\alpha) - \frac{3}{16} M_{000}(\alpha) M_{102}(\alpha) - \frac{3}{4}\zeta_3 M_{000}(\alpha)^2 - \frac{M_{013}(\alpha)}{2}\Bigg) \\ & + r(\alpha)^3\Bigg(\frac{1}{32} M_{000}(\alpha) M_{100}(\alpha)^2 - \frac{1}{8} M_{000}(\alpha) M_{111}(\alpha) - \frac{1}{32} M_{000}(\alpha)^2 M_{200}(\alpha) \end{aligned}$$

$$- \frac{1}{384} M_{000}(\alpha)^5 + \frac{1}{8} M_{011}(\alpha) M_{100}(\alpha) - \frac{3 M_{022}(\alpha)}{16} \Bigg)$$
$$+ r(\alpha) \left(-\frac{1}{4} \zeta_2 M_{000}(\alpha)^3 - \frac{15}{2} \zeta_4 M_{000}(\alpha) - \frac{1}{192} M_{000}(\alpha)^5 \right) \tag{3.15}$$

weight one	M_{000}
weight two	M_{100}
weight three	M_{011}, M_{200}
weight four	$M_{102}, M_{111}, M_{300}$
weight five	$M_{013}, M_{022}, M_{202}, M_{211}, M_{400}$

Table 3.2: The M_{kln} functions in the $(M + \zeta)$ basis

There is still one coefficient function that cannot be written in terms of these basis functions which is $B_5(\alpha)$. This function also has a new rational function which is not $r(\alpha)$ but $\frac{\alpha}{1-\alpha^2}$. We quote the result here for reference

$$\begin{aligned} B_5(\alpha) = \frac{\alpha}{1-\alpha^2} \Bigg(& \frac{3}{5} \zeta_2^2 \left(G_1(\alpha) - G_{-1}(\alpha) \right) + 2\zeta_3 (G_{-1,0}(\alpha) - G_{1,0}(\alpha)) \\ & - 4G_{-1,0,-1,0,0}(\alpha) + 4G_{-1,0,0,0,0}(\alpha) - 4G_{-1,0,1,0,0}(\alpha) \\ & + 4G_{1,0,-1,0,0}(\alpha) - 4G_{1,0,0,0,0}(\alpha) + 4G_{1,0,1,0,0}(\alpha) \Bigg). \end{aligned} \tag{3.16}$$

The symbol of the transcendental part of eq. (3.16) is

$$\mathcal{S} \left[\frac{1-\alpha^2}{\alpha} B_5(\alpha) \right] = 4\alpha \otimes \alpha \otimes \eta \otimes \alpha \otimes \frac{1+\alpha}{1-\alpha}. \tag{3.17}$$

Along with the expected letters α and η, we see a new symbol letter $y \equiv \frac{1+\alpha}{1-\alpha}$. It is clear from this new symbol that $B_5(\alpha)$ cannot be written in terms of the $M_{kln}(\alpha)$.

If we have any hope of constructing a general basis of functions for subtracted webs then we need to extend the $(M + \zeta)$ basis to include the new symbol y. In the next section we will do so by using known physical properties of Wilson-line correlators and will look to use the extension to perform prototypical bootstraps of some quantities.

3.2 Constructing the Basis

Let us now consider the general features of functions appearing in Wilson-line correlators. We can discuss the branch cuts of such functions by studying the branch cuts in normal Feynman diagrams. Branch cuts in Feynman integrals occur when centre of mass energy is at threshold and extend towards infinity. The energy for two incoming on-shell massive particles[1] with momentum p_i and p_j is given by $s_{ij} = (p_i + p_j)^2$ so that the threshold energy for particle creation is $4m^2$ and the cut extends over all real $s_{ij} > 4m^2$. Using eq. (3.1) and $p_i = m\beta_i$ we have

$$\frac{s_{ij}}{m^2} = \frac{(1-\alpha_{ij})^2}{-\alpha_{ij}} \implies s_{ij} \pm i\varepsilon \leftrightarrow \alpha_{ij} \pm i\varepsilon \tag{3.18}$$

which means that discontinuities in s_{ij} map to discontinuities in α_{ij} [116]. The specific map is shown in Figure 3.1. For a given polylogarithm, the first entry of

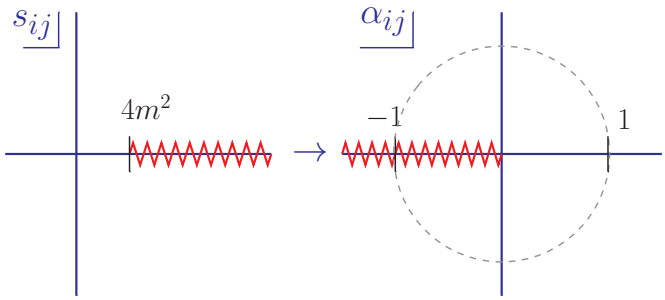

Figure 3.1: The map between the Mandelstam invariants s_{ij} to the α variables

its symbol captures its discontinuity. Our functions' symbols will have first entry α_{ij}, capturing the branch point at 0. This is known as a *first entry condition*. As can be seen from Table 3.1, all the M_{kln} functions obey this condition.

As observed in [64], any function appearing in subtracted webs that we want to construct $F(\alpha)$ has to obey $F(\alpha) = F(-\alpha)$ modulo terms from analytic continuation $(i\pi)$. The symbol should be invariant since it is blind to these $i\pi$ terms. This is crossing symmetry from spacelike to timelike kinematics. The letters previously mentioned $\log\alpha$, $\log\eta = \log\frac{\alpha}{1-\alpha^2}$ and $\log y = \log\frac{1+\alpha}{1-\alpha}$ have definite properties under this transformation, transforming to $\log\alpha$, $\log\eta$ and $-\log y$ respectively. These are natural symbol letters and our alphabet for our functions will be $\mathcal{A} = \{\alpha, \eta, y\}$. Functions that have this property are the harmonic polylogarithms (HPLs) [92], these are defined in Section 1.3.

[1] We are only considering two particle correlations where there will not be any intricate multi-particle discontinuities.

Along with the transcendental functions, the HPLs, subtracted webs will also have rational functions. As we have seen, the rational function

$$r(\alpha) = \frac{1+\alpha^2}{1-\alpha^2}, \tag{3.19}$$

appears many times in calculations of non-lightlike correlators, see eqs. (2.50a) and (2.99). The MGEW basis functions in eq. (3.2) only have this factor. However, in the three-loop cusp we have seen a new rational function eq. (3.16) which we will define as

$$s(\alpha) = \frac{\alpha}{1-\alpha^2}. \tag{3.20}$$

This factor comes from the topology involving the four-gluon vertex diagram that first appears at three loops [23]. Notice that both $r(\alpha)$ and $s(\alpha)$ diverge at $\alpha \to \pm 1$ which coincides with the divergences of the symbol letters y and η. A similar observation was made in the calculation of two-loop five-point QCD amplitudes in [121], where denominator factors of rationals were the same as symbol letters.

It is worthwhile to explain how the rational functions are generated. The factors $r(\alpha)$ and $s(\alpha)$ are related by

$$r(\alpha_{ij}) = -2 \times \underbrace{\beta_i \cdot \beta_j}_{\text{kinematics}} \times \underbrace{s(\alpha_{ij})}_{\text{integration}} . \tag{3.21}$$

The factor $s(\alpha)$ appears from the integral of the gluon propagator, see the leading singularity in eq. (2.44). Then multiplying this factor by $\beta_i \cdot \beta_j$ from the Feynman rules we arrive at $r(\alpha)$ as in eq. (3.21). There cannot be more scalar products $\beta_i \cdot \beta_j$ than factors of $s(\alpha)$. For MGEWs, this bound is saturated i.e. the number of $\beta_i \cdot \beta_j$ equals the number of $s(\alpha)$ which equals the number of $r(\alpha)$. The appearance of $s(\alpha)$ alone in $B_5(\alpha)$ of eq. (3.16) can be explained by the above. It is because the four-gluon-vertex diagram of the two-line cusp has for its kinematic part $(\beta_i \cdot \beta_j^2 - 1) \propto \frac{1}{s(\alpha)^2}$ and three loop integrals, each with a factor of $s(\alpha)$. Thus, overall, its rational factor is $s(\alpha)$.

A general function appearing in n-leg subtracted webs will schematically have the form

$$\text{subtracted webs} = \sum \prod_{(i,j)} r(\alpha_{ij})^a \times s(\alpha_{ij})^b \times \text{HPL}(\alpha_{ij}) \tag{3.22}$$

where the HPL has a symbol drawn from the alphabet $\mathcal{A}$, whose first entry is α and is of a prescribed weight. We conjecture that any function from non-lightlike Wilson-line correlators, where angle-dependence is factorisable, can be written in the form of eq. (3.22). We now explicitly construct a basis for subtracted webs by applying the $\alpha \to \frac{1}{\alpha}$ and $\alpha \to -\alpha$ symmetries to the general expression of eq. (3.22). We will see that the powers of a and b in eq. (3.22) are constrained and related to the transcendental function.

To be systematic in the construction of a basis we observe that there is a correspondence between the rational prefactor and the numbers of y and α entries in the symbol. For the correct property under $\alpha \to -\alpha$ we require the rational factor to be even/odd when the number of y entries is even/odd. Similarly for $\alpha \to \frac{1}{\alpha}$ we require the rational factor to be even/odd when the number of α entries is even/odd. Realising that,

$$r(\alpha)^2 - 4s(\alpha)^2 = 1, \tag{3.23}$$

there are then only four different types of rational factors. We summarise this analysis in Table 3.3 where we have eliminated any possibility of $s(\alpha)^{\text{even}}$ using eq. (3.23).

no. of y \ no. of α	odd	even
odd	$r(\alpha)^{\text{even}} s(\alpha)^{\text{odd}}$	$r(\alpha)^{\text{odd}} s(\alpha)^{\text{odd}}$
even	$r(\alpha)^{\text{odd}}$	$r(\alpha)^{\text{even}}$

Table 3.3: Rational to symbol correspondence, $r(\alpha)^{\text{odd}}$ means $r(\alpha)$ raised to an odd power.

As an illustration of the correspondence we consider an example symbol that can appear

$$\mathcal{S}\left[F(\alpha)\right] = \alpha \otimes \eta \otimes \alpha \otimes y. \tag{3.24}$$

Under $\alpha \to -\alpha$ we see that since the symbol drops $i\pi$ terms it is odd,

$$\begin{aligned} \mathcal{S}\left[F(-\alpha)\right] &= (-\alpha) \otimes \frac{-\alpha}{1-\alpha^2} \otimes (-\alpha) \otimes \frac{1}{y} \\ &= -(\alpha \otimes \eta \otimes \alpha \otimes y) \end{aligned} \tag{3.25}$$

Thus we need a rational factor that is odd under $\alpha \to -\alpha$ to cancel this minus

sign. From the choices it must be

$$s(\alpha)^{\text{odd}}. \tag{3.26}$$

Since we only need invariant functions up to $i\pi$ then the classification of odd/even number of y's is sufficient to ensure the $\alpha \to -\alpha$ property. We now move onto inversion, $\alpha \to \frac{1}{\alpha}$, which is an exact symmetry from the definition of α,

$$\begin{aligned}\mathcal{S}\left[F\left(\frac{1}{\alpha}\right)\right] &= \frac{1}{\alpha} \otimes (-\eta) \otimes \frac{1}{\alpha} \otimes (-y) \\ &= \alpha \otimes \eta \otimes \alpha \otimes y. \end{aligned} \tag{3.27}$$

So our symbol is even in inversion so our rational factor must be as well. Combining with eq. (3.26) we see that our rational factor should be

$$(r(\alpha)s(\alpha))^{\text{odd}}, \tag{3.28}$$

which is in agreement with the table.

Required for quantities up to three loops, all functions, with y present in the symbol, up to weight five have been constructed. They are given in Appendix B along with their respective symbols. We denote these as $w_i^{(j),k}$, which describes the i-th function at weight j corresponding to a rational factor which is the k-th element of the set

$$\{r(\alpha)^{\text{even}}, r(\alpha)^{\text{odd}}, r(\alpha)^{\text{even}}s(\alpha)^{\text{odd}}, r(\alpha)^{\text{odd}}s(\alpha)^{\text{odd}}\}. \tag{3.29}$$

One further constraint can be applied on these functions. We can observe that $M_{kln}(1) = 0$ for any k, l and n. This ensures finite results when combined with $r(\alpha)$ in $\alpha \to 1$, where the lines become one line. We can also redefine the new functions such that they obey this as well. For those with rational factor $r(\alpha)^{\text{even}}$, $w_i^{(n),1}$ a simple subtraction of a constant is needed. This constant is given with the functions in Appendix B. Those with factors $r(\alpha)^{\text{odd}}$ and $r(\alpha)^{\text{even}}s(\alpha)^{\text{odd}}$, $w_i^{(n),2}$ and $w_i^{(n),3}$ respectively, do not need subtraction, they already vanish at $\alpha = 1$. For those of $r(\alpha)^{\text{odd}}s(\alpha)^{\text{odd}}$ type, $w_i^{(n),4}$, a subtraction is needed. However, because of the odd number of y present in the symbol, see Table 3.3, any subtraction needs to also have an odd number of y otherwise it will spoil the $\alpha \to -\alpha$ property. We

demonstrate this by performing the subtraction

$$(r(\alpha)s(\alpha))^{\text{odd}} w_i^{(n),4}(\alpha) \to (r(\alpha)s(\alpha))^{\text{odd}} \left(w_i^{(n),4}(\alpha) - w_i^{(n),4}(1) \right). \tag{3.30}$$

This means that the difference is no longer solely terms from analytic continuation

$$\begin{aligned}(r(\alpha)s(\alpha))^{\text{odd}} \left(w_i^{(n),4}(\alpha) - w_i^{(n),4}(1) \right) - (r(-\alpha)s(-\alpha))^{\text{odd}} \left(w_i^{(n),4}(-\alpha) - w_i^{(n),4}(1) \right) \\ = (r(\alpha)s(\alpha))^{\text{odd}} \left(\text{analytic continuation} - 2w_i^{(n),4}(1) \right)\end{aligned} \tag{3.31}$$

The functions in Appendix B are general and do not have the vanishing property. However, we will discard the functions $w_i^{(n),4}$ entirely in future sections when we bootstrap the cusp anomalous dimensions and an individual integral.

As an example of the basis, we can write $B_5(\alpha)$, in eq. (3.16), in terms of these functions

$$B_5(\alpha) = s(\alpha) \left(4w_5^{(5),3}(\alpha) - \frac{24}{5}\log(2)\ w_1^{(4),3}(\alpha) - \frac{6}{5}\zeta_2 w_1^{(3),3}(\alpha) \right) \tag{3.32a}$$

$$\mathcal{S}[w_5^{(5),3}(\alpha)] = \alpha \otimes \alpha \otimes \eta \otimes \alpha \otimes y \tag{3.32b}$$

$$\mathcal{S}[w_1^{(4),3}(\alpha)] = \alpha \otimes \alpha \otimes \alpha \otimes y \tag{3.32c}$$

$$\mathcal{S}[w_1^{(3),3}(\alpha)] = \alpha \otimes \eta \otimes y \tag{3.32d}$$

where the new functions are drawn from those with a rational factor of the form $r(\alpha)^{\text{even}} s(\alpha)^{\text{odd}}$. We needed to add $\log(2)$ to reconstruct $B_5(\alpha)$. The constants $\text{Li}_4\left(\frac{1}{2}\right)$ and $\text{Li}_5\left(\frac{1}{2}\right)$ also show up in the functions. Powers of $\log(2)$, these constants and higher-weight generalisations thereof will be added to the basis. A full basis would involve these as well as the $(M + \zeta)$ basis in Table 3.2.

In the next two sections we use this full basis to create an ansatz for quantities and constrain it using known limits.

3.3 Towards Bootstrapping the Cusp Anomalous Dimension

In this section we explore the possibilities of bootstrapping the non-lightlike angle-dependent QCD cusp anomalous dimension Γ_{cusp}. This is the special two-leg case

of the general non-lightlike soft anomalous dimension, setting $n = 2$ in eq. (1.5). We have seen in Section 1.1 that this object governs the infrared behaviour of massive form factors. It also describes a heavy quark interacting with a potential in heavy quark effective theory (HQET) [23, 122–124]. A quark in the infinite mass limit will follow its classical trajectory and radiate gluons as a Wilson line. The velocity will transition from, say, β_1 to β_2 after interaction with the potential, thus a correlator of two Wilson lines.

Using the functions constructed in Section 3.2, we create an ansatz for the one-loop, two-loop and three-loop cases of Γ_{cusp} and constrain them using known limits. Although these functions are known, (see refs. [23, 79] for the detailed calculations) these are important steps to setup a bootstrap program to find the four loop result which is almost entirely unknown [23, 33, 125, 126] (see Table 1 in ref. [33] for an overview).

The object Γ_{cusp} is the anomalous dimension from renormalising the two-leg Wilson-line correlator in eq. (1.5) [79]. It only depends on the angle between the legs and we shall define α through eq. (3.1). As it only depends on this one variable, there are no other symmetries other than $\alpha \to \frac{1}{\alpha}$ and $\alpha \to -\alpha$ which were discussed in the previous section, Section 3.2.

The n-loop coefficient $\Gamma^{(n)}_{\text{cusp}}$ has a maximal weight of $2n-1$. Its colour structure is fairly straightforward and obeys Casimir scaling through to three loops,

$$\Gamma_{\text{cusp}} = C_R \left(\sum_{i=1}^{3} \left(\frac{\alpha_s}{4\pi} \right)^i \Gamma^{(i)}_{\text{cusp}} \right) + \mathcal{O}(\alpha_s^4) \tag{3.33}$$

with the quadratic Casimir defined by $\mathbf{T}^a\mathbf{T}^a = C_R\mathbf{1}$, with $\mathbf{T}$ being defined in Section 1.1. It is a singlet in colour space. A generalised version of this scaling occurs to all orders which accounts for quartic Casimirs which begin to contribute at four loops (see Section 4.5.2 for a detailed discussion).

In Section 3.3.1 we discuss the various limits we can use to constrain an ansatz for Γ_{cusp}. In Sections 3.3.2, 3.3.3 and 3.3.4 we look at the one-loop, two-loop and three-loop cases respectively.

3.3.1 Limits of Γ_{cusp}

As is clear from the structure of the definition of α in eq. (3.1), the limits that correspond to physical properties are $\alpha \to 0$, $\alpha \to -1$ and $\alpha \to 1$.

The first is the lightlike limit (see eq. (1.28)), where the Wilson lines become lightlike ($\beta_i^2 \to 0$). In this limit $\Gamma_{\text{cusp}}(\alpha)$ diverges as [79]

$$\lim_{\alpha\to 0} \Gamma_{\text{cusp}}(\alpha) = \gamma_{\text{cusp}} \log \alpha + \text{const.}, \tag{3.34}$$

where γ_{cusp} is the QCD lightlike cusp anomalous dimension which evaluates to

$$\begin{aligned}
\gamma_{\text{cusp}}(\alpha_s) &= \sum_{n=1}^{\infty} \left(\frac{\alpha_s}{\pi}\right)^n \gamma_{\text{cusp}}^{(n)} \\
&= \frac{\alpha_s}{\pi} C_i + \left(\frac{\alpha_s}{\pi}\right)^2 C_i \left[C_A \left(\frac{67}{36} - \frac{\zeta_2}{2} \right) - \frac{5}{9} n_f T_f \right] \\
&\quad + \left(\frac{\alpha_s}{\pi}\right)^3 C_i \left[C_A^2 \left(\frac{245}{96} - \frac{67}{36}\zeta_2 + \frac{11}{24}\zeta_3 + \frac{11}{8}\zeta_4 \right) \right. \\
&\qquad\qquad + C_A n_f T_f \left(-\frac{209}{216} + \frac{5}{9}\zeta_2 - \frac{7}{6}\zeta_3 \right) \\
&\qquad\qquad \left. + C_F n_f T_f \left(-\frac{55}{48} + \zeta_3 \right) - \frac{(n_f T_f)^2}{27} \right] + \mathcal{O}\left(\alpha_s^4\right),
\end{aligned} \tag{3.35}$$

where C_i, defined above, is the quadratic Casimir in the fundamental or the adjoint representation for quarks and gluons, respectively, n_f is the number of light quarks and the normalisation of the generators t^a in the fundamental representation, $\text{Tr}(t^a t^b) = T_f \delta_{ab}$, is conventionally set to $T_f = 1/2$. The three-loop value of γ_{cusp} was computed in [19]. After significant progress towards a four-loop determination [30–34] a complete result was recently calculated in refs. [35, 36]. Note we expand the quantity γ_{cusp} in terms of $\frac{\alpha_s}{\pi}$ whereas Γ_{cusp} is in terms of $\frac{\alpha_s}{4\pi}$.

The second limit $\alpha \to -1$ is when the three-velocities of the lines become anti-parallel. This is the case for heavy quark-antiquark production near threshold [23,33,123,127]. We shall use as a constraint that, up to three loops, Γ_{cusp} diverges as

$$\lim_{\alpha\to -1} \Gamma_{\text{cusp}}(\alpha) = \frac{V}{1+\alpha} + \mathcal{O}\left(\frac{\alpha_s^4 \log(1+\alpha)}{1+\alpha} \right) \tag{3.36}$$

but not any faster. As the coefficient V is found from $\Gamma_{\text{cusp}}(\alpha)$ we will not use its explicit expression but will use the fact that there are no terms $\frac{\log^k(1+\alpha)}{(\alpha+1)^n}$ for

$n \geq 2$ and any k in the limit.

The last limit is the $\alpha \to 1$ limit. In this case the lines become one single infinite line and all diagrams that span both legs become the self-energy type. These will be multi-loop generalisations of that seen at one-loop in Figure 2.1b. These cancel the self energies already present on the individual lines due to a Ward identity. As such as $\alpha \to 1$, Γ_{cusp} vanishes [79]. Due to the finiteness of the limit, one can expand the integrand in the limit and compute order by order in $(\alpha-1)^n$ the resulting integrals [33]. This will be the main source of information at higher loops. We will use this to reconstruct the full α dependence from this limit using the ansatz.

3.3.2 One loop

As the first entry of the symbol is α and we are restricted to weight one functions the only transcendental function available is $\log\alpha$. Looking at Table 3.3 the only rational piece is $r(\alpha)^{\text{odd}}$. Our ansatz for the one-loop correction to the cusp anomalous dimension is

$$\Gamma^{(1)}_{\text{cusp}}(\alpha) = c_1 r(\alpha)\log\alpha + c_2. \tag{3.37}$$

We exclude $r(\alpha)^3$ because, as explained in eq. (3.21), to generate that factor one would require three loop integrals. Let us expand the ansatz in eq. (3.37) for $\alpha \to 1$

$$\Gamma^{(1)}_{\text{cusp}}(\alpha) = (-c_1 + c_2) + \mathcal{O}(1-\alpha). \tag{3.38}$$

For vanishing $\alpha \to 1$ we require $c_1 = c_2$ which gives

$$\Gamma^{(1)}_{\text{cusp}}(\alpha) = c_1\bigg(r(\alpha)\log\alpha + 1\bigg). \tag{3.39}$$

The remaining constant can be fixed from the lightlike cusp,

$$\Gamma^{(1)}_{\text{cusp}}(\alpha) = c_1\log\alpha + \mathcal{O}(\alpha^2) = 4\gamma^{(1)}_{\text{cusp}}\log\alpha + \mathcal{O}(\alpha^2). \tag{3.40}$$

Using $\gamma^{(1)}_{\text{cusp}} = C_i$ in eq. (3.35) we find

$$\Gamma^{(1)}_{\text{cusp}}(\alpha) = 4C_i\bigg(r(\alpha)\log\alpha + 1\bigg), \tag{3.41}$$

Weight	Rational	Transcendental
zero	1	1
	r^2	1
one	1	$\log(2)$
	r	M_{000}
	r^2	$\log(2)$
two	1	$\zeta_2,\ M_{000}^2$
	r	$M_{100},\ M_{000}\log(2)$
	r^2	$\zeta_2,\ M_{000}^2$
three	1	$\zeta_3,\ M_{000}^2\log(2),\ M_{011},\ M_{000}M_{100}$
	r	$M_{200}, M_{000}\zeta_2,\ M_{100}\log(2),\ M_{000}^3$
	r^2	$\zeta_3,\ M_{000}^2\log(2),\ M_{011},\ M_{000}M_{100}$
	s	$w_1^{(3),3}$

Table 3.4: The list of functions in the ansatz for $\Gamma^{(2)}_{\text{cusp}}$ we have used shorthand notation that drops the functional argument.

replicating eq. (2.50b). Although a rather trivial example, it illustrates the powerfulness of the method since no explicit calculation was necessary, only the analytical properties of Γ_{cusp} and knowledge of its limits is required to reconstruct the full expression of eq. (3.41).

3.3.3 Two loop

Our ansatz at two loops includes the constants ζ_2, ζ_3 as well as $\log 2$, which is known to show up in computations involving massive particles. As there are two loop integrations, the maximal power of the rational function $r(\alpha)$ will be two. Including the possibility that the new functions with the letter y can appear, we find there are 24 functions that can appear up to weight three and these are displayed in Table 3.4.

We then apply constraints from $\alpha \to -1$, eq. (3.36), and $\alpha \to 0$, eq. (3.34), fitting to the two-loop lightlike cusp anomalous dimension in eq. (3.35). We give results for these series expansions of the transcendental functions in the ansatz in Table 3.5.

After the constraints from the $\alpha \to -1$, $\alpha \to 0$ and also requiring vanishing in $\alpha \to 1$ limits we find that there are still seven degrees of freedom. To fit the rest of them we use the $\alpha \to 1$ expansion. We would require explicit calculation of integrals in this limit. However as this is exploratory we will just expand the

$f(\alpha)$	$\lim_{\alpha\to 0} f(\alpha)$	$\lim_{\xi\to 0} f(\xi-1)$
M_{000}	$2\log(\alpha)$	$-2\xi+2i\pi$
M_{100}	$-2\log(\alpha)^2-2\zeta_2$	$4i\pi\log(\xi)+12\zeta_2+4i\pi\log(2)$
M_{011}	$-\frac{2}{3}\log(\alpha)^3-2\zeta_2\log(\alpha)-2\zeta_3$	$4\xi(-i\pi\log(\xi)-3\zeta_2+i\pi-4\pi\log(2))$
M_{200}	$\frac{8}{3}\log(\alpha)^3+8\zeta_2\log(\alpha)-4\zeta_3$	$8i\pi\log^2(\xi)+16\log(\xi)(4\zeta_2+i\pi\log(2))$ $+48\zeta_2\log(2)-\frac{4i\pi^3}{3}+8i\pi\log^2(2)$
$w_1^{(3),3}$	0	$-\frac{1}{2}i\pi\log^2(\xi)+\log(\xi)(i\pi\log(2)-3\zeta_2)$ $+3\zeta_2\log(2)+\frac{i\pi^3}{12}-\frac{1}{2}i\pi\log^2(2)$

Table 3.5: Transcendental functions in Table 3.4 expanded in the $\alpha\to 0$ limit and $\alpha\to -1$. For the latter, they are given up to the order required such that when combined with corresponding rational factors in Table 3.4 they can be expanded up to $\frac{1}{\alpha+1}=\frac{1}{\xi}$.

actual result in $\alpha\to 1$. The result, written in terms of the basis, is [79]

$$\Gamma^{(2)}_{\text{cusp}}(\alpha)=C_i\Bigg[C_A\left(-2M_{000}(\alpha)^2-16\zeta_2+\frac{196}{9}\right)-4C_AM_{011}(\alpha)r(\alpha)^2-\frac{80n_fT_f}{9}$$
$$r(\alpha)\Bigg(C_A\left(-8\zeta_2M_{000}(\alpha)-\frac{1}{3}M_{000}(\alpha)^3+\frac{134M_{000}(\alpha)}{9}-4M_{100}(\alpha)\right)$$
$$-\frac{40}{9}n_fT_fM_{000}(\alpha)\Bigg)\Bigg]. \quad (3.42)$$

The explicit functions M_{000} and M_{100} are given in eqs. (2.73) and (2.74) respectively. The expression for M_{011} can be found in eqs. (A.4) of ref. [65]. Comparing eq. (3.42) to the ansatz we find we need to go to $(\alpha-1)^8$ term in order to fit the remaining seven terms.

Some simplifications to the ansatz in Table 3.4 can be explored. One could be removing explicit appearances of log(2) in functions. This would remove six functions so that we would only have 18 functions in an ansatz. However doing this, we find we still need to go to $(\alpha-1)^8$ to fit all the coefficients.

3.3.4 Three loops and beyond

At three loops there are 137 functions in a general ansatz for the cusp. This is comprised of the $(M+\zeta)$ basis in Table 3.2 and the new functions with letter y in Appendix B. We only allow the possibility of log(2) to appear in products with the new functions. It is clear that this ansatz is large. To explore the practicalities of a potential bootstrap we instead only include functions that comprise the A_i and B_i in eqs. (3.5), (3.6), (3.8), (3.13) to (3.15) and (3.32a). After applying the

constraints from the $\alpha \to -1$ and $\alpha \to 0$ limits we find that we need to go to $\mathcal{O}\left((1-\alpha)^{20}\right)$ to fit the remaining terms.

Trying to fit the general ansatz, would require even higher orders. At four loops the ansatz would be greater and the required orders higher still. Of course, at four loops, this expansion is unknown and would need input from the actual integrals expanded in $(1-\alpha)$. This does not seem currently achievable as the authors of ref. [33] were able to calculate certain colour terms in the expansion of four loop integrals only to $\sim \mathcal{O}\left((1-\alpha)^6\right)$. Although for some colour terms the weight will be less than seven and the size of an ansatz would be comparable to three loops.

A greater understanding of the potential rational terms by maximal cuts would be one avenue to explore to limit the growth of the size of the ansatz when the loop order is increased. It will then control the required maximum term in the series expansion of the integrals around $\alpha = 1$.

3.4 Fitting the $[1,1,2,1]$-web

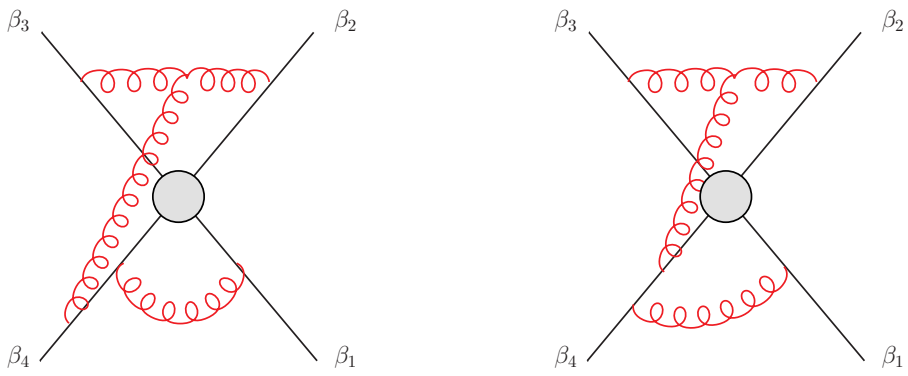

(a) A **(b)** B

Figure 3.2: Diagrams contributing to the $[1,1,2,1]$-web

In this section we use what we have learned about the new functions to construct an ansatz for the three-loop $[1,1,2,1]$-web. We then constrain the ansatz using known lightlike and collinear limits and fit remaining parameters numerically. A first attempt at this exercise was performed in [128], fitting solely to the MGEW basis functions M_{klm}. A subsequent fit was performed in [116] adding ζ_n values to the basis and using known constraints on the lightlike [78] and collinear limits [116] of the web.

We will produce an ansatz for the subtracted $[1,1,2,1]$-web, which is given by

$$\bar{w}_{1112}^{(3,-1)} = w_{1112}^{(3,-1)} - \frac{1}{2}\left[w_{3gv}^{(0)}, w^{(1,-1)}\right] + \frac{1}{2}\left[w_{3gv}^{(-1)}, w^{(1,0)}\right] \tag{3.43}$$

where $w_{3gv}^{(-1)}$ is given in eq. (2.98b) and $w^{(1,-1)}$ and $w^{(1,0)}$ are given in eqs. (2.51a) and (2.51b). The functions $w_{1121}^{(3,-1)}$ and $w_{3gv}^{(0)}$ are unknowns. Extracting the common colour term $-f^{ade}f^{bce}\mathbf{T}_1^a\mathbf{T}_2^b\mathbf{T}_3^c\mathbf{T}_4^d$ from each term in eq. (3.43) we can write the kinematic part of the subtracted web as

$$\bar{\mathcal{F}}_{1121}^{(-1)} = \frac{1}{2}\left(-\mathcal{F}_{1121,A}^{(-1)} + \mathcal{F}_{1121,B}^{(-1)}\right) - \frac{1}{2}\mathcal{F}_{3gv}^{(0)}\mathcal{F}^{(1,-1)} + \frac{1}{2}\mathcal{F}^{(1,0)}\mathcal{F}_{3gv}^{(-1)} \tag{3.44}$$

where $\mathcal{F}_{1121,A}$ and $\mathcal{F}_{1121,B}$ are the constituent diagrams to the $[1,1,2,1]$-web shown in Figure 3.2. It was shown in [128] that by integrating out the one-loop gluon exchange connecting β_1 and β_4 the subtracted web can be written as follows,

$$\bar{\mathcal{F}}_{1121}^{(-1)} = \frac{1}{3}r(\alpha_{14})\Big[t_1(\alpha_{23},\alpha_{24},\alpha_{34})M_{000}(\alpha_{14}) - 2t_0(\alpha_{23},\alpha_{24},\alpha_{34})M_{100}(\alpha_{14})\Big] \tag{3.45}$$

where t_0 is the kinematic function of $w_{3gv}^{(-1)}$ in eq. (2.98b),

$$t_0(\alpha_{23},\alpha_{24},\alpha_{34}) = -2\sum_{(i,j,k)\in\{2,3,4\}} \epsilon_{ijk}r(\alpha_{ij})\log(\alpha_{ij})\log^2(\alpha_{ik}). \tag{3.46}$$

We will construct an ansatz for the unknown function t_1. We will assume that the dependence of t_1 on the different variables factorises. These functions were the ones considered in Section 3.2. Along with the generic inversion ($\alpha \to \frac{1}{\alpha}$) and analytic ($\alpha \to -\alpha$) properties, t_1 also satisfies antisymmetry in $\beta_2 \leftrightarrow \beta_3$ from the three-gluon vertex. From which we have

$$t_1(\alpha_{23},\alpha_{24},\alpha_{34}) = -t_1(\alpha_{23},\alpha_{34},\alpha_{24}). \tag{3.47}$$

A collinear limit of the $[1,1,2,1]$-web is known. When $3||4$ it becomes the $[1,3,1]$-web which was computed in [116] by unitarity cut methods. To compute this limit, we first go to the physical region with β_4 incoming and the rest outgoing. Here, instead of all the $\alpha_{ij} > 0$, we have $\alpha_{23} > 0$ with the rest negative. Then we take the limit $\beta_4 \to -\beta_3$ because β_4 is incoming and β_3 is outgoing. As $\alpha_{34} \to 1$, t_1 goes to

$$t_1(\alpha_{23},\alpha_{24},\alpha_{34}) \to_{3||4} t_1(\alpha_{23},-\alpha_{23},1). \tag{3.48}$$

In order to connect with the previous result, we go back to the unphysical space,

where all entries are positive. Hence we know that $t_1(\alpha_{23}, \alpha_{23}, 1)$ is the $[1,3,1]$-web function which we quote here

$$\begin{aligned} t_1^{\rm coll}(\alpha_{23}) \equiv & t_1(\alpha_{23}, \alpha_{23}, 1) \\ = & r(\alpha_{23}) \left(M_{000}(\alpha_{23}) \left(-\frac{M_{011}(\alpha_{23})}{12} - \frac{\zeta_3}{2} \right) + \frac{1}{24} M_{000}(\alpha_{23})^2 M_{100}(\alpha_{23}) \right. \\ & \left. + \frac{1}{36} \left(24\zeta_2 M_{000}(\alpha_{23}) + M_{000}(\alpha_{23})^3 \right) - \frac{M_{102}(\alpha_{23})}{8} \right) \\ & + \frac{1}{12} M_{000}(\alpha_{23}) M_{100}(\alpha_{23}) - \frac{M_{011}(\alpha_{23})}{6} + \frac{4\zeta_2}{3} - \zeta_3. \end{aligned} \tag{3.49}$$

We have written the function $t_1^{\rm coll}(\alpha_{23})$ in the $(M + \zeta)$ basis of Table 3.2. The lightlike limit where all $\beta_i^2 \to 0$ ($\alpha_{ij} \to 0$) is also known [78]. This is a logarithmically divergent limit

$$\lim_{\alpha_{ij} \to 0} t_1(\alpha_{23}, \alpha_{24}, \alpha_{34}) \equiv t_1^{\rm ll}(\alpha_{23}, \alpha_{24}, \alpha_{34}) \tag{3.50}$$

$$\begin{aligned} = & \frac{1}{576} \Big(M_{000}(\alpha_{24}) - M_{000}(\alpha_{34}) \Big) \Big(4 M_{000}(\alpha_{23}) M_{000}(\alpha_{24}) M_{000}(\alpha_{34}) \\ & - 3 M_{000}(\alpha_{23})^2 M_{000}(\alpha_{24}) + M_{000}(\alpha_{23}) M_{000}(\alpha_{24})^2 - 3 M_{000}(\alpha_{23})^2 M_{000}(\alpha_{34}) \\ & + M_{000}(\alpha_{23}) M_{000}(\alpha_{34})^2 - 24\zeta_2 M_{000}(\alpha_{23}) - M_{000}(\alpha_{23})^3 \\ & - 3 M_{000}(\alpha_{24}) M_{000}(\alpha_{34})^2 - 3 M_{000}(\alpha_{24})^2 M_{000}(\alpha_{34}) + 24\zeta_2 M_{000}(\alpha_{24}) \\ & + M_{000}(\alpha_{24})^3 + 24\zeta_2 M_{000}(\alpha_{34}) + M_{000}(\alpha_{34})^3 - 96\zeta_3 \Big). \end{aligned} \tag{3.51}$$

It is a striking property of webs that connect the maximum number of lines at a given order are of uniform weight, see the previous results at two loops eqs. (2.72) and (2.98b) and other calculations [64, 65]. As the $[1,1,2,1]$-web connects the maximum number of lines at three loops, we shall assume that it is of uniform weight. We first construct an ansatz built from the $(M + \zeta)$ basis and write it as

$$t_1^{(\mathrm{M}+\zeta)\ \mathrm{ansatz}}(\alpha_{23}, \alpha_{24}, \alpha_{34}) = \sum_{i=1}^{5} c_i f_i(\alpha_{23}, \alpha_{24}, \alpha_{34}) + f_{\rm CL}(\alpha_{23}, \alpha_{24}, \alpha_{34}) \tag{3.52}$$

such that each f_i vanishes in both limits, with only $f_{\rm CL}$ replicating the limits. There are five remaining degrees of freedom. Explicitly the functions are

$$\begin{aligned} f_1 = & M_{000}(\alpha_{23})^2 (M_{100}(\alpha_{34}) r(\alpha_{34}) - M_{100}(\alpha_{24}) r(\alpha_{24})) \\ & + M_{000}(\alpha_{34})^2 (M_{100}(\alpha_{24}) r(\alpha_{24}) - M_{100}(\alpha_{23}) r(\alpha_{23})) \\ & + M_{000}(\alpha_{24})^2 (M_{100}(\alpha_{23}) r(\alpha_{23}) - M_{100}(\alpha_{34}) r(\alpha_{34})) \end{aligned}$$

$$
\begin{aligned}
f_2 = {} & M_{000}(\alpha_{23})(-6r(\alpha_{23})M_{011}(\alpha_{24}) - r(\alpha_{23})M_{000}(\alpha_{34})M_{100}(\alpha_{34}) \\
& \qquad + M_{100}(\alpha_{23})M_{000}(\alpha_{34})r(\alpha_{34}) + 6r(\alpha_{23})M_{011}(\alpha_{34})) \\
& + M_{000}(\alpha_{24})(M_{000}(\alpha_{23})r(\alpha_{23})M_{100}(\alpha_{24}) - M_{000}(\alpha_{23})M_{100}(\alpha_{23})r(\alpha_{24}) \\
& + 6M_{011}(\alpha_{23})r(\alpha_{24}) + r(\alpha_{24})M_{000}(\alpha_{34})M_{100}(\alpha_{34}) - M_{100}(\alpha_{24})M_{000}(\alpha_{34})r(\alpha_{34}) \\
& \qquad - 6r(\alpha_{24})M_{011}(\alpha_{34})) + 6M_{000}(\alpha_{34})r(\alpha_{34})(M_{011}(\alpha_{24}) - M_{011}(\alpha_{23}))
\end{aligned}
$$

$$
\begin{aligned}
f_3 = {} & M_{000}(\alpha_{24})^2 \left(r(\alpha_{23}) \left(M_{000}(\alpha_{23})^2 r(\alpha_{23}) + 2M_{100}(\alpha_{23})\right) - 2M_{100}(\alpha_{24})r(\alpha_{24})\right) \\
& + M_{000}(\alpha_{34})^2 \left(-M_{000}(\alpha_{23})^2 r(\alpha_{23})^2 - 2M_{100}(\alpha_{23})r(\alpha_{23}) + M_{000}(\alpha_{34})^2 r(\alpha_{34})^2 \right. \\
& \qquad \left. + 2M_{100}(\alpha_{34})r(\alpha_{34})\right) - M_{000}(\alpha_{24})^4 r(\alpha_{24})^2
\end{aligned}
$$

$$
\begin{aligned}
f_4 = {} & M_{000}(\alpha_{24})^2 \left(-M_{000}(\alpha_{23})^2 r(\alpha_{24})^2 - 2M_{100}(\alpha_{23})r(\alpha_{23}) + r(\alpha_{24})^2 M_{000}(\alpha_{34})^2 \right. \\
& \qquad \left. + 2M_{100}(\alpha_{24})r(\alpha_{24}) - M_{000}(\alpha_{34})^2 r(\alpha_{34})^2\right) \\
& + M_{000}(\alpha_{34})^2 \left(r(\alpha_{34}) \left(r(\alpha_{34}) \left(M_{000}(\alpha_{23})^2 - M_{000}(\alpha_{34})^2\right) - 2M_{100}(\alpha_{34})\right)\right. \\
& \qquad \left. + 2M_{100}(\alpha_{23})r(\alpha_{23})\right) + M_{000}(\alpha_{24})^4 r(\alpha_{24})^2
\end{aligned}
$$

$$
\begin{aligned}
f_5 = {} & M_{000}(\alpha_{23})r(\alpha_{23}) \left(12M_{011}(\alpha_{24}) - r(\alpha_{34})M_{000}(\alpha_{34})^3 - 12M_{011}(\alpha_{34})\right) \\
& + 12M_{000}(\alpha_{34})r(\alpha_{34})(M_{011}(\alpha_{23}) - M_{011}(\alpha_{24})) \\
& + M_{000}(\alpha_{24})r(\alpha_{24}) \left(-r(\alpha_{23})M_{000}(\alpha_{23})^3 - 12M_{011}(\alpha_{23}) + M_{000}(\alpha_{34})^3 r(\alpha_{34}) \right. \\
& \qquad \left. + 12M_{011}(\alpha_{34})\right) + M_{000}(\alpha_{24})^3 r(\alpha_{24})(M_{000}(\alpha_{23})r(\alpha_{23}) - M_{000}(\alpha_{34})r(\alpha_{34})) \\
& + M_{000}(\alpha_{23})^3 r(\alpha_{23})M_{000}(\alpha_{34})r(\alpha_{34})
\end{aligned}
$$

$$
\begin{aligned}
f_{\mathrm{CL}} = {} & r(\alpha_{24})\Bigg(\frac{1}{24}M_{000}(\alpha_{23})M_{100}(\alpha_{23})M_{000}(\alpha_{24}) - \frac{1}{12}M_{000}(\alpha_{24})M_{011}(\alpha_{34}) \\
& - \frac{1}{12}M_{000}(\alpha_{24})M_{011}(\alpha_{24}) - \frac{1}{32}5M_{000}(\alpha_{24})^2 M_{100}(\alpha_{24}) - \frac{1}{2}\zeta_3 M_{000}(\alpha_{24}) \\
& - \frac{M_{102}(\alpha_{24})}{8}\Bigg) + r(\alpha_{34})\Bigg(-\frac{1}{24}M_{000}(\alpha_{23})M_{100}(\alpha_{23})M_{000}(\alpha_{34}) + \frac{M_{102}(\alpha_{34})}{8} \\
& + \frac{1}{12}M_{011}(\alpha_{24})M_{000}(\alpha_{34}) + \frac{1}{12}M_{000}(\alpha_{34})M_{011}(\alpha_{34}) + \frac{1}{2}\zeta_3 M_{000}(\alpha_{34}) \\
& + \frac{5}{32}M_{000}(\alpha_{34})^2 M_{100}(\alpha_{34})\Bigg) + r(\alpha_{23})\Bigg(r(\alpha_{24})\Bigg[\frac{1}{3}\zeta_2 M_{000}(\alpha_{23})M_{000}(\alpha_{24}) \\
& - \frac{1}{192}M_{000}(\alpha_{23})M_{000}(\alpha_{24})M_{000}(\alpha_{34})^2 + \frac{11}{576}M_{000}(\alpha_{23})^3 M_{000}(\alpha_{24}) \\
& + \frac{43}{576}M_{000}(\alpha_{23})M_{000}(\alpha_{24})^3\Bigg] + r(\alpha_{34})\Bigg[\frac{1}{192}M_{000}(\alpha_{23})M_{000}(\alpha_{24})^2 M_{000}(\alpha_{34}) \\
& - \frac{1}{3}\zeta_2 M_{000}(\alpha_{23})M_{000}(\alpha_{34}) - \frac{11}{576}M_{000}(\alpha_{23})^3 M_{000}(\alpha_{34}) \\
& - \frac{43}{576}M_{000}(\alpha_{23})M_{000}(\alpha_{34})^3\Bigg] + \frac{1}{96}M_{100}(\alpha_{23})M_{000}(\alpha_{24})^2 \\
& + \frac{7}{48}M_{000}(\alpha_{23})M_{000}(\alpha_{24})M_{100}(\alpha_{24}) - \frac{1}{96}M_{100}(\alpha_{23})M_{000}(\alpha_{34})^2 \\
& - \frac{7}{48}M_{000}(\alpha_{23})M_{000}(\alpha_{34})M_{100}(\alpha_{34})\Bigg)
\end{aligned}
$$

$$+ r(\alpha_{24})^2 \left(-\frac{3}{32} M_{000}(\alpha_{24})^4 - \frac{1}{3}\zeta_2 M_{000}(\alpha_{24})^2 \right)$$
$$+ r(\alpha_{34})^2 \left(\frac{1}{3}\zeta_2 M_{000}(\alpha_{34})^2 + \frac{3 M_{000}(\alpha_{34})^4}{32} \right)$$

There have been previous, unsuccessful attempts at fitting this ansatz using solely functions from the M_{kln} basis [128] or the $(M + \zeta)$ basis [116]. Here, we now consider the extension given in Appendix B

$$t_1^{\text{full ansatz}} = t_1^{(\text{M}+\zeta)\text{ ansatz}} + \Delta\, t_1^{\text{new ansatz}}. \tag{3.53}$$

First we explore the combinations of any new functions not present in the $(M+\zeta)$ basis but can appear in an ansatz for t_1. We start with noting that any new function for t_1 has to be antisymmetric in $\beta_2 \leftrightarrow \beta_3$. Also, from the collinear limit $3||4$ where $\alpha_{34} \to 1$ and $\alpha_{24} = \alpha_{23}$ there is no letter y in the symbol in eq. (3.49). Therefore, if we were to include a new weight four function, including any rational factor, $K_4(\alpha)$ in t_1 then the combination we would need to have is

$$K_4(\alpha_{24}) - K_4(\alpha_{34}) \in \Delta\, t_1^{\text{new ansatz}}. \tag{3.54}$$

Taking $\alpha_{34} \to 1$, $\alpha_{24} = \alpha_{23}$ we see $K_4(\alpha_{23}) - K_4(1)$ would appear in the $[1,3,1]$-web. However, as noted above no new function does appear. Thus we can exclude any new function of weight four appearing in $\Delta\, t_1^{\text{new ansatz}}$.

A weight-three new function can appear when it is multiplied by M_{000}. For the weight-three new function, including a potential rational factor, we introduce two unknown functions that are either symmetric in inversion ($\alpha \to \frac{1}{\alpha}$), $K_{3\text{S}}(\alpha)$ or antisymmetric $K_{3\text{AS}}(\alpha)$. The antisymmetric new function $K_{3\text{AS}}(\alpha)$ can appear when multiplied by $M_{000}(\alpha)$ such that the overall product is symmetric. After applying the inversion symmetry in all variables and enforcing the antisymmetry in $\beta_2 \leftrightarrow \beta_3$ we find that there is the potential for five independent combinations

$$\begin{aligned}
\Delta\, t_1^{\text{new ansatz}} = {} & c_1 M_{000}(\alpha_{23}) r(\alpha_{23}) (K_{3S}(\alpha_{24}) - K_{3S}(\alpha_{34})) \\
& + c_2 (M_{000}(\alpha_{34}) K_{3\text{AS}}(\alpha_{34}) - M_{000}(\alpha_{24}) K_{3\text{AS}}(\alpha_{24})) \\
& + c_3 (M_{000}(\alpha_{24}) r(\alpha_{24}) K_{3\text{S}}(\alpha_{24}) - M_{000}(\alpha_{34}) r(\alpha_{34}) K_{3\text{S}}(\alpha_{34})) \\
& + c_4 (K_{3\text{S}}(\alpha_{34}) M_{000}(\alpha_{24}) r(\alpha_{24}) - M_{000}(\alpha_{34}) r(\alpha_{34}) K_{3\text{S}}(\alpha_{24})) \\
& + c_5 K_{3\text{S}}(\alpha_{23}) (M_{000}(\alpha_{24}) r(\alpha_{24}) - M_{000}(\alpha_{34}) r(\alpha_{34}))
\end{aligned} \tag{3.55}$$

where c_i are rational numbers. Now we take the collinear limit $\alpha_{34} \to 1$ and

$\alpha_{24} = \alpha_{23}$ of the above using $r(\alpha)M_{000}(\alpha) \to -2$ as $\alpha \to 1$,

$$\Delta\, t_1^{\text{new ansatz, collinear}} = 2(c_4 + c_5)K_{3\text{S}}(\alpha_{23}) + c_2 M_{000}(1)K_{3\text{AS}}(1) + 2c_3 K_{3\text{S}}(1)$$
$$+ M_{000}(\alpha_{23})\Big(r(\alpha_{23})\Big((c_1 + c_3 + c_5)K_{3\text{S}}(\alpha_{23}) + (c_4 - c_1)K_{3\text{S}}(1)\Big) - c_2 K_{3\text{AS}}(\alpha_{23})\Big) \tag{3.56}$$

As there are no new functions beyond the $(M + \zeta)$ basis in the actual collinear limit in eq. (3.49) all terms that depend on α_{23} in eq. (3.56) have to vanish. This leads to constraints on the coefficients of the functions $K_{3\text{S}}(\alpha_{23})$ and $K_{3\text{AS}}(\alpha_{23})$

$$c_1 + c_3 + c_5 = 0 \qquad c_2 = 0 \qquad c_4 + c_5 = 0. \tag{3.57}$$

This leaves just $\Delta\, t_1^{\text{new ansatz, collinear}} = c_3 K_{3\text{S}}(1)\,(2 + r(\alpha_{23})M_{000}(\alpha_{23}))$. There are then only two possible combinations from eq. (3.55) that are consistent with the collinear limit

$$\Delta\, t_1^{\text{new ansatz}} = \tag{3.58}$$
$$d_1(M_{000}(\alpha_{24})r(\alpha_{24}) - M_{000}(\alpha_{34})r(\alpha_{34}))(K_{3\text{S}}(\alpha_{23}) - K_{3\text{S}}(\alpha_{24}) - K_{3\text{S}}(\alpha_{34}))$$
$$+ d_2\Big[(M_{000}(\alpha_{34})r(\alpha_{34})(K_{3\text{S}}(\alpha_{23}) - K_{3\text{S}}(\alpha_{24}))$$
$$+ M_{000}(\alpha_{23})r(\alpha_{23})(K_{3\text{S}}(\alpha_{24}) - K_{3\text{S}}(\alpha_{34}))$$
$$+ M_{000}(\alpha_{24})r(\alpha_{24})(K_{3\text{S}}(\alpha_{34}) - K_{3\text{S}}(\alpha_{23}))\Big]. \tag{3.59}$$

If the constant $K_{3\text{S}}(1)$ is also not present in eq. (3.49) then we should remove the first of these combinations from an ansatz of t_1. There are two weight-three functions that involve the letter y, i.e. not present in the MGEW-basis. They are $w_1^{(3),3}(\alpha)$ and $w_1^{(3),4}(\alpha)$ which are given explicitly in Appendix B.1. The rational functions accompanying them are $r(\alpha)^{\text{even}}s(\alpha)^{\text{odd}}$ and $r(\alpha)^{\text{odd}}s(\alpha)^{\text{odd}}$. As discussed below eq. (3.28) we shall not consider the function $w_1^{(3),4}(\alpha)$. As the $[1,1,2,1]$-web is a three-loop integral we expect at most three powers of the rational function $r(\alpha)$. One is from the one-loop already integrated out in eq. (3.45) and another from the factors in eq. (3.58). We then deduce we only have one new function

$$K_{3\text{S}}(\alpha) = s(\alpha)w_1^{(3),3}(\alpha). \tag{3.60}$$

Taking the collinear limit ($\alpha \to 1$) we find

$$\lim_{\alpha\to 1} K_{3\mathrm{S}}(\alpha) = K_{3\mathrm{S}}(1) = \log(2) - \frac{1}{2}. \tag{3.61}$$

As there is no $\log(2)$ present in t_1^{coll} in eq. (3.49) we can set $d_1 = 0$ in eq. (3.58)

$$\begin{aligned}\Delta\, t_1^{\text{new ansatz}} = d_2 \Big[&(M_{000}(\alpha_{34}) r(\alpha_{34}) (K_{3\mathrm{S}}(\alpha_{23}) - K_{3\mathrm{S}}(\alpha_{24})) \\ &+ M_{000}(\alpha_{23}) r(\alpha_{23}) (K_{3\mathrm{S}}(\alpha_{24}) - K_{3\mathrm{S}}(\alpha_{34})) \\ &+ M_{000}(\alpha_{24}) r(\alpha_{24}) (K_{3\mathrm{S}}(\alpha_{34}) - K_{3\mathrm{S}}(\alpha_{23}))\Big].\end{aligned} \tag{3.62}$$

This function vanishes in the lightlike limit. As such we will call this f_6 and combine it with eq. (3.52) to arrive at an ansatz for $\bar{\mathcal{F}}^{(-1)}_{1121}$ in eq. (3.45)

$$\bar{\mathcal{F}}^{(-1)}_{1121} = r(\alpha_{14}) M_{000}(\alpha_{14}) \sum_{i=1}^{6} c_i f_i + \frac{1}{3} r(\alpha_{14}) \left(M_{000}(\alpha_{14}) f_{\mathrm{CL}} - 2 M_{100}(\alpha_{14}) t_0\right). \tag{3.63}$$

We can now fit the c_i based on numerical results. It is reminded that r, M_{000}, M_{100}, f_{CL}, f_i and t_0 are known functions and can be evaluated to arbitrary precision. The object that is unknown is $\bar{\mathcal{F}}^{(-1)}_{1121}$ for which numerical values are computed using `pySecDec` [129]. This implements the sector decomposition algorithm [130] to expand Feynman integrals in ϵ. The resultant integrals are then numerically integrated using the `CUBA` library where the algorithm `Vegas` [131] was chosen. It is a robust integrator giving trusted error estimates.

Several checks were performed on the numerical data. First we check the robustness of the results by changing the seed for random number generation. From an initial grid of 276 points in the $(\alpha_{14}, \alpha_{24}, \alpha_{23}, \alpha_{34})$-plane, 247 were within in the error range of the two data sets generated by two different seeds. Of these points, 158 had quoted errors of $<5\%$ in $\bar{\mathcal{F}}^{(-1)}_{1121}$. Further checks on this data were carried out. The values of $\mathcal{F}^{(1,-1)}$, $\mathcal{F}^{(1,0)}$ and $\mathcal{F}^{(-1)}_{3gv}$, were checked against the analytical results eqs. (2.51a), (2.51b) and (2.98b) respectively. The renormalisation condition of the cancelling of double poles eq. (1.19) was also checked

$$\frac{1}{2}\left(-\mathcal{F}^{(-2)}_{1121,A} + \mathcal{F}^{(-2)}_{1121,B}\right) = \frac{1}{6}\mathcal{F}^{(1,-1)}\mathcal{F}^{(-1)}_{3gv} \tag{3.64}$$

The most important check is the dependence on the regulator m. In eq. (3.44) there is no dependence on the regulator as this is the function that will contribute

	Estimate	Standard Error	P-Value
c_1	-966944.	196136.	$2.4243002938213373 \times 10^{-6}$
c_2	-9083.49	94130.4	0.923271
c_3	1.61558×10^7	4.83045	$3.716807937163101 \times 10^{-6}$
c_4	-1.53576×10^7	-4.83039	$3.7177658610870355 \times 10^{-6}$
c_5	475785.	121389.	0.000141816
c_6	-298514.	27636.3	$7.046531400600217 \times 10^{-20}$

Table 3.6: The estimated value, standard error and p-value of the outcome of a linear model fit on eq. (3.63)

to the anomalous dimension. This ensures that the correct combination of integrals is used. At the point $(\alpha_{14}, \alpha_{24}, \alpha_{23}, \alpha_{34}) = (0.1, 0.2, 0.15, 0.25)$, 20 random m values between 1 and 5 were used. These are plotted in Figure 3.3a, which clearly shows that $\bar{\mathcal{F}}^{(-1)}_{1121}$ does not depend on m.

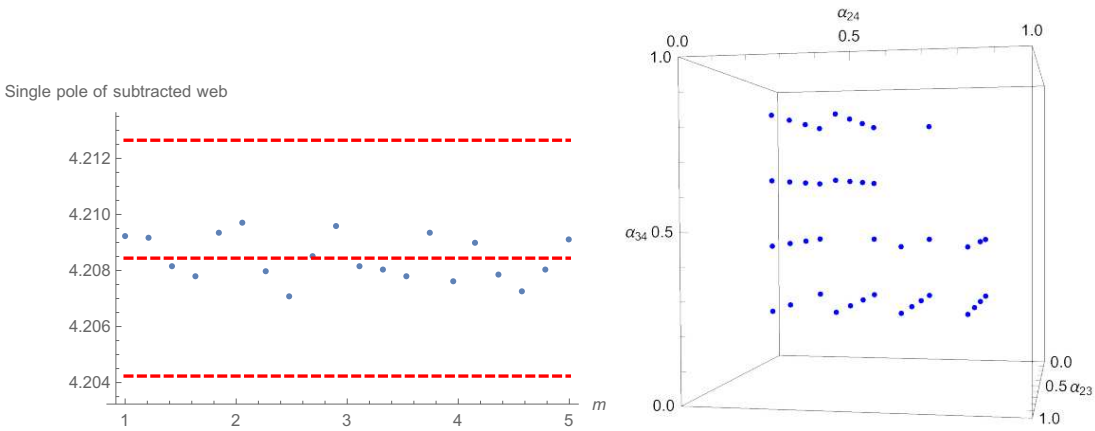

(a) **(b)**

Figure 3.3: **a)** Numerical values of $\bar{\mathcal{F}}^{(-1)}_{1121}$ as m varies. These are well within the red bands that indicate 0.1% deviation from the mean 4.2084. **b)** The phase points in the $(\alpha_{24}, \alpha_{23}, \alpha_{34})$-plane that give less than 5% error for $\bar{\mathcal{F}}^{(-1)}_{1121}$. Reliable data is scarce for the region $1 > \alpha_{24} > 0.5$, $1 > \alpha_{34} > 0.5$ and for extreme values.

We normalise the functions in eq. (3.63) by simply dividing by the sum of the numerical evaluations $f_i(x) \to \frac{f_i(x)}{\sum_j f_i(x_j)}$. After performing the checks and normalising we fit the c_i in eq. (3.63) using the `LinearModelFit` function in `Mathematica`. The results of this are displayed in Table 3.6. As can be seen from Table 3.6 the standard error in c_i is of the same order as the estimated value. Realistically, the results are inconclusive.

One of the issues of the fit is that we do not have accurate numerical values in all of the potential phase space. Figure 3.3b shows the space that is covered if 5% accuracy is sought. Improving this would improve the accuracy of the fit.

It may well be that the $[1,1,2,1]$-web does not evaluate to the basis functions and we would need to relax certain conditions. These would be uniform weight and the hypothesis that functions of different angles factorise. The first of which would be the first to test. We assumed that the (subtracted) web evaluates to a uniform weight function of weight five. It may not be the case and we would need to allow, in our ansatz, for lower weight terms. The second condition is a lot harder to implement. The study of the differential equations would be required to see what type of extra letters appear and the maximal cuts for the corresponding rational functions.

In this section we have constructed and constrained an ansatz for the $[1,1,2,1]$-web using the MGEW basis as well as the new functions constructed in Section 3.2. We found the potential for one these new functions to appear in the web in a particular combination. The remaining degrees of freedom were fitted to numerical results which gave disappointing results. Either better numerical results or an expansion of the ansatz or both will be required in future studies.

3.5 Conclusion

In this chapter we explored the function space arising in non-lightlike angle-dependent Wilson-line correlators. The functions we focused on were ones that factorised the dependence on multiple angles. The transcendental part of these functions are guided by the analytical behaviour of the correlators and are HPLs, i.e. their alphabet is $\{\alpha, \alpha \pm 1\}$. We restricted the rational functions to be of two known functions, $r(\alpha)$ and $s(\alpha)$. After mapping the alphabet to the convenient $\{\alpha, \eta, y\}$ we found an interesting interplay between the type of rational and symbol that can appear after analysing the $\alpha \to \frac{1}{\alpha}$ and $\alpha \to -\alpha$ behaviour of the functions. Along with the known functions of MGEW-type in eq. (3.2) there are new functions with the symbol letter y and are displayed up to weight five in Appendix B.

We then looked at the potential to bootstrap the non-lightlike cusp anomalous dimension (the two-line correlator). Using the limits of $\alpha \to -1$ and the lightlike limit to initially constrain an ansatz and then fit the rest using the finite $\alpha \to 1$ series expansion of the explicit integrals themselves. At higher loop orders the ansatz exponentially grows along with the required terms in the expansion.

We also examined the functions that could appear in the four-line three-loop $[1, 1, 2, 1]$-web. We discovered one function that has the symbol letter y that has the potential to be present in the web. We then constrained an ansatz based on the known lightlike and collinear limits and fitted the rest of the parameters numerically.

To improve both of the examples we may need to extend the basis. A greater understanding of the types of rationals that can appear would involve the computation of maximal cuts of multi-loop multi-leg diagrams. As was seen in the case of the two-loop three-line $[3gv]$-web, its maximal cut in eq. (2.87) may involve elliptic functions.

We can also look at ways to limit the growth of the ansatz. The only condition of the positions of letters in the symbol are that α appears in the first entry. There are other conditions that are a possibility for the future studies. One is that since the letter y does not appear to two loops (i.e. weight three) it can only appear starting in the fourth entry of the symbol [120].

Chapter 4

Lightlike Wilson lines

In this chapter we discuss and compare the factorisation properties of massless form factors (essentially two-leg scattering amplitudes) and the large-x limit of parton distribution functions. In the comparison we see that while the double poles are equivalent there is a difference in the single pole behaviour. We show that they exhibit the same hard-collinear behaviour so that this difference lies solely in the geometry of the underlying soft function. The main question we will answer is what is the Wilson-line correlator corresponding to $f_{\rm eik}$ in eq. (1.29), defined as the difference $\gamma_G^i - 2B_\delta^i$.

4.1 Initial Observations

Let us first note that the combination in (1.29) has a direct physical interpretation as the soft anomalous dimension associated with Drell-Yan production near partonic threshold [2–7], namely $\gamma_G^q - 2\,B_\delta^q = \frac{1}{2}\Gamma_{\rm DY}$. Similarly $\gamma_G^g - 2\,B_\delta^g$ is associated with Higgs production through gluon-gluon fusion near threshold. The corresponding soft function is defined *at cross-section level*, by replacing the energetic partons, which move in opposite lightlike directions (before annihilating at the hard interaction vertex), by Wilson lines that follow the same trajectory, in both the amplitude and its complex conjugate, see eq. (1.3). The cusp where the complex-conjugate amplitude Wilson lines meet is displaced by a timelike distance with respect to the amplitude: this distance is the Fourier conjugate

variable to the energy fraction carried by soft partons.[1] Initial-state radiation, namely the set of soft particles connecting the amplitude side to the complex-conjugate amplitude side, are described by cut propagators. This soft function admits an evolution equation governed by γ_{cusp} and Γ_{DY} (see e.g. eq. (9) in ref. [4], or eqs. (43-44) in ref. [7]). The latter was computed through three loops directly based on the aforementioned Wilson-line definition [21, 136], and the results agree with the combination of anomalous dimensions in (1.29), which were extracted from independent QCD computations of the form factor [84,85,137] and DGLAP splitting functions [138–145]. Thus, from this perspective, this physical quantity is well understood, and its Casimir-scaling property simply follows from the above-mentioned Wilson-line definition.

Our own investigation starts with the simple observation that the two-loop result for $\gamma_G - 2\,B_\delta$ in (1.30) *also agrees*, up to an overall factor of 4, with the result for the parallelogram Wilson loop made of four lightlike segments (see Figure 4.1c), which was computed in 1992 by Korchemsky and Korchemskaya [146]. It is a highly appealing proposition that[2]

$$f_{\text{eik}} \equiv \gamma_G - 2B_\delta = \frac{\Gamma_\square}{4}\,, \tag{4.1}$$

holds to all orders[3]. The parallelogram Wilson loop, is a very simple object: being compact it has no infrared divergences, so the singularities arise here from short distances, and the calculation can be done directly in dimensional regularisation. Importantly, in contrast to the Drell-Yan soft function described above, real corrections and cut propagators do not arise here. The natural questions to ask then are first, does the relation in (4.1) indeed hold to all orders, and second, can we see how a parallelogram Wilson loop arises from the definitions of the objects on the left-hand side of eq. (4.1), the form factor and the PDF. Establishing this relation is one of the main goals of this chapter.

The amplitude factorisation in eq. (1.20) gives rise to a different Wilson-line configuration, $\mathcal{S}_2$, which is a couple of *semi-infinite* lightlike Wilson lines (with different 4-velocities) meeting at the hard-interaction vertex, see Figure 4.1a. We

[1] An additional displacement of the two cusps in transverse space can be used to resum transverse-momentum logarithms [132]. The corresponding anomalous dimensions can be related to the DY soft function via a conformal transformation [77, 133–135].

[2] Note that we systematically omit the superscript q/g in (4.1) and below, and specify the representation only when needed.

[3] While the two-loop result for $\Gamma_\square$ has been known for a while, we are not aware that the proposition (4.1) was made before. Unfortunately, there is no *direct* three-loop computation of $\Gamma_\square$ available at this point.

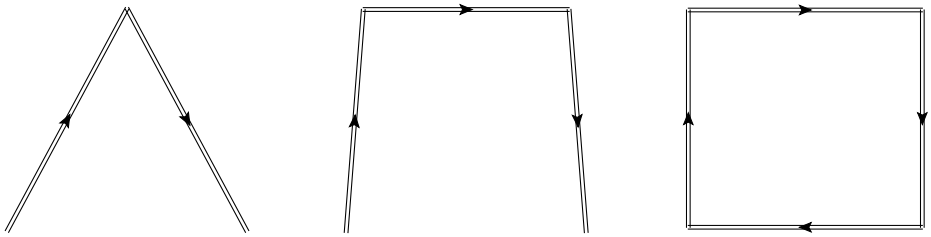

(a) $\wedge$ geometry **(b)** $\sqcap$ geometry **(c)** $\square$ geometry

Figure 4.1: Contours of lightlike Wilson loops that contain semi-infinite Wilson lines, which arise in the factorisation of the form factor (a) and the parton distribution function (b). Contour (c), the parallelogram, which consists of four *finite* lightlike segments, gives rise to the anomalous dimension on the right-hand-side of eq. (4.1).

shall refer to this contour as the $\wedge$ geometry. We emphasise that in contrast with the Drell-Yan soft function described above, where the cross section was considered [21, 136], here the Wilson-line configuration is defined at amplitude level. At a difference with the parallelogram of [146], the $\wedge$ geometry is non-compact, and thus gives rise to infrared divergences, in addition to ultraviolet ones, much like the non-lightlike soft function in Section 1.1. We shall return to the $\wedge$ geometry and its properties below. At this point it suffices to say that considering the infrared factorisation of the form factor, the origin of the relation between $\gamma_G - 2B_\delta$ and the parallelogram geometry remains obscure: the $\wedge$ geometry has no finite segments while the parallelogram consists exclusively of such.

An important step in explaining the eikonal nature of $f_{\rm eik}$ in (1.29), based on the infrared factorisation properties of the form factor and the PDF, was taken in 2008 in a paper by Dixon, Magnea and Sterman [147]. The fundamental explanation is that spin-dependent hard-collinear contributions are common to both γ_G and $2\,B_\delta$ and drop in the difference, leaving behind a purely eikonal component. This is the premise we shall follow. However, ref. [147] relied on the *assumption* that B_δ, as the coefficient of $\delta(1-x)$, is a purely virtual quantity and hence the factorisation of the PDF could be done at "amplitude level". According to the factorisation outlined in [147] the eikonal component of B_δ should correspond to Wilson lines with a $\wedge-$geometry, much like the form factor. Taking this at face value, if the eikonal components of γ_G and B_δ on the right-hand side of (4.1) indeed *both* correspond to the $\wedge-$geometry, one concludes that the $\wedge$ and the $\square$ anomalous dimensions must be proportional to each other, at least through two loops, or, put differently, one may deduce the anomalous dimension of the

$\wedge-$geometry from (1.30).

The first direct two-loop computation of $\wedge-$geometry Wilson loop was performed only in 2015, by Erdogan and Sterman [148]. This calculation is an important step forward also in the sense that it presents a new method for dealing directly with (semi)-infinite lightlike Wilson lines in configuration space (which a priori lead to scaleless integrals) without resorting to an extra regulator. This is done by cleverly using the exponentiation properties and isolating a well-defined integrand, before renormalising ultraviolet divergences by means of a suitable cutoff. We shall adopt and generalise this method in Section 4.4 below. The result of ref. [148] is that the anomalous dimension corresponding to the $\wedge-$geometry Wilson loop is given by

$$\Gamma_\wedge = \left(\frac{\alpha_s}{\pi}\right)^2 C_i \left[C_A \left(\frac{101}{54} - \frac{11}{24}\zeta_2 - \frac{1}{4}\zeta_3\right) + \left(-\frac{14}{27} + \frac{1}{6}\zeta_2\right) T_f n_f\right] + \mathcal{O}(\alpha_s^3), \tag{4.2}$$

where $C_i = C_F$ for Wilson lines in the fundamental representation and C_A for the adjoint. As with $f_{\rm eik}$ and $\Gamma_\wedge$ above, we omit the superscript q/g for $\Gamma_\wedge$ wherever it is not necessary. While the result in (4.2) bears a striking resemblance to $f_{\rm eik}$ in (1.30), it is evidently not identical; the coefficient of the ζ_3 term is entirely different. The authors of ref. [148] further provided a detailed diagrammatic analysis, comparing their calculation to that of the parallelogram in ref. [146], and explaining the origin of the difference in the coefficient of ζ_3 as emanating from endpoint contributions that are present in finite lightlike segments, but are absent in infinite ones. This conclusion can be confirmed by a momentum-space computation.

It is useful to bear in mind that infinite and semi-infinite Wilson-line configurations (but not finite ones!) are of direct relevance to partonic scattering amplitudes in the high-energy limit (the Regge limit) [12–15]. Also, the explicit two-loop combination in (4.2) appeared in the literature in that context long before the computation of the $\wedge$ configuration in ref. [148]. Specifically, considering $gg \to gg$, $qq \to qq$ or $qg \to qg$ scattering in the limit where the centre-of-mass energy is much larger than the momentum transfer, $s \gg -t$, the leading and next-to-leading logarithms in $s/(-t)$ in the (real part of the) amplitude exponentiate according to a simple replacement of the t-channel gluon propagator (dubbed gluon Reggeisation):

$$\frac{1}{t} \to \frac{1}{t}\left(\frac{s}{-t}\right)^{\alpha(t,\epsilon)}, \tag{4.3}$$

where $\alpha(t,\epsilon)$ is the gluon Regge trajectory[4] [150–154] given by:

$$\alpha(t,\epsilon) = \frac{\alpha_s}{\pi}\frac{\gamma_{\rm cusp}^{g\,(1)}}{2\epsilon} + \left(\frac{\alpha_s}{\pi}\right)^2 \frac{1}{4}\left(-\frac{C_A\hat{b}_0}{\epsilon^2} + \frac{\gamma_{\rm cusp}^{g\,(2)}}{\epsilon} + 2\Gamma_\wedge^{g\,(2)} + C_A\hat{b}_0\zeta_2\right) + \mathcal{O}(\alpha_s^3) \quad (4.4)$$

where $\alpha_s = \alpha_s(-t,\epsilon)$, with $\epsilon = (4-d)/2$ the dimensional regularisation parameter, $\hat{b}_0$ is the one-loop QCD beta function of (4.7a), $\gamma_{\rm cusp}^{g\,(n)}$ are the coefficient of the cusp anomalous dimension of eq. (3.35) for the gluon, and $\Gamma_\wedge^{g\,(2)}$ is the two-loop coefficient in eq. (4.2), again with $C_i = C_A$. We further recall that the overall similarity between the parallelogram Wilson loop in [146] and the gluon Regge trajectory in (4.4), as well as the peculiar difference between them in the coefficient of ζ_3, were already observed early on, in ref. [155], where an evolution equation for the Regge trajectory was derived, considering the forward limit of crossed Wilson lines. However, this raises no difficulty: as stressed above, it is the infinite Wilson-line geometry which is expected to be relevant for the factorisation of partonic scattering amplitudes, not the parallelogram.

A real puzzle arises, however, upon considering the explicit result for the $\wedge-$geometry anomalous dimension in eq. (4.2) in view of eq. (1.30), if the conclusion of ref. [147] is taken at face value. Given that the factorisation of the form factor is well understood, and the eikonal component of γ_G is determined by the $\wedge-$geometry, we are compelled to revisit the assumption of ref. [147] that B_δ is a purely virtual quantity, systematically establish the infrared factorisation of the PDFs at large x, and identify the eikonal component of B_δ, which clearly *must not* be proportional to $\Gamma_\wedge$.

We now review the factorisation properties of the form factor and parton distribution function separately.

4.2 Infrared Factorisation of the On-shell Form Factor

Let us first specialise the generic factorisation of massless scattering amplitudes in eq. (1.20) to the case of the QCD colour-singlet on-shell form factor of coloured massless particles (quarks or gluons). Historically this was known before that of

[4] See also a more recent observation in ref. [149] that the two-loop coefficient $\Gamma_\wedge^{g\,(2)}$ occurs also in the QCD impact factor.

the generic case [16, 17, 80, 85, 147, 156]. We label the external momenta by p_1 (incoming) and p_2 (outgoing) with the momentum transfer $Q^2 \equiv -(p_1-p_2)^2$, and, as usual, we renormalise all ultraviolet singularities in the $\overline{\text{MS}}$ scheme, denoting the renormalisation scale by μ^2.

The quark form factor is defined in terms of the electromagnetic vector current, proportional to $\bar{\psi}\gamma_\mu\psi$, which does not renormalise. The gluon form factor in turn is defined using an effective local interaction vertex with the Higgs field, $HG^a_{\mu\nu}G^{\mu\nu a}$, and it does renormalise, proportionally to the QCD beta function [84]. The distinct ultraviolet properties of the quark and gluon form factors will be of little relevance for us: we focus instead on the infrared singularities of the form factor, which have a rather similar structure for massless quarks and gluons.

For large Q^2 the form factor $F\left(Q^2/\mu^2, \alpha_s(\mu^2), \epsilon\right)$ features large logarithms in the ratio Q^2/μ^2, and fixed-order perturbation theory breaks down. These large logarithms can be resummed using a renormalisation-group equation (see e.g. [156]), giving the following all-order formula for the form factor,

$$F\left(1, \alpha_s(Q^2), \epsilon\right) = \exp\left[\frac{1}{2}\int_0^{Q^2}\frac{d\lambda^2}{\lambda^2}\left(G(1, \alpha_s(\lambda^2,\epsilon),\epsilon) - \gamma_{\text{cusp}}(\alpha_s(\lambda^2,\epsilon))\log\frac{Q^2}{\lambda^2}\right)\right], \tag{4.5}$$

where we set the renormalisation scale $\mu^2 = Q^2$ for simplicity. Note that we have absorbed into the function G any operator renormalisation terms — see [84, 85] for more details. Infrared singularities are generated in eq. (4.5) through an integration, from $\lambda^2 = 0$, over the $d = 4 - 2\epsilon$ dimensional running coupling $\alpha_s(\mu^2, \epsilon)$, which obeys

$$\frac{d}{d\ln\mu^2}\left(\frac{\alpha_s(\mu^2,\epsilon)}{\pi}\right) = -\epsilon\left(\frac{\alpha_s(\mu^2,\epsilon)}{\pi}\right) - \sum_{n=0}^{\infty}\hat{b}_n\left(\frac{\alpha_s(\mu^2,\epsilon)}{\pi}\right)^{n+2}. \tag{4.6}$$

We report the coefficients $\hat{b}_0$, $\hat{b}_1$ and $\hat{b}_2$ of the QCD beta function respectively at one [157–160], two [161–164] and three loops [165, 166], because we will use them in the rest of this chapter

$$\hat{b}_0 = \frac{11}{12}C_A - \frac{1}{3}T_f n_f, \tag{4.7a}$$

$$\hat{b}_1 = \frac{17}{24}C_A^2 - \frac{5}{12}C_A T_f n_f - \frac{1}{4}C_F T_f n_f, \tag{4.7b}$$

$$\hat{b}_2 = \frac{2857}{3456}C_A^3 - \frac{1415}{1728}C_A^2 T_f n_f - \frac{205}{576}C_A C_F T_f n_f + \frac{1}{32}C_F^2 T_f n_f + \frac{11}{144}C_F T_f^2 n_f^2 + \frac{79}{864}C_A T_f^2 n_f^2. \tag{4.7c}$$

Equation (4.5) applies for both quarks and gluons, but with distinct functions $\gamma_{\rm cusp}(\alpha_s)$ and $G(Q^2/\mu^2, \alpha_s, \epsilon)$, which do depend on the type of particles (although this is suppressed in our notation). The former, which captures all double poles, depends solely on the colour representation of the particles (fundamental and adjoint for quarks and gluons, respectively) while the latter, which controls single poles, depends also on their spin. This distinction will be crucial in what follows and it is a direct consequence of the fact that $\gamma_{\rm cusp}$ is an eikonal quantity, namely one that can be defined exclusively in terms of Wilson lines, while $G(Q^2/\mu^2, \alpha_s, \epsilon)$ instead, contains hard-collinear effects, which cannot fully be described by Wilson lines. Through three loops, the cusp anomalous dimension, much like other quantities that are defined exclusively in terms of Wilson lines, depends on the colour representation proportionally to the quadratic Casimir C_i, as in (3.35), adhering to the so-called *Casimir scaling* property. Starting at four loops quartic Casimirs, $d_{ij}^{(4)} \equiv d_i^{abcd} d_j^{abcd}$, appear as well, making the dependence of the colour representation more involved. Differently from $\gamma_{\rm cusp}$, the function $G(1, \alpha_s(\lambda^2, \epsilon), \epsilon)$ has an expansion both in α_s and ϵ, as follows

$$G\left(1, \alpha_s\left(\lambda^2, \epsilon\right), \epsilon\right) = \sum_{l=1}^{\infty} \sum_{n=0}^{\infty} G(l, n) \left(\frac{\alpha_s\left(\lambda^2, \epsilon\right)}{\pi}\right)^l \epsilon^n, \tag{4.8}$$

therefore it generates both infrared poles and non-negative powers of ϵ upon integrating over the scale λ^2 of the running coupling as in eq. (4.5). We isolate the divergent contribution order-by-order in α_s, by defining the anomalous dimension γ_G such that

$$\int_0^{\mu^2} \frac{d\lambda^2}{\lambda^2} G(1, \alpha_s(\lambda^2, \epsilon), \epsilon) = \int_0^{\mu^2} \frac{d\lambda^2}{\lambda^2} \left[\gamma_G\left(\alpha_s\left(\lambda^2, \epsilon\right)\right)\right] + \mathcal{O}\left(\epsilon^0\right), \tag{4.9}$$

where γ_G depends on ϵ only through the coupling. Once γ_G is defined, using eq. (4.5) the expression for the infrared poles $\Gamma_2^{\rm ll}$ in eq. (1.25) can be derived. The coefficients γ_G for the quark and for the gluon are well known in the literature; they are referred to sometimes as "collinear anomalous dimensions" and were denoted by $\widetilde{G}$ in [167], by $\mathcal{G}_0$ in [42] and by γ^q and γ^g in appendix I of [18]. The latter has a conventional factor of -2. In practice, we derive here γ_G to four loops by substituting the $d-$dimensional running coupling of eq. (4.6) into eq. (4.9) and

then identifying the singularities arising on the two sides of equation (4.9), getting

$$\begin{aligned}\gamma_G = &\frac{\alpha_s}{\pi} G(1,0) + \left(\frac{\alpha_s}{\pi}\right)^2 \Big[G(2,0) - \hat{b}_0\, G(1,1)\Big] \\ &+ \left(\frac{\alpha_s}{\pi}\right)^3 \Big[G(3,0) - \hat{b}_0\, G(2,1) - \hat{b}_1\, G(1,1) + \hat{b}_0^2\, G(1,2)\Big] \\ &+ \left(\frac{\alpha_s}{\pi}\right)^4 \Big[G(4,0) - \hat{b}_0\, G(3,1) - \hat{b}_1\, G(2,1) - \hat{b}_2\, G(1,1) + \hat{b}_0^2\, G(2,2) \\ &\qquad + 2\hat{b}_0\hat{b}_1\, G(1,2) - \hat{b}_0^3 G(1,3)\Big] + \mathcal{O}\left(\alpha_s^5\right) ,\end{aligned} \tag{4.10}$$

where $G(l,n)$ are defined in eq. (4.8) and their values can be extracted from refs. [84, 85, 137] where the form factors have been computed to three loops. For the purpose of this thesis we only need explicit results for the collinear anomalous dimensions through two loops, which read

$$\begin{aligned}\gamma_G^q = &\left(\frac{\alpha_s}{\pi}\right) \frac{3C_F}{2} + \left(\frac{\alpha_s}{\pi}\right)^2 \left\{ C_A C_F \left(\frac{11}{8}\zeta_2 - \frac{13}{4}\zeta_3 + \frac{961}{432}\right) \right. \\ &\left. + C_F^2 \left(-\frac{3}{2}\zeta_2 + 3\zeta_3 + \frac{3}{16}\right) - C_F T_f n_f \left(\frac{\zeta_2}{2} + \frac{65}{108}\right) \right\} + \mathcal{O}(\alpha_s^3) \\ \gamma_G^g = &\left(\frac{\alpha_s}{\pi}\right) 2\hat{b}_0 + \left(\frac{\alpha_s}{\pi}\right)^2 \left\{ C_A^2 \left(-\frac{11\zeta_2}{24} - \frac{\zeta_3}{4} + \frac{173}{54}\right) \right. \\ &\left. + C_A T_f n_f \left(\frac{\zeta_2}{6} - \frac{32}{27}\right) - \frac{C_F T_f n_f}{2} \right\} + \mathcal{O}(\alpha_s^3) ,\end{aligned} \tag{4.11}$$

where we added superscripts $i = q, g$ to distinguish between quarks and gluons.

4.2.1 Infrared factorisation

We specialise the general factorisation of massless scattering amplitudes in eq. (1.20) to that of the form factor

$$\begin{aligned}F\left(1, \alpha_s(Q^2), \epsilon\right) = &H\left(\frac{Q^2}{\mu^2}, \frac{(2p_i \cdot n_i)^2}{n_i^2 \mu^2}, \alpha_s(\mu^2)\right) \prod_{i=1}^{2} J_i\left(\frac{(2p_i \cdot n_i)^2}{n_i^2 \mu^2}, \alpha_s(\mu^2), \epsilon\right) \\ &\times \left(\frac{\mathcal{S}\left(\beta_1 \cdot \beta_2, \alpha_s(\mu^2), \epsilon\right)}{\prod_{k=1}^{2} \mathcal{J}_i\left(\frac{2(\beta_i \cdot n_i)^2}{n_i^2}, \alpha_s(\mu^2), \epsilon\right)}\right) .\end{aligned} \tag{4.12}$$

The operator definitions for J_i and $\mathcal{J}_i$ are given in eqs. (1.22) and (1.23) respectively and n_i is an auxiliary non-lightlike vector and the dependence on

its choice must cancel in eq. (4.12). The soft function is the two-leg specialisation of eq. (1.5) which for this chapter we simply name $\mathcal{S}$,

$$\mathcal{S}\left(\beta_1 \cdot \beta_2, \alpha_s(\mu^2), \epsilon\right) = \langle 0 | \mathrm{T}\Big[W_{\beta_1}(\infty, 0) W_{\beta_2}(0, \infty)\Big] | 0 \rangle \,, \tag{4.13}$$

and β_i in this context are lightlike lines $\beta_i^2 = 0$. The contour defining $\mathcal{S}$ is shown in Figure 4.1a. As mentioned in the context of the cusp anomalous dimension, one of the properties of eikonal quantities is that they admit Casimir scaling up to three loops; this is a consequence of non-Abelian exponentiation. Beyond three loops there are quartic (and eventually higher order) Casimir contributions, but given that the same Wilson-line diagrams contribute for quarks and gluons, differing just by the representations of the Wilson lines, one expects a relation between these quantities. Indeed, a conjectural relation was proposed in [30] based on partial four-loop computations; we shall return to this in Section 4.5.2 below.

The individual eikonal functions in eqs. (1.23) and (4.13) are heavily constrained by kinematic considerations, such as the dependence on the auxiliary vectors n_i, and by renormalisation group evolution. These constraints can be solved to give explicit formulae [72, 73],

$$\mathcal{J}_i = \exp\left\{ -\frac{1}{4} \int_0^{\mu^2} \frac{d\lambda^2}{\lambda^2} \left(\Gamma_{\mathcal{J}} \left(\alpha_s(\lambda^2, \epsilon) \right) + \gamma_{\text{cusp}}(\alpha_s(\lambda^2, \epsilon)) \log \frac{2(\beta_i \cdot n_i)^2 \mu^2}{n_i^2 \lambda^2} \right) \right\}, \tag{4.14}$$

$$\mathcal{S} = \exp\left\{ -\frac{1}{2} \int_0^{\mu^2} \frac{d\lambda^2}{\lambda^2} \left(\Gamma_{\wedge}(\alpha(\lambda^2, \epsilon)) + \gamma_{\text{cusp}}(\alpha_s(\lambda^2, \epsilon)) \log \left(\frac{\beta_1 \cdot \beta_2 \mu^2}{\lambda^2} \right) \right) \right\}, \tag{4.15}$$

where $\Gamma_{\mathcal{J}}$ and $\Gamma_{\wedge}$ are constants to be determined by direct calculation. Note that $\Gamma_{\wedge}$ was denoted in the literature [147, 148] as $-G_{\text{eik}}$. As in eq. (4.5), the infrared singularities of $\mathcal{J}_i$ and $\mathcal{S}$ are generated by integrating over the d dimensional running coupling $\alpha_s(\lambda^2, \epsilon)$ from $\lambda^2 = 0$. We notice that the soft function and the product of the eikonal jets share the same dependence on $\gamma_{\text{cusp}} \ln \mu^2/\lambda^2$, which is associated with the overlapping soft-collinear singularities of these two quantities. This fact ensures that the ratio $\frac{\mathcal{S}}{\mathcal{J}_1 \mathcal{J}_2}$ is free of overlapping divergences and depends only on the logarithm of the kinematic variable

$$\kappa = \frac{(\beta_1 \cdot \beta_2)^2 \, n_1^2 n_2^2}{4(\beta_1 \cdot n_1)^2 (\beta_2 \cdot n_2)^2}, \tag{4.16}$$

which is insensitive to the normalisation of the vectors β_i in the definition eq. (1.21). Using the factorisation equation eq. (4.12), we determine the partonic jet function by dividing the form factor in eq. (4.5) by the ratio $\frac{\mathcal{S}}{\mathcal{J}_1\mathcal{J}_2}$, yielding

$$J_i = \exp\left\{h_J + \frac{1}{2}\int_{\mu^2}^{p_n^2}\frac{d\lambda^2}{\lambda^2}\gamma_i(\alpha_s(\lambda^2)) + \frac{1}{4}\int_0^{p_n^2}\frac{d\lambda^2}{\lambda^2}\bigg(-\gamma_{\rm cusp}(\alpha_s(\lambda^2,\epsilon))\log\left(\frac{p_n^2}{\lambda^2}\right) + \Gamma_\wedge(\alpha_s(\lambda^2,\epsilon)) - \Gamma_{\mathcal{J}}(\alpha_s(\lambda^2,\epsilon)) + G(1,\alpha_s(\lambda^2,\epsilon),\epsilon)\bigg)\right\}, \tag{4.17}$$

where we introduced the variable $p_n^2 = \frac{(2p\cdot n)^2}{n^2}$. The function $h_J \equiv h_J(\alpha_s(p_n^2))$ is a matching coefficient that captures the finite parts of the jet function and γ_i, with $i = q$ for the quark and $i = g$ for the gluon, is the anomalous dimension of the field i in axial gauge. The latter is only concerned with the ultraviolet behaviour of the jet function and indeed it is not associated with any IR pole, because the contribution from the IR region $\lambda^2 \simeq 0$ is absent in the second term of eq. (4.17). All the IR poles of the form factor are generated by the second integral in the equation above, involving the anomalous dimensions $\gamma_{\rm cusp}$, $\Gamma_\wedge$, $\Gamma_{\mathcal{J}}$ and the resummation function $G(1,\alpha_s,\epsilon)$. The dependence on $\gamma_{\rm cusp}$ is such that the combination with $\frac{\mathcal{S}}{\mathcal{J}_1\mathcal{J}_2}$ reconstructs the kinematic dependence of the form factor eq. (4.5) through

$$2\log\left(\frac{Q^2}{\lambda^2}\right) = \log(\kappa) + \log\left(\frac{p_{n_1}^2}{\lambda^2}\right) + \log\left(\frac{p_{n_2}^2}{\lambda^2}\right). \tag{4.18}$$

4.2.2 Isolating hard-collinear singularities

The contribution of $\Gamma_{\mathcal{J}}$ in eq. (4.17) is associated to the soft singularities of J_i, which cancel in the ratio of J_i and $\mathcal{J}_i$ eq. (4.12). It is therefore convenient to focus on the poles of pure hard-collinear origin, defined as

$$J_{i/\mathcal{J}} \equiv \frac{J_i|_{\rm pole}}{\mathcal{J}_i}, \tag{4.19}$$

where $J_i|_{\rm pole}$ means only the poles of the jet function. We extract the function $J_{i/\mathcal{J}}$ for $i = q$ and $i = g$ from the form factor of the quark and of the gluon, respectively, thus providing the *process-independent* components containing the purely collinear singularities associated with massless external partons. In order to determine $J_{i/\mathcal{J}}$, we isolate the pole part of the jet function J_i, by replacing in eq. (4.17) the function $G(1,\alpha_s,\epsilon)$ with γ_G, according to the definition in eq. (4.9),

and we get the ratio

$$\begin{aligned}
&\log\left(\frac{J_i|_{\text{pole}}}{\mathcal{J}_i}\right)\\
=&\frac{1}{4}\int_0^{\mu^2}\frac{d\lambda^2}{\lambda^2}\left(\gamma_G(\alpha_s(\lambda^2,\epsilon))+\Gamma_\wedge(\alpha_s\left(\lambda^2,\epsilon\right))-\gamma_{\text{cusp}}\log\left(\frac{2(p_i\cdot n_i)^2}{(\beta_i\cdot n_i)^2\mu^2}\right)\right)\\
\equiv&\frac{1}{2}\int_0^{\mu^2}\frac{d\lambda^2}{\lambda^2}\left[\gamma_{J/\mathcal{J}}(\alpha_s(\lambda^2,\epsilon))-\frac{\gamma_{\text{cusp}}(\alpha_s(\lambda^2,\epsilon))}{2}\log\left(\frac{2(p_i\cdot n_i)^2}{(\beta_i\cdot n_i)^2\mu^2}\right)\right],
\end{aligned}\tag{4.20}$$

where on the last line we have defined the anomalous dimension $\gamma_{J/\mathcal{J}}$

$$2\gamma_{J/\mathcal{J}}=\gamma_G+\Gamma_\wedge.\tag{4.21}$$

As mentioned above, the collinear anomalous dimension γ_G is known to three loops [84, 85, 137] for both quarks and gluons, and we quoted the corresponding expressions through two loops in eq. (4.11). The anomalous dimension $\Gamma_\wedge$, in turn, is derived from the renormalisation of the soft function $\mathcal{S}$, that can be read off eq. (4.15)

$$\mu\frac{d}{d\mu}\log\mathcal{S}=-\int_0^{\mu^2}\frac{d\lambda^2}{\lambda^2}\gamma_{\text{cusp}}\left(\alpha_s(\lambda^2)\right)-\left[\Gamma_\wedge\left(\alpha_s(\mu^2)\right)+\gamma_{\text{cusp}}(\alpha_s(\mu^2))\log(\beta_1\cdot\beta_2)\right].\tag{4.22}$$

The equation above clarifies the meaning of the subscript $\wedge$, which symbolises the contour of the lightlike Wilson loop in the definition of the soft function in eq. (4.13) that defines $\Gamma_\wedge$. This notation will be used throughout this chapter and it will be generalised for different contours. $\Gamma_\wedge$ is known to two loops [148] by direct computation of the equation above

$$\Gamma_\wedge=\left(\frac{\alpha_s}{\pi}\right)^2\frac{C_i}{4}\left(-2\hat{b}_0\zeta_2-\frac{56}{27}T_f n_f+C_A\left[\frac{202}{27}-\zeta_3\right]\right)+\mathcal{O}(\alpha_s^3),\tag{4.23}$$

where C_i is the quadratic Casimir dependent on the representation of the Wilson lines in eq. (4.13). Using the results in eqs. (4.11) and (4.23) we determine $\gamma_{J/\mathcal{J}}$ to two loops. First for quarks we have

$$\begin{aligned}
\gamma^q_{J/\mathcal{J}}=&\left(\frac{\alpha_s}{\pi}\right)\frac{3C_F}{4}+\left(\frac{\alpha_s}{\pi}\right)^2\left\{C_AC_F\left(\frac{11\zeta_2}{24}-\frac{7\zeta_3}{4}+\frac{1769}{864}\right)\right.\\
&\left.+C_F^2\left(-\frac{3\zeta_2}{4}+\frac{3\zeta_3}{2}+\frac{3}{32}\right)-C_FT_fn_f\left(\frac{\zeta_2}{6}+\frac{121}{216}\right)\right\}+\mathcal{O}(\alpha_s^3).
\end{aligned}\tag{4.24}$$

Then for gluons,

$$\gamma^g_{J/\mathcal{J}} = \left(\frac{\alpha_s}{\pi}\right)\hat{b}_0 + \left(\frac{\alpha_s}{\pi}\right)^2 \left\{ C_A^2 \left(-\frac{11\zeta_2}{24} - \frac{\zeta_3}{4} + \frac{137}{54} \right) + C_A T_f n_f \left(\frac{\zeta_2}{6} - \frac{23}{27} \right) - \frac{C_F T_f n_f}{4} \right\} + \mathcal{O}(\alpha_s^3). \quad (4.25)$$

We have thus isolated the hard-collinear singularities of the form factor and found the quantity $\gamma_{J/\mathcal{J}}$ that governs this behaviour for quark and for gluons according to eq. (4.20). We emphasises that in contrast to the conventional collinear anomalous dimension γ_G given in eq. (4.11), which is specific to the form factor (recall eqs. (4.9) and (4.5)), the hard-collinear anomalous dimension $\gamma_{J/\mathcal{J}}$ defined here is *process independent*. This universality will now be put to use. In the next section we will consider the factorisation of parton distribution functions (PDFs) at large x where we will use the above two-loop results for $\gamma^q_{J/\mathcal{J}}$ and $\gamma^g_{J/\mathcal{J}}$ given in eqs. (4.24) and (4.25) respectively, and ultimately identify the eikonal anomalous dimension relevant to the PDF evolution.

4.3 Parton Distribution Functions at Large x

Parton distribution functions, $f_{AB}(x)$, describe the probability of finding parton A with momentum fraction x inside hadron (or parton) B. We will be interested here in PDF *evolution*, which is the same for the partonic and for the hadronic quantities, and will therefore consider partonic PDFs. PDFs are inherently defined at *cross-section* level with the need to combine real and virtual radiation to cancel soft singularities such that only pure collinear singularities associated with the massless initial-state parton are kept. We will see that in the elastic limit, $x \to 1$, the contributions from different regions factorise and claim that the hard-collinear behaviour of the initial-state partons is described by $\gamma_{J/\mathcal{J}}$, the same anomalous dimension we identified in the factorisation of the form factor.

4.3.1 Definition

The light-cone PDF for a quark (gluon) in a parton P of momentum p with longitudinal momentum fraction x is given by [168]

$$f_{qP}^{\text{bare}}(x,\epsilon) = \frac{1}{2}\int \frac{dy}{2\pi} e^{-iyxp\cdot u} \langle P|\bar{\psi}_q(yu)\gamma\cdot u W_u(y,0)\psi_q(0)|P\rangle \tag{4.26}$$

$$f_{gP}^{\text{bare}}(x,\epsilon) = \frac{1}{xp\cdot u}\int \frac{dy}{2\pi} e^{-iyxp\cdot u} \langle P|G_{\mu+}(yu)W_u(y,0)G^{+\mu}(0)|P\rangle\,. \tag{4.27}$$

The Wilson-line operator W_u is defined in eq. (1.6) and $|P\rangle$ is either an on-shell quark or gluon, $P = q, g$. We take the lightlike momentum p to be in the $(+)$ direction and then the velocity four-vector u is in the $(-)$ direction. It is worthwhile noting here that the bare PDFs $f_{j'j}^{\text{bare}}(x,\epsilon)$ are scaleless. This will be used later in the context of factorisation. They are renormalised through a convolution,

$$f_{jk}(x,\mu) = \sum_{j'}\int_x^1 \frac{dz}{z} Z_{jj'}(z,\alpha_s,\epsilon) f_{j'k}^{\text{bare}}(x/z,\epsilon), \tag{4.28}$$

where $Z_{jj'}$ is a renormalisation factor, removing the UV divergences from the bare PDF in the $\overline{\text{MS}}$ scheme and f_{jk} is the renormalised PDF. From $Z_{jj'}(x,\alpha_s,\epsilon)$ we can get the splitting functions,

$$\frac{d}{d\log\mu} Z_{jk}(x,\alpha_s,\epsilon) = 2\sum_{j'}\int_x^1 \frac{dz}{z} P_{jj'}(z,\alpha_s) Z_{j'k}(x/z,\alpha_s,\epsilon). \tag{4.29}$$

The RG evolution of the PDFs is governed by the DGLAP equations [81–83]:

$$\frac{d}{d\log\mu} f_{jk}(x,\mu) = 2\sum_{j'}\int_x^1 \frac{dz}{z} P_{jj'}(z,\alpha_s) f_{j'k}(x/z,\mu). \tag{4.30}$$

The DGLAP splitting kernels P_{jk} are known to three loops [19, 83, 138–145, 169–172] with some recent results at four loops [26, 28, 30].

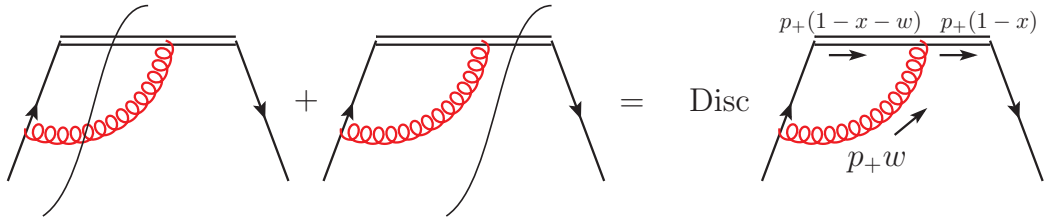

Figure 4.2: The vertex correction for the one-loop quark PDF. The left-hand side is the standard sum over cuts equating to the discontinuity of the amplitude. The double line is the Wilson line while the solid black line is a quark.

4.3.2 Perturbative calculation at large x

In the limit $x \to 1$ the diagonal terms in the splitting functions, P_{qq} and P_{gg}, feature divergent contributions [86, 173–175], namely

$$P_{ii} = \frac{\gamma_{\text{cusp}}}{(1-x)_+} + B_\delta^{(i)}\,\delta(1-x) \;+\; \mathcal{O}\left(\log(1-x)\right), \tag{4.31}$$

where the label $i = q, g$ indicates quarks and gluons, respectively, and the plus distribution is defined as usual, see e.g. [83].

The splitting functions are determined from the UV singularities of the PDFs defined in eqs. (4.26) and (4.27), which can be computed perturbatively. We can relate these definitions to time-ordered products by the discontinuity in x,

$$f_{qq}^{\text{bare}}(x,\epsilon) = \text{Disc}_x \frac{1}{2}\int \frac{dy}{2\pi} e^{-iyxp\cdot u}\,\langle p|T\left[\bar{\psi}_q(yu)\gamma\cdot u W_u(y,0)\psi_q(0)\right]|p\rangle\,. \tag{4.32}$$

This relation, which is illustrated diagrammatically in Figure 4.2, can be derived as follows. One first splits the Wilson line in eq. (4.26) into two Wilson lines that extend to infinity, $W_u(y,\infty)W_u(\infty,0)$, one then inserts a complete set of states between them and finally identifies the result as the discontinuity of the time-ordered product. This relies on the fact that the condition $x \leq 1$ selects the cuts with positive energy [17, 176]. One can think that the coefficient B_δ in eq. (4.31) is entirely determined by the contribution of the virtual diagrams, such as the second term in the left-handside in Figure 4.2, however the explicit calculation will lead to a different conclusion.

At one loop, the relevant diagram is shown in the right-hand side of Figure 4.2, which in Feynman gauge reads

$$f_{qq}^{\text{fig.1}} = \text{Disc}\frac{g_s^2}{\pi}C_F \int \frac{d^dq}{(2\pi)^d}\frac{p_+(p_+-q_+)}{(q^2)\left((p-q)^2\right)\left((p-k)\cdot u\right)\left((p-k-q)\cdot u\right)} \tag{4.33}$$

where we used p and k respectively to denote the incoming and outgoing quark momenta, and q the gluon momentum. For brevity, we also drop the superscript bare and the $+i0$ prescription on each propagator. It is straightforward to compute the integral over q_- by complex analysis. This places a bound on q_+ i.e. $p_+ > q_+ > 0$. The q_T integral is scaleless but as we are interested only in the UV divergence it is simply a matter of replacing,

$$\int \frac{d^{d-2}q_T}{(2\pi)^{d-2}} \frac{1}{q_T^2} \to \frac{e^{\epsilon\gamma_E}}{(4\pi)^{1-\epsilon}} \frac{1}{\epsilon}. \tag{4.34}$$

We then scale out p_+ by defining $q_+ = p_+ w$ to produce an elegant integral representation,

$$f_{qq}^{\text{fig.1}} = \text{Disc}\ \frac{i\alpha_s}{\pi} C_F \frac{1}{4\pi} \frac{1}{\epsilon} \int_0^1 dw \frac{1-w}{(1-x+i0)(1-x-w+i0)}, \tag{4.35}$$

where we have absorbed the $(e^{\gamma_E} 4\pi)^\epsilon$ factors in the $\overline{\text{MS}}$ coupling and reinstated the $+i0$ prescription. The representation in eq. (4.35) has the advantage of compactly displaying the sum over cuts: individual cuts can be isolated by computing the residues corresponding to each of the propagator poles. Using partial fractioning,

$$\frac{1}{1-x+i0} \frac{1}{1-x-w+i0} = \frac{1}{w} \left(\frac{1}{1-x-w+i0} - \frac{1}{1-x+i0} \right) \tag{4.36}$$

so the full discontinuity of the integrand equals,

$$\text{Disc} \frac{1}{1-x+i0} \frac{1}{1-x-w+i0} = \frac{1}{w} (-2\pi i) \left(\delta(1-x-w) - \delta(1-x) \right) \tag{4.37}$$

and we find

$$f_{qq}^{\text{fig.1}} = \frac{\alpha_s}{2\pi} \frac{C_F}{\epsilon} \left(\frac{x}{1-x} - \delta(1-x) \int_0^1 dw \frac{1-w}{w} \right). \tag{4.38}$$

Here the first term is a real emission cut, while the second, a virtual correction. As usual, the endpoint divergence in the first term is combined with the divergence as $w \to 0$ in the second to give,

$$f_{qq}^{\text{fig. 1}} = \frac{\alpha_s}{4\pi} C_F \frac{1}{\epsilon} \left(\frac{2}{(1-x)_+} + 2\delta(1-x) - 2 \right). \tag{4.39}$$

We emphasise that it is ambiguous to determine which cuts have contributed to the $\delta(1-x)$ term, as its coefficient is only finite after the cancellation of the soft

divergences between the real and the virtual cuts.

We combine eq. (4.39) with the mirror diagram representing the correction of the right vertex, which yields an identical result, and with the box-type diagram, which does not contribute to divergent terms at large x. We complete the calculation of the (bare) PDF by including the two diagrams featuring radiative corrections on the external legs

$$f_{qq}^{\text{SE}} = (Z_2 - 1)\,\delta(1-x) = -\frac{\alpha_s}{4\pi\epsilon} C_F\,\delta(1-x), \tag{4.40}$$

where we used the wavefunction renormalisation Z_2 at one loop. The expression of the UV singularities of the bare PDF at one loop reads

$$f_{qq}^{\text{bare}} = \delta(1-x) + \frac{\alpha_s(\mu^2)}{4\pi\epsilon} C_F \left(\frac{4}{(1-x)_+} + 3\delta(1-x) + \mathcal{O}((1-x)^0) \right) + \mathcal{O}(\alpha_s^2). \tag{4.41}$$

Following eq. (4.28), we derive the renormalisation factor Z_{qq} that cancels the ultraviolet divergence in the equation above

$$Z_{qq} = \delta(1-x) - \frac{\alpha_s(\mu^2)}{4\pi\epsilon} C_F \left(\frac{4}{(1-x)_+} + 3\delta(1-x) + \mathcal{O}((1-x)^0) \right) + \mathcal{O}(\alpha_s^2). \tag{4.42}$$

Finally, we obtain the splitting function by computing the derivative with respect to the renormalisation scale eq. (4.30), which yields the well-known result for the qq splitting function

$$P_{qq}(x) = \frac{\alpha_s}{4\pi} C_F \left(\frac{4}{(1-x)_+} + 3\delta(1-x) + \mathcal{O}((1-x)^0) \right) + \mathcal{O}(\alpha_s^2). \tag{4.43}$$

The one-loop calculation with on-shell states is straightforward but at two loops and beyond it becomes complicated to disentangle the UV from the IR in the transverse integrals. To regularise the IR we can take the initial states to be off-shell $p^2 \neq 0$. The intermediate expressions become more verbose but introduce no major conceptual issues. As the states are now unphysical the correlators become gauge dependent. It means that the running of the gauge parameter, $\xi \to Z_A \xi$ has to be taken into account in $\mathcal{O}(\epsilon^0)$ finite terms. A similar observation was made in [33]. Using this method we are able to arrive at the integral representation similar to eq. (4.35) for each two-loop diagram. For two loops it is a two parameter integral with integrals over the plus component of the two loop momenta. As an

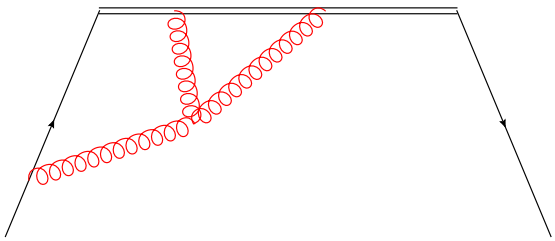

Figure 4.3: The diagram $f_{qq}^{(2),(e)}$.

example, the diagram in Figure 4.3 can be represented as

$$f_{qq}^{(2),(e)} = \text{Disc}\frac{i}{2\pi}C_A C_F \frac{\Gamma(\epsilon)\Gamma(2\epsilon)}{\Gamma(1+\epsilon)} \int_0^1 dydz\, y^{1-2\epsilon}(1-y)^{1-\epsilon}(1-z)^{-\epsilon}z^{-\epsilon} \times \frac{1-2z}{(1-x+i0)(1-x-y+i0)(1-x-yz+i0)}. \quad (4.44)$$

The three denominators correspond to the three Wilson-line propagators after integration over the $(-)$ and transverse components of the two loop momenta. We distinguish the contribution of the real emission and the ones of the virtual corrections by applying partial fractioning as in eq. (4.36). The discontinuity of the first propagator in eq. (4.44) is proportional to $\delta(1-x)$ and it determines the virtual contribution. The other two propagators in eq. (4.44) correspond to real emissions. Each term features infrared divergences, which cancel in the sum of all cuts. Furthermore, we notice that the real emission cuts yield UV poles that are proportional to $\delta(1-x)$ and therefore contribute to the P_{qq} splitting function. This particular calculation is detailed in Appendix C.1, where we also present the full two-loop results for quarks and gluons, diagram by diagram.

Our final result for the splitting functions eqs. (C.19) and (C.22) reproduces the known results [83, 138–145, 169–171]. These previous splitting function calculations have been performed using different methods, including extracting them from corresponding deep inelastic structure-function calculations [145], by means of the operator product expansion [138–141, 144, 169–171], by means of light-cone axial gauge [177,178], or by relating them to splitting amplitudes [179]. To our knowledge, our direct calculation is the first of its kind. This method has the advantage to show that not all the diagrams contribute to the singular behaviour of the splitting functions in eq. (4.31) and that the coefficient B_δ includes both the virtual and the real corrections.

4.3.3 Factorisation

As $x \to 1$ the momentum of the final-state parton tends to the initial-state one, meaning that the contribution from soft gluon radiation dominates. It then implies a factorisation of the renormalised PDFs at large x, allowing us to separate the hard-collinear divergences from the soft divergences [86,180]. In the following we shall only consider diagonal splitting functions and since the formulae apply to both quarks and gluons we shall drop the subscript jj on the partonic PDF and related quantities and only specialise when needed. To factorise the PDFs we shall transform into Mellin space,

$$\tilde{f}(N) = \int_0^1 dx x^{N-1} f(x), \tag{4.45}$$

where convolutions become products. In this space the divergent terms become,

$$\delta(1-x) \to 1 \qquad\qquad \frac{1}{(1-x)_+} \to -\log N - \gamma_E \,. \tag{4.46}$$

The large-x limit corresponds to the large-N limit. The factorisation works in much the same way as the form factor by defining two jet functions and two corresponding eikonal jet functions along with a soft function [86,180],

$$\tilde{f}(N,\mu) = H\left(\frac{(2p\cdot n)^2}{n^2\mu^2}, \alpha_s(\mu^2)\right) \prod_{i=L,R} \frac{J_i\left(\frac{(2p\cdot n)^2}{n^2\mu^2}, \alpha_s(\mu^2), \epsilon\right)}{\mathcal{J}_i\left(\frac{(2\beta\cdot n)^2}{n^2}, \alpha_s(\mu^2), \epsilon\right)} \times \tilde{S}_{\sqcap}\left(N, \frac{\beta\cdot u\mu}{p\cdot u}, \alpha_s(\mu^2), \epsilon\right) + \mathcal{O}\left(\frac{\log N}{N}\right) \tag{4.47}$$

where the four-velocity β is in the p direction and L and R indicate which side of the cut the jet functions are (see Figure 4.2). The renormalised parton distribution functions are defined as pure counterterms in minimal subtraction schemes, because they can only depend on the factorisation scale. Since the hard function H and the jet functions J_i are the only functions with finite terms it must mean that their non-divergent terms cancel such that eq. (4.47) contains

only poles,

$$\tilde{f}(N,\mu) = \left(\prod_{i=L,R} \frac{J_i\left(\frac{(2p\cdot n)^2}{n^2\mu^2}, \alpha_s(\mu^2), \epsilon\right)\Big|_{\text{pole}}}{\mathcal{J}_i\left(\frac{(2\beta\cdot n)^2}{n^2}, \alpha_s(\mu^2), \epsilon\right)} \right) \tilde{S}_{\sqcap}\left(N, \frac{\beta\cdot u\mu}{p\cdot u}, \alpha_s(\mu^2), \epsilon\right) + \mathcal{O}\left(\frac{\log N}{N}\right) \tag{4.48}$$

where $J|_{\text{pole}}$ has the same meaning as in eq. (4.19), that it is only the poles of the jet function. As in the case of the form factor, the soft function $\tilde{S}_{\sqcap}$ resums the emission of gluons with vanishing momenta in the eikonal approximation. We shall shortly see however that while its ultraviolet behaviour is qualitatively the same as that of the form-factor soft function in eq. (4.13), its infrared behaviour is qualitatively different, as it presents only single poles.

The function $\tilde{S}_{\sqcap}$ is defined by the Mellin transform of the $x-$space soft function

$$S_{\sqcap}\left(x, \frac{\beta\cdot u\mu}{p\cdot u}, \alpha_s(\mu^2), \epsilon\right) = (p\cdot u)\int \frac{dy}{2\pi}\, e^{iy(1-x)\,p\cdot u}\, W_{\sqcap}\left(\beta\cdot\, uy\mu, \alpha_s(\mu^2), \epsilon\right), \tag{4.49}$$

where $W_{\sqcap}$ is the Wilson loop with $\sqcap-$shaped contour, see Figure 4.1b (in ref. [86] it is defined in the axial gauge),

$$W_{\sqcap}\left(\beta\cdot u\, y\mu, \alpha_s(\mu^2), \epsilon\right) \equiv \langle 0|T\left[W_\beta(+\infty, y) W_u(y,0) W_\beta(0,-\infty)\right]|0\rangle\,. \tag{4.50}$$

Note that the time-ordering operation here acts on the product of the three Wilson lines together. The soft function can be written in this way, despite coming from a cross-section definition because of the particular relation between path-ordering and time-ordering [173].

The definition (4.49) determines two important properties concerning the analytic structure of $W_{\sqcap}$, as argued in [173]. First of all, the soft function has support in the physical region with $x \leq 1$ only if the singularities of $W_{\sqcap}$ are located on the positive imaginary axis in the complex $y-$plane. Indeed, if this is the case, for $x > 1$ we can close the integration contour in y in eq. (4.49) through the lower half-plane getting a vanishing result. Furthermore, the reality of the soft function implies that $W_{\sqcap}$ is unchanged by the transformation $y \to -y$ followed by complex conjugation. Both these conditions are satisfied if $W_{\sqcap}$ is a holomorphic function

in the variable

$$\rho(y) \equiv i(u \cdot \beta\, y - i0) = (\rho(-y))^* \,. \tag{4.51}$$

In Section 4.4 we show that we can write the renormalised $W_\sqcap$ as,

$$\log W_\sqcap = -\frac{1}{2}\int_0^{\mu^2} \frac{d\lambda^2}{\lambda^2}\left\{2\gamma_{\rm cusp}(\alpha_s\left(\lambda^2,\epsilon\right))\log\left(\frac{\rho(y)\mu}{\sqrt{2}}\right) + \Gamma_\sqcap(\alpha_s\left(\lambda^2,\epsilon\right))\right\}, \tag{4.52}$$

where the factor $\sqrt{2}$ was introduced in order to identify μ as the $\overline{\rm MS}$ renormalisation scale. The quantity $\Gamma_\sqcap$ will admit Casimir scaling to three loops and the scaling is determined by the representation of the Wilson lines in eq. (4.50). Following ref. [173], the soft function $\tilde{S}$ in the limit of large N, which is conjugate to the behaviour of $W_\sqcap$ at large y through the Fourier transform in eq. (4.49), is obtained to leading power in N by replacing $y \to -iN$ in eq. (4.52), which leads to

$$\begin{aligned}\log \tilde{S}_\sqcap = &-\frac{1}{2}\int_0^{\mu^2} \frac{d\lambda^2}{\lambda^2}\left\{2\gamma_{\rm cusp}(\alpha_s\left(\lambda^2,\epsilon\right))\log\left(\frac{N\mu\beta\cdot u}{\sqrt{2}p\cdot u}\right) + \Gamma_\sqcap(\alpha_s\left(\lambda^2,\epsilon\right))\right\} \\ &+ \mathcal{O}\left(\frac{\log N}{N}\right)\end{aligned} \tag{4.53}$$

so that $\tilde{S}_\sqcap$ admits the following evolution equation

$$\begin{aligned}\mu\frac{d}{d\mu}\log\tilde{S}_\sqcap = &-2\gamma_{\rm cusp}\left(\alpha_s\left(\mu^2\right)\right)\log\left(N\mu\frac{\beta\cdot u}{\sqrt{2}p\cdot u}\right) - \Gamma_\sqcap\left(\alpha_s\left(\mu^2\right)\right) \\ &- \int_0^{\mu^2}\frac{d\lambda^2}{\lambda^2}\gamma_{\rm cusp}\left(\alpha_s\left(\lambda^2,\epsilon\right)\right) + \mathcal{O}\left(\frac{\log N}{N}\right).\end{aligned} \tag{4.54}$$

Note that the UV behaviour of $\tilde{S}_\sqcap$ is *double* logarithmic: the right-hand side of eq. (4.54) is dominated by $\gamma_{\rm cusp}(\alpha_s(\mu^2))\log\mu^2$ and therefore it has the same UV behaviour as the one of the form-factor soft function $\mathcal{S}$ in eq. (4.15). However, in contrast with eq. (4.15), the argument of the logarithm in eq. (4.53) is independent of λ and thus the IR behaviour in eq. (4.54) is *single* logarithmic. Of course, it must be so also in view of eq. (4.48): there both the renormalised PDF on the left-hand side and the hard-collinear factor $J|_{\rm pole}/\mathcal{J}$ feature single poles. The distinct UV and IR behaviour in $\tilde{S}_\sqcap$ is associated to the presence of a length scale y in the definition of the soft function eq. (4.49). The soft function of the form factor does not involve any scale and therefore eq. (4.15) has double logarithmic behaviour both in the UV and in the IR.

As before with the form factor, we seek to isolate the hard-collinear and the purely soft contributions from the Mellin transform (4.45) of the splitting functions in eq. (4.29), $\tilde{P}(N,\alpha_s)$. The following argument is in the spirit of [147]. As mentioned earlier, the bare PDFs $\tilde{f}^{\text{bare}}(N,\epsilon)$ formally vanish because they are scaleless in dimensional regularisation [181]. They feature UV divergences which are renormalised by the splitting functions $\tilde{P}(N,\alpha_s)$ through $\tilde{Z}(N,\alpha_s,\epsilon)$, see eq. (4.28). They are also infrared divergent because there are massless on-shell incoming partons. The IR divergences are the same as in the renormalised PDFs described by eq. (4.48). In perturbation theory it must mean that in $\tilde{f}^{\text{bare}}(N,\epsilon)$ the IR poles match the UV poles. In a minimal subtraction scheme the factor Z in eq. (4.28) consists of only poles. We are then able to construct $\tilde{f}^{\text{bare}}(N,\epsilon)$ in a way that separates the UV from the IR,

$$\tilde{f}^{\text{bare}}(N) = \underbrace{\tilde{Z}(N)^{-1}}_{\text{UV}} \underbrace{\left\{ \left(\prod_{i=L,R} \frac{J_i|_{\text{pole}}}{\mathcal{J}_i} \right) \tilde{S}_{\sqcap}(N) + \mathcal{O}\left(\frac{\log N}{N}\right) \right\}}_{\text{IR}}, \tag{4.55}$$

where we have suppressed the dependence on α_s, the renormalisation scale μ, the kinematic dependence of the functions and ϵ. Let us now consider the logarithm of both sides of eq. (4.55) and compute the derivative with respect to $\log(\mu)$, using the evolution equation for the ratio of jet functions in eq. (4.20). The terms of the form

$$\int_0^{\mu^2} \frac{d\lambda^2}{\lambda^2} \gamma_{\text{cusp}}\left(\alpha_s\left(\lambda^2,\epsilon\right)\right), \tag{4.56}$$

cancel between $\mu\frac{d}{d\mu}\log\tilde{S}_{\sqcap}$ and $\mu\frac{d}{d\mu}\log\frac{J}{\mathcal{J}}$. The bare PDFs do not depend on the renormalisation scale so by using eqs. (4.54), (4.30), and (4.20) we get,

$$\begin{aligned} 0 &= \mu\frac{d}{d\mu}\log\tilde{f}^{\text{bare}}(N) \\ &= -2\tilde{P}(N) + 2\gamma_{J/\mathcal{J}} - 2\gamma_{\text{cusp}}\log\left(\frac{\sqrt{2}p\cdot n}{\beta\cdot n}\frac{\beta\cdot u}{\sqrt{2}p\cdot u}N\right) - \Gamma_{\sqcap} + \mathcal{O}\left(\frac{\log N}{N}\right) \end{aligned} \tag{4.57}$$

The kinematic dependence in the argument of the logarithm cancels upon identifying $\frac{p\cdot n}{\beta\cdot n} = \frac{p\cdot u}{\beta\cdot u} = \frac{p^+}{\beta^+}$. We now require the Mellin transform of eq. (4.31) at large N [86, 173–175],

$$\tilde{P}(N) = -\gamma_{\text{cusp}}\log N + B_\delta + \mathcal{O}\left(\frac{\log N}{N}\right). \tag{4.58}$$

Substituting this into eq. (4.57) the dependence on γ_{cusp} drops. This shows that the factor $\sqrt{2}$ present in eq. (4.52) is indeed necessary for μ to be identified as $\overline{\text{MS}}$ scale. Comparing the non-logarithmic terms in eqs. (4.57) and (4.58) we finally arrive at the relation,

$$2B_\delta = 2\gamma_{J/\mathcal{J}} - \Gamma_\sqcap. \tag{4.59}$$

The above equation mirrors the form factor equation for γ_G in eq. (4.21). In both equations the same hard-collinear anomalous dimension $\gamma_{J/\mathcal{J}}$ is present. We now proceed to use its universality to extract $\Gamma_\sqcap$ at two loops from the above equation. As in the form factor case to specialise to quarks or gluons we simply add a superscript $i = q, g$. Up to two loops the expressions for B_δ may be read off the results in eq. (C.19) and eq. (C.22) of the calculation in the appendix, in agreement with refs. [138–145]. They read

$$\begin{aligned}
B_\delta^q &= \left(\frac{\alpha_s}{\pi}\right)\frac{3}{4}C_F + \left(\frac{\alpha_s}{\pi}\right)^2\left\{C_A C_F\left(\frac{11\zeta_2}{12} - \frac{3\zeta_3}{4} + \frac{17}{96}\right)\right. \\
&\quad \left. + C_F^2\left(-\frac{3\zeta_2}{4} + \frac{3\zeta_3}{2} + \frac{3}{32}\right) - C_F T_f n_f\left(\frac{\zeta_2}{3} + \frac{1}{24}\right)\right\} + \mathcal{O}(\alpha_s^3), \\
B_\delta^g &= \left(\frac{\alpha_s}{\pi}\right)\hat{b}_0 + \left(\frac{\alpha_s}{\pi}\right)^2\left\{C_A^2\left(\frac{3\zeta_3}{4} + \frac{2}{3}\right) - \frac{C_A T_f n_f}{3} - \frac{C_F T_f n_f}{4}\right\} + \mathcal{O}(\alpha_s^3).
\end{aligned} \tag{4.60}$$

Substituting these results into eq. (4.59) along with the values of $\gamma^i_{J/\mathcal{J}}$ calculated in eq. (4.24) and eq. (4.25) we arrive at the *same quantity* for $\Gamma_\sqcap$ for quarks and gluons up to an overall Casimir scaling:

$$\Gamma_\sqcap = \left(\frac{\alpha_s}{\pi}\right)^2\left\{\frac{C_i}{2}\left(-2\hat{b}_0\zeta_2 - \frac{56}{27}T_f n_f + C_A\left[\frac{202}{27} - 4\zeta_3\right]\right)\right\} + \mathcal{O}(\alpha_s^3). \tag{4.61}$$

The fact that Casimir scaling is recovered is expected of course, as this quantity is defined by Wilson lines. Nevertheless, recovering it by subtracting non-eikonal quantities is a non-trivial consistency check. It is worthwhile noting that only the ζ_3 term is different between $\frac{\Gamma_\sqcap}{2}$ and $\Gamma_\wedge$ in eq. (4.23). The factor of two is present because there are two cusp contributions for the $\sqcap$ contour as opposed to one for the $\wedge$ contour. The different coefficient in front of ζ_3 will be discussed further in Section 4.5.

We have found the anomalous dimension that controls the non-collinear soft divergences of the diagonal DGLAP kernels by separating it from the hard-collinear behaviour that is identical to that in the form factor. We shall now

verify the above result, eq. (4.61), by computing it directly.

4.4 Explicit Calculation of $\Gamma_\sqcap$

In this section we derive the integral representation (4.52) of the renormalised Wilson loop $W_\sqcap$ defined in eq. (4.50) and we verify the two-loop result of eq. (4.61) for the anomalous dimension $\Gamma_\sqcap$ with a direct calculation. This provides a consistency check of eq. (4.59), which follows from the all-order factorisation in eq. (4.47).

The derivation of eq. (4.52) consists of two parts: firstly we will compute the bare diagrams and the UV counterterms related to the renormalisation of the QCD coupling constant, then we will subtract the short-distance singularities associated with the Wilson-line operators, thus completing the renormalisation of $\log W_\sqcap$. The non-Abelian exponentiation theorem [59–61, 182] allows us to determine directly $\log W_\sqcap$ by computing only the *webs* that capture the maximally non-Abelian colour factors of each Feynman diagram, as defined in [182]. Moreover, $\log W_\sqcap$ has a simpler singularity structure compared to $W_\sqcap$, which allows us to setup the renormalisation procedure directly at the level of the webs.

We introduce the following parameterisation for the contour of the Wilson loop $W_\sqcap$

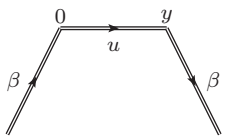

$$x^\mu(t) = \begin{cases} \beta^\mu t & t \in (-\infty, 0) \\ u^\mu t & t \in (0, y) \\ y u^\mu + \beta^\mu (t - y) & t \in (y, +\infty) \end{cases} \tag{4.62}$$

We use the following Feynman rules in configuration space (c.f. the momentum space rule in eq. (2.31)) for the gluon propagator in Feynman gauge and for the gluon emission from the eikonal lines, respectively

$$= \frac{\mathcal{N}}{\left[-x^2 + i0\right]^{1-\epsilon}} g_{\mu\nu} \,, \tag{4.63}$$

$$= i g_s \, \mathbf{T}^a \, v^\mu \int d^d z \int_0^\infty d\lambda \, \delta^d(z - x_0 - \lambda v), \tag{4.64}$$

where $\mathbf{T}^a$ is the SU(N) generator in the appropriate representation and $\mathcal{N} = -\frac{\Gamma(1-\epsilon)}{4\pi^{2-\epsilon}}$.

In Section 4.4.1 we consider the one-loop calculation of $\log(W_\sqcap)$ and then establish its general form before and after renormalisation. In Section 4.4.3 we perform the calculation at two loops, verifying the general structure and obtaining an explicit result for $\Gamma_\sqcap$ consistent with eq. (4.61).

4.4.1 One-loop calculation

As a direct consequence of the Feynman rules given above, all the diagrams that feature a gluon exchange between two lines with the same lightlike velocity v are proportional to v^2 and therefore they are automatically zero. At one loop there will be only two non-vanishing webs contributing to $\log(W_\sqcap)$

$d_A^{(1)} =$ 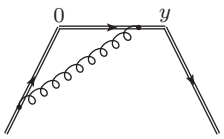

, $d_B^{(1)} =$ 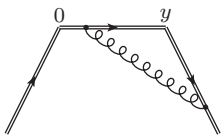

which differ only by a translation and therefore yield the same result

$$d^{(1)}(\alpha_s, \beta\cdot uy, \epsilon) = \frac{\alpha_s}{\pi}(\mu^2\pi)^\epsilon\,(u\cdot\beta)\;C_i\,\Gamma(1-\epsilon)\int_0^\infty dt\int_0^y ds\,(-2\beta\cdot u\,ts+i0)^{-1+\epsilon}, \tag{4.65}$$

where C_i, with $i = A, F$ is the quadratic Casimir in the adjoint or in the fundamental representation. We notice that the integral over the parameter t diverges both in the UV limit $t \to 0$ and in the IR regime $t \to \infty$. This fact is a consequence of the absence of any scale associated with the integration over an infinite Wilson line and it implies that the bare diagram in eq. (4.65) yields a vanishing contribution. Nevertheless, the diagram is non-trivial after the renormalisation procedure, which subtracts the divergence for $t \to 0$ and allows us to define uniquely the integrand in eq. (4.65). In order to expose the analytic structure of eq. (4.65) in terms of the variable ρ defined in eq. (4.51), we rotate the path along the negative imaginary axis in the complex $t-$plane. Then we change variables $t = -i\sqrt{2}\lambda$, $s = -i\sqrt{2}\frac{\sigma}{u\cdot\beta}$, obtaining

$$d^{(1)}(\alpha_s, \rho, \epsilon) = -\frac{\alpha_s}{\pi}(4\pi\mu^2)^\epsilon C_i\frac{\Gamma(1-\epsilon)}{2}\int_0^\infty\frac{d\lambda}{\lambda^{1-\epsilon}}\int_0^{\frac{\rho}{\sqrt{2}}}\frac{d\sigma}{\sigma^{1-\epsilon}}. \tag{4.66}$$

The complete result for $\log(W_\sqcap)$ at one loop is given by twice the contribution of eq. (4.66). It is convenient to write it with the factor $(4\pi e^{\gamma_E})^\epsilon$ absorbed into

the $\overline{\text{MS}}$ running coupling as follows

$$\log W_{\sqcap}^{\text{bare}} = -\frac{\alpha_s(\mu^2)}{\pi} e^{-\epsilon\gamma_E}\, C_i \Gamma(1-\epsilon) \int_0^\infty \frac{d\lambda}{\lambda} \int_0^{\frac{\rho}{\sqrt{2}}} \frac{d\sigma}{\sigma}\, \left(\lambda\sigma\mu^2\right)^\epsilon + \mathcal{O}(\alpha_s^2). \quad (4.67)$$

The label "bare" reminds us that eq. (4.67) still has the UV divergences associated to the cusps of the Wilson loop in eq. (4.62), which must be subtracted before IR singularities can be identified. Indeed, it is convenient to show explicitly that eq. (4.67) is independent on the renormalisation scale, by writing the running coupling as

$$\alpha_s\left(\mu^2\right) = \left(\mu^2\lambda\sigma\right)^{-\epsilon} \alpha_s\left(\frac{1}{\lambda\sigma}\right) + \frac{\hat{b}_0}{\epsilon}(\mu^2\lambda\sigma)^{-2\epsilon}\left(1-(\mu^2\lambda\sigma)^\epsilon\right)\alpha_s\left(\frac{1}{\lambda\sigma}\right)^2 + \mathcal{O}(\alpha_s^3), \quad (4.68)$$

which leads to the expression

$$\log W_{\sqcap}^{\text{bare}} = -C_i \int_0^\infty \frac{d\lambda}{\lambda} \int_0^{\frac{\rho}{\sqrt{2}}} \frac{d\sigma}{\sigma}\, \frac{\alpha_s\left(\frac{1}{\lambda\sigma}\right)}{\pi}\, e^{-\epsilon\gamma_E}\Gamma(1-\epsilon) + \mathcal{O}(\alpha_s^2). \quad (4.69)$$

4.4.2 Exponentiation and renormalisation

The integrand in eq. (4.69) is finite in the limit $\epsilon \to 0$ and the singularities of $\log W_{\sqcap}$ arise only after the integration over λ, σ. In particular, following the coordinate-space analysis of refs. [148, 183, 184], we distinguish three possible types of singular behaviour: *cusp singularities*, which are associated to the limit $\lambda \simeq \sigma \to 0$ in which all the vertices approach a cusp of the Wilson loop; *collinear* singularities, which arise if either λ or σ approaches the cusp, while the other parameter stays finite; finally, the large-distance region with $\lambda \to \infty$, which determines the IR pole. At higher perturbative orders, individual diagrams feature soft and collinear subdivergences when a subset of the vertices approaches one of these limits, which give rise to poles of higher order compared to those in eq. (4.69). However, owing to its exponentiation property, upon considering the logarithm of the Wilson-line correlator, all the subdivergences cancel in the sum of webs at each perturbative order [148, 180, 184–186]. It is always possible to organise the calculation of $\log(W_{\sqcap})$ such that the integral over the position of the vertex that is located at the largest distance along the infinite Wilson line is performed last. Thus, the single infrared pole will be generated only in the final integration, while all the subdivergences of individual diagrams cancel in the sum of webs. This procedure, which follows the prescriptions of ref. [148], allows us

to generalise the representation of eq. (4.69) to all orders

$$\log W_{\sqcap}^{\text{bare}} = \int_0^{\infty} \frac{d\lambda}{\lambda} \int_0^{\frac{\rho}{\sqrt{2}}} \frac{d\sigma}{\sigma} w\left(\alpha_s\left(\frac{1}{\lambda\sigma}\right), \epsilon\right), \tag{4.70}$$

where the integrand w has an expansion in ϵ that involves only non-negative powers

$$w\left(\alpha_s\left(\frac{1}{\lambda\sigma}\right), \epsilon\right) = \sum_{n=0}^{\infty} w_n\left(\alpha_s\left(\frac{1}{\lambda\sigma}\right)\right) \epsilon^n. \tag{4.71}$$

The representation eq. (4.70) is analogous to the one derived in [148] for the soft function of the form factor, defined in eq. (4.13), with the difference that in the latter case the integrals over both the parameters are unbounded. This is consistent with the presence of a double pole of long-distance origin in the form factor, as compared to the single pole of this type arising in eq. (4.52).

We now proceed with the renormalisation of the singularities of short-distance origin that are present in the bare expression of eq. (4.70). Following [148], we notice that the integral of w_0 in eq. (4.70) generates double UV poles, which are subtracted by cutting the integration domain with $\lambda < \frac{1}{\mu}$, $\sigma < \frac{1}{\mu}$ in eq. (4.70), where μ defines the subtraction point. The contributions of w_i with $i \geq 1$ generate at most one UV singularity, which we subtract in the last integration. In conclusion we derive the representation for the sum of renormalised webs in configuration space

$$\log\left(W_{\sqcap}^{\text{ren}}\right) = -\int_{\frac{1}{\mu}}^{\infty} \frac{d\lambda}{\lambda} \int_{\frac{1}{\mu}}^{\frac{\rho}{\sqrt{2}}} \frac{d\sigma}{\sigma} \gamma_{\text{cusp}}\left(\alpha_s\left(\frac{1}{\lambda\sigma}\right)\right) - \int_{\frac{1}{\mu}}^{\infty} \frac{d\lambda}{\lambda} \Gamma_{\sqcap}\left(\alpha_s\left(\frac{1}{\lambda^2}\right)\right), \tag{4.72}$$

where we performed the integral over σ by expanding the coupling constant $\alpha_s\left(\frac{1}{\lambda\sigma}\right)$ at the scale $\frac{1}{\lambda^2}$, as in eq. (4.68)

$$\alpha_s\left(\frac{1}{\lambda\sigma}\right) = \alpha_s\left(\frac{1}{\lambda^2}\right)\left(\frac{\lambda}{\sigma}\right)^{-\epsilon} + \left(\alpha_s\left(\frac{1}{\lambda^2}\right)\right)^2 \frac{\hat{b}_0}{\epsilon}\left(\frac{\lambda}{\sigma}\right)^{-2\epsilon}\left[1 - \left(\frac{\lambda}{\sigma}\right)^{\epsilon}\right] + \mathcal{O}(\alpha_s^3). \tag{4.73}$$

Eq. (4.72) directly leads to the result eq. (4.52) from the web integrals in coordinate space and it allows us to extract the coefficients γ_{cusp} and $\Gamma_{\sqcap}$. At one-loop order, we expand the web in eq. (4.69) and we get

$$w\left(\alpha_s\left(\frac{1}{\lambda\sigma}\right), \epsilon\right) = -\frac{\alpha_s\left(\frac{1}{\lambda\sigma}\right)}{\pi} C_i\left[1 + \mathcal{O}\left(\epsilon^2\right)\right] + \mathcal{O}\left(\alpha_s^2\right). \tag{4.74}$$

Applying the renormalisation procedure described above we find

$$\begin{aligned}\log W_{\sqcap}^{\text{ren}} &= -\frac{C_i}{\pi}\int_{1/\mu}^{\infty}\frac{d\lambda}{\lambda}\int_{1/\mu}^{\frac{\rho}{\sqrt{2}}}\frac{d\sigma}{\sigma}\alpha_s\left(\frac{1}{\lambda\sigma}\right)+\mathcal{O}(\alpha_s^2)\\ &= \frac{\alpha_s(\mu^2)}{\pi}\frac{C_i}{\epsilon}\log\left(\frac{\rho\mu}{\sqrt{2}}\right)+\mathcal{O}(\alpha_s^2),\end{aligned} \tag{4.75}$$

where we have used the fact that $W_{\sqcap}$ consists of pure poles. The pole is infrared and is exactly the one that replicates the soft divergence of the PDF. We compare eq. (4.75) with the poles of eq. (4.52) getting

$$\begin{aligned}\gamma_{\text{cusp}} &= \frac{\alpha_s}{\pi}C_i+\mathcal{O}\left(\alpha_s^2\right),\\ \Gamma_{\sqcap} &= 0\cdot\alpha_s+\mathcal{O}\left(\alpha_s^2\right).\end{aligned} \tag{4.76}$$

4.4.3 Two-loop calculation

We now apply the renormalisation procedure to the two-loop webs. Only a few diagrams contribute to this order and they are represented below

$d_{\text{SE}}^{(2)} =$ 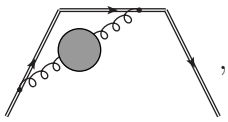 , $d_{X_2}^{(2)} =$ 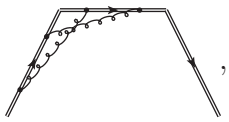 , $d_{X_3}^{(2)} =$ 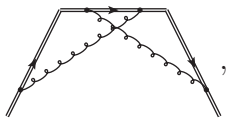 ,

$d_{Y_s}^{(2)} =$ 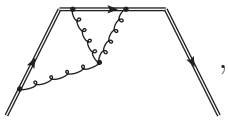 , $d_{Y_L}^{(2)} =$ 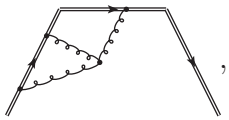 , $d_{3s}^{(2)} =$ 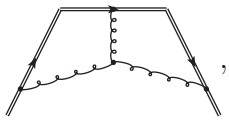 , (4.77)

where we omit the configurations that are simply obtained by mirror symmetry. The diagrams in the first row of eq. (4.77) are computed following the same steps as the one-loop case. As in the one-loop case, we write the bare webs using the representation in eq. (4.70) and we define the integrand $w_i^{(2)}$ of diagram $d_i^{(2)}$ as,

$$d_i^{(2)}(\alpha_s,\rho,\epsilon) = \int_0^{\infty}\frac{d\lambda}{\lambda}\int_0^{\frac{\rho}{\sqrt{2}}}\frac{d\sigma}{\sigma}\left(\frac{\alpha_s\left(1/\lambda\sigma\right)}{\pi}e^{-\epsilon\gamma_E}\right)^2 w_i^{(2)}(\epsilon). \tag{4.78}$$

From now on we drop the arguments on d_i and w_i which are understood to have the above arguments unless otherwise stated. The first diagram, $d_{\text{SE}}^{(2)}$ is obtained from eq. (4.65) by replacing the gluon propagator eq. (4.63) with the one-loop

expression

$$D^{(1)}_{\mu\nu}(x) = -\frac{\alpha_s}{16\pi^3}\left(\pi^2\mu^2\right)^{\epsilon}\frac{\Gamma^2(1-\epsilon)}{\epsilon(1-2\epsilon)(3-2\epsilon)}\Big[C_A(5-3\epsilon)-4n_f T_f(1-\epsilon)\Big] \times\left[-x^2+i\,0\right]^{-1+2\epsilon} g_{\mu\nu}, \tag{4.79}$$

where we discarded the longitudinal components of the propagator, that are proportional to $\partial_\mu\partial_\nu$, because they decouple from the amplitude via Ward identities [148]. The result is

$$w^{(2)}_{\rm SE} = -C_i\frac{\Gamma^2(1-\epsilon)}{8\epsilon(1-2\epsilon)(3-2\epsilon)}\Big[C_A(5-3\epsilon)-4n_f T_f(1-\epsilon)\Big], \tag{4.80}$$

in agreement with the results of [146, 148]. We notice immediately that, at two-loop level, the representation eq. (4.78) of the individual webs has subdivergences, which are manifest as explicit poles in the integrand w_i. In this case the subdivergence is cancelled by the coupling renormalisation in the QCD Lagrangian of eq. (1.1) that will be taken into account later in this section. The double gluon exchange diagrams give

$$w^{(2)}_{X_2} = -C_i\,C_A\frac{\Gamma^2(1-\epsilon)}{8\epsilon^2}\,, \tag{4.81}$$

$$w^{(2)}_{X_3} = -C_i\,C_A\frac{\Gamma^2(1-\epsilon)}{2\epsilon}\left[\frac{1}{\epsilon}-B(\epsilon,1+\epsilon)\right]. \tag{4.82}$$

Both results are in agreement with the maximally non-Abelian contributions of the diagrams W_c and W_d reported in [146]. The integrand of the diagram $d^{(2)}_{X_2}$ in eq. (4.81) has poles of short-distance origin, associated to the configuration shown below, where the two innermost vertices on the Wilson lines are in proximity of the cusp

$w^{(2),\rm subdiv}_{X_2} =$ 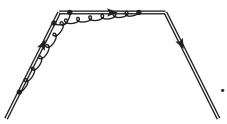 .

These subdivergences are not related to QCD renormalisation and they will cancel in the sum of all webs. Eq. (4.82) is finite when $\epsilon \to 0$ as we discuss more in detail in Appendix C.2.2. The diagrams in the second row of eq. (4.77) involve

the three-gluon vertex, whose Feynman rule in configuration space reads

$$V^{a_1a_2a_3}_{\mu_1\mu_2\mu_3}(x_1,x_2,x_3) = g_s f^{a_1a_2a_3}\Bigg[\left(-i\frac{\partial}{\partial x_1^{\mu_3}}+i\frac{\partial}{\partial x_2^{\mu_3}}\right)g_{\mu_1\mu_2} + \left(-i\frac{\partial}{\partial x_2^{\mu_1}}+i\frac{\partial}{\partial x_3^{\mu_1}}\right)g_{\mu_2\mu_3}+\left(-i\frac{\partial}{\partial x_3^{\mu_2}}+i\frac{\partial}{\partial x_1^{\mu_2}}\right)g_{\mu_3\mu_1}\Bigg]. \tag{4.83}$$

We notice that the diagrams $d^{(2)}_{Y_s}$ and $d^{(2)}_{Y_L}$ are not related by symmetry transformations, because the former has two gluon attachments on the segment of finite length y, while the latter has two emissions from the semi-infinite line. We begin with the calculation of $d^{(2)}_{Y_s}$

$$d^{(2)}_{Y_s} = K_Y\int d^dz\int_{-\infty}^0 dt_3 u\cdot\left\{\int_0^y ds_1\int_{s_1}^y ds_2\left(\frac{\partial}{\partial s_2 u}\right)-\int_0^y ds_2\int_0^{s_2} ds_1\left(\frac{\partial}{\partial s_1 u}\right)\right\} \times\left[-(us_2-z)^2+i0\right]^{-1+\epsilon}\left[-(us_1-z)^2+i0\right]^{-1+\epsilon}\left[-(\beta t_3-z)^2+i0\right]^{-1+\epsilon}, \tag{4.84}$$

where we introduced the normalisation factor $K_Y = ig_s^4\frac{C_iC_A}{2}\mathcal{N}^3u\cdot\beta$. We write the differential operators in eq. (4.84) in terms of total derivatives as follows

$$u\cdot\frac{\partial}{\partial s_2\,u}\left[-z^2+2z\cdot us_2+i0\right]^{-1+\epsilon} = \frac{d}{ds_2}\left[-z^2+2z\cdot us_2+i0\right]^{-1+\epsilon}, \tag{4.85}$$

which allows us to perform immediately the integrals over s_2 and over s_1, respectively in the first and in the second term in curly brackets, by evaluating the appropriate propagator at the endpoints of the integration interval. Eq. (4.84) becomes

$$d^{(2)}_{Y_s} = d^{(2)}_E(y\,u,u\cdot\beta)+d^{(2)}_E(0,u\cdot\beta)-2d^{(2)}_B(u\cdot\beta), \tag{4.86}$$

in terms of the functions

$$d^{(2)}_E(v,u\cdot\beta) = K_Y\int d^dz\int_{-\infty}^0 dt\int_0^y ds\left[-(\beta t-z)^2\right]^{\epsilon-1} \times\left[-(us-z)^2\right]^{\epsilon-1}\left[-(v-z)^2\right]^{\epsilon-1}, \tag{4.87}$$

$$d^{(2)}_B(u\cdot\beta) = K_Y\int d^dz\int_{-\infty}^0 dt\int_0^y ds\left[-(\beta t-z)^2\right]^{\epsilon-1}\left[-(us-z)^2\right]^{2\epsilon-2}, \tag{4.88}$$

where the prescription $+i0$ is understood in every factor appearing in the integrals. Each function has a clear diagrammatic interpretation, because the

integrands are products of scalar propagators in coordinate space. Thus, $d^{(2)}_{Y_s}$ is decomposed in a sum of diagrams, as discussed in [148], giving in one-to-one correspondence with the three terms in eq. (4.86)

$$d^{(2)}_{Y_s} = \quad + \quad - 2 \quad , \tag{4.89}$$

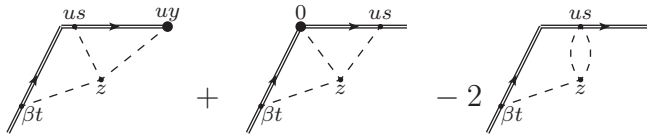

where the dashed lines represent scalar propagators and dotted vertices on the Wilson line indicate that the position of the endpoint of the propagator is not be integrated over. We integrate eqs. (4.87) and (4.88) over the position z of the three-gluon vertex and write the results in the two-dimensional integral representation in eq. (4.78). We obtain

$$w^{(2)}_E(y\,u, u\cdot\beta) = C_i C_A \frac{\Gamma(1-2\epsilon)}{16\epsilon}\Big[B(-\epsilon, 1-\epsilon) - B(-\epsilon, 1+\epsilon)\Big], \tag{4.90a}$$

$$w^{(2)}_E(0, u\cdot\beta) = C_i C_A \frac{\Gamma(1-\epsilon)\Gamma(1-2\epsilon)}{16\epsilon}\Gamma(\epsilon), \tag{4.90b}$$

$$w^{(2)}_B(u\cdot\beta) = C_i C_A \frac{\Gamma^2(1-\epsilon)}{16\epsilon(1-2\epsilon)}. \tag{4.90c}$$

Let us discuss the singularity structure of the separate integrals above. The only one which is separately finite is eq. (4.90a), which corresponds to the integrand of the first diagram in eq. (4.89). Eq. (4.90b) has single and double poles that will cancel the corresponding singularities in eq. (4.81). Indeed, the second diagram in eq. (4.89), which is associated to the integrand in eq. (4.90b), has subdivergences of short distance origin when the three-gluon vertex approaches the cusp, similarly to the behaviour shown by diagram $d^{(2)}_{X_2}$. The single pole in eq. (4.90c) is entirely due to the presence of a one-particle-irreducible UV divergent subgraph in the last diagram in eq. (4.89). Therefore, this singularity is removed by the counterterms of the QCD Lagrangian. Using these results, the total contribution of the diagram $d^{(2)}_{Y_s}$ in eq. (4.86) agrees with the corresponding expression for diagram W_e in [146] and in the notation of eq. (4.78) it reads

$$w^{(2)}_{Y_s} = -C_i C_A \frac{\Gamma(1-\epsilon)}{16\epsilon^2(1-2\epsilon)}\Big[\Gamma(1-\epsilon) - 2\Gamma(2-2\epsilon)\Gamma(1+\epsilon)\Big]. \tag{4.91}$$

The next diagram, $d^{(2)}_{Y_L}$, differs from eq. (4.84) only by the presence of the two gluon attachments on the semi-infinite Wilson line rather than on the finite one.

Once again, we write the three gluon vertex in terms of total derivative and we decompose the diagram as

$$d^{(2)}_{Y_L} = d^{(2)}_E(0, u\cdot\beta) - 2d^{(2)}_B(u\cdot\beta) \equiv$$ 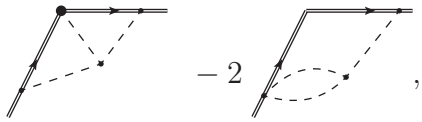 , (4.92)

where we have used the functions defined in eqs. (4.87) and (4.88). The comparison of eqs. (4.86) and (4.92) shows that two diagrams differ only by the term featuring a scalar propagator connected to the endpoint of the Wilson line. In the case of $d^{(2)}_{Y_L}$, the Wilson line is infinite and this term is absent. This result was shown in [148], by introducing a cutoff on the infinite line and carefully taking the limit to infinity, which does not commute with the integration over z. The same conclusion is found by computing $d^{(2)}_{Y_L}$ in momentum space, as shown in Appendix C.2.1. Using eqs. (4.90a), (4.90b) and (4.90c) we get

$$w^{(2)}_{Y_L} = C_i C_A \frac{\Gamma(1-\epsilon)}{8\epsilon}\left[\frac{\Gamma(1-2\epsilon)\Gamma(\epsilon)}{2} - \frac{\Gamma(1-\epsilon)}{1-2\epsilon}\right]. \tag{4.93}$$

By construction, the expression above has the same singularities as $w^{(2)}_{Y_s}$, because the integrand of the diagram $d^{(2)}_{Y_L}$ differs from $d^{(2)}_{Y_s}$ only by the function in eq. (4.90a), which is finite.

We compute the diagram $d^{(2)}_{3s}$ using the same procedure

$$d^{(2)}_{3s} = 2\, d^{(2)}_E(yu, u\cdot\beta) \equiv$$ 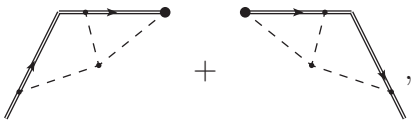 , (4.94)

getting

$$w^{(2)}_{3s} = C_i C_A \frac{\Gamma(1-2\epsilon)}{8\epsilon}\Big[B(-\epsilon, 1-\epsilon) - B(-\epsilon, 1+\epsilon)\Big], \tag{4.95}$$

which is finite because it involves only the function in eq. (4.90a). We renormalise the UV divergences associated with the QCD vertices and propagators by means of the one-loop counterterm

$$d^{(2)}_{\rm ct} = -\frac{\alpha_s}{4\pi\epsilon}\left[\frac{11}{3}C_A - \frac{4}{3}T_f n_f\right] d^{(1)}, \tag{4.96}$$

where $d^{(1)}$ is the result of the one-loop diagram eq. (4.66).

Finally, we sum all the diagrams depicted in eq. (4.77), including the symmetric configurations which are not shown there, getting

$$\begin{aligned}\log W_{\sqcap}^{\text{bare}} &= 2d^{(1)} + \Big(2d_{\text{SE}}^{(2)} + 2d_{Y_s}^{(2)} + 2d_{Y_L}^{(2)} + 2d_{X_2}^{(2)} + d_{3s}^{(2)} + d_{X_3}^{(2)} + 2d_{ct}^{(2)}\Big), \\ &= 2\Big\{d^{(1)} + d_{\text{SE}}^{(2)} + 2d_{Y_L}^{(2)} + d_{X_2}^{(2)} + d_{ct}^{(2)}\Big\} + 2d_{3s}^{(2)} + d_{X_3}^{(2)}, \end{aligned} \tag{4.97}$$

where to get to the second line we used the identity $2d_{Y_s}^{(2)} = 2d_{Y_L}^{(2)} + d_{3s}^{(2)}$ that is obtained by comparing eqs. (4.89), (4.92) and eq. (4.94). The terms in curly brackets in the final expression are the same that appear in the calculation of the cusped Wilson loop with two semi-infinite lightlike lines, discussed in [148]. The last two contributions in eq. (4.97) are special to the configuration of $W_{\sqcap}$, where the semi-infinite lines are connected by a finite lightlike segment. The final expression in eq. (4.97) follows the decomposition of polygon-shaped Wilson loops presented in [148]. The distinction between the terms inside and outside the curly brackets in eq. (4.97) stems from the structure of their singularities. The former ones give rise to cusp configurations characterised by double UV poles and therefore they can be written in terms of the representation in eq. (4.70) with a finite integrand. The last contributions in eq (4.97) generate at most a single pole, associated to the configurations where all the vertices simultaneously approach a lightlike segment, and therefore their combination will give rise to an integrand of order ϵ in eq. (4.70), as we verify by expanding eqs. (4.82) and (4.95)

$$2w_{3s}^{(2)} + w_{X_3}^{(2)} = \frac{3}{2}\epsilon\, C_i C_A\, \zeta_3. \tag{4.98}$$

Substituting the results in eqs. (4.80), (4.81), (4.82), (4.93) and (4.95) into eq. (4.97), the integral representation of the bare diagrams reads

$$\begin{aligned}\log W_{\sqcap}^{\text{bare}} = C_i \int_0^\infty \frac{d\lambda}{\lambda} \int_0^{\frac{\rho}{\sqrt{2}}} \frac{d\sigma}{\sigma} \Bigg\{ &\frac{\alpha_s\left(\frac{1}{\lambda\sigma}\right)}{\pi}\kappa\Gamma(1-\epsilon)\Bigg[-1 + \frac{\alpha_s\left(\frac{1}{\lambda\sigma}\right)}{\pi}\frac{\hat{b}_0}{\epsilon}\Bigg] \\ &+ \left(\frac{\alpha_s\left(\frac{1}{\lambda\sigma}\right)}{\pi}\kappa\right)^2 \Bigg[C_A\left(\frac{3(-4+3\epsilon)\Gamma(1-\epsilon)\Gamma(2-\epsilon)}{4\epsilon^2(3-8\epsilon+4\epsilon^2)} - \pi\Gamma(-2\epsilon)\cot\left(\frac{\pi\epsilon}{2}\right)\right) \\ &- T_f n_f \frac{\Gamma(2-\epsilon)\Gamma(-\epsilon)}{3-8\epsilon+4\epsilon^2}\Bigg]\Bigg\} \end{aligned} \tag{4.99}$$

where $\kappa = e^{-\epsilon\gamma_E}$. By expanding the equation above in ϵ we get

$$\log W_{\sqcap}^{\text{bare}} = -\int_0^\infty \frac{d\lambda}{\lambda} \int_0^{\frac{\rho}{\sqrt{2}}} \frac{d\sigma}{\sigma} \Bigg\{ \left(\frac{\alpha_s\left(\frac{1}{\lambda\sigma}\right)}{\pi}\right)\left[1 + \frac{\epsilon^2}{2}\zeta_2 + \mathcal{O}(\epsilon^3)\right]$$

$$+\left(\frac{\alpha_s\left(\frac{1}{\lambda\sigma}\right)}{\pi}\right)^2\left[\gamma^{(2)}_{\text{cusp}}+\epsilon\left(\Gamma^{(2)}_{\sqcap}+\frac{3\hat{b}_0\zeta_2}{2}\right)+\mathcal{O}(\epsilon^2)\right]\Bigg\}, \tag{4.100}$$

where $\Gamma^{(2)}_{\sqcap}$ is the two-loop contribution to $\Gamma_{\sqcap}$ eq. (4.61),

$$\Gamma^{(2)}_{\sqcap}=\frac{C_i}{2}\left(-2\hat{b}_0\zeta_2-\frac{56}{27}T_f n_f+C_A\left[\frac{202}{27}-4\zeta_3\right]\right). \tag{4.101}$$

Now we renormalise using the procedure outlined in the one-loop case, see eq. (4.72). For the terms of $\mathcal{O}(\epsilon^0)$, the cusp terms, we integrate from $1/\mu$ on both integrals. For all the subsequent terms, the σ integral is performed first, integrating from 0 to $\frac{\rho}{\sqrt{2}}$. Then the parameter λ integrated from $\frac{1}{\mu}$. By doing this we get,

$$\begin{aligned}\log W_{\sqcap} =& \alpha_s(\mu^2)\frac{1}{\epsilon}\log\left(\frac{\rho\mu}{\sqrt{2}}\right)\\ &+\alpha_s(\mu^2)^2\Bigg\{-\frac{\hat{b}_0}{2\epsilon^2}\log\left(\frac{\rho\mu}{\sqrt{2}}\right)+\frac{1}{\epsilon}\left(\frac{1}{4}\Gamma^{(2)}_{\sqcap}+\frac{1}{2}\gamma^{(2)}_{\text{cusp}}\log\left(\frac{\rho\mu}{\sqrt{2}}\right)\right)\Bigg\}.\end{aligned} \tag{4.102}$$

Again it is reminded that we have used the fact that $W_{\sqcap}$ consists of pure poles. The above is reproduced by eq. (4.52)

$$\log W_{\sqcap}=-\frac{1}{2}\int_0^{\mu^2}\frac{d\xi^2}{\xi^2}\Bigg\{2\gamma_{\text{cusp}}(\alpha_s(\xi^2,\epsilon))\log\left(\frac{\rho\mu}{\sqrt{2}}\right)+\Gamma_{\sqcap}(\alpha_s(\xi^2,\epsilon))\Bigg\}. \tag{4.103}$$

By this point we have determined the anomalous dimension $\Gamma_{\sqcap}$ in two different ways, first by extracting it from the evolution of PDFs using the universality of the hard-collinear poles $J/\mathcal{J}$ and now by a direct computation of the renormalisation of the corresponding Wilson-line correlator.

4.5 Relating Wilson-line Geometries to Physical Quantities

In this section we establish a set of relations between different physical quantities, based on the properties of the Wilson loops discussed in Section 4.4. In Section 4.5.1 we will show that the single infrared poles in the quark and in

the gluon form factors are related to the corresponding diagonal term in the DGLAP kernels by a precise eikonal quantity that is associated to the geometry of the Wilson loops with lightlike lines. The latter emerges as the difference between the anomalous dimensions associated with a wedged Wilson loop with two semi-infinite lines and a $\sqcap-$shaped Wilson loop. This difference, in turn, can be expressed as the anomalous dimension associated with a parallelogram (or more generally) a polygon with lightlike segments. In Section 4.5.2 we use this relation to extract the anomalous dimensions associated with a polygon Wilson loop to three loops, which is related to the soft anomalous dimension appearing in the resummation of threshold logarithms in the Drell-Yan process. Finally we extract the fermionic components of the four-loop result in the planar limit.

4.5.1 Relating the form factor with the DGLAP kernels

The direct calculation of the anomalous dimension $\Gamma_{\sqcap}$ in Section 4.4 confirms the identity in eq. (4.59)

$$2B_{\delta} = 2\gamma_{J/\mathcal{J}} - \Gamma_{\sqcap}, \tag{4.104}$$

which follows from the factorisation of the parton distribution functions for large x. This identity is interpreted as a decomposition of B_{δ}, which was defined in eq. (4.58) as the coefficient of the delta distribution in the splitting functions in the limit $x \to 1$, into the contribution of the hard-collinear radiation, $\gamma_{J/\mathcal{J}}$, and the purely soft one, which is encoded by $\Gamma_{\sqcap}$. In eq. (4.104) we suppressed the dependence on the external parton: the relation holds for both quarks and gluons. The hard-collinear contribution $\gamma_{J/\mathcal{J}}$ is process independent, as discussed in Section 4.2.2 in the context of the infrared factorisation of the form factor. Indeed, eq. (4.21) provides the analogue of eq. (4.104)

$$\gamma_G = 2\gamma_{J/\mathcal{J}} - \Gamma_{\wedge}, \tag{4.105}$$

where γ_G is the anomalous dimension that determines the single poles of the form factor. By comparing eq. (4.104) and eq. (4.105) we derive the relation

$$\gamma_G - 2B_{\delta} = \Gamma_{\sqcap} - \Gamma_{\wedge}, \tag{4.106}$$

which connects the single poles in the form factor with the diagonal DGLAP kernels. The two quantities appearing on the left-hand side of eq. (4.106) depend on both the spin and the colour representation of the external particles in a non-

trivial way. In contrast, the right-hand side involves the anomalous dimensions of two eikonal quantities, which depend only on the colour representation of the particles and obey Casimir scaling up to three loops. Therefore, eq. (4.106) allows us to interpret the function $f_{\rm eik}$ eq. (1.29), which was introduced in [84,85] as the difference $f_{\rm eik} \equiv \gamma_G - 2B_\delta$, in terms of the anomalous dimensions of Wilson-line correlators. By substituting the two-loop expressions of $\Gamma_\sqcap$ and $\Gamma_\wedge$ from direct calculations, respectively in eqs. (4.61) and (4.23), into the right-hand side of eq. (4.106) we reproduced the two-loop result obtained from the difference of γ_G and B_δ in ref. [85], namely

$$f_{\rm eik} = \left(\frac{\alpha_s}{\pi}\right)^2 C_i \left[C_A \left(-\frac{11\zeta_2}{24} - \frac{7}{4}\zeta_3 + \frac{101}{54} \right) + T_f n_f \left(\frac{\zeta_2}{6} - \frac{14}{27} \right) \right] + \mathcal{O}\left(\alpha_s^3\right), \tag{4.107}$$

thus verifying eq. (4.106) through two loops.

The difference of anomalous dimensions appearing on the right-hand side of eq. (4.106) has also a geometric interpretation, which suggests to define it as universal quantity. Following the analysis of the singularities of the Wilson loops with lightlike lines detailed in ref. [148] and the calculation in Section 4.4 above, the anomalous dimensions $\Gamma_\sqcap$ and $\Gamma_\wedge$ receive contributions only from the singular configurations, in which all the vertices approach one lightlike line. In this sense, these anomalous dimensions depend only on the features of each lightlike line separately and they are insensitive to the global shape of the Wilson loop. Both $\Gamma_\sqcap$ and $\Gamma_\wedge$ encode the collinear singularities associated with the two semi-infinite lightlike lines, but the former receives an additional contribution from the configurations that are collinear to the finite segment. Such singularities differ from the ones originating from infinite lines by the presence of endpoint contributions, as we showed by computing the diagrams $d^{(2)}_{Y_s}$ and $d^{(2)}_{Y_L}$ in eqs. (4.89) and (4.92). It is therefore useful to define the difference of $\Gamma_\sqcap$ and $\Gamma_\wedge$ as the anomalous dimension that captures the collinear singularities of a finite lightlike segment. Similarly, we define also the collinear anomalous dimension associated to infinite lines in terms of $\Gamma_\wedge$ only

$$\Gamma^{\rm fin}_{\rm co} \equiv \Gamma_\sqcap - \Gamma_\wedge \,, \tag{4.108}$$

$$\Gamma^{\rm inf}_{\rm co} \equiv \frac{\Gamma_\wedge}{2} \,. \tag{4.109}$$

The two-loop expression of $\Gamma^{\rm fin}_{\rm co}$ coincides with the right-hand side of eq. (4.107), while $\Gamma^{\rm inf}_{\rm co}$ to the same order is obtained from eq. (4.23). Comparing the two

expressions we get

$$\Gamma_{\text{co}}^{\text{fin}} = 2\,\Gamma_{\text{co}}^{\text{inf}} - \frac{3}{2}\left(\frac{\alpha_s}{\pi}\right)^2 C_i C_A\,\zeta_3 + \mathcal{O}\left(\alpha_s^3\right). \tag{4.110}$$

The factor of two multiplying $\Gamma_{\text{co}}^{\text{inf}}$ is consistent with the fact that the finite Wilson line is obtained as a contour involving two semi-infinite lines. The remaining discrepancy proportional to ζ_3 is related to the endpoint contributions in eq. (4.98).

The geometric interpretation of $\Gamma_{\text{co}}^{\text{fin}}$ and $\Gamma_{\text{co}}^{\text{inf}}$ allows one to derive the anomalous dimensions of Wilson loops with the contour consisting of arbitrary, possibly open, polygons with lightlike lines. The first example is the parallelogram-shaped Wilson loop $W_\square$ that features four lightlike segments of finite length (see Figure 4.1c), whose renormalisation was given in [146]

$$\mu\frac{d\log\left(W_\square\right)}{d\mu} = -2\gamma_{\text{cusp}}\left[\log\left(\mu^2(x\cdot y + i\varepsilon)\right) + \log\left(\mu^2(-x\cdot y + i\varepsilon)\right)\right] - \Gamma_\square, \tag{4.111}$$

where x and y are the four-vectors that define the sides of the parallelogram. $\Gamma_\square$ receives contributions from the collinear divergences of four finite segments in lightlike directions, therefore it is

$$\Gamma_\square = 4\,\Gamma_{\text{co}}^{\text{fin}} = 4\left(\Gamma_\sqcap - \Gamma_\wedge\right). \tag{4.112}$$

By replacing in the equation above the two-loop value of $\Gamma_{\text{co}}^{\text{fin}}$ in eq. (4.107), we reproduce the results of $\Gamma_\square$ in ref. [146]. In the case of a generic polygonal Wilson loop W_i with lightlike lines the evolution equation in eq. (4.111) generalises [146, 148]

$$\mu\frac{d\log\,W_i}{d\mu} = -\sum_a \gamma_{\text{cusp}}\log\left(\mu^2 x_a\cdot x_{a-1}\right) - \Gamma_i, \tag{4.113}$$

where the sum is extended over all the cusps in the contour and x_a, x_{a-1} define the sides adjacent to the cusp a. The anomalous dimension Γ_i collects all the collinear contributions and it can be derived by summing the appropriate multiples of $\Gamma_{\text{co}}^{\text{fin}}$ and $\Gamma_{\text{co}}^{\text{inf}}$, given by the number of finite and infinite sides, respectively.

Finally, having identified the difference $\Gamma_\sqcap - \Gamma_\wedge = \frac{\Gamma_\square}{4}$ in eq. (4.112), we may notice that eq. (4.106) provides yet another identity relating the form factor, the

DGLAP kernel and the Wilson loop $W_\square$ computed in ref. [146], namely

$$\gamma_G - 2B_\delta = \frac{\Gamma_\square}{4}, \tag{4.114}$$

thus explaining the numerical agreement of these two quantities computed respectively in ref. [85] and in ref. [146].

4.5.2 The Drell-Yan soft function and $\Gamma_\square$ beyond two loops

We move to relate the abstract $W_\square$ to a physical quantity relevant for soft-gluon resummation. It is known that the Drell-Yan *cross-section* factorises near threshold [2–6] (see also the more recent literature in the Soft Collinear Effective Theory [7, 18]). The hard-collinear region is described by the PDFs, the hard function by a squared timelike form factor and the soft region by Wilson lines in the DY configuration [136]. See eq. (1.3) for the schematic formulation. This leads to the all-order relation $\gamma_G - 2B_\delta = \Gamma_{\rm DY}/2$, where $\Gamma_{\rm DY}$ is the anomalous dimension associated to the DY configuration of Wilson lines (see e.g. [6, 7]). Using eq. (4.114) we have,

$$2\Gamma_{\rm DY} = \Gamma_\square. \tag{4.115}$$

The ideas in Section 4.5.1 will allow us to test the identification in eq. (4.115). The three-loop value for $\gamma_G - 2B_\delta$ was first extracted in [85] using the three-loop results for γ_G and B_δ. If we expand $\Gamma_\square$ as,

$$\Gamma_\square = \sum_{n=0}^{\infty} \left(\frac{\alpha_s}{\pi}\right)^n \Gamma_\square^{(n)}, \tag{4.116}$$

using the values in [85] we can then state

$$\Gamma_\square^{(1)} = 0 \tag{4.117}$$

$$\Gamma_\square^{(2)} = C_i \left[C_A \left(-\frac{11\zeta_2}{6} - 7\zeta_3 + \frac{202}{27} \right) + T_f n_f \left(\frac{2\zeta_2}{3} - \frac{56}{27} \right) \right] \tag{4.118}$$

$$\begin{aligned}\Gamma_\square^{(3)} = C_i \Bigg[& C_A^2 \left(\frac{22\zeta_2^2}{5} + \frac{11\zeta_2\zeta_3}{3} - \frac{6325\zeta_2}{648} - \frac{329\zeta_3}{12} + 12\zeta_5 + \frac{136781}{11664} \right) \\ & + C_A n_f T_f \left(-\frac{12\zeta_2^2}{5} + \frac{707\zeta_2}{162} + \frac{91\zeta_3}{27} - \frac{5921}{2916} \right) \\ & + C_F n_f T_f \left(\frac{4\zeta_2^2}{5} + \frac{\zeta_2}{2} + \frac{38\zeta_3}{9} - \frac{1711}{216} \right)\end{aligned}$$

$$+ n_f^2 T_f^2 \left(-\frac{10\zeta_2}{27} + \frac{28\zeta_3}{27} - \frac{520}{729} \right) \Bigg]. \tag{4.119}$$

As mentioned in Section 4.5.1, the two-loop $\Gamma_{\square}^{(2)}$ was calculated explicitly using Wilson lines in [146] and agrees with the extracted value in eq. (4.118). The three-loop $\Gamma_{\square}^{(3)}$ displayed in eq. (4.119) should be regarded as a prediction to be verified by direct calculation. For the Drell-Yan configuration of Wilson lines, $\Gamma_{\rm DY}$ was computed at two loops in [136] and three loops in [21]. The three-loop $\Gamma_{\rm DY}$ coincides with eq. (4.119). This is a non-trivial three-loop test of the identification in eq. (4.115), we arrive at the same value for $\Gamma_{\square}^{(3)}$ by two different paths: the difference $\gamma_G - 2B_\delta = \Gamma_\sqcap - \Gamma_\wedge = \Gamma_\square/4$ and the explicit calculation of $\Gamma_{\rm DY}$.

At four loops the complete picture in QCD for $\Gamma_\square$ is unknown but in planar $\mathcal{N} = 4$ super Yang-Mills the four-loop result for the difference $\gamma_G - 2B_\delta$ was found in [42]. We identify this as $\Gamma_{\square}^{\text{planar } \mathcal{N}=4}$ and quote the result here,

$$\begin{aligned}\Gamma_{\square}^{\text{planar } \mathcal{N}=4} = &- \left(\frac{\alpha_s}{\pi} C_A\right)^2 7\zeta_3 + \left(\frac{\alpha_s}{\pi} C_A\right)^3 \left(12\zeta_5 + \frac{11}{3}\zeta_2\zeta_3\right) \\ &- \left(\frac{\alpha_s}{\pi} C_A\right)^4 \left(\frac{425}{16}\zeta_7 + \frac{13}{2}\zeta_2\zeta_5 + \frac{45}{4}\zeta_3\zeta_4\right) + \mathcal{O}(\alpha_s^5)\end{aligned} \tag{4.120}$$

It is well-known that to reach the above result one can simply take the QCD result and take the limit $N_c \to \infty$ and the maximal transcendental weight term at each order in α_s. We can do this at two and three loops by looking at eqs. (4.107) and (4.119) respectively.

Above three loops, strict Casimir scaling has been proven to fail [28, 29, 38]. As such, we need to distinguish between quarks and gluons or rather particles in the fundamental and adjoint representation. We focus on the quark case. To compute $\Gamma_{\square}^{(4),q}$ we need B_δ^q and γ_G^q at four loops. The state of the art is that some colour structures are known for both B_δ^q [26, 28] and γ_G^q [27] in the planar limit, $N_c \to \infty$. Using the values in [27, 28] we can extract the following terms in that limit for $\Gamma_{\square}^{(4),q}$,

$$\begin{aligned}\Gamma_{\square}^{(4),q}|_{N_c^3 n_f} = &- \frac{247315}{55296} + \frac{51529\zeta_2}{11664} + \frac{102205\zeta_3}{31104} - \frac{7589\zeta_4}{768} \\ &- \frac{185\zeta_5}{288} - \frac{103\zeta_2\zeta_3}{144} + \frac{15611\zeta_6}{3456} + \frac{22\zeta_3^2}{9}\end{aligned} \tag{4.121}$$

$$\Gamma_{\square}^{(4),q}|_{N_c^2 n_f^2} = \frac{329069}{2239488} - \frac{22447\zeta_2}{93312} + \frac{6325\zeta_3}{7776} + \frac{35\zeta_4}{96} - \frac{107\zeta_5}{144} - \frac{11\zeta_2\zeta_3}{72} \tag{4.122}$$

$$\Gamma^{(4),q}_{\Box}|_{N_c n_f^3} = -\frac{505}{26244} - \frac{\zeta_2}{648} - \frac{25\zeta_3}{1944} + \frac{\zeta_4}{27} \tag{4.123}$$

where we have used $T_f = \frac{1}{2}$. We are unable to deduce the $N_c^4 n_f^0$ term as it is unknown for γ_G but it is known for B_δ [28]. In the planar limit $N_c \to \infty$ the quartic Casimirs $d^{(4)}_{FF} \equiv \left(d_F^{abcd}\right)^2$ contribute to the colour factor in eq. (4.121) since,

$$n_f \frac{d^{(4)}_{FF}}{N_F} = n_f T_f^4 \left(\frac{N_c^3}{6} - \frac{7N_c}{6} + \frac{4}{N_c} - \frac{3}{N_c^3} \right). \tag{4.124}$$

It means that we are unable to fully construct the Casimir scaling of $N_c^3 n_f$. The full (planar and non-planar) contribution of the quartic Casimir colour factor $d^{(4)}_{FF}$ to γ_G is known [31] but not to B_δ. Only the low-N values of the splitting functions or γ_{cusp} is known [30, 33]. In [30] it was also found that, within numerical errors, quartic Casimir contribution to the cusp anomalous dimension did not depend on the representation, i.e. it is the same for gluons and quarks. It was conjectured that although Casimir scaling is violated there is a generalised version where quartic factors are simply exchanged depending on gluon or quarks,

$$\begin{gathered} \text{quarks} \leftrightarrow \text{gluons} \\ \frac{d^{(4)}_{FA}}{N_F} \leftrightarrow \frac{d^{(4)}_{AA}}{N_A} \\ n_f \frac{d^{(4)}_{FF}}{N_F} \leftrightarrow n_f \frac{d^{(4)}_{FA}}{N_A} \end{gathered} \tag{4.125}$$

where $N_{F/A}$ denote the dimensions of the corresponding representations, namely $N_F = N_c = C_A$ and $N_A = N_c^2 - 1 = 2N_c C_F$. The relation in eq. (4.106) may be used as an interesting test for a generalised Casimir scaling extension to the anomalous dimension $\Gamma_\Box$.

However, the quartic Casimirs do not appear in the n_f^2 or n_f^3 terms of eqs. (4.122) and (4.123). We are then able to use these terms for a leading-N_c, Casimir-scaling part of $\Gamma^{(4)}_\Box$. We put these terms together with the conjectured generalised scaling to create an ansatz for $\Gamma^{(4)}_\Box$,

$$\begin{aligned} \Gamma^{(4)}_\Box = C_i \Bigg[& n_f^3 \left(-\frac{505}{13122} - \frac{\zeta_2}{324} - \frac{25\zeta_3}{972} + \frac{2\zeta_4}{27} \right) \\ & + N_c n_f^2 \left(\frac{329069}{1119744} - \frac{22447\zeta_2}{46656} + \frac{6325\zeta_3}{3888} + \frac{35\zeta_4}{48} - \frac{107\zeta_5}{72} - \frac{11\zeta_2\zeta_3}{36} \right) + \cdots \Bigg] \end{aligned}$$

$$+ n_f \frac{d^{(4)}_{Fi}}{N_i} \Gamma^{(4),dFi}_{\square} + \frac{d^{(4)}_{Ai}}{N_i} \Gamma^{(4),dAi}_{\square}, \tag{4.126}$$

where the ellipsis represents all terms subleading in N_c, including the n_f^1 and n_f^0 terms, which are not found from the quartic Casimirs when they are expanded in N_c.

4.6 Conclusion

In this chapter we have presented a detailed study of the infrared factorisation of form factors and PDFs at large x using a common formalism. By identifying the universal contributions from the hard-collinear region in both quantities, those controlled by the anomalous dimension $\gamma_{J/\mathcal{J}}$, we were able to derive the relation in eq. (4.106),

$$\boxed{\gamma_G - 2B_\delta = \Gamma_\sqcap - \Gamma_\wedge = \frac{\Gamma_\square}{4}\,.} \tag{4.127}$$

That is, the difference between anomalous dimension describing single poles in the on-shell form factor of quarks (gluons) and that associated with the $\delta(1-x)$ term in the large-x limit of the quark (gluon) diagonal DGLAP splitting function, reduces to a difference between corresponding eikonal quantities, $\Gamma_\wedge$ and $\Gamma_\sqcap$ defined directly in terms of Wilson loops. Furthermore, based on the configuration-space origin of the contributions to these two eikonal quantities we concluded that their difference simply corresponds to the anomalous dimension associated with a closed polygonal Wilson loop, such as the parallelogram analysed first in ref. [146]. The contributions of the semi-infinite Wilson lines in $W_\sqcap$ and $W_\wedge$ cancel in the difference. We emphasise that while each of the quantities on the left-hand side of eq. (4.127) depends in a non-trivial way on the spin of the partons, in addition to their colour representations, yielding very different results for quarks and for gluons, the eikonal quantities, by definition, depend only on the colour representation of these partons, and in particular admit Casimir scaling through three loops. We stress that the relation in eq. (4.127) is expected to hold to all orders in perturbation theory. An obvious next step is to compute $\Gamma_\square$ to three loops in order to check it explicitly to this order.

In establishing the relation between $\Gamma_\square$ and $\Gamma_\sqcap - \Gamma_\wedge$ we used the fact that singularities arise only from configurations where all the vertices approach a cusp or one where they all approach a particular lightlike segment [148]. This underlies

the cancellation of the two infinite segments, isolating a remaining finite segment. The very same logic may be applied to other, more complicated Wilson-line geometries involving both finite and semi-infinite lightlike segments. Specifically, the double pole is always governed by γ_{cusp} while the single-pole anomalous dimension is written as a sum of terms, building blocks, each corresponding to either a finite or semi-infinite segment, which contribute $\Gamma_{\text{co}}^{\text{fin}}$ and $\Gamma_{\text{co}}^{\text{inf}}$, respectively. An example of such a construction with only finite segments can be found in refs. [187–189], where polygons of up to six sides were computed to two loops. Following our discussion in Section 4.5.1 it may interesting to explicitly compute other Wilson-line configurations involving both finite and infinite segments. A simple example of direct relevance to physics is the non-forward amplitude, generalising the $\sqcap$ configuration.

One interesting aspect that we have encountered is that $W_{\sqcap}$ behaves very differently in the ultraviolet as compared to the infrared, as can be seen explicitly in eq. (4.103). In the ultraviolet, one encounters a double logarithmic dependence on the scale μ^2, originating from the cusp singularity, while in the infrared there is just a single pole. This stands in sharp contrast to the $W_{\wedge}$, corresponding to the soft function of the form factor (4.15) (or more generally, in soft functions corresponding to multi-leg amplitudes) where the infrared behaviour entails a double pole, mirroring the ultraviolet. The absence of any distance scale in the relevant Wilson-line contour implies such mirroring. Indeed the symmetry between the ultraviolet and the infrared is broken in $W_{\sqcap}$ due to the presence of the scale $\beta \cdot y$. The single-pole character of $W_{\sqcap}$ can be seen as intermediate in comparing $W_{\square}$, which lacking infinite rays, is infrared finite, to $W_{\wedge}$, which is double logarithmic.

The relation in eq. (4.115) between the soft anomalous dimension in Drell-Yan production and the parallelogram $W_{\square}$ is interesting in its own right. The Drell-Yan soft function involves real gluon emission diagrams where the propagators connecting the amplitude side to the complex-conjugate one are cut, while in $W_{\square}$ there are no cut propagators. A possible way to explain[5] this is to recall that a parallelogram made of four lightlike segments features two cusps where the exchanged gluons span timelike distances and two others where gluons span spacelike distances. The latter correspond to diagrams that feature in *virtual* corrections to the Drell-Yan process (these propagators are not cut). In turn, the former are naturally time-ordered, because there path-ordering coincides with

[5]We would like to thank Gregory Korchemsky for proposing this explanation.

time-ordering (just as in the case of the $W_{\sqcap}$, discussed below eq. (4.50)) and could be computed using either cut propagators or ordinary ones, giving the same answer. This way the calculation of the parallelogram can be mapped into that of the Drell-Yan soft function. It would be interesting to turn this argument into a proof relating the two Wilson line configurations directly. It would also be interesting to explore in this context the conformal mapping techniques of ref. [77, 135].

Another interesting direction to explore is the connection between partonic amplitudes in the Regge limit and anomalous dimensions of Wilson lines. In particular, one would like to derive the relation between the Regge trajectory and $W_{\wedge}$ in eq. (4.4) and understand its generalisation to higher orders.

Chapter 5

Concluding Remarks

In this thesis we studied the infrared divergent properties of scattering amplitudes by examining Wilson line correlators. The correlators appear in factorisation formula, see eqs. (1.10) and (1.20), which can be computed in perturbation theory. One main use for the study of infrared singularities is the ability to resum large logarithms that appear in special kinematic limits of processes.

Aside from the phenomenological motivation, the correlators themselves exhibit interesting mathematical structure. For non-lightlike lines we have calculated the first orders in the perturbative expansion of the n-leg soft function $\mathcal{S}_n$, defined in eq. (1.5). Although the two-loop result has been known for some time [115], in Chapter 2 we calculated it using the novel differential equations method. We found that the regulator employed complicates the resulting system. Focusing solely on the contribution to the physical quantity, the single pole, allowed for its calculation. However, if one was to employ this method at three loops we need higher order terms in the ϵ expansion and similar simplifications would not be seen.

With three loop calculations of multiple non-lightlike Wilson line correlators in mind we looked at another approach, which was called *bootstrapping*. In Chapter 3 we presented new observations on the types of functions that can appear, which extended the known work applying to multiple gluon exchange webs [64, 65]. We saw an interesting interplay between the rational and transcendental part of the functions. Bypassing the Feynman integral expansion entirely and concentrating solely on the analytical structure of the correlators is clearly the efficient method. Greater understanding of the function space, including rational factors, is needed

to limit the growth of a potential ansatz at high loop orders.

In Chapter 4 we switched attention to the factorisation of massless scattering amplitudes. Here, lightlike Wilson line correlators capture the relevant divergences. In studying an often misunderstood relation between single poles of form factors and of $\delta(1-x)$ in diagonal splitting functions, we found an intriguing result about the singular regions of these correlators, see eq. (4.113). They are completely localised, either at a cusp or collinear to a line. They do not depend on the global geometrical configuration of the lines.

Continuing to improve our understanding of Wilson line correlators, whether that be the types of functions that appear or the origin of divergences, will aid the deeper question of infrared singularities and give insights into some aspects of the rich mathematical structure of scattering amplitudes.

Appendix A

Differential Equation Details

A.1 $[1,2,1]$-web Differential Equation

In this section we give the explicit constituents of the differential equation for the $[1,2,1]$-web in eq. (2.58).

A.1.1 Uniform weight basis

The integrals in the uniform weight basis $\mathbf{g}^{[1,2,1]}$ written in terms of the $I^{[1,2,1]}$ family are

$$g_1^{[1,2,1]} = -\epsilon^2(2\epsilon-1)^2 I^{[1,2,1]}_{1111}$$

$$g_2^{[1,2,1]} = -\frac{1}{3}\epsilon(2\epsilon-1)(4\epsilon-3)(4\epsilon-1) I^{[1,2,1]}_{11001}$$

$$g_3^{[1,2,1]} = \frac{(2\epsilon-1)^2\epsilon^2 I^{[1,2,1]}_{11101}}{3(\alpha_{12}-1)} + \frac{\epsilon^2 I^{[1,2,1]}_{11102}(\alpha_{12}\epsilon+3\epsilon-1)}{6\alpha_{12}} - \frac{(2\epsilon-1)(4\epsilon-3)\epsilon I^{[1,2,1]}_{11001}(4\alpha_{12}\epsilon-\alpha_{12}-6\epsilon+1)}{6(\alpha_{12}-1)}$$

$$g_4^{[1,2,1]} = \frac{(3\epsilon-1)\epsilon^2 I^{[1,2,1]}_{11102}}{3s(\alpha_{12})} + \frac{2(\alpha_{12}+1)(2\epsilon-1)(4\epsilon-3)\epsilon^2 I^{[1,2,1]}_{11001}}{3(\alpha_{12}-1)} + \frac{2(\alpha_{12}+1)(2\epsilon-1)^2\epsilon^2 I^{[1,2,1]}_{11101}}{3(\alpha_{12}-1)}$$

$$g_5^{[1,2,1]} = \frac{\epsilon^3 I^{[1,2,1]}_{11102}}{s(\alpha_{12})} + \frac{(2\epsilon-1)\epsilon^3 I^{[1,2,1]}_{11111}}{s(\alpha_{12})}$$

$$g_6^{[1,2,1]} = \frac{\epsilon^3(2\epsilon-1) I^{[1,2,1]}_{111101}}{s(\alpha_{23})}$$

$$g_7^{[1,2,1]} = -\frac{(2\epsilon-1)\epsilon^2 I^{[1,2,1]}_{110011}\left(\alpha_{23}^2\epsilon-3\epsilon+1\right)}{3(\alpha_{23}-1)\alpha_{23}} - \frac{\epsilon^2 I^{[1,2,1]}_{110012}(\alpha_{23}\epsilon+3\epsilon-1)}{6\alpha_{23}} - \frac{(2\epsilon-1)(4\epsilon-3)\epsilon I^{[1,2,1]}_{11001}(4\alpha_{23}\epsilon-\alpha_{23}-6\epsilon+1)}{6(\alpha_{23}-1)}$$

$$g_8^{[1,2,1]} = \frac{2(\alpha_{23}+1)(2\epsilon-1)\epsilon^2 I^{[1,2,1]}_{110011}\left(3\alpha_{23}^2\epsilon-\alpha_{23}^2-4\alpha_{23}\epsilon+\alpha_{23}+3\epsilon-1\right)}{3(\alpha_{23}-1)\alpha_{23}} - \frac{(3\epsilon-1)\epsilon^2 I^{[1,2,1]}_{110012}}{3s(\alpha_{23})} + \frac{2(\alpha_{23}+1)(2\epsilon-1)(4\epsilon-3)\epsilon^2 I^{[1,2,1]}_{11001}}{3(\alpha_{23}-1)}$$

$$g_9^{[1,2,1]} = \frac{(\alpha_{12}-1)\epsilon^3 I^{[1,2,1]}_{111021}}{2\alpha_{12}s(\alpha_{23})} + \frac{(4\epsilon-1)\epsilon^3 I^{[1,2,1]}_{111011}}{2s(\alpha_{23})} + \frac{\epsilon^3 I^{[1,2,1]}_{111012}}{2s(\alpha_{23})}$$

$$g_{10}^{[1,2,1]} = -\frac{\epsilon^3 I^{[1,2,1]}_{111021}}{2\alpha_{23}s(\alpha_{12})} - \frac{\epsilon^3 I^{[1,2,1]}_{111012}}{2s(\alpha_{12})}$$

$$g_{11}^{[1,2,1]} = \frac{3\epsilon^3 I^{[1,2,1]}_{111021}}{4s(\alpha_{12})s(\alpha_{23})}$$

$$g_{12}^{[1,2,1]} = \frac{\epsilon^4 I^{[1,2,1]}_{111111}}{s(\alpha_{12})s(\alpha_{23})}$$

A.1.2 Matrices

The dlog matrices $c_i^{[1,2,1]}$ corresponding to the uniform weight basis in eq. (2.59) are

$$c_1^{[1,2,1]} = \begin{pmatrix}
0&0&0&0&0&0&0&0&0&0&0&0\\
0&0&0&0&0&0&0&0&0&0&0&0\\
0&0&-2&0&0&0&0&0&0&0&0&0\\
0&0&0&-2&0&0&0&0&0&0&0&0\\
0&0&0&0&2&0&0&0&0&0&0&0\\
0&0&0&0&0&0&0&0&0&0&0&0\\
0&0&0&0&0&0&0&0&0&0&0&0\\
0&0&0&0&0&0&0&0&0&0&0&0\\
0&0&0&0&0&0&0&0&0&0&-\frac{2}{3}&0\\
0&0&0&0&0&0&0&0&0&2&0&0\\
0&0&0&0&0&0&0&0&0&0&2&0\\
0&0&0&0&0&0&0&0&0&0&0&2
\end{pmatrix} \qquad c_2^{[1,2,1]} = \begin{pmatrix}
0&0&0&0&0&0&0&0&0&0&0&0\\
0&0&0&0&0&0&0&0&0&0&0&0\\
0&1&0&-\frac{1}{2}&0&0&0&0&0&0&0&0\\
0&4&-4&1&0&0&0&0&0&0&0&0\\
-2&-6&12&-3&-2&0&0&0&0&0&0&0\\
0&0&0&0&0&0&0&0&0&0&0&0\\
0&0&0&0&0&0&0&0&0&0&0&0\\
0&0&0&0&0&0&0&0&0&0&0&0\\
0&0&0&0&0&0&0&-\frac{3}{2}&0&0&\frac{2}{3}&0\\
-\frac{1}{2}&0&3&-\frac{3}{2}&0&0&-3&0&-1&-1&-\frac{2}{3}&0\\
0&0&0&0&0&0&0&\frac{9}{4}&3&0&1&0\\
0&0&0&0&0&2&0&0&-4&0&-\frac{4}{3}&-2
\end{pmatrix} \tag{A.1a}$$

$$c_3^{[1,2,1]} = \begin{pmatrix}
0&0&0&0&0&0&0&0&0&0&0&0\\
0&0&0&0&0&0&0&0&0&0&0&0\\
0&0&0&\frac{1}{2}&0&0&0&0&0&0&0&0\\
0&0&0&2&0&0&0&0&0&0&0&0\\
0&0&0&0&2&0&0&0&0&0&0&0\\
0&0&0&0&0&0&0&0&0&0&0&0\\
0&0&0&0&0&0&0&0&0&0&0&0\\
0&0&0&0&0&0&0&0&0&0&0&0\\
0&0&0&0&0&0&0&0&0&0&-\frac{2}{3}&0\\
0&0&0&0&0&0&0&0&0&2&0&0\\
0&0&0&0&0&0&0&0&0&0&2&0\\
0&0&0&0&0&0&0&0&0&0&0&2
\end{pmatrix} \qquad c_4^{[1,2,1]} = \begin{pmatrix}
0&0&0&0&0&0&0&0&0&0&0&0\\
0&0&0&0&0&0&0&0&0&0&0&0\\
0&0&0&0&0&0&0&0&0&0&0&0\\
0&0&0&0&0&0&0&0&0&0&0&0\\
0&0&0&0&0&0&0&0&0&0&0&0\\
0&0&0&0&0&0&0&0&0&0&0&0\\
0&0&0&0&0&0&0&-2&0&0&0&0\\
0&0&0&0&0&0&0&0&-2&0&0&0\\
0&0&0&0&0&0&0&0&2&0&0&0\\
0&0&0&0&0&0&0&0&0&0&-\frac{2}{3}&0\\
0&0&0&0&0&0&0&0&0&0&2&0\\
0&0&0&0&0&0&0&0&0&0&-\frac{4}{3}&0
\end{pmatrix} \tag{A.1b}$$

$$c_5^{[1,2,1]}=\begin{pmatrix}
0&0&0&0&0&0&0&0&0&0&0&0\\
0&0&0&0&0&0&0&0&0&0&0&0\\
0&0&0&0&0&0&0&0&0&0&0&0\\
0&0&0&0&0&0&0&0&0&0&0&0\\
0&0&0&0&0&0&0&0&0&0&0&0\\
-2&0&0&0&0&-1&0&0&0&0&0&0\\
0&1&0&0&0&0&0&-\frac{1}{2}&0&0&0&0\\
0&4&0&0&0&0&-4&1&0&0&0&0\\
-\frac{1}{2}&0&-3&0&0&0&3&-\frac{3}{2}&-1&-1&-\frac{2}{3}&0\\
0&0&0&-\frac{3}{2}&0&0&0&0&0&0&\frac{2}{3}&0\\
0&0&0&\frac{9}{4}&0&0&0&0&0&3&1&0\\
0&0&0&0&1&0&0&0&0&2&\frac{4}{3}&-1
\end{pmatrix}
\qquad
c_6^{[1,2,1]}=\begin{pmatrix}
0&0&0&0&0&0&0&0&0&0&0&0\\
0&0&0&0&0&0&0&0&0&0&0&0\\
0&0&0&0&0&0&0&0&0&0&0&0\\
0&0&0&0&0&0&0&0&0&0&0&0\\
0&0&0&0&0&0&0&0&0&0&0&0\\
0&0&0&0&0&0&2&0&0&0&0&0\\
0&0&0&0&0&0&0&\frac{1}{2}&0&0&0&0\\
0&0&0&0&0&0&0&2&0&0&0&0\\
0&0&0&0&0&0&0&0&2&0&0&0\\
0&0&0&0&0&0&0&0&0&0&-\frac{2}{3}&0\\
0&0&0&0&0&0&0&0&0&0&2&0\\
0&0&0&0&0&0&0&0&0&0&0&2
\end{pmatrix}$$

(A.1c)

$$c_7^{[1,2,1]}=\begin{pmatrix}
0&0&0&0&0&0&0&0&0&0&0&0\\
0&0&0&0&0&0&0&0&0&0&0&0\\
0&0&0&0&0&0&0&0&0&0&0&0\\
0&0&0&0&0&0&0&0&0&0&0&0\\
0&0&0&0&0&0&0&0&0&0&0&0\\
0&0&0&0&0&0&0&0&0&0&0&0\\
0&0&0&0&0&0&0&0&0&0&0&0\\
0&0&0&0&0&0&0&0&0&0&0&0\\
-\frac{1}{2}&-3&3&0&0&0&3&0&-1&-1&0&0\\
-\frac{1}{2}&-3&3&0&0&0&3&0&-1&-1&0&0\\
\frac{3}{4}&\frac{9}{2}&-\frac{9}{2}&0&0&0&-\frac{9}{2}&0&\frac{3}{2}&\frac{3}{2}&0&0\\
0&0&0&0&0&0&0&0&0&0&0&0
\end{pmatrix}
\qquad
c_8^{[1,2,1]}=\begin{pmatrix}
0&0&0&0&0&0&0&0&0&0&0&0\\
0&0&0&0&0&0&0&0&0&0&0&0\\
0&0&0&0&0&0&0&0&0&0&0&0\\
0&0&0&0&0&0&0&0&0&0&0&0\\
0&0&0&0&0&0&0&0&0&0&0&0\\
0&0&0&0&0&0&0&0&0&0&0&0\\
0&0&0&0&0&0&0&0&0&0&0&0\\
0&0&0&0&0&0&0&0&0&0&0&0\\
0&0&0&0&0&0&0&0&0&0&0&0\\
\frac{1}{2}&3&-3&\frac{3}{2}&0&0&-3&0&1&-1&\frac{2}{3}&0\\
-\frac{3}{4}&-\frac{9}{2}&\frac{9}{2}&-\frac{9}{4}&0&0&\frac{9}{2}&0&-\frac{3}{2}&\frac{3}{2}&-1&0\\
0&0&0&0&0&0&0&0&0&0&0&0
\end{pmatrix}$$

(A.1d)

$$c_9^{[1,2,1]}=\begin{pmatrix}
0&0&0&0&0&0&0&0&0&0&0&0\\
0&0&0&0&0&0&0&0&0&0&0&0\\
0&0&0&0&0&0&0&0&0&0&0&0\\
0&0&0&0&0&0&0&0&0&0&0&0\\
0&0&0&0&0&0&0&0&0&0&0&0\\
0&0&0&0&0&0&0&0&0&0&0&0\\
0&0&0&0&0&0&0&0&0&0&0&0\\
0&0&0&0&0&0&0&0&0&0&0&0\\
\frac{1}{2}&3&-3&0&0&0&-3&\frac{3}{2}&-1&1&\frac{2}{3}&0\\
0&0&0&0&0&0&0&0&0&0&0&0\\
-\frac{3}{4}&-\frac{9}{2}&\frac{9}{2}&0&0&0&\frac{9}{2}&-\frac{9}{4}&\frac{3}{2}&-\frac{3}{2}&-1&0\\
0&0&0&0&0&0&0&0&0&0&0&0
\end{pmatrix}
\qquad
c_{10}^{[1,2,1]}=\begin{pmatrix}
0&0&0&0&0&0&0&0&0&0&0&0\\
0&0&0&0&0&0&0&0&0&0&0&0\\
0&0&0&0&0&0&0&0&0&0&0&0\\
0&0&0&0&0&0&0&0&0&0&0&0\\
0&0&0&0&0&0&0&0&0&0&0&0\\
0&0&0&0&0&0&0&0&0&0&0&0\\
0&0&0&0&0&0&0&0&0&0&0&0\\
0&0&0&0&0&0&0&0&0&0&0&0\\
0&0&0&0&0&0&0&0&0&0&0&0\\
0&0&0&0&0&0&0&0&0&0&0&0\\
\frac{3}{4}&\frac{9}{2}&-\frac{9}{2}&\frac{9}{4}&0&0&-\frac{9}{2}&\frac{9}{4}&-\frac{3}{2}&-\frac{3}{2}&-2&0\\
0&0&0&0&0&0&0&0&0&0&0&0
\end{pmatrix}$$

(A.1e)

A.1.3 ϵ^4 term of $g_{12}^{[1,2,1]}$

The integral $g_{12}^{[1,2,1]}$ evaluates to eqs. (2.67) and (2.68) at order ϵ^2 and ϵ^3 respectively. The order ϵ^4 result is

$$
\begin{aligned}
g_{12}^{[1,2,1],(4)} = & -8\zeta_3(5G(0,\alpha_{12})+G(0,\alpha_{23})-2G(1,\alpha_{23}))+32G(-1,-1,0,\alpha_{12})G(0,\alpha_{23}) \\
& -32G(-1,0,0,\alpha_{12})G(0,\alpha_{23})+32G(-1,1,0,\alpha_{12})G(0,\alpha_{23})-32G(0,-1,0,\alpha_{12})G(0,\alpha_{23}) \\
& -32G(0,1,0,\alpha_{12})G(0,\alpha_{23})+16G(0,\alpha_{23})G\left(0,\tfrac{1}{1-\alpha_{23}},0,\alpha_{12}\right)-16G(0,\alpha_{23})G(0,1-\alpha_{23},0,\alpha_{12}) \\
& -16G(0,\alpha_{23})G\left(0,\tfrac{\alpha_{23}-1}{\alpha_{23}},0,\alpha_{12}\right)+16G(0,\alpha_{23})G\left(0,\tfrac{\alpha_{23}}{\alpha_{23}-1},0,\alpha_{12}\right) \\
& +32G(1,-1,0,\alpha_{12})G(0,\alpha_{23})-32G(1,0,0,\alpha_{12})G(0,\alpha_{23})+32G(1,1,0,\alpha_{12})G(0,\alpha_{23}) \\
& -\tfrac{8}{3}i\pi^3(G(0,\alpha_{12})-G(1,\alpha_{23}))+16G(0,0,\alpha_{12})(G(0,0,\alpha_{23})-2G(-1,0,\alpha_{23})) \\
& +\tfrac{4}{3}\pi^2\Big(G(0,\alpha_{12})(3G(0,\alpha_{23})+2i\pi)+2G\left(0,\tfrac{1}{1-\alpha_{23}},\alpha_{12}\right)+2G(0,1-\alpha_{23},\alpha_{12})-2G\left(0,\tfrac{\alpha_{23}-1}{\alpha_{23}},\alpha_{12}\right) \\
& \qquad -2G\left(0,\tfrac{\alpha_{23}}{\alpha_{23}-1},\alpha_{12}\right)-2i\pi G(1,\alpha_{23})+2G(0,0,\alpha_{23})-2G(0,1,\alpha_{23})-2G(1,0,\alpha_{23})+\pi^2\Big) \\
& +32G(-1,0,\alpha_{12})(G(-1,0,\alpha_{23})-G(1,0,\alpha_{23}))+32G(1,0,\alpha_{12})(G(-1,0,\alpha_{23})-G(1,0,\alpha_{23})) \\
& -16(G(0,0,\alpha_{23})-G(1,0,\alpha_{23}))G\left(0,\tfrac{\alpha_{23}-1}{\alpha_{23}},\alpha_{12}\right)-16(G(0,0,\alpha_{23})-G(1,0,\alpha_{23}))G\left(0,\tfrac{\alpha_{23}}{\alpha_{23}-1},\alpha_{12}\right) \\
& +16G(1,0,\alpha_{23})G\left(0,\tfrac{1}{1-\alpha_{23}},\alpha_{12}\right)+16G(1,0,\alpha_{23})G(0,1-\alpha_{23},\alpha_{12}) \\
& -\tfrac{8}{3}\pi^2\Big(-3G(0,\alpha_{12})G(-1,\alpha_{23})+G(0,\alpha_{12})G(0,\alpha_{23})+G(0,\alpha_{12})G(1,\alpha_{23})+G(-1,\alpha_{12})G(0,\alpha_{23}) \\
& \quad +G(1,\alpha_{12})G(0,\alpha_{23})+2G(0,1-\alpha_{23},\alpha_{12})+2G\left(0,\tfrac{\alpha_{23}}{\alpha_{23}-1},\alpha_{12}\right)-3G(-1,0,\alpha_{12})+G(0,0,\alpha_{12}) \\
& \qquad -3G(1,0,\alpha_{12})+G(-1,0,\alpha_{23})-2G(0,0,\alpha_{23})+3G(1,0,\alpha_{23})-2G(1,1,\alpha_{23})\Big) \\
& +16G(0,\alpha_{12})(2G(-1,-1,0,\alpha_{23})-2G(-1,1,0,\alpha_{23})+G(0,1,0,\alpha_{23})-2G(1,-1,0,\alpha_{23}) \\
& \qquad +G(1,0,0,\alpha_{23}))+16G\left(0,\tfrac{1}{1-\alpha_{23}},0,0,\alpha_{12}\right) \\
& -16G\left(0,\tfrac{1}{1-\alpha_{23}},1,0,\alpha_{12}\right)+16G(0,1-\alpha_{23},1,0,\alpha_{12})-16G\left(0,\tfrac{\alpha_{23}-1}{\alpha_{23}},1,0,\alpha_{12}\right) \\
& -16G\left(0,\tfrac{\alpha_{23}}{\alpha_{23}-1},0,0,\alpha_{12}\right)+16G\left(0,\tfrac{\alpha_{23}}{\alpha_{23}-1},1,0,\alpha_{12}\right)+64\log^2(2)G(0,\alpha_{12})G(0,\alpha_{23}) \\
& +\tfrac{16}{3}\log(2)\left(\left(-12G(-1,0,\alpha_{12})+12G(0,0,\alpha_{12})-12G(1,0,\alpha_{12})+\pi^2\right)G(0,\alpha_{23})\right. \\
& \qquad \left.-3G(0,\alpha_{12})\left(4G(-1,0,\alpha_{23})-4G(1,0,\alpha_{23})+\pi^2\right)\right) \\
& +16G(0,0,0,0,\alpha_{23})-16G(0,0,1,0,\alpha_{23})-16G(0,1,0,0,\alpha_{23})+16G(0,1,1,0,\alpha_{23}) \\
& -16G(1,0,0,0,\alpha_{23})+16G(1,0,1,0,\alpha_{23})+16G(1,1,0,0,\alpha_{23})-32G(1,1,1,0,\alpha_{23})+\tfrac{4\pi^4}{15}
\end{aligned}
$$

which has been checked numerically using `pySecDec` [129].

A.2 $[3gv]$-web Differential Equation

In this section we solve the lower sectors of the $[3gv]$-web system. One set of basis integrals for this 20-dimensional system are the first 20 integrals in eq. (2.92). We shall label these 20 as $\mathbf{f}^{[3gv]}$. Proceeding as before we find a transformation to a uniform weight basis $\mathbf{f}^{[3gv]} = T\mathbf{g}^{[3gv]}$. The new basis satisfies the differential equation

$$
\mathrm{d}\mathbf{g}^{[3gv]} = \sum_{i=1}^{|\mathcal{A}^{[3gv]}|} c_i \mathrm{d}\log\left(\mathcal{A}_i^{[3gv]}\right)\mathbf{g}^{[3gv]}. \tag{A.2}
$$

The alphabet is

$$\begin{aligned}\mathcal{A}^{[3gv]} =\{&\alpha_{12}-1,\alpha_{12},\alpha_{12}+1,\alpha_{13}-1,\alpha_{13},\alpha_{13}+1,\alpha_{12}+\alpha_{13}-1,\alpha_{12}\alpha_{13}-\alpha_{12}+1,\\ &\alpha_{12}\alpha_{13}-\alpha_{13}+1,\alpha_{12}\alpha_{13}-\alpha_{12}-\alpha_{13},\alpha_{23}-1,\alpha_{23},\alpha_{23}+1,\alpha_{12}+\alpha_{23}-1,\\ &\alpha_{13}+\alpha_{23}-1,\alpha_{12}\alpha_{23}-\alpha_{12}+1,\alpha_{12}\alpha_{23}-\alpha_{23}+1,\alpha_{12}\alpha_{23}-\alpha_{12}-\alpha_{23},\\ &\alpha_{13}\alpha_{23}-\alpha_{13}+1,\alpha_{13}\alpha_{23}-\alpha_{23}+1,\alpha_{13}\alpha_{23}-\alpha_{13}-\alpha_{23}\}\end{aligned} \tag{A.3}$$

with $|\mathcal{A}^{[3gv]}|= 21$. Note that this is just the alphabet for the lower integrals. The 20 uniform weight integals are

$$g_1^{[3gv]} = \frac{1}{3}\epsilon\left(32\epsilon^3-48\epsilon^2+22\epsilon-3\right)I_{0111}^{[3gv]}$$

$$g_2^{[3gv]} = (1-2\epsilon)^2\epsilon^2 I_{11011}^{[3gv]} - \frac{1}{3}\epsilon(2\epsilon-1)\left(16\epsilon^2-16\epsilon+3\right)I_{0111}^{[3gv]}$$

$$g_3^{[3gv]} = -\frac{(1-2\epsilon)^2\epsilon^2 I_{10111}^{[3gv]}}{3(\alpha_{12}-1)} - \frac{\epsilon^2 I_{10112}^{[3gv]}((\alpha_{12}+3)\epsilon-1)}{6\alpha_{12}} + \frac{\left(8\epsilon^2-10\epsilon+3\right)\epsilon I_{0111}^{[3gv]}(\alpha_{12}(4\epsilon-1)-6\epsilon+1)}{6(\alpha_{12}-1)}$$

$$g_4^{[3gv]} = -\frac{2(\alpha_{12}+1)\left(8\epsilon^2-10\epsilon+3\right)\epsilon^2 I_{0111}^{[3gv]}}{3(\alpha_{12}-1)} - \frac{2(\alpha_{12}+1)(1-2\epsilon)^2\epsilon^2 I_{10111}^{[3gv]}}{3(\alpha_{12}-1)} - \frac{(3\epsilon-1)\epsilon^2 I_{10112}^{[3gv]}}{3s(\alpha_{12})}$$

$$g_5^{[3gv]} = -\frac{\epsilon^4 I_{11111}^{[3gv]}}{s(\alpha_{12})}$$

$$g_6^{[3gv]} = -\frac{(1-2\epsilon)^2\epsilon^2 I_{110101}^{[3gv]}}{3(\alpha_{13}-1)} - \frac{\epsilon^2 I_{110102}^{[3gv]}((\alpha_{13}+3)\epsilon-1)}{6\alpha_{13}} + \frac{\left(8\epsilon^2-10\epsilon+3\right)\epsilon I_{0111}^{[3gv]}(\alpha_{13}(4\epsilon-1)-6\epsilon+1)}{6(\alpha_{13}-1)}$$

$$g_7^{[3gv]} = -\frac{2(\alpha_{13}+1)\left(8\epsilon^2-10\epsilon+3\right)\epsilon^2 I_{0111}^{[3gv]}}{3(\alpha_{13}-1)} - \frac{2(\alpha_{13}+1)(1-2\epsilon)^2\epsilon^2 I_{110101}^{[3gv]}}{3(\alpha_{13}-1)} - \frac{(3\epsilon-1)\epsilon^2 I_{110102}^{[3gv]}}{3s(\alpha_{13})}$$

$$g_8^{[3gv]} = -\frac{\epsilon^4 I_{111101}^{[3gv]}}{s(\alpha_{13})}$$

$$g_9^{[3gv]} = -\frac{(1-2\epsilon)^2\epsilon^2 I_{110011}^{[3gv]}}{3(\alpha_{23}-1)} - \frac{\epsilon^2 I_{110012}^{[3gv]}((\alpha_{23}+3)\epsilon-1)}{6\alpha_{23}} + \frac{\left(8\epsilon^2-10\epsilon+3\right)\epsilon I_{0111}^{[3gv]}(\alpha_{23}(4\epsilon-1)-6\epsilon+1)}{6(\alpha_{23}-1)}$$

$$g_{10}^{[3gv]} = -\frac{2(\alpha_{23}+1)\left(8\epsilon^2-10\epsilon+3\right)\epsilon^2 I_{0111}^{[3gv]}}{3(\alpha_{23}-1)} - \frac{2(\alpha_{23}+1)(1-2\epsilon)^2\epsilon^2 I_{110011}^{[3gv]}}{3(\alpha_{23}-1)} - \frac{(3\epsilon-1)\epsilon^2 I_{110012}^{[3gv]}}{3s(\alpha_{23})}$$

$$g_{11}^{[3gv]} = -\frac{\epsilon^4 I_{111011}^{[3gv]}}{s(\alpha_{23})}$$

$$g_{12}^{[3gv]} = \frac{(\alpha_{13}-1)\epsilon^3 I_{110112}^{[3gv]}}{2\alpha_{13}s(\alpha_{23})} + \frac{(4\epsilon-1)\epsilon^3 I_{110111}^{[3gv]}}{2s(\alpha_{23})} + \frac{\epsilon^3 I_{110121}^{[3gv]}}{2s(\alpha_{23})}$$

$$g_{13}^{[3gv]} = \frac{3\epsilon^3 I_{110112}^{[3gv]}}{4s(\alpha_{13})s(\alpha_{23})}$$

$$g_{14}^{[3gv]} = -\frac{\epsilon^3 I_{110112}^{[3gv]}}{2\alpha_{23}s(\alpha_{13})} - \frac{\epsilon^3 I_{110121}^{[3gv]}}{2s(\alpha_{13})}$$

$$g_{15}^{[3gv]} = \frac{(\alpha_{23}-1)\epsilon^3 I_{101121}^{[3gv]}}{2\alpha_{23} s(\alpha_{12})} + \frac{(4\epsilon-1)\epsilon^3 I_{101111}^{[3gv]}}{2s(\alpha_{12})} + \frac{\epsilon^3 I_{101211}^{[3gv]}}{2s(\alpha_{12})}$$

$$g_{16}^{[3gv]} = \frac{3\epsilon^3 I_{101121}^{[3gv]}}{4s(\alpha_{12})s(\alpha_{23})}$$

$$g_{17}^{[3gv]} = -\frac{\epsilon^3 I_{101121}^{[3gv]}}{2\alpha_{12} s(\alpha_{23})} - \frac{\epsilon^3 I_{101211}^{[3gv]}}{2s(\alpha_{23})}$$

$$g_{18}^{[3gv]} = \frac{(\alpha_{12}-1)\epsilon^3 I_{011211}^{[3gv]}}{2\alpha_{12} s(\alpha_{13})} + \frac{(4\epsilon-1)\epsilon^3 I_{011111}^{[3gv]}}{2s(\alpha_{13})} + \frac{\epsilon^3 I_{011112}^{[3gv]}}{2s(\alpha_{13})}$$

$$g_{19}^{[3gv]} = -\frac{\epsilon^3 I_{011211}^{[3gv]}}{2\alpha_{13} s(\alpha_{12})} - \frac{\epsilon^3 I_{011112}^{[3gv]}}{2s(\alpha_{12})}$$

$$g_{20}^{[3gv]} = \frac{3\epsilon^3 I_{011211}^{[3gv]}}{4s(\alpha_{12})s(\alpha_{13})}$$

The boundary for solving the system is chosen to be $\alpha_{12} = 1$, $\alpha_{13} = 1$ and $\alpha_{23} = 1$. Defining the boundary vector $\mathbf{b}^{[3gv]}$ to be $\mathbf{g}^{[3gv]}$ evaluated at the boundary we find

$$\begin{aligned} b_1^{[3gv]} =& -\frac{2}{3} + \frac{8}{3}\epsilon\log(2) + \epsilon^2\left(-\pi^2 - \frac{16}{3}\log^2(2)\right) \\ &+ \epsilon^3\left(\frac{124\zeta_3}{9} + \frac{64\log^3(2)}{9} + 4\pi^2\log(2)\right) + \mathcal{O}(\epsilon^4) \qquad \text{(A.4a)} \\ b_2^{[3gv]} =& \frac{14}{3} - \frac{56}{3}\epsilon\log(2) + \epsilon^2\left(\frac{13\pi^2}{3} + \frac{112\log^2(2)}{3}\right) \\ &+ \epsilon^3\left(-\frac{292\zeta_3}{9} - \frac{448}{9}\log^3(2) - \frac{52}{3}\pi^2\log(2)\right) + \mathcal{O}(\epsilon^4) \qquad \text{(A.4b)} \\ b_i^{[3gv]} =& \mathcal{O}(\epsilon^4) \qquad \forall i \geq 3 \qquad \text{(A.4c)} \end{aligned}$$

and, as a simple check, we notice that they are of uniform weight. The specific matrices that appear in eq. (A.2) are

$$c_1^{[3gv]} = \begin{pmatrix}
0&0&0&0&0&0&0&0&0&0&0&0&0&0&0&0&0&0&0&0\\
0&0&0&0&0&0&0&0&0&0&0&0&0&0&0&0&0&0&0&0\\
0&0&-2&0&0&0&0&0&0&0&0&0&0&0&0&0&0&0&0&0\\
0&0&0&-2&0&0&0&0&0&0&0&0&0&0&0&0&0&0&0&0\\
0&0&0&0&2&0&0&0&0&0&0&0&0&0&0&0&0&0&0&0\\
0&0&0&0&0&0&0&0&0&0&0&0&0&0&0&0&0&0&0&0\\
0&0&0&0&0&0&0&0&0&0&0&0&0&0&0&0&0&0&0&0\\
0&0&0&0&0&0&0&0&0&0&0&0&0&0&0&0&0&0&0&0\\
0&0&0&0&0&0&0&0&0&0&0&0&0&0&0&0&0&0&0&0\\
0&0&0&0&0&0&0&0&0&0&0&0&0&0&0&0&0&0&0&0\\
0&0&0&0&0&0&0&0&0&0&0&0&0&0&0&0&0&0&0&0\\
0&0&0&0&0&0&0&0&0&0&0&0&0&0&0&0&0&0&0&0\\
0&0&0&0&0&0&0&0&0&0&0&0&0&0&0&0&0&0&0&0\\
0&0&0&0&0&0&0&0&0&0&0&0&0&0&0&0&0&0&0&0\\
0&0&0&0&0&0&0&0&0&0&0&0&0&0&2&0&0&0&0&0\\
0&0&0&0&0&0&0&0&0&0&0&0&0&0&0&2&0&0&0&0\\
0&0&0&0&0&0&0&0&0&0&0&0&0&0&0&-\frac{2}{3}&0&0&0&0\\
0&0&0&0&0&0&0&0&0&0&0&0&0&0&0&0&0&0&0&-\frac{2}{3}\\
0&0&0&0&0&0&0&0&0&0&0&0&0&0&0&0&0&0&2&0\\
0&0&0&0&0&0&0&0&0&0&0&0&0&0&0&0&0&0&0&2
\end{pmatrix} \qquad c_2^{[3gv]} = \begin{pmatrix}
0&0&0&0&0&0&0&0&0&0&0&0&0&0&0&0&0&0&0&0\\
0&0&0&0&0&0&0&0&0&0&0&0&0&0&0&0&0&0&0&0\\
1&0&0&-\frac{1}{2}&0&0&0&0&0&0&0&0&0&0&0&0&0&0&0&0\\
4&0&-4&1&0&0&0&0&0&0&0&0&0&0&0&0&0&0&0&0\\
\frac{7}{2}&\frac{1}{2}&-6&\frac{3}{2}&-2&0&0&0&0&0&0&0&0&0&0&0&0&0&0&0\\
0&0&0&0&0&0&0&0&0&0&0&0&0&0&0&0&0&0&0&0\\
0&0&0&0&0&0&0&0&0&0&0&0&0&0&0&0&0&0&0&0\\
0&0&0&0&0&0&0&0&0&0&0&0&0&0&0&0&0&0&0&0\\
0&0&0&0&0&0&0&0&0&0&0&0&0&0&0&0&0&0&0&0\\
0&0&0&0&0&0&0&0&0&0&0&0&0&0&0&0&0&0&0&0\\
0&0&0&0&0&0&0&0&0&0&0&0&0&0&0&0&0&0&0&0\\
0&0&0&0&0&0&0&0&0&0&0&0&0&0&0&0&0&0&0&0\\
0&0&0&0&0&0&0&0&0&0&0&0&0&0&0&0&0&0&0&0\\
0&0&0&0&0&0&0&0&0&0&0&0&0&0&0&0&0&0&0&0\\
\frac{1}{2}&\frac{1}{2}&-3&\frac{3}{2}&0&0&0&0&3&0&0&0&0&0&-1&-\frac{2}{3}&-1&0&0&0\\
0&0&0&0&0&0&0&0&0&-\frac{9}{4}&0&0&0&0&0&1&3&0&0&0\\
0&0&0&0&0&0&0&0&0&\frac{3}{2}&0&0&0&0&0&\frac{2}{3}&0&0&0&0\\
0&0&0&0&0&0&\frac{3}{2}&0&0&0&0&0&0&0&0&0&0&0&0&\frac{2}{3}\\
\frac{1}{2}&\frac{1}{2}&-3&\frac{3}{2}&0&3&0&0&0&0&0&0&0&0&0&0&0&-1&-1&-\frac{2}{3}\\
0&0&0&0&0&0&-\frac{9}{4}&0&0&0&0&0&0&0&0&0&0&3&0&1
\end{pmatrix}$$

(A.5a)

$$c_3^{[3gv]}=$$

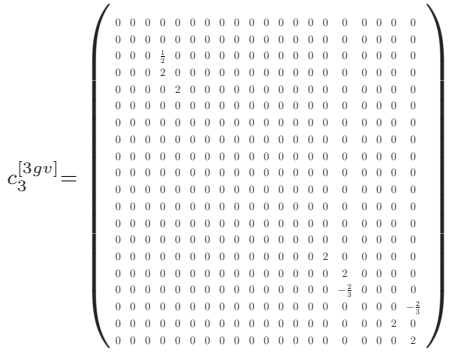

$$c_4^{[3gv]}=$$

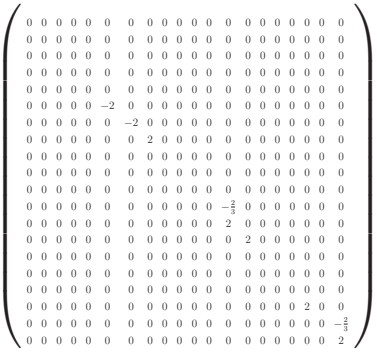

(A.5b)

$$c_5^{[3gv]}=$$

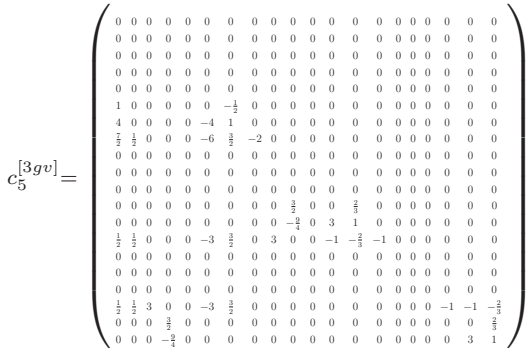

$$c_6^{[3gv]}=$$

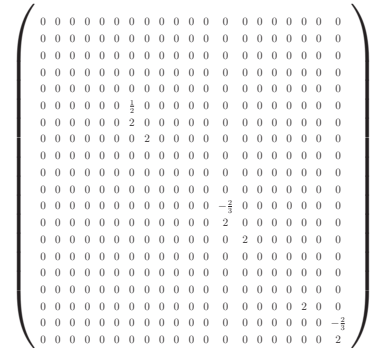

(A.5c)

$$c_7^{[3gv]}=$$

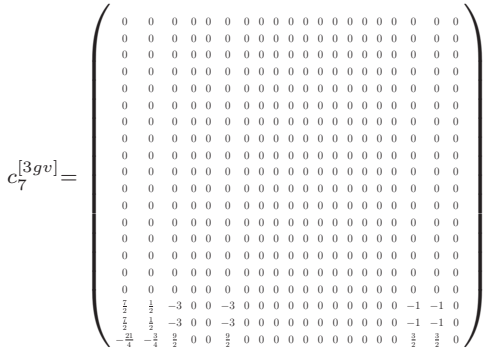

$$c_8^{[3gv]}=$$

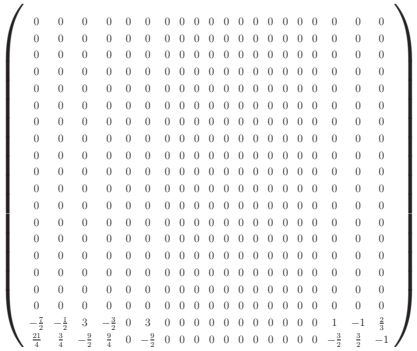

(A.5d)

$$c_9^{[3gv]}=$$

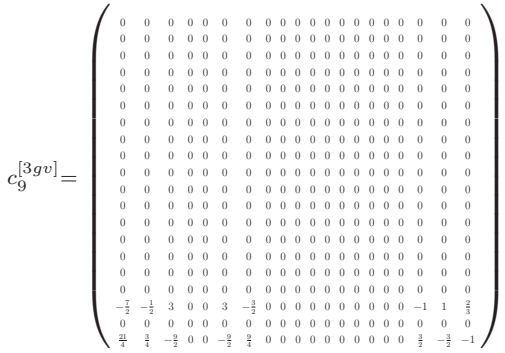

$$c_{10}^{[3gv]}=$$

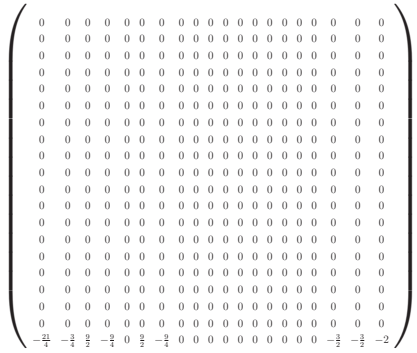

(A.5e)

$$c_{11}^{[3gv]}=$$

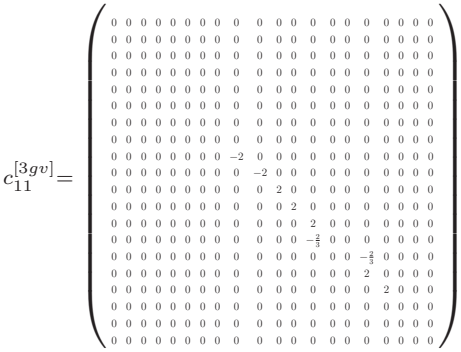

$$c_{12}^{[3gv]}=$$

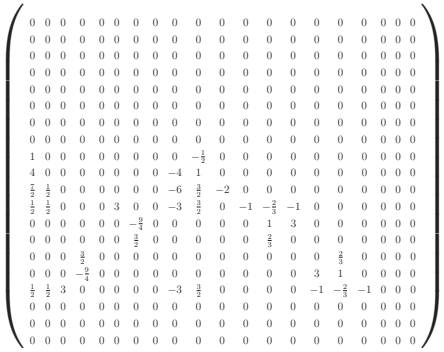

(A.5f)

$$c_{13}^{[3gv]}=$$

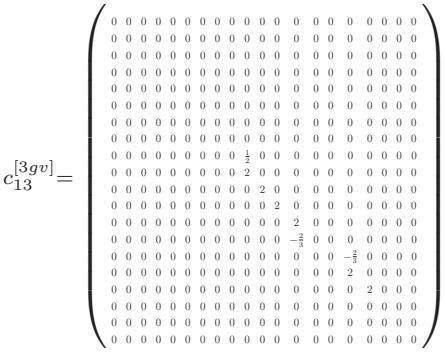

$$c_{14}^{[3gv]}=$$

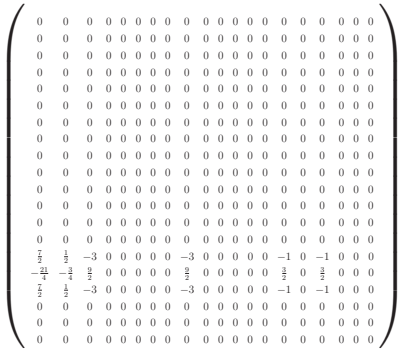

(A.5g)

$$c_{15}^{[3gv]}=$$

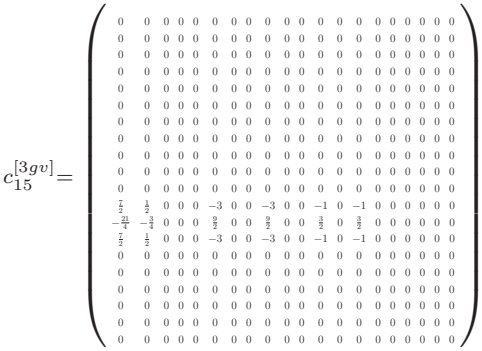

$$c_{16}^{[3gv]}=$$

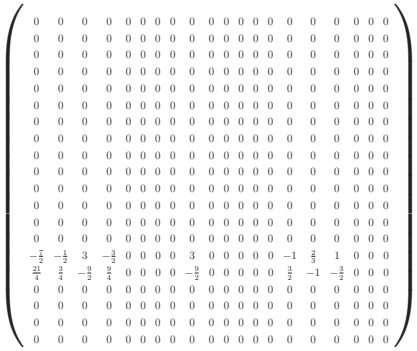

(A.5h)

$$c_{17}^{[3gv]}=$$

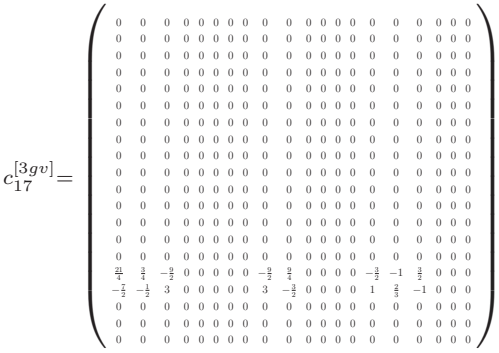

$$c_{18}^{[3gv]}=$$

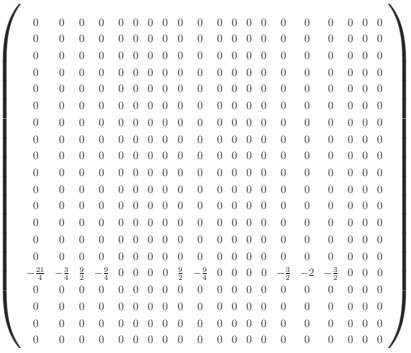

(A.5i)

$$c_{19}^{[3gv]}=\left(\begin{array}{cccccccccccccccccccc}
0 & 0 & 0 & 0 & 0 & 0 & 0 & 0 & 0 & 0 & 0 & 0 & 0 & 0 & 0 & 0 & 0 & 0 & 0 & 0 \\
0 & 0 & 0 & 0 & 0 & 0 & 0 & 0 & 0 & 0 & 0 & 0 & 0 & 0 & 0 & 0 & 0 & 0 & 0 & 0 \\
0 & 0 & 0 & 0 & 0 & 0 & 0 & 0 & 0 & 0 & 0 & 0 & 0 & 0 & 0 & 0 & 0 & 0 & 0 & 0 \\
0 & 0 & 0 & 0 & 0 & 0 & 0 & 0 & 0 & 0 & 0 & 0 & 0 & 0 & 0 & 0 & 0 & 0 & 0 & 0 \\
0 & 0 & 0 & 0 & 0 & 0 & 0 & 0 & 0 & 0 & 0 & 0 & 0 & 0 & 0 & 0 & 0 & 0 & 0 & 0 \\
0 & 0 & 0 & 0 & 0 & 0 & 0 & 0 & 0 & 0 & 0 & 0 & 0 & 0 & 0 & 0 & 0 & 0 & 0 & 0 \\
0 & 0 & 0 & 0 & 0 & 0 & 0 & 0 & 0 & 0 & 0 & 0 & 0 & 0 & 0 & 0 & 0 & 0 & 0 & 0 \\
0 & 0 & 0 & 0 & 0 & 0 & 0 & 0 & 0 & 0 & 0 & 0 & 0 & 0 & 0 & 0 & 0 & 0 & 0 & 0 \\
0 & 0 & 0 & 0 & 0 & 0 & 0 & 0 & 0 & 0 & 0 & 0 & 0 & 0 & 0 & 0 & 0 & 0 & 0 & 0 \\
0 & 0 & 0 & 0 & 0 & 0 & 0 & 0 & 0 & 0 & 0 & 0 & 0 & 0 & 0 & 0 & 0 & 0 & 0 & 0 \\
0 & 0 & 0 & 0 & 0 & 0 & 0 & 0 & 0 & 0 & 0 & 0 & 0 & 0 & 0 & 0 & 0 & 0 & 0 & 0 \\
0 & 0 & 0 & 0 & 0 & 0 & 0 & 0 & 0 & 0 & 0 & 0 & 0 & 0 & 0 & 0 & 0 & 0 & 0 & 0 \\
\frac{21}{4} & \frac{3}{4} & 0 & 0 & 0 & -\frac{9}{2} & \frac{9}{4} & 0 & -\frac{9}{2} & 0 & 0 & -\frac{3}{2} & -1 & \frac{3}{2} & 0 & 0 & 0 & 0 & 0 & 0 \\
-\frac{7}{2} & -\frac{1}{2} & 0 & 0 & 0 & 3 & -\frac{3}{2} & 0 & 3 & 0 & 0 & 1 & \frac{2}{3} & -1 & 0 & 0 & 0 & 0 & 0 & 0 \\
0 & 0 & 0 & 0 & 0 & 0 & 0 & 0 & 0 & 0 & 0 & 0 & 0 & 0 & 0 & 0 & 0 & 0 & 0 & 0 \\
0 & 0 & 0 & 0 & 0 & 0 & 0 & 0 & 0 & 0 & 0 & 0 & 0 & 0 & 0 & 0 & 0 & 0 & 0 & 0 \\
0 & 0 & 0 & 0 & 0 & 0 & 0 & 0 & 0 & 0 & 0 & 0 & 0 & 0 & 0 & 0 & 0 & 0 & 0 & 0 \\
0 & 0 & 0 & 0 & 0 & 0 & 0 & 0 & 0 & 0 & 0 & 0 & 0 & 0 & 0 & 0 & 0 & 0 & 0 & 0 \\
0 & 0 & 0 & 0 & 0 & 0 & 0 & 0 & 0 & 0 & 0 & 0 & 0 & 0 & 0 & 0 & 0 & 0 & 0 & 0 \\
0 & 0 & 0 & 0 & 0 & 0 & 0 & 0 & 0 & 0 & 0 & 0 & 0 & 0 & 0 & 0 & 0 & 0 & 0 & 0
\end{array}\right)
\qquad
c_{20}^{[3gv]}=\left(\begin{array}{cccccccccccccccccccc}
0 & 0 & 0 & 0 & 0 & 0 & 0 & 0 & 0 & 0 & 0 & 0 & 0 & 0 & 0 & 0 & 0 & 0 & 0 & 0 \\
0 & 0 & 0 & 0 & 0 & 0 & 0 & 0 & 0 & 0 & 0 & 0 & 0 & 0 & 0 & 0 & 0 & 0 & 0 & 0 \\
0 & 0 & 0 & 0 & 0 & 0 & 0 & 0 & 0 & 0 & 0 & 0 & 0 & 0 & 0 & 0 & 0 & 0 & 0 & 0 \\
0 & 0 & 0 & 0 & 0 & 0 & 0 & 0 & 0 & 0 & 0 & 0 & 0 & 0 & 0 & 0 & 0 & 0 & 0 & 0 \\
0 & 0 & 0 & 0 & 0 & 0 & 0 & 0 & 0 & 0 & 0 & 0 & 0 & 0 & 0 & 0 & 0 & 0 & 0 & 0 \\
0 & 0 & 0 & 0 & 0 & 0 & 0 & 0 & 0 & 0 & 0 & 0 & 0 & 0 & 0 & 0 & 0 & 0 & 0 & 0 \\
0 & 0 & 0 & 0 & 0 & 0 & 0 & 0 & 0 & 0 & 0 & 0 & 0 & 0 & 0 & 0 & 0 & 0 & 0 & 0 \\
0 & 0 & 0 & 0 & 0 & 0 & 0 & 0 & 0 & 0 & 0 & 0 & 0 & 0 & 0 & 0 & 0 & 0 & 0 & 0 \\
0 & 0 & 0 & 0 & 0 & 0 & 0 & 0 & 0 & 0 & 0 & 0 & 0 & 0 & 0 & 0 & 0 & 0 & 0 & 0 \\
0 & 0 & 0 & 0 & 0 & 0 & 0 & 0 & 0 & 0 & 0 & 0 & 0 & 0 & 0 & 0 & 0 & 0 & 0 & 0 \\
0 & 0 & 0 & 0 & 0 & 0 & 0 & 0 & 0 & 0 & 0 & 0 & 0 & 0 & 0 & 0 & 0 & 0 & 0 & 0 \\
-\frac{7}{2} & -\frac{1}{2} & 0 & 0 & 0 & 3 & 0 & 0 & 3 & -\frac{3}{2} & 0 & -1 & \frac{2}{3} & 1 & 0 & 0 & 0 & 0 & 0 & 0 \\
\frac{21}{4} & \frac{3}{4} & 0 & 0 & 0 & -\frac{9}{2} & 0 & 0 & -\frac{9}{2} & \frac{9}{4} & 0 & \frac{3}{2} & -1 & -\frac{3}{2} & 0 & 0 & 0 & 0 & 0 & 0 \\
0 & 0 & 0 & 0 & 0 & 0 & 0 & 0 & 0 & 0 & 0 & 0 & 0 & 0 & 0 & 0 & 0 & 0 & 0 & 0 \\
0 & 0 & 0 & 0 & 0 & 0 & 0 & 0 & 0 & 0 & 0 & 0 & 0 & 0 & 0 & 0 & 0 & 0 & 0 & 0 \\
0 & 0 & 0 & 0 & 0 & 0 & 0 & 0 & 0 & 0 & 0 & 0 & 0 & 0 & 0 & 0 & 0 & 0 & 0 & 0 \\
0 & 0 & 0 & 0 & 0 & 0 & 0 & 0 & 0 & 0 & 0 & 0 & 0 & 0 & 0 & 0 & 0 & 0 & 0 & 0 \\
0 & 0 & 0 & 0 & 0 & 0 & 0 & 0 & 0 & 0 & 0 & 0 & 0 & 0 & 0 & 0 & 0 & 0 & 0 & 0 \\
0 & 0 & 0 & 0 & 0 & 0 & 0 & 0 & 0 & 0 & 0 & 0 & 0 & 0 & 0 & 0 & 0 & 0 & 0 & 0 \\
0 & 0 & 0 & 0 & 0 & 0 & 0 & 0 & 0 & 0 & 0 & 0 & 0 & 0 & 0 & 0 & 0 & 0 & 0 & 0
\end{array}\right) \tag{A.5j}$$

$$c_{21}^{[3gv]}=\left(\begin{array}{cccccccccccccccccccc}
0 & 0 & 0 & 0 & 0 & 0 & 0 & 0 & 0 & 0 & 0 & 0 & 0 & 0 & 0 & 0 & 0 & 0 & 0 & 0 \\
0 & 0 & 0 & 0 & 0 & 0 & 0 & 0 & 0 & 0 & 0 & 0 & 0 & 0 & 0 & 0 & 0 & 0 & 0 & 0 \\
0 & 0 & 0 & 0 & 0 & 0 & 0 & 0 & 0 & 0 & 0 & 0 & 0 & 0 & 0 & 0 & 0 & 0 & 0 & 0 \\
0 & 0 & 0 & 0 & 0 & 0 & 0 & 0 & 0 & 0 & 0 & 0 & 0 & 0 & 0 & 0 & 0 & 0 & 0 & 0 \\
0 & 0 & 0 & 0 & 0 & 0 & 0 & 0 & 0 & 0 & 0 & 0 & 0 & 0 & 0 & 0 & 0 & 0 & 0 & 0 \\
0 & 0 & 0 & 0 & 0 & 0 & 0 & 0 & 0 & 0 & 0 & 0 & 0 & 0 & 0 & 0 & 0 & 0 & 0 & 0 \\
0 & 0 & 0 & 0 & 0 & 0 & 0 & 0 & 0 & 0 & 0 & 0 & 0 & 0 & 0 & 0 & 0 & 0 & 0 & 0 \\
0 & 0 & 0 & 0 & 0 & 0 & 0 & 0 & 0 & 0 & 0 & 0 & 0 & 0 & 0 & 0 & 0 & 0 & 0 & 0 \\
0 & 0 & 0 & 0 & 0 & 0 & 0 & 0 & 0 & 0 & 0 & 0 & 0 & 0 & 0 & 0 & 0 & 0 & 0 & 0 \\
0 & 0 & 0 & 0 & 0 & 0 & 0 & 0 & 0 & 0 & 0 & 0 & 0 & 0 & 0 & 0 & 0 & 0 & 0 & 0 \\
0 & 0 & 0 & 0 & 0 & 0 & 0 & 0 & 0 & 0 & 0 & 0 & 0 & 0 & 0 & 0 & 0 & 0 & 0 & 0 \\
0 & 0 & 0 & 0 & 0 & 0 & 0 & 0 & 0 & 0 & 0 & 0 & 0 & 0 & 0 & 0 & 0 & 0 & 0 & 0 \\
-\frac{21}{4} & -\frac{3}{4} & 0 & 0 & 0 & \frac{9}{2} & -\frac{9}{4} & 0 & \frac{9}{2} & -\frac{9}{4} & 0 & -\frac{3}{2} & -2 & -\frac{3}{2} & 0 & 0 & 0 & 0 & 0 & 0 \\
0 & 0 & 0 & 0 & 0 & 0 & 0 & 0 & 0 & 0 & 0 & 0 & 0 & 0 & 0 & 0 & 0 & 0 & 0 & 0 \\
0 & 0 & 0 & 0 & 0 & 0 & 0 & 0 & 0 & 0 & 0 & 0 & 0 & 0 & 0 & 0 & 0 & 0 & 0 & 0 \\
0 & 0 & 0 & 0 & 0 & 0 & 0 & 0 & 0 & 0 & 0 & 0 & 0 & 0 & 0 & 0 & 0 & 0 & 0 & 0 \\
0 & 0 & 0 & 0 & 0 & 0 & 0 & 0 & 0 & 0 & 0 & 0 & 0 & 0 & 0 & 0 & 0 & 0 & 0 & 0 \\
0 & 0 & 0 & 0 & 0 & 0 & 0 & 0 & 0 & 0 & 0 & 0 & 0 & 0 & 0 & 0 & 0 & 0 & 0 & 0 \\
0 & 0 & 0 & 0 & 0 & 0 & 0 & 0 & 0 & 0 & 0 & 0 & 0 & 0 & 0 & 0 & 0 & 0 & 0 & 0 \\
0 & 0 & 0 & 0 & 0 & 0 & 0 & 0 & 0 & 0 & 0 & 0 & 0 & 0 & 0 & 0 & 0 & 0 & 0 & 0
\end{array}\right) \tag{A.5k}$$

A.3 Parameterisation of the $[3gv]$-web Integrand

In this appendix we explain in more detail the parameterisation used in eq. (2.83c). We first decompose β_1 in terms of two lightlike vectors p_1 and p_2

$$\beta_1 = p_1 + p_2. \tag{A.6}$$

Since $\beta_1^2 = 1$ we have $2p_1{\cdot}p_2 = 1$. Next, we parameterise β_2 as a linear combination of these vectors. As we define the α variables through $2\beta_1 \cdot \beta_2 = -\left(\frac{1}{\alpha_{12}} - \alpha_{12}\right)$ then

$$\beta_2 = -\frac{p_1}{\alpha_{12}} - \alpha_{12} p_2. \tag{A.7}$$

We have one Wilson line left to parameterise, β_3. The vectors p_1 and p_2 do not span fully the space occupied by β_1 and β_2. We need vectors other than p_1 and p_2 in order to do so. To achieve this we will use the constituent spinors of p_1 and p_2 to define the new vectors. The following formalism is referred to the *spinor-helicity formalism* (see eg. [190] for a more detailed introduction). Since both are lightlike we can write them as

$$p_i^\mu \sigma_\mu^{\alpha\dot{\alpha}} = \lambda_i^\alpha \tilde{\lambda}_i^{\dot{\alpha}} \tag{A.8}$$

where $\sigma^\mu = (1, \boldsymbol{\sigma})$ is the usual four-dimensional Pauli matrices and λ_i and $\tilde{\lambda}_i$ are two-dimensional vectors. In eq. (A.8) we use the fact that rank 1 matrices can be written as a product of two vectors. We then define new vectors from these spinors, $\lambda_1\tilde{\lambda}_2$ and $\lambda_2\tilde{\lambda}_1$. These are both orthogonal to p_1 and p_2 which allows us to parameterise β_3 in terms of all of them

$$\beta_3 = a_1 p_1 + a_2 p_2 + a_3 \frac{\langle 23\rangle}{\langle 13\rangle}\lambda_1\tilde{\lambda}_2 + a_4 \frac{\langle 13\rangle}{\langle 23\rangle}\lambda_2\tilde{\lambda}_1. \tag{A.9}$$

The a_i are given in eqs. (2.84a) and (2.84b). We have also used the angle-bracket notation where $\lambda_i^{\dot{\alpha}} \to |i\rangle^{\dot{\alpha}}$ and $\langle ij\rangle = \langle i|_{\dot{\alpha}}\, |j\rangle^{\dot{\alpha}}$. The explicit appearance of the spinor products in eq. (A.9) keeps it little group invariant without the need to transform the pararmeters a_i. In the spinor language, this transformation is $\lambda_i \to \frac{\lambda_i}{t}$ and $\tilde{\lambda}_i \to t\tilde{\lambda}_i$.

Appendix B

Functions with letter y

In this section we present the functions that have at least one occurence of the letter y in their symbol. These are constructed in Section 3.2. Each pure polylogarithm functions in this class is labelled as $w_i^{(j),k}$, which describes the i-th function at weight j corresponding to a rational factor which is the k-th element of the set

$$\{r(\alpha)^{\text{even}}, r(\alpha)^{\text{odd}}, r(\alpha)^{\text{even}}s(\alpha)^{\text{odd}}, r(\alpha)^{\text{odd}}s(\alpha)^{\text{odd}}\}. \tag{B.1}$$

The $w_i^{(j),k}$ functions are written in terms of MPLs and for brevity of the expressions we drop the functional argument i.e. $G_{a_1\cdots a_n} \equiv G_{a_1\cdots a_n}(\alpha)$.

For those of the first type $w_i^{(n),1}$ we give its value at $\alpha = 1$. The types $w_i^{(n),2}$ and $w_i^{(n),3}$ already vanish at $\alpha = 1$. As explained in Section 3.2 subtraction constants for the fourth type $w_i^{(n),4}$ are not consistent with symmetries.

B.1 Weight Three Functions

There are two functions at weight three. The only function at weight 3 with rational factor $r(\alpha)^{\text{even}}s(\alpha)^{\text{odd}}$ is

$$\begin{aligned} w_1^{(3),3} = &-G_{-1,-1,0} + G_{-1,0,0} - G_{-1,1,0} + G_{1,-1,0} - G_{1,0,0} + G_{1,1,0} \\ &+ 2\log(2)G_{-1,0} - 2\log(2)G_{1,0} + \frac{1}{2}\zeta_2 G_{-1} - \frac{1}{2}\zeta_2 G_1 \end{aligned}$$

$$\mathcal{S}[w_1^{(3),3}] = \alpha \otimes \eta \otimes y$$

The only function at weight three with rational factor $r(\alpha)^{\text{odd}}(\alpha)s^{\text{odd}}$ is

$$w_1^{(3),4} = G_{-1,0,0} - G_{1,0,0}$$

$$\mathcal{S}[w_1^{(3),4}] = \alpha \otimes \alpha \otimes y$$

B.2 Weight Four Functions

There are nine functions at weight four.

The only function at weight four with rational factor $r(\alpha)^{\text{even}}$ is

$$w_1^{(4),1} = G_{-1,-1,0,0} - G_{-1,1,0,0} - G_{1,-1,0,0} + G_{1,1,0,0} + \frac{7}{4}\zeta_3 G_{-1} - \frac{7}{4}\zeta_3 G_0 + \frac{7}{4}\zeta_3 G_1$$

$$w_1^{(4),1}(1) = -4\text{Li}_4\left(\frac{1}{2}\right) + \zeta_2 \log^2(2) + \frac{53}{16}\zeta_4 - \frac{1}{6}\log^4(2)$$

$$\mathcal{S}[w_1^{(4),1}] = \alpha \otimes \alpha \otimes y \otimes y$$

The only function at weight four with rational factor $r(\alpha)^{\text{odd}}$ is

$$\begin{aligned} w_1^{(4),2} = & -G_{-1,-1,-1,0} + G_{-1,-1,0,0} - G_{-1,-1,1,0} + G_{-1,1,-1,0} - G_{-1,1,0,0} + G_{-1,1,1,0} + G_{1,-1,-1,0} - G_{1,-1,0,0} \\ & + G_{1,-1,1,0} - G_{1,1,-1,0} + G_{1,1,0,0} - G_{1,1,1,0} + 2\log^2(2) G_{-1,0} - 2\log^2(2) G_{0,0} + 2\log^2(2) G_{1,0} \\ & - 12\log(2) G_{-1,-1,0} + 14\log(2) G_{-1,0,0} - 16\log(2) G_{-1,1,0} + 14\log(2) G_{0,-1,0} + 14\log(2) G_{0,1,0} \\ & - 16\log(2) G_{1,-1,0} + 14\log(2) G_{1,0,0} - 12\log(2) G_{1,1,0} + \tfrac{53}{20}\zeta_2 G_{-1,0} + \tfrac{1}{2}\zeta_2 G_{-1,-1} - \tfrac{1}{2}\zeta_2 G_{-1,1} \\ & - \tfrac{53}{20}\zeta_2 G_{0,0} - \tfrac{1}{2}\zeta_2 G_{1,-1} + \tfrac{53}{20}\zeta_2 G_{1,0} + \tfrac{1}{2}\zeta_2 G_{1,1} + 7\zeta_2 \log(2) G_{-1} + 7\zeta_2 \log(2) G_1 - 4\text{Li}_4\left(\tfrac{1}{2}\right) - \tfrac{\log^4(2)}{6} \end{aligned}$$

$$\mathcal{S}[w_1^{(4),2}] = \alpha \otimes \eta \otimes y \otimes y$$

There are three functions at weight four with rational factor $r(\alpha)^{\text{even}}s(\alpha)^{\text{odd}}$ are

$$w_1^{(4),3} = G_{-1,0,0,0} - G_{1,0,0,0} - \tfrac{1}{2}\zeta_2 G_{-1,0} + \tfrac{1}{2}\zeta_2 G_{1,0}$$

$$\mathcal{S}[w_1^{(4),3}] = \alpha \otimes \alpha \otimes \alpha \otimes y$$

$$w_2^{(4),3} = G_{0,-1,0,0} - G_{0,1,0,0} + \tfrac{3}{2}\zeta_2 G_{-1,0} - \tfrac{3}{2}\zeta_2 G_{1,0}$$

$$\mathcal{S}[w_2^{(4),3}] = \alpha \otimes \alpha \otimes y \otimes \alpha$$

$$w_3^{(4),3}=3G_{-1,-1,-1,0}-3G_{-1,-1,0,0}+3G_{-1,-1,1,0}-2G_{-1,0,-1,0}+2G_{-1,0,0,0}-2G_{-1,0,1,0}+G_{-1,1,-1,0}$$
$$-G_{-1,1,0,0}+G_{-1,1,1,0}-G_{0,-1,-1,0}+G_{0,-1,0,0}-G_{0,-1,1,0}+G_{0,1,-1,0}-G_{0,1,0,0}+G_{0,1,1,0}$$
$$-G_{1,-1,-1,0}+G_{1,-1,0,0}-G_{1,-1,1,0}+2G_{1,0,-1,0}-2G_{1,0,0,0}+2G_{1,0,1,0}-3G_{1,1,-1,0}$$
$$+3G_{1,1,0,0}-3G_{1,1,1,0}-4\log^2(2)G_{-1,0}+4\log^2(2)G_{1,0}-2\log(2)G_{-1,-1,0}+2\log(2)G_{-1,1,0}$$
$$+2\log(2)G_{0,-1,0}-2\log(2)G_{0,1,0}-2\log(2)G_{1,-1,0}+2\log(2)G_{1,1,0}-\tfrac{3}{2}\zeta_2 G_{-1,-1}+\tfrac{1}{2}\zeta_2 G_{-1,0}$$
$$-\tfrac{1}{2}\zeta_2 G_{-1,1}+\tfrac{1}{2}\zeta_2 G_{0,-1}-\tfrac{1}{2}\zeta_2 G_{0,1}+\tfrac{1}{2}\zeta_2 G_{1,-1}-\tfrac{1}{2}\zeta_2 G_{1,0}+\tfrac{3}{2}\zeta_2 G_{1,1}-\tfrac{1}{2}\zeta_3 G_{-1}+\tfrac{1}{2}\zeta_3 G_1$$

$$\mathcal{S}[w_3^{(4),3}] = \alpha\otimes\eta\otimes y\otimes\eta + 2\alpha\otimes\eta\otimes\eta\otimes y$$

There are four functions at weight four with rational factor $r(\alpha)^{\rm odd}s(\alpha)^{\rm odd}$ are

$$w_1^{(4),4}=-G_{-1,-1,0,0}+G_{-1,0,0,0}-G_{-1,1,0,0}+G_{1,-1,0,0}-G_{1,0,0,0}+G_{1,1,0,0}-\tfrac{1}{4}\zeta_3 G_{-1}+\tfrac{1}{4}\zeta_3 G_1$$

$$\mathcal{S}[w_1^{(4),4}] = \alpha\otimes\alpha\otimes\eta\otimes y$$

$$w_2^{(4),4}=-G_{-1,-1,0,0}+G_{-1,1,0,0}+G_{0,-1,0,0}-G_{0,1,0,0}-G_{1,-1,0,0}+G_{1,1,0,0}-\tfrac{7}{4}\zeta_3 G_{-1}+\tfrac{7}{4}\zeta_3 G_1$$

$$\mathcal{S}[w_2^{(4),4}] = \alpha\otimes\alpha\otimes y\otimes\eta$$

$$w_3^{(4),4}=-G_{0,-1,-1,0}+G_{0,-1,0,0}-G_{0,-1,1,0}+G_{0,1,-1,0}-G_{0,1,0,0}$$
$$+G_{0,1,1,0}+2\log(2)G_{0,-1,0}-2\log(2)G_{0,1,0}+\tfrac{1}{2}\zeta_2 G_{0,-1}-\tfrac{1}{2}\zeta_2 G_{0,1}$$

$$\mathcal{S}[w_3^{(4),4}] = \alpha\otimes\eta\otimes y\otimes\alpha$$

$$w_4^{(4),4}=-G_{-1,0,-1,0}+G_{-1,0,0,0}-G_{-1,0,1,0}+G_{1,0,-1,0}-G_{1,0,0,0}$$
$$+G_{1,0,1,0}+\tfrac{1}{2}\zeta_2 G_{-1,0}-\tfrac{1}{2}\zeta_2 G_{1,0}+\tfrac{1}{2}\zeta_3 G_{-1}-\tfrac{1}{2}\zeta_3 G_1$$

$$\mathcal{S}[w_4^{(4),4}] = \alpha\otimes\eta\otimes\alpha\otimes y$$

B.3 Weight Five Functions

There are 32 functions at weight five.

There are six functions at weight five with rational factor $r(\alpha)^{\rm even}$ are

$$w_1^{(5),1}=-G_{-1,-1,-1,0,0}+G_{-1,-1,1,0,0}+G_{-1,1,-1,0,0}-G_{-1,1,1,0,0}+G_{0,-1,-1,0,0}-G_{0,-1,1,0,0}$$
$$-G_{0,1,-1,0,0}+G_{0,1,1,0,0}-G_{1,-1,-1,0,0}+G_{1,-1,1,0,0}+G_{1,1,-1,0,0}-G_{1,1,1,0,0}-\tfrac{1}{6}\log^4(2)G_{-1}$$
$$+\tfrac{1}{6}\log^4(2)G_0-\tfrac{1}{6}\log^4(2)G_1+2\log^2(2)G_{-1,0,0}-2\log^2(2)G_{0,-1,0}-2\log^2(2)G_{0,1,0}$$
$$+2\log^2(2)G_{1,0,0}-4\mathrm{Li}_4\left(\tfrac{1}{2}\right)G_{-1}+4\mathrm{Li}_4\left(\tfrac{1}{2}\right)G_0-4\mathrm{Li}_4\left(\tfrac{1}{2}\right)G_1+\tfrac{53}{40}\zeta_2^2 G_{-1}+\tfrac{53}{40}\zeta_2^2 G_1$$
$$+\tfrac{53}{20}\zeta_2 G_{-1,0,0}-\tfrac{53}{20}\zeta_2 G_{0,-1,0}-\tfrac{53}{20}\zeta_2 G_{0,1,0}+\tfrac{53}{20}\zeta_2 G_{1,0,0}+\zeta_2\log^2(2)G_{-1}+\zeta_2\log^2(2)G_1$$
$$-\tfrac{7}{4}\zeta_3 G_{-1,-1}+\tfrac{7}{4}\zeta_3 G_{-1,0}-\tfrac{7}{4}\zeta_3 G_{-1,1}+\tfrac{7}{4}\zeta_3 G_{0,-1}+\tfrac{7}{4}\zeta_3 G_{0,1}-\tfrac{7}{4}\zeta_3 G_{1,-1}+\tfrac{7}{4}\zeta_3 G_{1,0}-\tfrac{7}{4}\zeta_3 G_{1,1}$$

$$w_1^{(5),1}(1)=8\mathrm{Li}_5\left(\tfrac{1}{2}\right)-\tfrac{159\zeta_2\zeta_3}{80}+\tfrac{2}{3}\zeta_2\log^3(2)+\tfrac{53}{8}\zeta_4\log(2)-\tfrac{217\zeta_5}{32}-\tfrac{3}{2}\zeta_3\log^2(2)-\tfrac{1}{15}\log^5(2)$$

$$\mathcal{S}[w_1^{(5),1}] = \alpha\otimes\alpha\otimes y\otimes y\otimes\eta$$

$$w_2^{(5),1}=-G_{-1,-1,-1,0,0}+G_{-1,-1,1,0,0}+G_{-1,0,-1,0,0}-G_{-1,0,1,0,0}-G_{-1,1,-1,0,0}+G_{-1,1,1,0,0}+G_{1,-1,-1,0,0}$$
$$-G_{1,-1,1,0,0}-G_{1,0,-1,0,0}+G_{1,0,1,0,0}+G_{1,1,-1,0,0}-G_{1,1,1,0,0}+\frac{9}{8}\zeta_2^2G_{-1}+\frac{9}{8}\zeta_2^2G_1+\frac{9}{4}\zeta_2G_{-1,0,0}$$
$$-\frac{9}{4}\zeta_2G_{0,-1,0}-\frac{9}{4}\zeta_2G_{0,1,0}+\frac{9}{4}\zeta_2G_{1,0,0}-\frac{7}{4}\zeta_3G_{-1,-1}+\frac{7}{4}\zeta_3G_{-1,1}+\frac{7}{4}\zeta_3G_{1,-1}-\frac{7}{4}\zeta_3G_{1,1}$$

$$w_2^{(5),1}(1)=-\frac{27\zeta_2\zeta_3}{16}+\frac{45}{8}\zeta_4\log(2)-\frac{31\zeta_5}{32}$$

$$\mathcal{S}[w_2^{(5),1}]=\alpha\otimes\alpha\otimes y\otimes\eta\otimes y$$

$$w_3^{(5),1}=-G_{-1,-1,-1,0,0}+G_{-1,-1,0,0,0}-G_{-1,-1,1,0,0}+G_{-1,1,-1,0,0}-G_{-1,1,0,0,0}+G_{-1,1,1,0,0}$$
$$+G_{1,-1,-1,0,0}-G_{1,-1,0,0,0}+G_{1,-1,1,0,0}-G_{1,1,-1,0,0}+G_{1,1,0,0,0}-G_{1,1,1,0,0}$$
$$+\frac{1}{6}\log^4(2)G_{-1}-\frac{1}{6}\log^4(2)G_0+\frac{1}{6}\log^4(2)G_1-2\log^2(2)G_{-1,0,0}+2\log^2(2)G_{0,-1,0}$$
$$+2\log^2(2)G_{0,1,0}-2\log^2(2)G_{1,0,0}+4\mathrm{Li}_4\left(\tfrac{1}{2}\right)G_{-1}-4\mathrm{Li}_4\left(\tfrac{1}{2}\right)G_0+4\mathrm{Li}_4\left(\tfrac{1}{2}\right)G_1$$
$$-\frac{53}{40}\zeta_2^2G_{-1}-\frac{53}{40}\zeta_2^2G_1-\frac{53}{20}\zeta_2G_{-1,0,0}+\frac{53}{20}\zeta_2G_{0,-1,0}+\frac{53}{20}\zeta_2G_{0,1,0}-\frac{53}{20}\zeta_2G_{1,0,0}$$
$$-\zeta_2\log^2(2)G_{-1}-\zeta_2\log^2(2)G_1-\frac{1}{4}\zeta_3G_{-1,-1}+\frac{1}{4}\zeta_3G_{-1,1}+\frac{1}{4}\zeta_3G_{1,-1}-\frac{1}{4}\zeta_3G_{1,1}$$

$$w_3^{(5),1}(1)=-16\mathrm{Li}_5\left(\tfrac{1}{2}\right)+\frac{159\zeta_2\zeta_3}{80}-\frac{4}{3}\zeta_2\log^3(2)-\frac{53}{4}\zeta_4\log(2)+\frac{31\zeta_5}{2}+\frac{3}{2}\zeta_3\log^2(2)+\frac{2\log^5(2)}{15}$$

$$\mathcal{S}[w_3^{(5),1}]=\alpha\otimes\alpha\otimes\eta\otimes y\otimes y$$

$$w_4^{(5),1}=-G_{-1,-1,0,-1,0}+G_{-1,-1,0,0,0}-G_{-1,-1,0,1,0}+G_{-1,1,0,-1,0}-G_{-1,1,0,0,0}+G_{-1,1,0,1,0}$$
$$+G_{1,-1,0,-1,0}-G_{1,-1,0,0,0}+G_{1,-1,0,1,0}-G_{1,1,0,-1,0}+G_{1,1,0,0,0}-G_{1,1,0,1,0}-\frac{9}{8}\zeta_2^2G_{-1}$$
$$-\frac{9}{8}\zeta_2^2G_1+\frac{1}{2}\zeta_2G_{-1,-1,0}-\frac{9}{4}\zeta_2G_{-1,0,0}-\frac{1}{2}\zeta_2G_{-1,1,0}+\frac{9}{4}\zeta_2G_{0,-1,0}+\frac{9}{4}\zeta_2G_{0,1,0}$$
$$-\frac{1}{2}\zeta_2G_{1,-1,0}-\frac{9}{4}\zeta_2G_{1,0,0}+\frac{1}{2}\zeta_2G_{1,1,0}+\frac{1}{2}\zeta_3G_{-1,-1}-\frac{1}{2}\zeta_3G_{-1,1}-\frac{1}{2}\zeta_3G_{1,-1}+\frac{1}{2}\zeta_3G_{1,1}$$

$$w_4^{(5),1}(1)=\frac{41\zeta_2\zeta_3}{16}+\frac{1}{8}(-45)\zeta_4\log(2)-\frac{31\zeta_5}{32}$$

$$\mathcal{S}[w_4^{(5),1}]=\alpha\otimes\eta\otimes\alpha\otimes y\otimes y$$

$$w_5^{(5),1}=-G_{-1,0,-1,-1,0}+G_{-1,0,-1,0,0}-G_{-1,0,-1,1,0}+G_{-1,0,1,-1,0}-G_{-1,0,1,0,0}+G_{-1,0,1,1,0}$$
$$+G_{1,0,-1,-1,0}-G_{1,0,-1,0,0}+G_{1,0,-1,1,0}-G_{1,0,1,-1,0}+G_{1,0,1,0,0}-G_{1,0,1,1,0}-\frac{1}{3}\log^4(2)G_{-1}$$
$$+\frac{1}{3}\log^4(2)G_0-\frac{1}{3}\log^4(2)G_1+4\log^2(2)G_{-1,0,0}-4\log^2(2)G_{0,-1,0}-4\log^2(2)G_{0,1,0}+4\log^2(2)G_{1,0,0}$$
$$+\log(16)G_{-1,-1,0,0}+\log(16)G_{1,1,0,0}+\log(4)G_{-1,0,-1,0}-\log(4)G_{-1,0,1,0}-\log(4)G_{1,0,-1,0}$$
$$+\log(4)G_{1,0,1,0}-4\log(2)G_{-1,1,0,0}-4\log(2)G_{1,-1,0,0}-8\mathrm{Li}_4\left(\tfrac{1}{2}\right)G_{-1}+8\mathrm{Li}_4\left(\tfrac{1}{2}\right)G_0-8\mathrm{Li}_4\left(\tfrac{1}{2}\right)G_1$$
$$+\frac{151}{40}\zeta_2^2G_{-1}+\frac{151}{40}\zeta_2^2G_1+\frac{1}{2}\zeta_2G_{-1,0,-1}+\frac{151}{20}\zeta_2G_{-1,0,0}-\frac{1}{2}\zeta_2G_{-1,0,1}-\frac{151}{20}\zeta_2G_{0,-1,0}$$
$$-\frac{151}{20}\zeta_2G_{0,1,0}-\frac{1}{2}\zeta_2G_{1,0,-1}+\frac{151}{20}\zeta_2G_{1,0,0}+\frac{1}{2}\zeta_2G_{1,0,1}+2\zeta_2\log^2(2)G_{-1}+2\zeta_2\log^2(2)G_1$$

$$w_5^{(5),1}(1)=\frac{8\log(2)^3\zeta_2}{3}-3\log(2)^2\zeta_3-\frac{4\log(2)^5}{15}+\frac{257\log(2)\zeta_4}{8}+32\mathrm{Li}_5\left(\tfrac{1}{2}\right)-\frac{593\zeta_2\zeta_3}{80}-\frac{465\zeta_5}{16}$$

$$\mathcal{S}[w_5^{(5),1}]=\alpha\otimes\eta\otimes y\otimes\alpha\otimes y$$

$$w_6^{(5),1}=-G_{0,-1,-1,-1,0}+G_{0,-1,-1,0,0}-G_{0,-1,-1,1,0}+G_{0,-1,1,-1,0}-G_{0,-1,1,0,0}+G_{0,-1,1,1,0}+G_{0,1,-1,-1,0}$$
$$-G_{0,1,-1,0,0}+G_{0,1,-1,1,0}-G_{0,1,1,-1,0}+G_{0,1,1,0,0}-G_{0,1,1,1,0}-\frac{1}{6}\log^4(2)G_0-2\log^2(2)G_{-1,0,0}$$
$$+2\log^2(2)G_{0,-1,0}+2\log^2(2)G_{0,1,0}-2\log^2(2)G_{1,0,0}+12\log(2)G_{-1,-1,0,0}-14\log(2)G_{-1,0,0,0}$$
$$+16\log(2)G_{-1,1,0,0}-12\log(2)G_{0,-1,-1,0}-16\log(2)G_{0,-1,1,0}+14\log(2)G_{0,0,-1,0}$$
$$+14\log(2)G_{0,0,1,0}-16\log(2)G_{0,1,-1,0}-12\log(2)G_{0,1,1,0}+16\log(2)G_{1,-1,0,0}-14\log(2)G_{1,0,0,0}$$
$$+12\log(2)G_{1,1,0,0}-4\mathrm{Li}_4\left(\tfrac{1}{2}\right)G_0-\frac{53}{20}\zeta_2G_{-1,0,0}+\frac{1}{2}\zeta_2G_{0,-1,-1}+\frac{53}{20}\zeta_2G_{0,-1,0}-\frac{1}{2}\zeta_2G_{0,-1,1}$$
$$-\frac{1}{2}\zeta_2G_{0,1,-1}+\frac{53}{20}\zeta_2G_{0,1,0}+\frac{1}{2}\zeta_2G_{0,1,1}-\frac{53}{20}\zeta_2G_{1,0,0}+7\zeta_2\log(2)G_{0,-1}+7\zeta_2\log(2)G_{0,1}$$

$$w_6^{(5),1}(1)=-2\log(2)^3\zeta_2+\frac{3\log(2)^2\zeta_3}{2}+\frac{\log(2)^5}{3}+8\log(2)\mathrm{Li}_4\left(\tfrac{1}{2}\right)-\frac{67\log(2)\zeta_4}{8}+\frac{229\zeta_2\zeta_3}{80}-\frac{31\zeta_5}{32}$$

$$\mathcal{S}[w_6^{(5),1}] = \alpha \otimes \eta \otimes y \otimes y \otimes \alpha$$

There are 4 functions at weight 5 with rational factor $r(\alpha)^{\text{odd}}$ are

$$\begin{aligned} w_1^{(5),2} =& G_{-1,-1,0,0,0} - G_{-1,1,0,0,0} - G_{1,-1,0,0,0} + G_{1,1,0,0,0} - \tfrac{1}{2}\zeta_2 G_{-1,-1,0} + \tfrac{1}{2}\zeta_2 G_{-1,1,0} \\ &+ \tfrac{1}{2}\zeta_2 G_{1,-1,0} - \tfrac{1}{2}\zeta_2 G_{1,1,0} + \tfrac{7}{2}\zeta_3 G_{-1,0} - \tfrac{7}{2}\zeta_3 G_{0,0} + \tfrac{7}{2}\zeta_3 G_{1,0} - \tfrac{31\zeta_5}{16} \end{aligned}$$

$$\mathcal{S}[w_1^{(5),2}] = \alpha \otimes \alpha \otimes \alpha \otimes y \otimes y$$

$$\begin{aligned} w_2^{(5),2} =& G_{-1,0,-1,0,0} - G_{-1,0,1,0,0} - G_{1,0,-1,0,0} + G_{1,0,1,0,0} + \tfrac{3}{2}\zeta_2 G_{-1,-1,0} - \tfrac{3}{2}\zeta_2 G_{-1,1,0} \\ &- \tfrac{3}{2}\zeta_2 G_{1,-1,0} + \tfrac{3}{2}\zeta_2 G_{1,1,0} - \tfrac{35}{4}\zeta_3 G_{-1,0} + \tfrac{35}{4}\zeta_3 G_{0,0} - \tfrac{35}{4}\zeta_3 G_{1,0} + \tfrac{31\zeta_5}{4} \end{aligned}$$

$$\mathcal{S}[w_2^{(5),2}] = \alpha \otimes \alpha \otimes y \otimes \alpha \otimes y$$

$$w_3^{(5),2} = G_{0,-1,-1,0,0} - G_{0,-1,1,0,0} - G_{0,1,-1,0,0} + G_{0,1,1,0,0} + \tfrac{7}{4}\zeta_3 G_{0,-1} - \tfrac{7}{4}\zeta_3 G_{0,0} + \tfrac{7}{4}\zeta_3 G_{0,1} - \tfrac{31\zeta_5}{16}$$

$$\mathcal{S}[w_3^{(5),2}] = \alpha \otimes \alpha \otimes y \otimes y \otimes \alpha$$

$$\begin{aligned} w_4^{(5),2} =& -\log^2(2)\zeta_2 G_{-1} + 4\mathrm{Li}_4\left(\tfrac{1}{2}\right) G_{-1} + \tfrac{1}{6}\log^4(2) G_{-1} + 4G_{-1,-1,-1,-1,0} - 4G_{-1,-1,-1,0,0} + 4G_{-1,-1,-1,1,0} \\ &- 2G_{-1,-1,0,-1,0} + 2G_{-1,-1,0,0,0} - 2G_{-1,-1,0,1,0} - G_{-1,0,-1,-1,0} + G_{-1,0,-1,0,0} - G_{-1,0,-1,1,0} \\ &+ G_{-1,0,1,-1,0} - G_{-1,0,1,0,0} + G_{-1,0,1,1,0} - 2G_{-1,1,-1,-1,0} + 2G_{-1,1,-1,0,0} - 2G_{-1,1,-1,1,0} \\ &+ 2G_{-1,1,0,-1,0} - 2G_{-1,1,0,0,0} + 2G_{-1,1,0,1,0} - 2G_{-1,1,1,-1,0} + 2G_{-1,1,1,0,0} - 2G_{-1,1,1,1,0} \\ &- G_{0,-1,-1,-1,0} + G_{0,-1,-1,0,0} - G_{0,-1,-1,1,0} + G_{0,-1,1,-1,0} - G_{0,-1,1,0,0} + G_{0,-1,1,1,0} \\ &+ G_{0,1,-1,-1,0} - G_{0,1,-1,0,0} + G_{0,1,-1,1,0} - G_{0,1,1,-1,0} + G_{0,1,1,0,0} - G_{0,1,1,1,0} - 2G_{1,-1,-1,-1,0} \\ &+ 2G_{1,-1,-1,0,0} - 2G_{1,-1,-1,1,0} + 2G_{1,-1,0,-1,0} - 2G_{1,-1,0,0,0} + 2G_{1,-1,0,1,0} - 2G_{1,-1,1,-1,0} \\ &+ 2G_{1,-1,1,0,0} - 2G_{1,-1,1,1,0} + G_{1,0,-1,-1,0} - G_{1,0,-1,0,0} + G_{1,0,-1,1,0} - G_{1,0,1,-1,0} + G_{1,0,1,0,0} \\ &- G_{1,0,1,1,0} - 2G_{1,1,0,-1,0} + 2G_{1,1,0,0,0} - 2G_{1,1,0,1,0} + 4G_{1,1,1,-1,0} - 4G_{1,1,1,0,0} + 4G_{1,1,1,1,0} \\ &- 2G_{-1,-1,-1}\zeta_2 - \tfrac{43}{20}G_{-1,-1,0}\zeta_2 + \tfrac{1}{2}G_{-1,0,-1}\zeta_2 + \tfrac{53}{20}G_{-1,0,0}\zeta_2 - \tfrac{1}{2}G_{-1,0,1}\zeta_2 + G_{-1,1,-1}\zeta_2 \\ &- \tfrac{63}{20}G_{-1,1,0}\zeta_2 + G_{-1,1,1}\zeta_2 + \tfrac{1}{2}G_{0,-1,-1}\zeta_2 + \tfrac{53}{20}G_{0,-1,0}\zeta_2 - \tfrac{1}{2}G_{0,-1,1}\zeta_2 - \tfrac{1}{2}G_{0,1,-1}\zeta_2 + \tfrac{53}{20}G_{0,1,0}\zeta_2 \\ &+ \tfrac{1}{2}G_{0,1,1}\zeta_2 + G_{1,-1,-1}\zeta_2 - \tfrac{63}{20}G_{1,-1,0}\zeta_2 + G_{1,-1,1}\zeta_2 - \tfrac{1}{2}G_{1,0,-1}\zeta_2 + \tfrac{53}{20}G_{1,0,0}\zeta_2 + \tfrac{1}{2}G_{1,0,1}\zeta_2 \\ &- \tfrac{43}{20}G_{1,1,0}\zeta_2 - 2G_{1,1,1}\zeta_2 - G_1\log^2(2)\zeta_2 - 6G_{-1,-1}\log(2)\zeta_2 - 8G_{-1,1}\log(2)\zeta_2 + 7G_{0,-1}\log(2)\zeta_2 \\ &+ 7G_{0,1}\log(2)\zeta_2 - 8G_{1,-1}\log(2)\zeta_2 - 6G_{1,1}\log(2)\zeta_2 - \tfrac{31\zeta_5}{32} - \tfrac{1}{2}G_{-1,-1}\zeta_3 + \tfrac{123}{40}G_{-1,0}\zeta_3 \\ &+ \tfrac{1}{2}G_{-1,1}\zeta_3 - \tfrac{123}{40}G_{0,0}\zeta_3 + \tfrac{1}{2}G_{1,-1}\zeta_3 + \tfrac{123}{40}G_{1,0}\zeta_3 - \tfrac{1}{2}G_{1,1}\zeta_3 + 4G_1\mathrm{Li}_4\left(\tfrac{1}{2}\right) + \tfrac{1}{6}G_1\log^4(2) \\ &+ 8G_{-1,-1,-1}\log(2) - 12G_{-1,-1,0,0}\log(2) + 16G_{-1,-1,1,0}\log(2) - 12G_{-1,0,-1,0}\log(2) \\ &+ \tfrac{21}{4}G_{-1,0,0,0}\log(2) - 16G_{-1,0,1,0}\log(2) + 16G_{-1,1,-1,0}\log(2) - 16G_{-1,1,0,0}\log(2) \\ &+ 16G_{-1,1,1,0}\log(2) - 12G_{0,-1,-1,0}\log(2) + \tfrac{35}{4}G_{0,-1,0,0}\log(2) - 16G_{0,-1,1,0}\log(2) \\ &+ 14G_{0,0,-1,0}\log(2) + 14G_{0,0,1,0}\log(2) - 16G_{0,1,-1,0}\log(2) + \tfrac{35}{4}G_{0,1,0,0}\log(2) - 12G_{0,1,1,0}\log(2) \\ &+ 16G_{1,-1,-1,0}\log(2) - 16G_{1,-1,0,0}\log(2) + 16G_{1,-1,1,0}\log(2) - 16G_{1,0,-1,0}\log(2) \\ &+ \tfrac{21}{4}G_{1,0,0,0}\log(2) - 12G_{1,0,1,0}\log(2) + 16G_{1,1,-1,0}\log(2) - 12G_{1,1,0,0}\log(2) + 8G_{1,1,1,0}\log(2) \end{aligned}$$

$$\mathcal{S}[w_4^{(5),2}] = \alpha \otimes \eta \otimes y \otimes y \otimes \eta + \alpha \otimes \eta \otimes y \otimes \eta \otimes y + 2\alpha \otimes \eta \otimes \eta \otimes y \otimes y$$

There are 11 functions at weight 5 with rational factor $r(\alpha)^{\text{even}}s(\alpha)^{\text{odd}}$ are

$$\begin{aligned}w_1^{(5),3}=&-G_{-1,-1,0,0,0}+G_{-1,1,0,0,0}+G_{0,-1,0,0,0}-G_{0,1,0,0,0}-G_{1,-1,0,0,0}+G_{1,1,0,0,0}+\tfrac{1}{2}\zeta_2 G_{-1,-1,0}\\&-\tfrac{1}{2}\zeta_2 G_{-1,1,0}-\tfrac{1}{2}\zeta_2 G_{0,-1,0}+\tfrac{1}{2}\zeta_2 G_{0,1,0}+\tfrac{1}{2}\zeta_2 G_{1,-1,0}-\tfrac{1}{2}\zeta_2 G_{1,1,0}-\tfrac{7}{4}\zeta_3 G_{-1,0}+\tfrac{7}{4}\zeta_3 G_{1,0}\end{aligned}$$

$$\mathcal{S}[w_1^{(5),3}] = \alpha\otimes\alpha\otimes\alpha\otimes y\otimes\eta$$

$$\begin{aligned}w_2^{(5),3}=&-G_{-1,-1,0,0,0}+G_{-1,0,0,0,0}-G_{-1,1,0,0,0}+G_{1,-1,0,0,0}-G_{1,0,0,0,0}+G_{1,1,0,0,0}\\&+\tfrac{8}{5}\log(2)G_{-1,0,0,0}-\tfrac{8}{5}\log(2)G_{1,0,0,0}+\tfrac{1}{10}\zeta_2 G_{-1,-1,0}-\tfrac{1}{10}\zeta_2 G_{-1,0,0}\\&+\tfrac{1}{10}\zeta_2 G_{-1,1,0}-\tfrac{1}{10}\zeta_2 G_{1,-1,0}+\tfrac{1}{10}\zeta_2 G_{1,0,0}-\tfrac{1}{10}\zeta_2 G_{1,1,0}-\tfrac{1}{4}\zeta_3 G_{-1,0}+\tfrac{1}{4}\zeta_3 G_{1,0}\end{aligned}$$

$$\mathcal{S}[w_2^{(5),3}] = \alpha\otimes\alpha\otimes\alpha\otimes\eta\otimes y$$

$$\begin{aligned}w_3^{(5),3}=&-G_{-1,0,-1,0,0}+G_{-1,0,1,0,0}+G_{0,0,-1,0,0}-G_{0,0,1,0,0}-G_{1,0,-1,0,0}+G_{1,0,1,0,0}\\&+\log(64)G_{1,0,0,0}-6\log(2)G_{-1,0,0,0}-\tfrac{3}{2}\zeta_2 G_{-1,-1,0}+\tfrac{3}{2}\zeta_2 G_{-1,1,0}\\&+\tfrac{3}{2}\zeta_2 G_{0,-1,0}-\tfrac{3}{2}\zeta_2 G_{0,1,0}-\tfrac{3}{2}\zeta_2 G_{1,-1,0}+\tfrac{3}{2}\zeta_2 G_{1,1,0}+\tfrac{7}{2}\zeta_3 G_{-1,0}-\tfrac{7}{2}\zeta_3 G_{1,0}\end{aligned}$$

$$\mathcal{S}[w_3^{(5),3}] = \alpha\otimes\alpha\otimes y\otimes\alpha\otimes\eta$$

$$\begin{aligned}w_4^{(5),3}=&-G_{0,-1,-1,0,0}+G_{0,-1,1,0,0}+G_{0,0,-1,0,0}-G_{0,0,1,0,0}-G_{0,1,-1,0,0}\\&+G_{0,1,1,0,0}+\log(64)G_{-1,0,0,0}-6\log(2)G_{1,0,0,0}-\tfrac{7}{4}\zeta_3 G_{0,-1}+\tfrac{7}{4}\zeta_3 G_{0,1}\end{aligned}$$

$$\mathcal{S}[w_4^{(5),3}] = \alpha\otimes\alpha\otimes y\otimes\eta\otimes\alpha$$

$$\begin{aligned}w_5^{(5),3}=&-G_{-1,0,-1,0,0}+G_{-1,0,0,0,0}-G_{-1,0,1,0,0}+G_{1,0,-1,0,0}-G_{1,0,0,0,0}+G_{1,0,1,0,0}\\&+\tfrac{6}{5}\log(2)G_{-1,0,0,0}-\tfrac{6}{5}\log(2)G_{1,0,0,0}-\tfrac{3}{10}\zeta_2 G_{-1,-1,0}+\tfrac{3}{10}\zeta_2 G_{-1,0,0}\\&-\tfrac{3}{10}\zeta_2 G_{-1,1,0}+\tfrac{3}{10}\zeta_2 G_{1,-1,0}-\tfrac{3}{10}\zeta_2 G_{1,0,0}+\tfrac{3}{10}\zeta_2 G_{1,1,0}+\tfrac{1}{2}\zeta_3 G_{-1,0}-\tfrac{1}{2}\zeta_3 G_{1,0}\end{aligned}$$

$$\mathcal{S}[w_5^{(5),3}] = \alpha\otimes\alpha\otimes\eta\otimes\alpha\otimes y$$

$$\begin{aligned}w_6^{(5),3}=&-G_{0,-1,-1,0,0}+G_{0,-1,0,0,0}-G_{0,-1,1,0,0}+G_{0,1,-1,0,0}-G_{0,1,0,0,0}\\&+G_{0,1,1,0,0}+\log(64)G_{1,0,0,0}-6\log(2)G_{-1,0,0,0}-\tfrac{1}{4}\zeta_3 G_{0,-1}+\tfrac{1}{4}\zeta_3 G_{0,1}\end{aligned}$$

$$\mathcal{S}[w_6^{(5),3}] = \alpha\otimes\alpha\otimes\eta\otimes y\otimes\alpha$$

$$\begin{aligned}w_7^{(5),3}=&-G_{-1,0,0,-1,0}+G_{-1,0,0,0,0}-G_{-1,0,0,1,0}+G_{1,0,0,-1,0}-G_{1,0,0,0,0}+G_{1,0,0,1,0}\\&-\tfrac{6}{5}\log(2)G_{-1,0,0,0}+\tfrac{6}{5}\log(2)G_{1,0,0,0}+\tfrac{3}{10}\zeta_2 G_{-1,-1,0}+\tfrac{1}{5}\zeta_2 G_{-1,0,0}\\&+\tfrac{3}{10}\zeta_2 G_{-1,1,0}-\tfrac{3}{10}\zeta_2 G_{1,-1,0}-\tfrac{1}{5}\zeta_2 G_{1,0,0}-\tfrac{3}{10}\zeta_2 G_{1,1,0}+\tfrac{3}{2}\zeta_3 G_{-1,0}-\tfrac{3}{2}\zeta_3 G_{1,0}\end{aligned}$$

$$\mathcal{S}[w_7^{(5),3}] = \alpha\otimes\eta\otimes\alpha\otimes\alpha\otimes y$$

$$\begin{aligned}w_8^{(5),3}=&-G_{0,-1,0,-1,0}+G_{0,-1,0,0,0}-G_{0,-1,0,1,0}+G_{0,1,0,-1,0}-G_{0,1,0,0,0}+G_{0,1,0,1,0}\\&+\tfrac{1}{2}\zeta_2 G_{0,-1,0}-\tfrac{1}{2}\zeta_2 G_{0,1,0}-\tfrac{7}{2}\zeta_3 G_{-1,0}+\tfrac{1}{2}\zeta_3 G_{0,-1}-\tfrac{1}{2}\zeta_3 G_{0,1}+\tfrac{7}{2}\zeta_3 G_{1,0}\end{aligned}$$

$$\mathcal{S}[w_8^{(5),3}] = \alpha\otimes\eta\otimes\alpha\otimes y\otimes\alpha$$

$$\begin{aligned}w_9^{(5),3}=&-G_{0,0,-1,-1,0}+G_{0,0,-1,0,0}-G_{0,0,-1,1,0}+G_{0,0,1,-1,0}-G_{0,0,1,0,0}+G_{0,0,1,1,0}\\&+\log(4)G_{0,0,-1,0}-\log(4)G_{0,0,1,0}+\tfrac{1}{2}\zeta_2 G_{0,0,-1}-\tfrac{1}{2}\zeta_2 G_{0,0,1}+\tfrac{7}{4}\zeta_3 G_{-1,0}-\tfrac{7}{4}\zeta_3 G_{1,0}\end{aligned}$$

$$\mathcal{S}[w_9^{(5),3}] = \alpha \otimes \eta \otimes y \otimes \alpha \otimes \alpha$$

$$\begin{aligned}
w_{10}^{(5),3} =& -4\mathrm{Li}_4\left(\tfrac{1}{2}\right)G_{-1} - \tfrac{1}{6}\log^4(2)G_{-1} - G_{-1,-1,-1,-1,0} + G_{-1,-1,-1,0,0} - G_{-1,-1,-1,1,0} + G_{-1,-1,1,-1,0} \\
& - G_{-1,-1,1,0,0} + G_{-1,-1,1,1,0} + G_{-1,1,-1,-1,0} - G_{-1,1,-1,0,0} + G_{-1,1,-1,1,0} - G_{-1,1,1,-1,0} \\
& + G_{-1,1,1,0,0} - G_{-1,1,1,1,0} + G_{1,-1,-1,-1,0} - G_{1,-1,-1,0,0} + G_{1,-1,-1,1,0} - G_{1,-1,1,-1,0} \\
& + G_{1,-1,1,0,0} - G_{1,-1,1,1,0} - G_{1,1,-1,-1,0} + G_{1,1,-1,0,0} - G_{1,1,-1,1,0} + G_{1,1,1,-1,0} - G_{1,1,1,0,0} \\
& + G_{1,1,1,1,0} + \tfrac{1}{2}G_{-1,-1,-1}\zeta_2 + \tfrac{53}{20}G_{-1,-1,0}\zeta_2 - \tfrac{1}{2}G_{-1,-1,1}\zeta_2 - \tfrac{53}{20}G_{-1,0,0}\zeta_2 - \tfrac{1}{2}G_{-1,1,-1}\zeta_2 \\
& + \tfrac{53}{20}G_{-1,1,0}\zeta_2 + \tfrac{1}{2}G_{-1,1,1}\zeta_2 - \tfrac{1}{2}G_{1,-1,-1}\zeta_2 - \tfrac{53}{20}G_{1,-1,0}\zeta_2 + \tfrac{1}{2}G_{1,-1,1}\zeta_2 + \tfrac{53}{20}G_{1,0,0}\zeta_2 \\
& + \tfrac{1}{2}G_{1,1,-1}\zeta_2 - \tfrac{53}{20}G_{1,1,0}\zeta_2 - \tfrac{1}{2}G_{1,1,1}\zeta_2 + \tfrac{21}{2}G_{-1,-1}\log(2)\zeta_2 + \tfrac{7}{2}G_{-1,1}\log(2)\zeta_2 - \tfrac{7}{2}G_{0,-1}\log(2)\zeta_2 \\
& + \tfrac{7}{2}G_{0,1}\log(2)\zeta_2 - \tfrac{7}{2}G_{1,-1}\log(2)\zeta_2 - \tfrac{21}{2}G_{1,1}\log(2)\zeta_2 - \tfrac{1}{4}G_{-1,0}\zeta_3 + \tfrac{1}{4}G_{1,0}\zeta_3 + 4G_1\mathrm{Li}_4\left(\tfrac{1}{2}\right) \\
& + G_{1,-1,-1,0}\log(32) + \tfrac{1}{6}G_1\log^4(2) + 24G_{-1,0}\log^3(2) - 24G_{1,0}\log^3(2) + 16G_{-1,-1,0}\log^2(2) \\
& - 2G_{-1,0,0}\log^2(2) - 12G_{-1,1,0}\log^2(2) - 14G_{0,-1,0}\log^2(2) + 14G_{0,1,0}\log^2(2) + 12G_{1,-1,0}\log^2(2) \\
& + 2G_{1,0,0}\log^2(2) - 16G_{1,1,0}\log^2(2) - 19G_{-1,-1,-1,0}\log(2) + 21G_{-1,-1,0,0}\log(2) \\
& - 23G_{-1,-1,1,0}\log(2) + 14G_{-1,0,-1,0}\log(2) - \tfrac{53}{5}G_{-1,0,0,0}\log(2) + 14G_{-1,0,1,0}\log(2) \\
& - 9G_{-1,1,-1,0}\log(2) + 7G_{-1,1,0,0}\log(2) - 5G_{-1,1,1,0}\log(2) + 7G_{0,-1,-1,0}\log(2) + 7G_{0,-1,1,0}\log(2) \\
& - 7G_{0,1,-1,0}\log(2) - 7G_{0,1,1,0}\log(2) - 7G_{1,-1,0,0}\log(2) + 9G_{1,-1,1,0}\log(2) - 14G_{1,0,-1,0}\log(2) \\
& + \tfrac{53}{5}G_{1,0,0,0}\log(2) - 14G_{1,0,1,0}\log(2) + 23G_{1,1,-1,0}\log(2) - 21G_{1,1,0,0}\log(2) + 19G_{1,1,1,0}\log(2)
\end{aligned}$$

$$\mathcal{S}[w_{10}^{(5),3}] = \alpha \otimes \eta \otimes y \otimes y \otimes y$$

$$\begin{aligned}
w_{11}^{(5),3} =& -\tfrac{1}{2}\log(2)\zeta_2 G_{-1,-1} + \tfrac{5}{4}\zeta_3 G_{-1,-1} - 6G_{-1,-1,-1,-1,0} + 6G_{-1,-1,-1,0,0} - 6G_{-1,-1,-1,1,0} \\
& + 5G_{-1,-1,0,-1,0} - 5G_{-1,-1,0,0,0} + 5G_{-1,-1,0,1,0} - 4G_{-1,-1,1,-1,0} + 4G_{-1,-1,1,0,0} - 4G_{-1,-1,1,1,0} \\
& + 4G_{-1,0,-1,-1,0} - 4G_{-1,0,-1,0,0} + 4G_{-1,0,-1,1,0} - 3G_{-1,0,0,-1,0} + 3G_{-1,0,0,0,0} - 3G_{-1,0,0,1,0} \\
& + 2G_{-1,0,1,-1,0} - 2G_{-1,0,1,0,0} + 2G_{-1,0,1,1,0} - 2G_{-1,1,-1,-1,0} + 2G_{-1,1,-1,0,0} - 2G_{-1,1,-1,1,0} \\
& + G_{-1,1,0,-1,0} - G_{-1,1,0,0,0} + G_{-1,1,0,1,0} + 3G_{0,-1,-1,-1,0} - 3G_{0,-1,-1,0,0} + 3G_{0,-1,-1,1,0} \\
& - 2G_{0,-1,0,-1,0} + 2G_{0,-1,0,0,0} - 2G_{0,-1,0,1,0} + G_{0,-1,1,-1,0} - G_{0,-1,1,0,0} + G_{0,-1,1,1,0} \\
& - G_{0,0,-1,-1,0} + G_{0,0,-1,0,0} - G_{0,0,-1,1,0} + G_{0,0,1,-1,0} - G_{0,0,1,0,0} + G_{0,0,1,1,0} - G_{0,1,-1,-1,0} \\
& + G_{0,1,-1,0,0} - G_{0,1,-1,1,0} + 2G_{0,1,0,-1,0} - 2G_{0,1,0,0,0} + 2G_{0,1,0,1,0} - 3G_{0,1,1,-1,0} + 3G_{0,1,1,0,0} \\
& - 3G_{0,1,1,1,0} - G_{1,-1,0,-1,0} + G_{1,-1,0,0,0} - G_{1,-1,0,1,0} + 2G_{1,-1,1,-1,0} - 2G_{1,-1,1,0,0} + 2G_{1,-1,1,1,0} \\
& - 2G_{1,0,-1,-1,0} + 2G_{1,0,-1,0,0} - 2G_{1,0,-1,1,0} + 3G_{1,0,0,-1,0} - 3G_{1,0,0,0,0} + 3G_{1,0,0,1,0} - 4G_{1,0,1,-1,0} \\
& + 4G_{1,0,1,0,0} - 4G_{1,0,1,1,0} + 4G_{1,1,-1,-1,0} - 4G_{1,1,-1,0,0} + 4G_{1,1,-1,1,0} - 5G_{1,1,0,-1,0} + 5G_{1,1,0,0,0} \\
& - 5G_{1,1,0,1,0} + 6G_{1,1,1,-1,0} - 6G_{1,1,1,0,0} + 6G_{1,1,1,1,0} + 3G_{-1,-1,-1}\zeta_2 - \tfrac{13}{20}G_{-1,-1,0}\zeta_2 + 2G_{-1,-1,1}\zeta_2 \\
& - 2G_{-1,0,-1}\zeta_2 + \tfrac{3}{20}G_{-1,0,0}\zeta_2 - G_{-1,0,1}\zeta_2 + G_{-1,1,-1}\zeta_2 + \tfrac{7}{20}G_{-1,1,0}\zeta_2 - \tfrac{3}{2}G_{0,-1,-1}\zeta_2 + \tfrac{1}{2}G_{0,-1,0}\zeta_2 \\
& - \tfrac{1}{2}G_{0,-1,1}\zeta_2 + \tfrac{1}{2}G_{0,0,-1}\zeta_2 - \tfrac{1}{2}G_{0,0,1}\zeta_2 + \tfrac{1}{2}G_{0,1,-1}\zeta_2 - \tfrac{1}{2}G_{0,1,0}\zeta_2 + \tfrac{3}{2}G_{0,1,1}\zeta_2 - \tfrac{7}{20}G_{1,-1,0}\zeta_2 \\
& - G_{1,-1,1}\zeta_2 + G_{1,0,-1}\zeta_2 - \tfrac{3}{20}G_{1,0,0}\zeta_2 + 2G_{1,0,1}\zeta_2 - 2G_{1,1,-1}\zeta_2 + \tfrac{13}{20}G_{1,1,0}\zeta_2 - 3G_{1,1,1}\zeta_2 \\
& + \tfrac{1}{2}G_{-1,1}\log(2)\zeta_2 + \tfrac{1}{2}G_{0,-1}\log(2)\zeta_2 - \tfrac{1}{2}G_{0,1}\log(2)\zeta_2 - \tfrac{1}{2}G_{1,-1}\log(2)\zeta_2 + \tfrac{1}{2}G_{1,1}\log(2)\zeta_2 \\
& + \tfrac{1}{4}G_{-1,1}\zeta_3 - \tfrac{1}{2}G_{0,-1}\zeta_3 + \tfrac{1}{2}G_{0,1}\zeta_3 - \tfrac{1}{4}G_{1,-1}\zeta_3 - \tfrac{5}{4}G_{1,1}\zeta_3 + G_{-1,-1,-1,0}\log(8) - G_{-1,1,1,0}\log(8) \\
& - G_{0,-1,-1,0}\log(8) + G_{0,1,1,0}\log(8) + G_{1,-1,-1,0}\log(8) - G_{1,1,1,0}\log(8) - G_{-1,0,-1,0}\log(4) \\
& + G_{-1,0,1,0}\log(4) + G_{0,0,-1,0}\log(4) - G_{0,0,1,0}\log(4) - G_{1,0,-1,0}\log(4) + G_{1,0,1,0}\log(4) \\
& + 4G_{-1,0}\log^3(2) - 4G_{1,0}\log^3(2) + 2G_{-1,-1,0}\log^2(2) - 2G_{-1,1,0}\log^2(2) - 2G_{0,-1,0}\log^2(2) \\
& + 2G_{0,1,0}\log^2(2) + 2G_{1,-1,0}\log^2(2) - 2G_{1,1,0}\log^2(2) - G_{-1,-1,0,0}\log(2) - G_{-1,-1,1,0}\log(2) \\
& - \tfrac{27}{5}G_{-1,0,0,0}\log(2) + G_{-1,1,-1,0}\log(2) + G_{-1,1,0,0}\log(2) + G_{0,-1,1,0}\log(2) - G_{0,1,-1,0}\log(2) \\
& - G_{1,-1,0,0}\log(2) - G_{1,-1,1,0}\log(2) + \tfrac{27}{5}G_{1,0,0,0}\log(2) + G_{1,1,-1,0}\log(2) + G_{1,1,0,0}\log(2)
\end{aligned}$$

$$\mathcal{S}[w_{11}^{(5),3}] = \alpha \otimes \eta \otimes y \otimes \eta \otimes \eta + 2\alpha \otimes \eta \otimes \eta \otimes y \otimes \eta + 3\alpha \otimes \eta \otimes \eta \otimes \eta \otimes y$$

There are 11 functions at weight 5 with rational factor $r(\alpha)^{\text{odd}}s(\alpha)^{\text{odd}}$ are

$$w_1^{(5),4}=G_{-1,0,0,0,0}-G_{1,0,0,0,0}$$

$$\mathcal{S}[w_1^{(5),4}] = \alpha\otimes\alpha\otimes\alpha\otimes\alpha\otimes y$$

$$w_2^{(5),4}=G_{0,-1,0,0,0}-G_{0,1,0,0,0}-\tfrac{1}{2}\zeta_2 G_{0,-1,0}+\tfrac{1}{2}\zeta_2 G_{0,1,0}$$

$$\mathcal{S}[w_2^{(5),4}] = \alpha\otimes\alpha\otimes\alpha\otimes y\otimes\alpha$$

$$w_3^{(5),4}=G_{0,0,-1,0,0}-G_{0,0,1,0,0}+\tfrac{3}{2}\zeta_2 G_{0,-1,0}-\tfrac{3}{2}\zeta_2 G_{0,1,0}$$

$$\mathcal{S}[w_3^{(5),4}] = \alpha\otimes\alpha\otimes y\otimes\alpha\otimes\alpha$$

$$\begin{aligned}w_4^{(5),4}=&G_{-1,-1,-1,0,0}-G_{-1,-1,1,0,0}-G_{-1,1,-1,0,0}+G_{-1,1,1,0,0}-G_{1,-1,-1,0,0}\\&+G_{1,-1,1,0,0}+G_{1,1,-1,0,0}-G_{1,1,1,0,0}+\tfrac{1}{6}\log^4(2)G_{-1}-\tfrac{1}{6}\log^4(2)G_1\\&+4\mathrm{Li}_4\left(\tfrac{1}{2}\right)G_{-1}-4\mathrm{Li}_4\left(\tfrac{1}{2}\right)G_1-\tfrac{53}{40}\zeta_2^2G_{-1}+\tfrac{53}{40}\zeta_2^2G_1-\zeta_2\log^2(2)G_{-1}+\zeta_2\log^2(2)G_1\\&+\tfrac{7}{4}\zeta_3G_{-1,-1}-\tfrac{7}{4}\zeta_3G_{-1,0}+\tfrac{7}{4}\zeta_3G_{-1,1}-\tfrac{7}{4}\zeta_3G_{1,-1}+\tfrac{7}{4}\zeta_3G_{1,0}-\tfrac{7}{4}\zeta_3G_{1,1}\end{aligned}$$

$$\mathcal{S}[w_4^{(5),4}] = \alpha\otimes\alpha\otimes y\otimes y\otimes y$$

$$\begin{aligned}w_5^{(5),4}=&G_{-1,-1,-1,0,0}-G_{-1,-1,1,0,0}-G_{-1,0,-1,0,0}+G_{-1,0,1,0,0}+G_{-1,1,-1,0,0}-G_{-1,1,1,0,0}\\&-G_{0,-1,-1,0,0}+G_{0,-1,1,0,0}+G_{0,0,-1,0,0}-G_{0,0,1,0,0}-G_{0,1,-1,0,0}+G_{0,1,1,0,0}\\&+G_{1,-1,-1,0,0}-G_{1,-1,1,0,0}-G_{1,0,-1,0,0}+G_{1,0,1,0,0}+G_{1,1,-1,0,0}-G_{1,1,1,0,0}-\tfrac{9}{8}\zeta_2^2G_{-1}\\&+\tfrac{9}{8}\zeta_2^2G_1+\tfrac{7}{4}\zeta_3G_{-1,-1}-\tfrac{7}{4}\zeta_3G_{-1,1}-\tfrac{7}{4}\zeta_3G_{0,-1}+\tfrac{7}{4}\zeta_3G_{0,1}+\tfrac{7}{4}\zeta_3G_{1,-1}-\tfrac{7}{4}\zeta_3G_{1,1}\end{aligned}$$

$$\mathcal{S}[w_5^{(5),4}] = \alpha\otimes\alpha\otimes y\otimes\eta\otimes\eta$$

$$\begin{aligned}w_6^{(5),4}=&G_{-1,-1,-1,0,0}-G_{-1,-1,0,0,0}+G_{-1,-1,1,0,0}-G_{-1,1,-1,0,0}+G_{-1,1,0,0,0}-G_{-1,1,1,0,0}\\&-G_{0,-1,-1,0,0}+G_{0,-1,0,0,0}-G_{0,-1,1,0,0}+G_{0,1,-1,0,0}-G_{0,1,0,0,0}+G_{0,1,1,0,0}+G_{1,-1,-1,0,0}\\&-G_{1,-1,0,0,0}+G_{1,-1,1,0,0}-G_{1,1,-1,0,0}+G_{1,1,0,0,0}-G_{1,1,1,0,0}-\tfrac{1}{6}\log^4(2)G_{-1}\\&+\tfrac{1}{6}\log^4(2)G_1-4\mathrm{Li}_4\left(\tfrac{1}{2}\right)G_{-1}+4\mathrm{Li}_4\left(\tfrac{1}{2}\right)G_1+\tfrac{53}{40}\zeta_2^2G_{-1}-\tfrac{53}{40}\zeta_2^2G_1+\zeta_2\log^2(2)G_{-1}\\&-\zeta_2\log^2(2)G_1+\tfrac{1}{4}\zeta_3G_{-1,-1}-\tfrac{1}{4}\zeta_3G_{-1,1}-\tfrac{1}{4}\zeta_3G_{0,-1}+\tfrac{1}{4}\zeta_3G_{0,1}+\tfrac{1}{4}\zeta_3G_{1,-1}-\tfrac{1}{4}\zeta_3G_{1,1}\end{aligned}$$

$$\mathcal{S}[w_6^{(5),4}] = \alpha\otimes\alpha\otimes\eta\otimes y\otimes\eta$$

$$\begin{aligned}w_7^{(5),4}=&G_{-1,-1,-1,0,0}-G_{-1,-1,0,0,0}+G_{-1,-1,1,0,0}-G_{-1,0,-1,0,0}+G_{-1,0,0,0,0}-G_{-1,0,1,0,0}\\&+G_{-1,1,-1,0,0}-G_{-1,1,0,0,0}+G_{-1,1,1,0,0}-G_{1,-1,-1,0,0}+G_{1,-1,0,0,0}-G_{1,-1,1,0,0}\\&+G_{1,0,-1,0,0}-G_{1,0,0,0,0}+G_{1,0,1,0,0}-G_{1,1,-1,0,0}+G_{1,1,0,0,0}-G_{1,1,1,0,0}-\tfrac{3}{40}\zeta_2^2G_{-1}\\&+\tfrac{3}{40}\zeta_2^2G_1+\tfrac{1}{4}\zeta_3G_{-1,-1}-\tfrac{1}{4}\zeta_3G_{-1,0}+\tfrac{1}{4}\zeta_3G_{-1,1}-\tfrac{1}{4}\zeta_3G_{1,-1}+\tfrac{1}{4}\zeta_3G_{1,0}-\tfrac{1}{4}\zeta_3G_{1,1}\end{aligned}$$

$$\mathcal{S}[w_7^{(5),4}] = \alpha\otimes\alpha\otimes\eta\otimes\eta\otimes y$$

$$\begin{aligned}w_8^{(5),4}=&G_{-1,-1,0,-1,0}-G_{-1,-1,0,0,0}+G_{-1,-1,0,1,0}-G_{-1,1,0,-1,0}+G_{-1,1,0,0,0}-G_{-1,1,0,1,0}\\&-G_{0,-1,0,-1,0}+G_{0,-1,0,0,0}-G_{0,-1,0,1,0}+G_{0,1,0,-1,0}-G_{0,1,0,0,0}+G_{0,1,0,1,0}\\&+G_{1,-1,0,-1,0}-G_{1,-1,0,0,0}+G_{1,-1,0,1,0}-G_{1,1,0,-1,0}+G_{1,1,0,0,0}-G_{1,1,0,1,0}+\tfrac{9}{8}\zeta_2^2G_{-1}\\&-\tfrac{9}{8}\zeta_2^2G_1-\tfrac{1}{2}\zeta_2G_{-1,-1,0}+\tfrac{1}{2}\zeta_2G_{-1,1,0}+\tfrac{1}{2}\zeta_2G_{0,-1,0}-\tfrac{1}{2}\zeta_2G_{0,1,0}-\tfrac{1}{2}\zeta_2G_{1,-1,0}\\&+\tfrac{1}{2}\zeta_2G_{1,1,0}-\tfrac{1}{2}\zeta_3G_{-1,-1}+\tfrac{1}{2}\zeta_3G_{-1,1}+\tfrac{1}{2}\zeta_3G_{0,-1}-\tfrac{1}{2}\zeta_3G_{0,1}-\tfrac{1}{2}\zeta_3G_{1,-1}+\tfrac{1}{2}\zeta_3G_{1,1}\end{aligned}$$

$$\mathcal{S}[w_8^{(5),4}] = \alpha \otimes \eta \otimes \alpha \otimes y \otimes \eta$$

$$\begin{aligned}w_9^{(5),4}=&G_{-1,-1,0,-1,0}-G_{-1,-1,0,0,0}+G_{-1,-1,0,1,0}-G_{-1,0,0,-1,0}+G_{-1,0,0,0,0}-G_{-1,0,0,1,0}+G_{-1,1,0,-1,0}\\&-G_{-1,1,0,0,0}+G_{-1,1,0,1,0}-G_{1,-1,0,-1,0}+G_{1,-1,0,0,0}-G_{1,-1,0,1,0}+G_{1,0,0,-1,0}-G_{1,0,0,0,0}\\&+G_{1,0,0,1,0}-G_{1,1,0,-1,0}+G_{1,1,0,0,0}-G_{1,1,0,1,0}+\tfrac{11}{40}\zeta_2^2G_{-1}-\tfrac{11}{40}\zeta_2^2G_1-\tfrac{1}{2}\zeta_2G_{-1,-1,0}-\tfrac{1}{2}\zeta_2G_{-1,1,0}\\&+\tfrac{1}{2}\zeta_2G_{1,-1,0}+\tfrac{1}{2}\zeta_2G_{1,1,0}-\tfrac{1}{2}\zeta_3G_{-1,-1}+\tfrac{1}{2}\zeta_3G_{-1,0}-\tfrac{1}{2}\zeta_3G_{-1,1}+\tfrac{1}{2}\zeta_3G_{1,-1}-\tfrac{1}{2}\zeta_3G_{1,0}+\tfrac{1}{2}\zeta_3G_{1,1}\end{aligned}$$

$$\mathcal{S}[w_9^{(5),4}] = \alpha \otimes \eta \otimes \alpha \otimes \eta \otimes y$$

$$\begin{aligned}w_{10}^{(5),4}=&G_{-1,0,-1,-1,0}-G_{-1,0,-1,0,0}+G_{-1,0,-1,1,0}-G_{-1,0,1,-1,0}+G_{-1,0,1,0,0}-G_{-1,0,1,1,0}\\&-G_{0,0,-1,-1,0}+G_{0,0,-1,0,0}-G_{0,0,-1,1,0}+G_{0,0,1,-1,0}-G_{0,0,1,0,0}+G_{0,0,1,1,0}+G_{1,0,-1,-1,0}\\&-G_{1,0,-1,0,0}+G_{1,0,-1,1,0}-G_{1,0,1,-1,0}+G_{1,0,1,0,0}-G_{1,0,1,1,0}+\tfrac{1}{3}\log^4(2)G_{-1}\\&-\tfrac{1}{3}\log^4(2)G_1-8\log^2(2)G_{0,-1,0}+8\log^2(2)G_{0,1,0}+\log(16)G_{-1,1,0,0}+\log(16)G_{0,-1,-1,0}\\&+\log(16)G_{0,-1,1,0}+\log(16)G_{1,1,0,0}-\log(4)G_{-1,0,-1,0}+\log(4)G_{-1,0,1,0}+\log(4)G_{0,0,-1,0}\\&-\log(4)G_{0,0,1,0}-\log(4)G_{1,0,-1,0}+\log(4)G_{1,0,1,0}-4\log(2)G_{-1,-1,0,0}-4\log(2)G_{0,1,-1,0}\\&-4\log(2)G_{0,1,1,0}-4\log(2)G_{1,-1,0,0}+8\mathrm{Li}_4\left(\tfrac{1}{2}\right)G_{-1}-8\mathrm{Li}_4\left(\tfrac{1}{2}\right)G_1-\tfrac{151}{40}\zeta_2^2G_{-1}\\&+\tfrac{151}{40}\zeta_2^2G_1-\tfrac{1}{2}\zeta_2G_{-1,0,-1}+\tfrac{1}{2}\zeta_2G_{-1,0,1}+\tfrac{1}{2}\zeta_2G_{0,0,-1}-\tfrac{1}{2}\zeta_2G_{0,0,1}-\tfrac{1}{2}\zeta_2G_{1,0,-1}\\&+\tfrac{1}{2}\zeta_2G_{1,0,1}-2\zeta_2\log^2(2)G_{-1}+2\zeta_2\log^2(2)G_1-2\zeta_2\log(2)G_{0,-1}+2\zeta_2\log(2)G_{0,1}\end{aligned}$$

$$\mathcal{S}[w_{10}^{(5),4}] = \alpha \otimes \eta \otimes y \otimes \alpha \otimes \eta$$

$$\begin{aligned}w_{11}^{(5),4}=&-2G_{-1,0,-1,-1,0}+2G_{-1,0,-1,0,0}-2G_{-1,0,-1,1,0}+2G_{-1,0,0,-1,0}-2G_{-1,0,0,0,0}+2G_{-1,0,0,1,0}\\&-2G_{-1,0,1,-1,0}+2G_{-1,0,1,0,0}-2G_{-1,0,1,1,0}+3G_{0,-1,-1,-1,0}-3G_{0,-1,-1,0,0}+3G_{0,-1,-1,1,0}\\&-2G_{0,-1,0,-1,0}+2G_{0,-1,0,0,0}-2G_{0,-1,0,1,0}+G_{0,-1,1,-1,0}-G_{0,-1,1,0,0}+G_{0,-1,1,1,0}-G_{0,0,-1,-1,0}\\&+G_{0,0,-1,0,0}-G_{0,0,-1,1,0}+G_{0,0,1,-1,0}-G_{0,0,1,0,0}+G_{0,0,1,1,0}-G_{0,1,-1,-1,0}+G_{0,1,-1,0,0}\\&-G_{0,1,-1,1,0}+2G_{0,1,0,-1,0}-2G_{0,1,0,0,0}+2G_{0,1,0,1,0}-3G_{0,1,1,-1,0}+3G_{0,1,1,0,0}-3G_{0,1,1,1,0}\\&+2G_{1,0,-1,-1,0}-2G_{1,0,-1,0,0}+2G_{1,0,-1,1,0}-2G_{1,0,0,-1,0}+2G_{1,0,0,0,0}-2G_{1,0,0,1,0}+2G_{1,0,1,-1,0}\\&-2G_{1,0,1,0,0}+2G_{1,0,1,1,0}-4\log^2(2)G_{0,-1,0}+4\log^2(2)G_{0,1,0}-\log(4)G_{0,-1,-1,0}+\log(4)G_{0,-1,1,0}\\&+\log(4)G_{0,0,-1,0}-\log(4)G_{0,0,1,0}-\log(4)G_{0,1,-1,0}+\log(4)G_{0,1,1,0}+\tfrac{1}{4}\zeta_2^2G_{-1}-\tfrac{1}{4}\zeta_2^2G_1+\zeta_2G_{-1,0,-1}\\&+\zeta_2G_{-1,0,1}-\tfrac{3}{2}\zeta_2G_{0,-1,-1}+\tfrac{1}{2}\zeta_2G_{0,-1,0}-\tfrac{1}{2}\zeta_2G_{0,-1,1}+\tfrac{1}{2}\zeta_2G_{0,0,-1}-\tfrac{1}{2}\zeta_2G_{0,0,1}+\tfrac{1}{2}\zeta_2G_{0,1,-1}\\&-\tfrac{1}{2}\zeta_2G_{0,1,0}+\tfrac{3}{2}\zeta_2G_{0,1,1}-\zeta_2G_{1,0,-1}-\zeta_2G_{1,0,1}+\tfrac{1}{2}\zeta_3G_{-1,0}-\tfrac{1}{2}\zeta_3G_{0,-1}+\tfrac{1}{2}\zeta_3G_{0,1}-\tfrac{1}{2}\zeta_3G_{1,0}\end{aligned}$$

$$\mathcal{S}[w_{11}^{(5),4}] = \alpha \otimes \eta \otimes y \otimes \eta \otimes \alpha + 2\alpha \otimes \eta \otimes \eta \otimes y \otimes \alpha - 2\alpha \otimes \eta \otimes \eta \otimes \alpha \otimes y$$

Appendix C

Lightlike Wilson-line Calculations

C.1 Direct Calculation of the Splitting Functions at Large x

In this appendix we present a calculation for parton distribution splitting functions directly using the definitions (4.26) and (4.27). As explained in the main text we take incoming partons to be off shell $p^2 \neq 0$ but with zero transverse momentum $p = (p_+, \frac{p^2}{2p_+}, \mathbf{0}_{d-2})$. This regulates the infrared such that we are only exposed to UV poles.

To calculate a single diagram there is a general strategy talked through in the main text with a slight change for the off shell case:

- Write down the integral using Feynman rules
- Integrate over the minus component of all loop momenta using Cauchy's residue theorem. This provides constraints on the plus component of loop momenta due to the location of the poles.
- Integrate over the transverse component of all loop momenta. As we are only interested in the UV divergent terms, this can be simplified to just calculating iterated bubbles at two loops. Although we do need to calculate the finite terms of one loop graphs to perform the renormalisation.

- Rescale the plus component to arrive at a general form such as,

$$\text{Disc}\int_0^1 dydz\frac{N(x,y,z,\epsilon)}{(1-x+i\varepsilon)(1-x-y+i\varepsilon)(1-x-yz+i\varepsilon)}. \tag{C.1}$$

  The denominators correspond to the Wilson line propagators.

- Now we take the discontinuity in x and perform the final integrations. Often these integrals evaluate to ${}_2F_1$ functions at two loops.

- Finally we expand in ϵ using,

$$(1-x)^{-1-m\epsilon} = -\frac{1}{m\epsilon}\delta(1-x) + \frac{1}{(1-x)_+} + \sum_{n=1}^{\infty}\frac{(-m\epsilon)^n}{n!}\left(\frac{\log(1-x)^n}{1-x}\right)_+. \tag{C.2}$$

For brevity of results we shall define,

$$\delta = \delta(1-x) \qquad P = \frac{1}{(1-x)_+} \qquad L^n = \frac{\log^n(1-x)}{(1-x)_+}. \tag{C.3}$$

Also, all the following expressions are valid up to but not including terms that diverge as slowly as $\log(1-x)$.

For PDFs we expand in powers of $\left(\frac{\alpha_s}{4\pi}\right)$,

$$f_{ii} = \sum_{n=0}^{\infty}\left(\frac{\alpha_s}{4\pi}\right)^n f_{ii}^{(n)}. \tag{C.4}$$

Example. Let us illustrate the above steps. For this we choose the two loop diagram in Figure C.1e. The Feynman rules for the diagram, in Feynman gauge, give,

$$\text{Disc}\frac{ig_s^4}{2\pi}C_AC_F\int\frac{d^dq_1}{(2\pi)^d}\int\frac{d^dq_2}{(2\pi)^d}\frac{p_+(p_+-q_{1+})(2q_{2+}-q_{1+})}{q_2^2q_1^2(q_1-q_2)^2(p-q_1)^2} \times\frac{1}{(p-k)\cdot u\ \ (p-k-q_1)\cdot u\ \ (p-k-q_2)\cdot u}, \tag{C.5}$$

where $k\cdot u = xp_+$ and the $+i\varepsilon$ prescription is implied. It is reminded that the Wilson line direction u is in the (-) direction, $u=(0,1,\mathbf{0}_{d-2})$.

We shall define $f_{qq}^{(2),(e)}$ to be the contribution to $f_{qq}^{(2)}$ of diagram C.1e. When

integrating the q_{1-} and q_{2-} components using the residue theorem, constraints are placed on the plus momenta,

$$p_+ > q_{1+} > q_{2+} > 0. \tag{C.6}$$

The integrations over the transverse components are just iterated bubbles. Rescaling the plus component we arrive at,

$$f_{qq}^{(2),(e)} = \text{Disc}\frac{i}{2\pi}C_A C_F \frac{\Gamma(\epsilon)\Gamma(2\epsilon)}{\Gamma(1+\epsilon)}\int_0^1 dydzy^{1-2\epsilon}(1-y)^{1-\epsilon}(1-z)^{-\epsilon}z^{-\epsilon} \times \frac{1-2z}{(1-x+i\varepsilon)(1-x-y+i\varepsilon)(1-x-yz+i\varepsilon)}. \tag{C.7}$$

Taking the discontinuity we use,

$$\text{Disc}\,\frac{i}{2\pi}\,\frac{1}{(1-x+i\varepsilon)(1-x-y+i\varepsilon)(1-x-yz+i\varepsilon)} = \left(\frac{\delta(1-x)}{(1-x-y)(1-x-yz)} + \frac{\delta(1-x-y)}{(1-x)(1-x-yz)} + \frac{\delta(1-x-yz)}{(1-x)(1-x-y)}\right). \tag{C.8}$$

There are three separate terms now to calculate. The first is the *virtual* cut and evaluates to,

$$f_{qq}^{(2),(e),(V)} = C_A C_F\left(\frac{1}{4\epsilon^4} + \frac{1}{\epsilon^3} + \frac{1}{\epsilon^2}\left(\frac{7}{2} - \frac{\zeta_2}{4}\right) + \frac{1}{\epsilon}\left(-\zeta_2 - \frac{8\zeta_3}{3} + \frac{23}{2}\right)\right)\delta \tag{C.9}$$

The second and third are *real* cuts,

$$f_{qq}^{(2),(e),(R1)} = C_A C_F\Bigg(-\frac{\delta}{4\epsilon^4} + \frac{P-\delta}{2\epsilon^3} + \frac{1}{\epsilon^2}\left(\left(-\frac{\zeta_2}{4}-1\right)\delta + P - L\right) + \frac{1}{\epsilon}\left(\delta\left(-\frac{\zeta_2}{2} + \frac{7\zeta_3}{6} - 2\right) + \left(\frac{\zeta_2}{2}+2\right)P - 2L + L^2\right)\Bigg) \tag{C.10}$$

$$f_{qq}^{(2),(e),(R2)} = C_A C_F\Bigg(\frac{-\delta - P}{2\epsilon^3} + \frac{1}{\epsilon^2}\left((\zeta_2 - 1)\delta + \frac{1}{2}P + \frac{3}{2}L\right) + \frac{1}{\epsilon}\left(\delta\left(-\frac{\zeta_2}{2} + \zeta_3 - 2\right) + \left(1 - \frac{5\zeta_2}{2}\right)P - \frac{1}{2}L - \frac{7}{4}L^2\right)\Bigg) \tag{C.11}$$

In the sum we find,

$$f_{qq}^{(2),(e)} = C_A C_F\Bigg(\frac{1}{\epsilon^2}\left(\left(\frac{\zeta_2}{2}+\frac{3}{2}\right)\delta + \frac{3}{2}P + \frac{1}{2}L\right)$$

$$+\frac{1}{\epsilon}\left(\delta\left(-2\zeta_2-\frac{\zeta_3}{2}+\frac{15}{2}\right)+(3-2\zeta_2)P-\frac{5}{2}L-\frac{3}{4}L^2\right)\Bigg) \tag{C.12}$$

Above we see a salient feature of two loop diagrams: individual cuts are ϵ^{-4} and ϵ^{-3} divergent. These are poles from when the emitted gluon goes soft and cancel in the sum of real and virtual cuts. The remaining divergences are UV, whose renormalisation gives the splitting functions. The L and L^2 terms are present in individual diagrams but cancel in the combination such that the splitting functions diverge as in eq. (4.58).

Another feature is that we found that the real cuts, eqs. (C.10) and (C.11), contribute to B_δ. Rather than inferring the coefficient of δ from sum or momentum conservation rules, we are able to state that for the off-shell extraction of the splitting functions, real cuts contribute to $\delta(1-x)$.

We now calculate the two loop diagonal splitting functions at large x for quarks and gluons.

C.1.1 Calculating P_{qq}

The one loop contributions are Figures C.1a and C.1b and the self energy on each external leg. They sum to,

$$\begin{aligned} f_{qq}^{(1)} &= f_{qq}^{(1),(a)} + 2f_{qq}^{(1),(b)} + f_{qq}^{(1),\text{SE ext}} \\ &= C_F\left(\frac{1}{\epsilon}\left(4P-(\xi-3)\delta\right)-\delta(\xi+4\zeta_2-7)+(\xi-1)P-4L\right), \end{aligned} \tag{C.13}$$

where ξ is the gauge parameter in a general covariant gauge. The two loop contributions are shown in Figures C.1c–C.1m. They exclude self energies on external legs. Their calculation was performed in Feynman gauge $\xi=1$ and the results are,

$$\begin{aligned} f_{qq}^{(2),(c)} &= C_F(C_A-2C_F)\left[\frac{1}{\epsilon^2}\left(2\zeta_2\delta\right)+\frac{1}{\epsilon}\left(-4\zeta_3\delta-4\zeta_2P\right)\right] \\ f_{qq}^{(2),(d)} &= C_F^2\left[\frac{1}{\epsilon^2}\left((4-8\zeta_2)\delta+8P+8L\right)\right. \\ &\qquad\left.+\frac{1}{\epsilon}\left((16-8\zeta_2)\delta+(8\zeta_2+16)P-8L-12L^2\right)\right] \end{aligned}$$

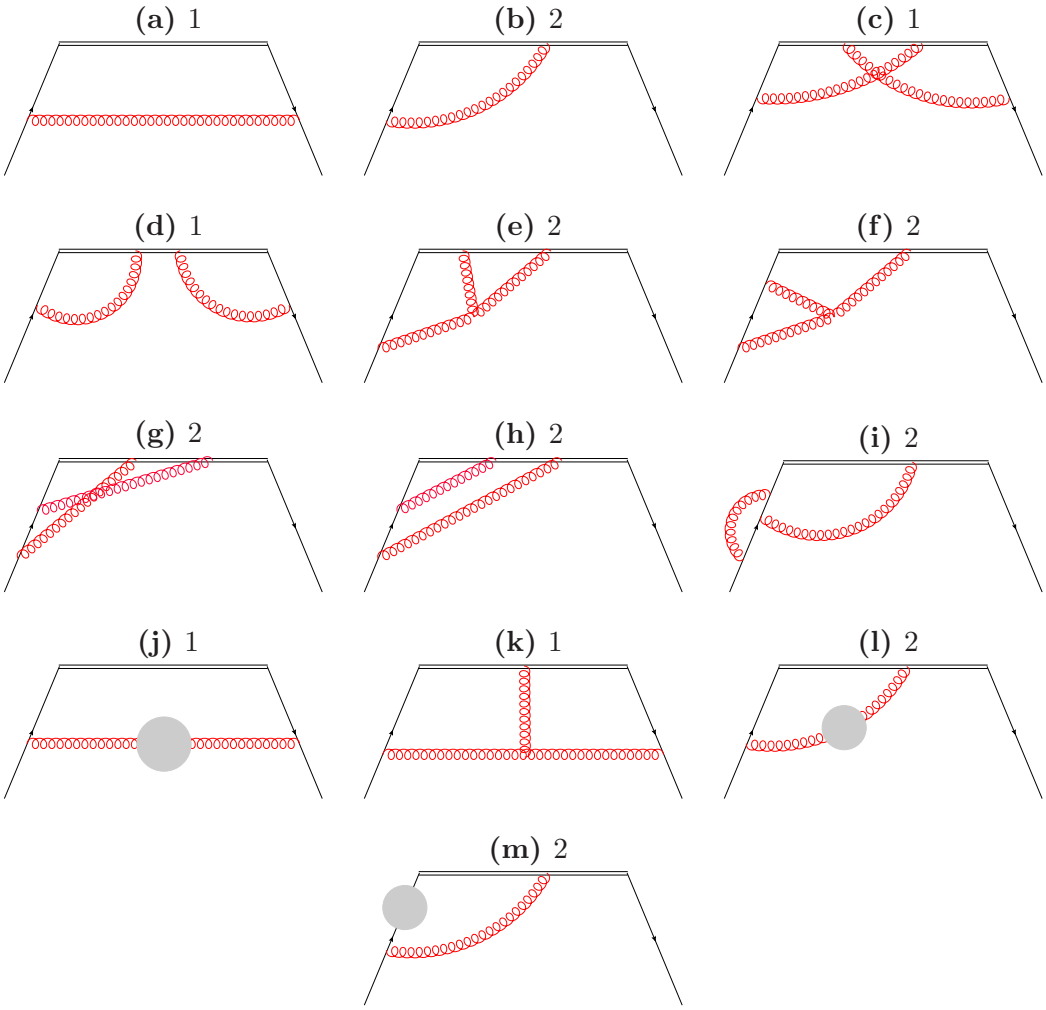

Figure C.1: Large-x divergent contributions to the quark-quark parton distribution up to two loops. The grey blob represents a self energy insertion. Each diagram has a multiple factor displayed. Insertions on external legs are excluded.

$$
\begin{aligned}
f_{qq}^{(2),(e)} &= C_A C_F \left[\frac{1}{\epsilon^2} \left(\left(\frac{\zeta_2}{2} + \frac{3}{2} \right) \delta + \frac{3}{2} P + \frac{1}{2} L \right) \right. \\
&\quad \left. + \frac{1}{\epsilon} \left(\delta \left(-2\zeta_2 - \frac{\zeta_3}{2} + \frac{15}{2} \right) + (3 - 2\zeta_2) P - \frac{5}{2} L - \frac{3}{4} L^2 \right) \right] \\
f_{qq}^{(2),(f)} &= C_A C_F \left[\frac{1}{\epsilon^2} \left(\delta + 2P + \frac{1}{2} L \right) \right. \\
&\quad \left. + \frac{1}{\epsilon} \left(\delta \left(-\frac{5\zeta_2}{2} - \zeta_3 + 3 \right) + \left(\frac{7}{2} - \zeta_2 \right) P - 3L - \frac{3}{4} L^2 \right) \right] \\
f_{qq}^{(2),(g)} &= C_F (C_A - 2C_F) \left[\frac{1}{\epsilon^2} \left((1 - \zeta_2) \delta + P + L \right) \right. \\
&\quad \left. + \frac{1}{\epsilon} \left(\delta(-2\zeta_2 - 3\zeta_3 + 5) + 2P - L - \frac{3}{2} L^2 \right) \right] \\
f_{qq}^{(2),(h)} &= C_F^2 \left[\frac{1}{\epsilon^2} \left((2 - 2\zeta_2) \delta + 2P + 2L \right) \right. \\
&\quad \left. + \frac{1}{\epsilon} \left(\delta(-4\zeta_2 - 6\zeta_3 + 10) + 4P - 2L - 3L^2 \right) \right] \\
f_{qq}^{(2),(i)} &= C_F (C_A - 2C_F) \left[\frac{1}{\epsilon^2} \left(\left(\zeta_2 - \frac{1}{2} \right) \delta + \frac{1}{2} P \right) \right. \\
&\quad \left. + \frac{1}{\epsilon} \left(\delta \left(-\frac{\zeta_2}{2} + 7\zeta_3 - 4 \right) + \frac{1}{2} P - \frac{1}{2} L \right) \right] \\
f_{qq}^{(2),(j)} &= C_F \left[\frac{1}{\epsilon^2} \left(\delta \left(\frac{2 n_f T_f}{3} - \frac{5 C_A}{6} \right) \right) \right. \\
&\quad \left. + \frac{1}{\epsilon} \left(\delta \left(\frac{7 C_A}{9} - \frac{8 n_f T_f}{9} \right) + P \left(\frac{5 C_A}{3} - \frac{4 n_f T_f}{3} \right) \right) \right] \\
f_{qq}^{(2),(k)} &= C_A C_F \left(\frac{1}{\epsilon^2} \left(\zeta_2 \delta \right) + \frac{1}{\epsilon} \left(\zeta_3 \delta - 2\zeta_2 P \right) \right) \\
f_{qq}^{(2),(l)} &= C_F \left[\frac{1}{\epsilon^2} \left(\delta \left(\frac{5 C_A}{3} - \frac{4 n_f T_f}{3} \right) + P \left(\frac{5 C_A}{3} - \frac{4 n_f T_f}{3} \right) \right) \right. \\
&\quad + \frac{1}{\epsilon} \left(\delta \left(-\frac{5 C_A \zeta_2}{3} + \frac{61 C_A}{9} + \frac{4}{3} n_f T_f \zeta_2 - \frac{44 n_f T_f}{9} \right) \right. \\
&\quad \left. \left. + P \left(\frac{16 C_A}{9} - \frac{8 n_f T_f}{9} \right) + L \left(\frac{8 n_f T_f}{3} - \frac{10 C_A}{3} \right) \right) \right] \\
f_{qq}^{(2),(m)} &= C_F^2 \left(-\frac{1}{\epsilon^2} \left(\delta + P \right) + \frac{1}{\epsilon} \left((2\zeta_2 - 4) \delta - P + L \right) \right) \\
f_{qq}^{(2),\text{SE ext}} &= \frac{1}{\epsilon^2} \left(-2 \left(C_A C_F + 3 C_F^2 \right) \delta - 8 C_F^2 P \right) \\
&\quad + \frac{1}{\epsilon} \left(\frac{1}{2} \delta \left(-25 C_A C_F + 16 C_F^2 \zeta_2 - 37 C_F^2 + 4 C_F n_f T_f \right) \right. \\
&\quad \left. - 8 C_F^2 P + 8 C_F^2 L \right)
\end{aligned}
$$

Summing the two loop contributions with the factors shown in Figure C.1 we find,

$$f_{qq}^{(2)} = \frac{C_F}{\epsilon^2}\Bigg[\delta\left(\frac{9C_A}{2} + C_F(2-8\zeta_2) - 2n_fT_f\right) + P\left(\frac{22C_A}{3} + 8C_F^2 - \frac{8n_fT_f}{3}\right) + 16C_FL\Bigg] + \frac{C_F}{\epsilon}\Bigg[\delta\Bigg(C_A\left(-\frac{22\zeta_2}{3} - 6\zeta_3 + \frac{125}{6}\right) + C_F\left(-14\zeta_2 - 4\zeta_3 + \frac{27}{2}\right) + n_fT_f\left(\frac{8\zeta_2}{3} - \frac{26}{3}\right)\Bigg) + P\left(C_A\left(\frac{119}{9} - 4\zeta_2\right) + 24C_F - \frac{28n_fT_f}{9}\right) + L\left(-\frac{44C_A}{3} - 8C_F + \frac{16n_fT_f}{3}\right) - 24C_FL^2\Bigg] \tag{C.14}$$

At two loops we need to take into account the running from the one loop contribution, $\frac{\alpha_s}{4\pi}f_{qq}^{(1)} \to \frac{\alpha_s}{4\pi}f_{qq}^{(1),R}$. This is found by replacing $\xi \to \left(1 + \frac{\alpha_s}{4\pi\epsilon}\left(\frac{10}{6}C_A - \frac{4}{3}T_fn_f\right)\right)\xi$ and $\alpha_s \to (1 + \frac{\alpha_s\hat{b}_0}{\pi\epsilon})\alpha_s$. We then specialise to Feynman gauge $\xi = 1$.

We then find the Z_{qq} that minimally subtracts the divergences in $\delta + \frac{\alpha_s}{4\pi}f_{qq}^{(1),R} + \left(\frac{\alpha_s}{4\pi}\right)^2 f_{qq}^{(2)}$. As the renormalisation is multiplicative, convolutions need to be taken into account for one loop squared terms. For example,

$$P \otimes L = -\zeta_2 P + \frac{3}{2}L^2 + \zeta_3\delta. \tag{C.15}$$

Equivalently the renormalisation can be transformed to Mellin space, eq. 4.45, where the convolutions become products ensuring that,

$$\tilde{Z}_{qq}\left(1 + \frac{\alpha_s}{4\pi}\tilde{f}_{qq}^{(1),R} + \left(\frac{\alpha_s}{4\pi}\right)^2\tilde{f}_{qq}^{(2)}\right) \tag{C.16}$$

is finite in ϵ. We can then extract the splitting functions to two loops from,

$$\tilde{P}_{qq} = \left(-\epsilon\alpha_s - \alpha_s^2\frac{\hat{b}_0}{\pi}\right)\frac{d}{d\alpha_s}\log(\tilde{Z}_{qq}Z_q), \tag{C.17}$$

where Z_q is the wavefunction renormalisation in $\overline{\text{MS}}$ for the quark. Up to two loops,

$$Z_q = 1 - \left(\frac{\alpha_s}{4\pi}\right)\frac{C_F}{\epsilon} + \left(\frac{\alpha_s}{4\pi}\right)^2 C_F\left(\frac{1}{\epsilon^2}\left(C_A + \frac{C_F}{2}\right) + \frac{1}{\epsilon}\left(-\frac{17C_A}{4} + \frac{3C_F}{4} + T_fn_f\right)\right). \tag{C.18}$$

Converting back to x space we find,

$$\begin{aligned}P_{qq} =& \frac{\alpha_s}{4\pi} C_F \left(3\delta + 4P\right) \\ &+ \left(\frac{\alpha_s}{4\pi}\right)^2 \Bigg[\delta\Bigg(C_A C_F \left(\frac{44\zeta_2}{3} - 12\zeta_3 + \frac{17}{6}\right) + C_F^2 \left(-12\zeta_2 + 24\zeta_3 + \frac{3}{2}\right) \\ &\quad - C_F T_f n_f \left(\frac{16\zeta_2}{3} + \frac{2}{3}\right)\Bigg) + P\left(C_A C_F \left(\frac{268}{9} - 8\zeta_2\right) - \frac{80 C_F n_f T_f}{9}\right)\Bigg]\end{aligned} \tag{C.19}$$

Notice that we find that all L^n terms cancel. This reproduces B_δ^q, the coefficient of δ in eq. (4.60), and shows that the coefficient of P is γ_{cusp} as in eq. (3.35).

C.1.2 Calculating P_{gg}

The one loop contributions for the gluon gluon distribution function are shown in Figures C.2a and C.2b. The total one loop contributions are,

$$\begin{aligned}f_{gg}^{(1)} =& \frac{1}{\epsilon}\left[\delta\left(-\frac{C_A\xi}{2} + \frac{35C_A}{6} - \frac{8n_f T_f}{3}\right) + 4C_A P\right] \\ &+ \delta\left(-4C_A\zeta_2 + \frac{98C_A}{9} - \frac{40n_f T_f}{9}\right) + (C_A\xi - C_A)P - 4C_A L.\end{aligned} \tag{C.20}$$

The two loop contributions are shown in Figures C.2c–C.2p. The two loop contributions are,

$$\begin{aligned}f_{gg}^{(2),(c)} =& C_A^2\left(\frac{1}{\epsilon^2}\left(-\frac{9}{4}P\right) + \frac{1}{\epsilon}\left(\frac{9}{4}\zeta_2\delta - \frac{9}{2}P + \frac{9}{4}L\right)\right) \\ f_{gg}^{(2),(d)} =& C_A^2\left(\frac{1}{\epsilon^2}\left(2\zeta_2\delta\right) + \frac{1}{\epsilon}\left(-4\zeta_3\delta - 4\zeta_2 P\right)\right) \\ f_{gg}^{(2),(e)} =& C_A^2\Bigg[\frac{1}{\epsilon^2}\left((1 - 8\zeta_2)\delta + 4P + 8L\right) \\ &\quad + \frac{1}{\epsilon}\left((4 - 4\zeta_2)\delta + (8\zeta_2 + 8)P - 4L - 12L^2\right)\Bigg] \\ f_{gg}^{(2),(f)} =& C_A^2\Bigg[\frac{1}{\epsilon^2}\left(\left(\frac{\zeta_2}{2} + \frac{3}{4}\right)\delta + \frac{5}{4}P + \frac{1}{2}L\right) \\ &\quad + \frac{1}{\epsilon}\left(\delta\left(-\frac{3\zeta_2}{2} - \frac{\zeta_3}{2} + \frac{15}{4}\right) + \left(\frac{5}{2} - 2\zeta_2\right)P - \frac{9}{4}L - \frac{3}{4}L^2\right)\Bigg] \\ f_{gg}^{(2),(g)} =& C_A^2\left(\frac{1}{\epsilon^2}\left(-\frac{9}{8}\delta - \frac{9}{8}P\right) + \frac{1}{\epsilon}\left(\left(\frac{9\zeta_2}{4} - \frac{45}{8}\right)\delta - \frac{9}{4}P + \frac{9}{8}L\right)\right)\end{aligned}$$

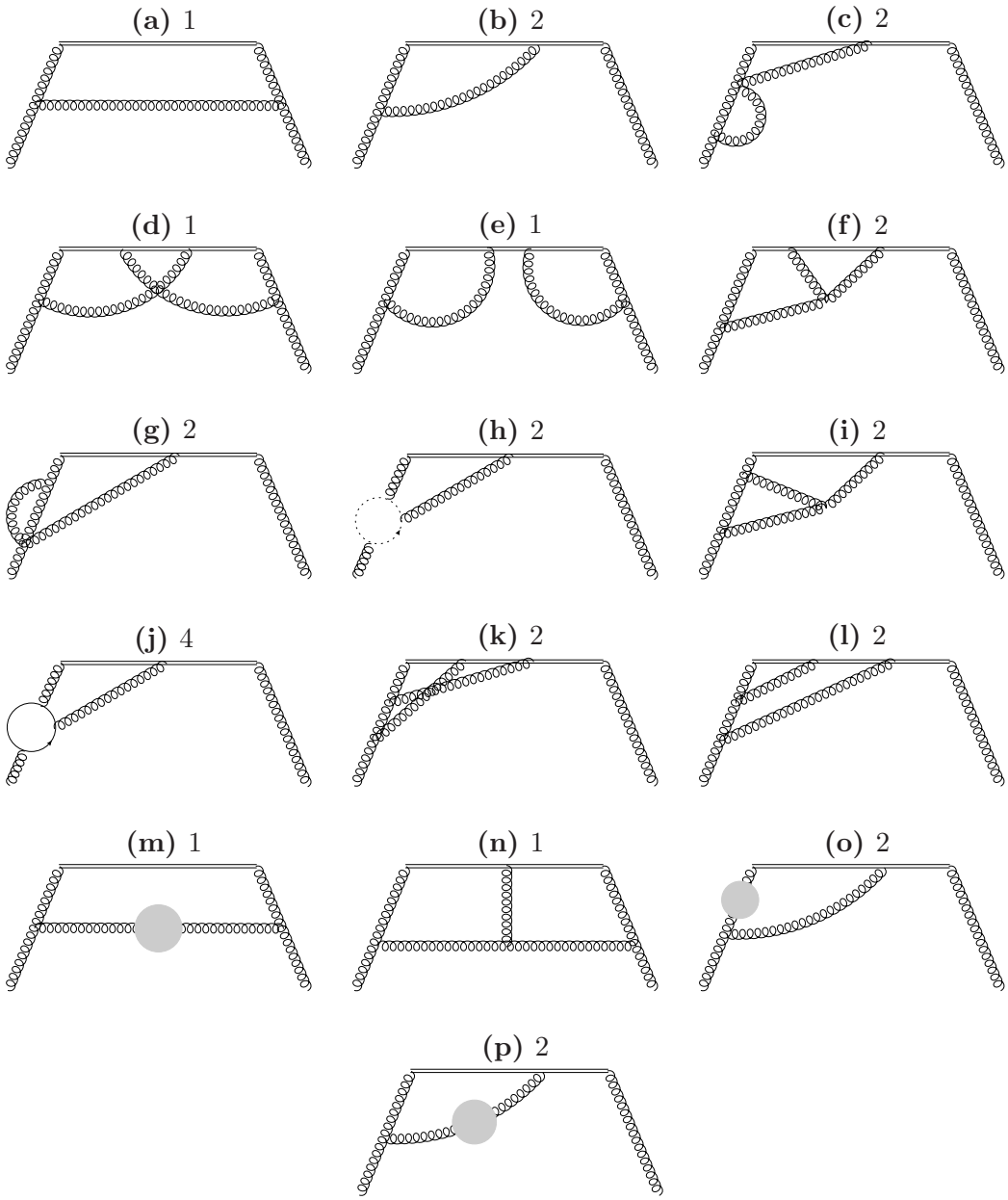

Figure C.2: Large-x divergent contributions to the gluon-gluon parton distribution up to two loops. The grey blob represents a self energy insertion. Insertions on external legs are excluded. The clockwise ghost is included in h).

$$
\begin{aligned}
f_{gg}^{(2),(h)} =& C_A^2 \left(\frac{1}{\epsilon^2}\left(-\frac{1}{48}\delta - \frac{1}{24}P\right) + \frac{1}{\epsilon}\left(\left(\frac{\zeta_2}{24} - \frac{31}{288}\right)\delta - \frac{1}{9}P + \frac{1}{24}L\right)\right) \\
f_{gg}^{(2),(i)} =& C_A^2 \left[\frac{1}{\epsilon^2}\left(\left(\frac{3\zeta_2}{4} + \frac{5}{16}\right)\delta + 3P + \frac{1}{2}L\right)\right. \\
&\left. + \frac{1}{\epsilon}\left(\delta\left(-\frac{35\zeta_2}{8} + \frac{17\zeta_3}{4} + \frac{65}{96}\right) + \left(\frac{71}{12} - \zeta_2\right)P - 4L - \frac{3}{4}L^2\right)\right] \\
f_{gg}^{(2),(j)} =& C_A n_f T_f \left(\frac{1}{\epsilon^2}\left(\frac{1}{3}\delta + \frac{2}{3}P\right) + \frac{1}{\epsilon}\left(\left(\frac{59}{36} - \frac{2\zeta_2}{3}\right)\delta + \frac{10}{9}P - \frac{2}{3}L\right)\right) \\
f_{gg}^{(2),(k)} =& C_A^2 \left[\frac{1}{\epsilon^2}\left(\left(\frac{3}{4} - \frac{5\zeta_2}{4}\right)\delta + \frac{1}{2}P + L\right)\right. \\
&\left. + \frac{1}{\epsilon}\left(\delta\left(-\zeta_2 - \frac{19\zeta_3}{4} + \frac{15}{4}\right) + P - \frac{1}{2}L - \frac{3}{2}L^2\right)\right] \\
f_{gg}^{(2),(l)} =& C_A^2 \left[\frac{1}{\epsilon^2}\left(-\frac{3}{2}\zeta_2\delta + P + 2L\right)\right. \\
&\left. + \frac{1}{\epsilon}\left(\delta\left(-2\zeta_2 - \frac{5\zeta_3}{2}\right) + 2P - L - 3L^2\right)\right] \\
f_{gg}^{(2),(m)} =& \frac{1}{\epsilon^2}\left(\delta\left(\frac{2C_A n_f T_f}{3} - \frac{5C_A^2}{6}\right)\right) \\
&+ \frac{1}{\epsilon}\left(\delta\left(\frac{7C_A^2}{9} - \frac{8C_A n_f T_f}{9}\right) + P\left(\frac{5C_A^2}{3} - \frac{4C_A n_f T_f}{3}\right)\right) \\
f_{gg}^{(2),(n)} =& C_A^2 \left(\frac{1}{\epsilon^2}\left(\zeta_2\delta\right) + \frac{1}{\epsilon}\left(-2\zeta_2 P + \zeta_3\delta\right)\right) \\
f_{gg}^{(2),(o)} =& \frac{1}{\epsilon^2}\left(\delta\left(-\frac{7C_A n_f T_f}{9} + \frac{35C_A^2}{36}\right) + P\left(-\frac{4C_A n_f T_f}{3} + \frac{5C_A^2}{3}\right)\right) \\
&+ \frac{1}{\epsilon}\left[\delta\left(-\frac{10C_A^2\zeta_2}{3} + \frac{133C_A^2}{27} + \frac{8}{3}C_A n_f T_f \zeta_2 - \frac{98C_A n_f T_f}{27}\right)\right. \\
&\left. + P\left(-\frac{20C_A n_f T_f}{9} + \frac{31C_A^2}{9}\right) + L\left(-\frac{5C_A^2}{3} + \frac{4C_A n_f T_f}{3}\right)\right] \\
f_{gg}^{(2),(p)} =& \frac{1}{\epsilon^2}\left(\delta\left(-\frac{13C_A n_f T_f}{18} + \frac{65C_A^2}{72}\right) + P\left(-\frac{4C_A n_f T_f}{3} + \frac{5C_A^2}{3}\right)\right) \\
&+ \frac{1}{\epsilon}\left[\delta\left(-\frac{5C_A^2\zeta_2}{3} + \frac{1931C_A^2}{432} + \frac{4}{3}C_A n_f T_f \zeta_2 - \frac{355C_A n_f T_f}{108}\right)\right. \\
&\left. + P\left(-\frac{8C_A n_f T_f}{9} + \frac{16C_A^2}{9}\right) + L\left(-\frac{10C_A^2}{3} + \frac{8C_A n_f T_f}{3}\right)\right] \\
f_{gg}^{(2)\text{SE ext}} =& \frac{1}{\epsilon^2}\left(\delta\left(\frac{95C_A^2}{6} - \frac{58C_A n_f T_f}{3} + \frac{16n_f^2 T_f^2}{3}\right) + P\left(\frac{20C_A^2}{3} - \frac{16C_A n_f T_f}{3}\right)\right) \\
&+ \frac{1}{\epsilon}\left[\delta\left(-\frac{1}{3}20C_A^2\zeta_2 + \frac{2311C_A^2}{36} + \frac{16}{3}C_A n_f T_f \zeta_2 - \frac{637C_A n_f T_f}{9}\right.\right. \\
&\left.\left. - 4C_F n_f T_f + \frac{160n_f^2 T_f^2}{9}\right) + P\left(\frac{124C_A^2}{9} - \frac{80C_A n_f T_f}{9}\right)\right.
\end{aligned}
$$

$$+ L\left(\frac{16C_An_fT_f}{3} - \frac{20C_A^2}{3}\right)\Bigg]$$

The total two loop contribution is,

$$\begin{aligned} f^{(2)} =& \frac{1}{\epsilon}\Bigg[\delta\Bigg(C_A^2\left(-36\zeta_2 - 10\zeta_3 + \frac{7591}{72}\right) + C_An_fT_f\left(16\zeta_2 - \frac{527}{6}\right) - 4C_Fn_fT_f \\ &+ \frac{160n_f^2T_f^2}{9}\Bigg) + P\left(C_A^2\left(-4\zeta_2 + \frac{496}{9}\right) - \frac{176C_An_fT_f}{9}\right) \\ &+ L\left(16C_An_fT_f - 36C_A^2\right) - 24C_A^2L^2\Bigg] \\ &+ \frac{1}{\epsilon^2}\Bigg[\delta\left(C_A^2\left(-8\zeta_2 + \frac{101}{4}\right) - \frac{71C_An_fT_f}{3} + \frac{16n_f^2T_f^2}{3}\right) \\ &+ P\left(\frac{86C_A^2}{3} - \frac{40C_An_fT_f}{3}\right) + 16C_A^2L\Bigg] \end{aligned}$$

The extraction of the splitting function from above is the same as in the quark case. Instead of Z_q we use the gluon field renormalisation in $\overline{\text{MS}}$,

$$\begin{aligned} Z_A =& 1 + \frac{\alpha_s}{4\pi}\frac{1}{\epsilon}\left(\frac{5C_A}{3} - \frac{4n_fT_f}{3}\right) \\ &+ \left(\frac{\alpha_s}{4\pi}\right)^2\left[\frac{1}{\epsilon}\left(\frac{23C_A^2}{8} - \frac{5C_An_fT_f}{2} - 2C_Fn_fT_f\right) + \frac{1}{\epsilon^2}\left(\frac{5C_An_fT_f}{3} - \frac{25C_A^2}{12}\right)\right] \end{aligned} \tag{C.21}$$

Performing those steps we find,

$$\begin{aligned} P_{gg} =& \frac{\alpha_s}{4\pi}\left(\delta\left(\frac{11C_A}{3} - \frac{4n_fT_f}{3}\right) + 4C_AP\right) \\ &+ \left(\frac{\alpha_s}{4\pi}\right)^2\Bigg[\delta\left(12C_A^2\zeta_3 + \frac{32C_A^2}{3} - \frac{16C_An_fT_f}{3} - 4C_Fn_fT_f\right) \\ &+ P\left(-8C_A^2\zeta_2 + \frac{268C_A^2}{9} - \frac{80C_An_fT_f}{9}\right)\Bigg]. \end{aligned} \tag{C.22}$$

Again this aligns with B_δ^g in eq. (4.60) and γ_{cusp} in eq. (3.35).

We have replicated previous splitting function calculations at large x directly from the definitions (4.26) and (4.27) in a covariant gauge. By taking the incoming partons off shell, $p^2 \neq 0$, we regulate the infrared divergences allowing the extraction of the UV poles of the PDFs. Although the divergent terms remain gauge independent the finite terms become gauge dependent. It means that we need to take into account the running of the gauge parameter $\xi \to Z_A\xi$ in finite terms, even when working in Feynman gauge.

C.2 Particular Two-loop Diagrams Contributing to $W_{\sqcap}$

In this appendix we elaborate on aspects of the calculation of $W_{\sqcap}$ presented in Section 4.4. We consider two specific diagrams where some subtle points arise. In Section C.2.1 we discuss the endpoint contributions in diagram $d^{(2)}_{Y_L}$ in Figure 4.77 using momentum space, and in Section C.2.2 we show the single IR divergent behaviour of $d^{(2)}_{X_3}$.

C.2.1 Endpoint contribution in the diagram $d^{(2)}_{Y_L}$

In Section 4.4 we revisited the analysis of non-Abelian contributions to the correlators of finite and semi-infinite Wilson lines [148]. Specifically, we derived the representations of the two-loop diagrams that contain a three-gluon vertex and made a clear distinction between ones where two gluons are emitted from a finite Wilson-line segment as compared to the case where two emissions emerge from a semi-infinite line, corresponding respectively to diagrams $d^{(2)}_{Y_s}$ and $d^{(2)}_{Y_L}$ in (4.77). The difference is that in the former case both endpoint contributions appear, as in (4.89), while in the latter case there is no endpoint contribution from infinity, so the representation of $d^{(2)}_{Y_L}$ simplifies to (4.92). Let us now present this calculation in detail using momentum space and show explicitly that this endpoint contribution is indeed absent.

Using the Feynman rules given in Section 4.4, diagram $d^{(2)}_{Y_L}$ in (4.77) reads

$$\begin{aligned} d^{(2)}_{Y_L} = K_Y \int d^d z \int_{-\infty}^{0} ds_1 \int_{s_1}^{0} ds_2 \int_{0}^{y} dt_3 \left[\beta \cdot \frac{\partial}{\partial s_2 \beta} - \beta \cdot \frac{\partial}{\partial s_1 \beta}\right] \\ \times \left[-(s_1\beta - z)^2 + i0\right]^{-1+\epsilon} \left[-(s_2\beta - z)^2 + i0\right]^{-1+\epsilon} \left[-(ut_3 - z)^2 + i0\right]^{-1+\epsilon}, \end{aligned} \tag{C.23}$$

which is analogous to eq. (4.84). In the equation above, we integrate over z using the momentum-space representation of the propagators

$$\mathcal{N}\left[-x^2 + i0\right]^{-1+\epsilon} = -i \int \frac{d^d k}{(2\pi)^d} \frac{e^{-ik\cdot x}}{k^2 + i0}, \tag{C.24}$$

obtaining

$$d^{(2)}_{Y_L} = ig_s^4 \frac{C_i C_A}{2} u\cdot\beta \int \frac{d^dk_1 d^dk_2}{(2\pi)^{2d}} \int_{-\infty}^{0} ds_1 \int_{s_1}^{0} ds_2 \int_0^y dt_3 \left[\beta\cdot\frac{\partial}{\partial s_2\beta} - \beta\cdot\frac{\partial}{\partial s_1\beta}\right] \times (-i)^3 \frac{e^{-ik_1\cdot\beta s_1} e^{-ik_2\cdot\beta s_2} e^{i(k_1+k_2)\cdot u t_3}}{k_1^2 k_2^2 (k_1+k_2)^2}. \tag{C.25}$$

After taking the derivatives with respect to $s_1\beta$, $s_2\beta$ and integrating over the infinite line we get

$$d^{(2)}_{Y_L} = ig_s^4 \frac{C_i C_A}{2} u\cdot\beta \int \frac{d^dk_1 d^dk_2}{(2\pi)^{2d}} \int_0^y dt_3 \frac{(-i)^3 e^{i(k_1+k_2)\cdot u t_3}}{k_1^2 k_2^2 (k_1+k_2)^2} \frac{k_2\cdot\beta - k_1\cdot\beta}{k_2\cdot\beta + i0} \times \left\{ \frac{1}{-i(k_1\cdot\beta + i0)} - \frac{1}{-i\left[(k_1+k_2)\cdot\beta + i0\right]} \right\}, \tag{C.26}$$

where the prescription $+i0$ in the denominators ensures the convergence of the integrals for $s_1 \to -\infty$. The expression above may be conveniently rewritten as

$$d^{(2)}_{Y_L} = ig_s^4 \frac{C_i C_A}{2} u\cdot\beta \int \frac{d^dk_1 d^dk_2}{(2\pi)^{2d}} \int_0^y dt_3\, e^{i(k_1+k_2)\cdot u t_3} \frac{(-i)^3}{k_1^2 k_2^2 (k_1+k_2)^2} \times \left\{ \frac{1}{-i(k_1\cdot\beta + i0)} - \frac{2}{-i\left[(k_1+k_2)\cdot\beta + i0\right]} \right\}. \tag{C.27}$$

This directly leads to the representation of eq. (4.92), as we now show. Upon introducing an auxiliary integration constrained by momentum conservation we obtain:

$$d^{(2)}_{Y_L} = ig_s^4 \frac{C_i C_A}{2} u\cdot\beta \int \frac{d^dk_1 d^dk_2 d^dk_3}{(2\pi)^{3d}} (2\pi)^d \delta^d(k_1+k_2+k_3) \frac{(-i)^3}{k_1^2 k_2^2 k_3^2} \times \left\{ \int_0^y dt_3 \int_{-\infty}^{0} ds_1\, e^{-ik_3\cdot u t_3} \left[e^{-ik_1\cdot\beta s_1} - 2\, e^{-i(k_1+k_2)\cdot\beta s_1} \right] \right\}. \tag{C.28}$$

The representation of the delta function $(2\pi)^d\delta^d(k_1+k_2+k_3) = \int d^dz\, e^{i(k_1+k_2+k_3)\cdot z}$ is interpreted as an integral over the position of the scalar "three gluon" vertex in eq. (4.92). Using eq. (C.24) we recover the expression of the three gluon propagators in coordinate space, carrying momenta k_1, k_2 and k_3, obtaining

$$d^{(2)}_{Y_L} = K_Y \int d^dz \int_0^y dt_3 \int_{-\infty}^{0} ds_1 \left[-(z-ut_3)^2 + i0\right]^{\epsilon-1} \times \left\{ \left[-(z-\beta s_1)^2 + i0\right]^{\epsilon-1} \left[-z^2 + i0\right]^{\epsilon-1} - 2 \left[-(z-\beta s_1)^2 + i0\right]^{2\epsilon-2} \right\}. \tag{C.29}$$

Substituting the definitions in eqs. (4.90a), (4.90b) and (4.90c) we verify the result in eq. (4.92).

C.2.2 The diagram $d^{(2)}_{X_3}$ connecting three Wilson lines

In this section we derive the representation of eq. (4.82) of the diagram $d^{(2)}_{X_3}$ that connects two cusps with a lightlike segment of finite length. Following the discussion of ref. [148], the singularities of the webs of this kind are associated with the configuration where all the vertices approach the lightlike segment of finite length. These webs do not contribute to the cusp singularities because there is not any region of configuration space where all the vertices are in proximity of the cusp. By using the Feynman rules in eq. (4.63), the diagram $d^{(2)}_{X_3}$ reads

$$\begin{aligned} d^{(2)}_{X_3} = & -g_s^4 \mu^{4\epsilon} \frac{C_A C_F}{2} \mathcal{N}^2 (\beta \cdot u)^2 \int_0^{+\infty} dt_1 \int_0^{+\infty} dt_3 \int_0^y ds_1 \int_{s_1}^y ds_2 \\ & \times \left[-2\beta \cdot u t_1 s_2 + i0 \right]^{\epsilon-1} \left[-2\beta \cdot u t_3 (s_1 - y) + i0 \right]^{\epsilon-1} , \end{aligned} \tag{C.30}$$

where the factor $-\frac{C_A C_F}{2}$ corresponds to the maximally non-Abelian part of the colour factor of the diagram, which is exponentiated [59–61, 182]. We expose the overall infrared singularity in the last integration by rewriting the integration domain using $\theta(t_1 - t_3) + \theta(t_3 - t_1) = 1$ and changing the order of integrations. Thus we obtain

$$\begin{aligned} d^{(2)}_{X_3} = & -g_s^4 \mu^{4\epsilon} \, C_A C_F \mathcal{N}^2 (\beta \cdot u)^2 \int_0^{+\infty} dt \int_0^t dt' (t\, t')^{-1+\epsilon} \int_0^y ds_1 \int_{s_1}^y ds_2 \\ & \times \left[-2\beta \cdot u s_2 + i0 \right]^{\epsilon-1} \left[-2\beta \cdot u (s_1 - y) + i0 \right]^{\epsilon-1} . \end{aligned} \tag{C.31}$$

We stress that the expression above still has infrared singularities from the limit $t \to \infty$ in the upper bound of the t' integral. Therefore we decouple the infrared contributions by applying the changes of variables

$$t' = t \left(\frac{s}{y} \right)^2 , \quad s_1 = y\, a_1, \quad s_2 = y\, a_2, \tag{C.32}$$

which yields

$$d^{(2)}_{X_3} = g_s^4 \mu^{4\epsilon} \, C_A C_F \mathcal{N}^2 (\beta \cdot u) \int_0^{+\infty} dt \int_0^y ds \left[-2\beta \cdot u t s + i0 \right]^{2\epsilon-1}$$

$$\times \int_0^1 \frac{da_1}{(1-a_1)^{1-\epsilon}} \int_{a_1}^1 \frac{da_2}{a_2^{1-\epsilon}}. \tag{C.33}$$

The parameters a_1 and a_2 are integrated immediately, leading to

$$\begin{aligned} d_{X_3}^{(2)} = & g_s^4 \mu^{4\epsilon} C_A C_F \mathcal{N}^2 (\beta \cdot u) \frac{1}{\epsilon} \left[\frac{1}{\epsilon} - B(\epsilon, 1+\epsilon) \right] \\ & \times \int_0^{+\infty} dt \int_0^y ds \left[-2\beta \cdot uts + i0 \right]^{2\epsilon - 1}. \end{aligned} \tag{C.34}$$

Thus we apply the change of variables introduced before eq. (4.66) and we get

$$\begin{aligned} d_{X_3}^{(2)} = & -g_s^4 \mu^{4\epsilon} \frac{C_A C_F}{2} \mathcal{N}^2 \frac{1}{\epsilon} \left[\frac{1}{\epsilon} - B(\epsilon, 1+\epsilon) \right] \\ & \times \int_0^{+\infty} \frac{d\tau}{\tau} \int_0^{\frac{\rho}{\sqrt{2}}} \frac{d\sigma}{\sigma} \left(4\tau\sigma\mu^2 \right)^{2\epsilon}. \end{aligned} \tag{C.35}$$

By replacing the normalisation $\mathcal{N} = -\frac{\Gamma(1-\epsilon)}{4\pi^{2-\epsilon}}$, we absorb the factor $(4\pi e^{\gamma_E})^\epsilon$ into the coupling constant, which we expand at the scale $\frac{1}{\tau\sigma}$ by means of eq. (4.68), thus getting

$$\begin{aligned} d_{X_3}^{(2)} = & -C_A C_F \frac{\Gamma^2(1-\epsilon)}{2\epsilon} \left[\frac{1}{\epsilon} - B(\epsilon, 1+\epsilon) \right] \\ & \times \int_0^{+\infty} \frac{d\tau}{\tau} \int_0^{\frac{\rho}{\sqrt{2}}} \frac{d\sigma}{\sigma} \left(\frac{\alpha_s\left(\frac{1}{\tau\sigma}\right)}{\pi} e^{-\epsilon\gamma_E} \right)^2, \end{aligned} \tag{C.36}$$

which is written in terms of the representation in eq. (4.78) and reproduces the result of eq. (4.82). By expanding the integrand for $\epsilon \to 0$ we get

$$w_{X_3}^{(2)} = -C_A C_F \left[\frac{\zeta_2}{2} - \epsilon\zeta_3 \right]. \tag{C.37}$$

We notice that the first term in the equation above, once integrated with λ and $\sigma \to 0$, would yield a double UV pole, which is expected to arise only from single cusp singularities. By summing the contribution of $w_{X_3}^{(2)}$ above with the one originated from the other webs connecting three lines, namely $w_{3s}^{(2)}$, we verify that the cusp term cancels, leaving only the subleading pole in eq. (4.98) associated with collinear configurations around the finite segment.

Bibliography

[1] G. Falcioni, E. Gardi and C. Milloy, *Relating amplitude and PDF factorisation through Wilson-line geometries*, *JHEP* **11** (2019) 100 [1909.00697].

[2] G. F. Sterman, *Summation of Large Corrections to Short Distance Hadronic Cross-Sections*, *Nucl. Phys.* **B281** (1987) 310.

[3] S. Catani and L. Trentadue, *Resummation of the QCD Perturbative Series for Hard Processes*, *Nucl. Phys.* **B327** (1989) 323.

[4] G. P. Korchemsky and G. Marchesini, *Resummation of large infrared corrections using Wilson loops*, *Phys. Lett.* **B313** (1993) 433.

[5] H. Contopanagos, E. Laenen and G. F. Sterman, *Sudakov factorization and resummation*, *Nucl. Phys.* **B484** (1997) 303 [hep-ph/9604313].

[6] E. Laenen and L. Magnea, *Threshold resummation for electroweak annihilation from DIS data*, *Phys. Lett.* **B632** (2006) 270 [hep-ph/0508284].

[7] T. Becher, M. Neubert and G. Xu, *Dynamical Threshold Enhancement and Resummation in Drell-Yan Production*, *JHEP* **07** (2008) 030 [0710.0680].

[8] I. I. Balitsky and L. N. Lipatov, *The Pomeranchuk Singularity in Quantum Chromodynamics*, *Sov. J. Nucl. Phys.* **28** (1978) 822.

[9] E. A. Kuraev, L. N. Lipatov and V. S. Fadin, *Multi - Reggeon Processes in the Yang-Mills Theory*, *Sov. Phys. JETP* **44** (1976) 443.

[10] V. S. Fadin, E. A. Kuraev and L. N. Lipatov, *On the Pomeranchuk Singularity in Asymptotically Free Theories*, *Phys. Lett.* **60B** (1975) 50.

[11] L. N. Lipatov, *Reggeization of the Vector Meson and the Vacuum Singularity in Nonabelian Gauge Theories*, *Sov. J. Nucl. Phys.* **23** (1976) 338.

[12] I. A. Korchemskaya and G. P. Korchemsky, *High-energy scattering in QCD and cross singularities of Wilson loops*, *Nucl. Phys.* **B437** (1995) 127 [hep-ph/9409446].

[13] I. Balitsky, *Operator expansion for high-energy scattering*, *Nucl. Phys.* **B463** (1996) 99 [hep-ph/9509348].

[14] S. Caron-Huot, *When does the gluon reggeize?*, *JHEP* **05** (2015) 093 [1309.6521].

[15] S. Caron-Huot, E. Gardi and L. Vernazza, *Two-parton scattering in the high-energy limit*, *JHEP* **06** (2017) 016 [1701.05241].

[16] J. C. Collins, *Sudakov form-factors*, *Adv. Ser. Direct. High Energy Phys.* **5** (1989) 573 [hep-ph/0312336].

[17] J. Collins, *Foundations of perturbative QCD*, *Camb. Monogr. Part. Phys. Nucl. Phys. Cosmol.* **32** (2011) 1.

[18] T. Becher, A. Broggio and A. Ferroglia, *Introduction to Soft-Collinear Effective Theory*, *Lect. Notes Phys.* **896** (2015) pp.1 [1410.1892].

[19] S. Moch, J. A. M. Vermaseren and A. Vogt, *The Three loop splitting functions in QCD: The Nonsinglet case*, *Nucl. Phys.* **B688** (2004) 101 [hep-ph/0403192].

[20] S. Moch, J. A. M. Vermaseren and A. Vogt, *Higher-order corrections in threshold resummation*, *Nucl. Phys.* **B726** (2005) 317 [hep-ph/0506288].

[21] Y. Li, A. von Manteuffel, R. M. Schabinger and H. X. Zhu, *Soft-virtual corrections to Higgs production at N^3LO*, *Phys. Rev.* **D91** (2015) 036008 [1412.2771].

[22] A. Grozin, J. M. Henn, G. P. Korchemsky and P. Marquard, *Three Loop Cusp Anomalous Dimension in QCD*, *Phys. Rev. Lett.* **114** (2015) 062006 [1409.0023].

[23] A. Grozin, J. M. Henn, G. P. Korchemsky and P. Marquard, *The three-loop cusp anomalous dimension in QCD and its supersymmetric extensions*, *JHEP* **01** (2016) 140 [1510.07803].

[24] O. Almelid, C. Duhr and E. Gardi, *Three-loop corrections to the soft anomalous dimension in multileg scattering*, *Phys. Rev. Lett.* **117** (2016) 172002 [1507.00047].

[25] O. Almelid, C. Duhr, E. Gardi, A. McLeod and C. D. White, *Bootstrapping the QCD soft anomalous dimension*, *JHEP* **09** (2017) 073 [1706.10162].

[26] J. Davies, A. Vogt, B. Ruijl, T. Ueda and J. A. M. Vermaseren, *Large-n_f contributions to the four-loop splitting functions in QCD*, *Nucl. Phys.* **B915** (2017) 335 [1610.07477].

[27] J. M. Henn, A. V. Smirnov, V. A. Smirnov and M. Steinhauser, *A planar four-loop form factor and cusp anomalous dimension in QCD*, *JHEP* **05** (2016) 066 [1604.03126].

[28] S. Moch, B. Ruijl, T. Ueda, J. A. M. Vermaseren and A. Vogt, *Four-Loop Non-Singlet Splitting Functions in the Planar Limit and Beyond*, *JHEP* **10** (2017) 041 [1707.08315].

[29] A. Grozin, J. Henn and M. Stahlhofen, *On the Casimir scaling violation in the cusp anomalous dimension at small angle*, *JHEP* **10** (2017) 052 [1708.01221].

[30] S. Moch, B. Ruijl, T. Ueda, J. A. M. Vermaseren and A. Vogt, *On quartic colour factors in splitting functions and the gluon cusp anomalous dimension*, *Phys. Lett.* **B782** (2018) 627 [1805.09638].

[31] R. N. Lee, A. V. Smirnov, V. A. Smirnov and M. Steinhauser, *Four-loop quark form factor with quartic fundamental colour factor*, *JHEP* **02** (2019) 172 [1901.02898].

[32] J. M. Henn, T. Peraro, M. Stahlhofen and P. Wasser, *Matter dependence of the four-loop cusp anomalous dimension*, *Phys. Rev. Lett.* **122** (2019) 201602 [1901.03693].

[33] R. Brüser, A. Grozin, J. M. Henn and M. Stahlhofen, *Matter dependence of the four-loop QCD cusp anomalous dimension: from small angles to all angles*, *JHEP* **05** (2019) 186 [1902.05076].

[34] A. von Manteuffel and R. M. Schabinger, *Quark and gluon form factors in four loop QCD: The N_f^2 and $N_{q\gamma}N_f$ contributions*, *Phys. Rev. D* **99** (2019) 094014 [1902.08208].

[35] J. M. Henn, G. P. Korchemsky and B. Mistlberger, *The full four-loop cusp anomalous dimension in $\mathcal{N} = 4$ super Yang-Mills and QCD*, *JHEP* **04** (2020) 018 [1911.10174].

[36] A. von Manteuffel, E. Panzer and R. M. Schabinger, *Cusp and collinear anomalous dimensions in four-loop QCD from form factors*, *Phys. Rev. Lett.* **124** (2020) 162001 [2002.04617].

[37] N. Beisert, B. Eden and M. Staudacher, *Transcendentality and Crossing*, *J. Stat. Mech.* **0701** (2007) P01021 [hep-th/0610251].

[38] R. H. Boels, T. Huber and G. Yang, *Four-Loop Nonplanar Cusp Anomalous Dimension in N=4 Supersymmetric Yang-Mills Theory*, *Phys. Rev. Lett.* **119** (2017) 201601 [1705.03444].

[39] D. Fioravanti, P. Grinza and M. Rossi, *Beyond cusp anomalous dimension from integrability*, *Phys. Lett.* **B675** (2009) 137 [0901.3161].

[40] L. Freyhult and S. Zieme, *The virtual scaling function of AdS/CFT*, *Phys. Rev.* **D79** (2009) 105009 [0901.2749].

[41] L. Freyhult, A. Rej and M. Staudacher, *A Generalized Scaling Function for AdS/CFT*, *J. Stat. Mech.* **0807** (2008) P07015 [0712.2743].

[42] L. J. Dixon, *The Principle of Maximal Transcendentality and the Four-Loop Collinear Anomalous Dimension*, *JHEP* **01** (2018) 075 [1712.07274].

[43] S. Moch and A. Vogt, *Higher-order soft corrections to lepton pair and Higgs boson production*, *Phys. Lett. B* **631** (2005) 48 [hep-ph/0508265].

[44] M. Beneke, A. Broggio, M. Garny, S. Jaskiewicz, R. Szafron, L. Vernazza et al., *Leading-logarithmic threshold resummation of the Drell-Yan process at next-to-leading power*, *JHEP* **03** (2019) 043 [1809.10631].

[45] M. Beneke, A. Broggio, S. Jaskiewicz and L. Vernazza, *Threshold factorization of the Drell-Yan process at next-to-leading power*, *JHEP* **20** (2020) 078 [1912.01585].

[46] N. Bahjat-Abbas, D. Bonocore, J. Sinninghe Damsté, E. Laenen, L. Magnea, L. Vernazza et al., *Diagrammatic resummation of leading-logarithmic threshold effects at next-to-leading power*, *JHEP* **11** (2019) 002 [1905.13710].

[47] J.-w. Qiu and G. F. Sterman, *Power corrections in hadronic scattering. 1. Leading 1/Q**2 corrections to the Drell-Yan cross-section*, *Nucl. Phys. B* **353** (1991) 105.

[48] J.-w. Qiu and G. F. Sterman, *Power corrections to hadronic scattering. 2. Factorization*, *Nucl. Phys. B* **353** (1991) 137.

[49] F. Bloch and A. Nordsieck, *Note on the radiation field of the electron*, *Phys. Rev.* **52** (1937) 54.

[50] T. Kinoshita, *Mass singularities of feynman amplitudes*, *Journal of Mathematical Physics* **3** (1962) 650 [https://doi.org/10.1063/1.1724268].

[51] T. D. Lee and M. Nauenberg, *Degenerate systems and mass singularities*, *Phys. Rev.* **133** (1964) B1549.

[52] N. Kidonakis, *Resummation for heavy quark and jet cross-sections*, *Int. J. Mod. Phys. A* **15** (2000) 1245 [hep-ph/9902484].

[53] A. Bassetto, M. Ciafaloni and G. Marchesini, *Jet Structure and Infrared Sensitive Quantities in Perturbative QCD*, *Phys. Rept.* **100** (1983) 201.

[54] S. Catani and M. Seymour, *A General algorithm for calculating jet cross-sections in NLO QCD*, *Nucl. Phys. B* **485** (1997) 291 [hep-ph/9605323].

[55] A. Polyakov, *Gauge fields as rings of glue*, *Nuclear Physics B* **164** (1980) 171 .

[56] R. A. Brandt, F. Neri and M.-a. Sato, *Renormalization of loop functions for all loops*, *Phys. Rev. D* **24** (1981) 879.

[57] D. Yennie, S. Frautschi and H. Suura, *The infrared divergence phenomena and high-energy processes*, *Annals of Physics* **13** (1961) 379 .

[58] S. Weinberg, *Infrared photons and gravitons*, *Phys. Rev.* **140** (1965) B516.

[59] G. F. Sterman, *Infrared divergences in perturbative QCD*, *AIP Conf. Proc.* **74** (1981) 22.

[60] J. G. M. Gatheral, *Exponentiation of Eikonal Cross-sections in Nonabelian Gauge Theories*, *Phys. Lett.* **133B** (1983) 90.

[61] J. Frenkel and J. C. Taylor, *Nonabelian eikonal exponentiation*, *Nucl. Phys.* **B246** (1984) 231.

[62] E. Gardi, J. M. Smillie and C. D. White, *The Non-Abelian Exponentiation theorem for multiple Wilson lines*, *JHEP* **06** (2013) 088 [1304.7040].

[63] E. Gardi, J. M. Smillie and C. D. White, *On the renormalization of multiparton webs*, *JHEP* **09** (2011) 114 [1108.1357].

[64] E. Gardi, *From Webs to Polylogarithms*, *JHEP* **04** (2014) 044 [1310.5268].

[65] G. Falcioni, E. Gardi, M. Harley, L. Magnea and C. D. White, *Multiple Gluon Exchange Webs*, *JHEP* **10** (2014) 10 [1407.3477].

[66] S. Catani, *The Singular behavior of QCD amplitudes at two loop order*, *Phys. Lett.* **B427** (1998) 161 [hep-ph/9802439].

[67] G. F. Sterman and M. E. Tejeda-Yeomans, *Multiloop amplitudes and resummation*, *Phys. Lett.* **B552** (2003) 48 [hep-ph/0210130].

[68] S. M. Aybat, L. J. Dixon and G. F. Sterman, *The Two-loop anomalous dimension matrix for soft gluon exchange*, *Phys. Rev. Lett.* **97** (2006) 072001 [hep-ph/0606254].

[69] S. M. Aybat, L. J. Dixon and G. F. Sterman, *The Two-loop soft anomalous dimension matrix and resummation at next-to-next-to leading pole*, *Phys. Rev.* **D74** (2006) 074004 [hep-ph/0607309].

[70] T. Becher and M. Neubert, *Infrared singularities of scattering amplitudes in perturbative QCD*, *Phys. Rev. Lett.* **102** (2009) 162001 [0901.0722].

[71] T. Becher and M. Neubert, *On the Structure of Infrared Singularities of Gauge-Theory Amplitudes*, *JHEP* **06** (2009) 081 [0903.1126].

[72] E. Gardi and L. Magnea, *Factorization constraints for soft anomalous dimensions in QCD scattering amplitudes*, *JHEP* **03** (2009) 079 [0901.1091].

[73] E. Gardi and L. Magnea, *Infrared singularities in QCD amplitudes*, *Nuovo Cim.* **C32N5-6** (2009) 137 [0908.3273].

[74] T. Becher and M. D. Schwartz, *Direct photon production with effective field theory*, *JHEP* **02** (2010) 040 [0911.0681].

[75] T. Becher and G. Bell, *The gluon jet function at two-loop order*, *Phys. Lett.* **B695** (2011) 252 [1008.1936].

[76] L. Magnea, E. Maina, G. Pelliccioli, C. Signorile-Signorile, P. Torrielli and S. Uccirati, *Factorisation and Subtraction beyond NLO*, *JHEP* **12** (2018) 062 [1809.05444].

[77] A. Vladimirov, *Structure of rapidity divergences in multi-parton scattering soft factors*, *JHEP* **04** (2018) 045 [1707.07606].

[78] O. Almelid, *The three-loop soft anomalous dimension of massless multi-leg scattering*, *Thesis* (2016) .

[79] G. P. Korchemsky and A. V. Radyushkin, *Renormalization of the Wilson Loops Beyond the Leading Order*, *Nucl. Phys.* **B283** (1987) 342.

[80] A. H. Mueller, ed., *Perturbative Quantum Chromodynamics*, vol. 5. WSP, Singapore, 1989, 10.1142/0494.

[81] Y. L. Dokshitzer, *Calculation of the Structure Functions for Deep Inelastic Scattering and e+ e- Annihilation by Perturbation Theory in Quantum Chromodynamics.*, *Sov. Phys. JETP* **46** (1977) 641.

[82] V. N. Gribov and L. N. Lipatov, *Deep inelastic e p scattering in perturbation theory*, *Sov. J. Nucl. Phys.* **15** (1972) 438.

[83] G. Altarelli and G. Parisi, *Asymptotic Freedom in Parton Language*, *Nucl. Phys.* **B126** (1977) 298.

[84] V. Ravindran, J. Smith and W. L. van Neerven, *Two-loop corrections to Higgs boson production*, *Nucl. Phys.* **B704** (2005) 332 [hep-ph/0408315].

[85] S. Moch, J. A. M. Vermaseren and A. Vogt, *Three-loop results for quark and gluon form-factors*, *Phys. Lett.* **B625** (2005) 245 [hep-ph/0508055].

[86] G. P. Korchemsky, *Asymptotics of the Altarelli-Parisi-Lipatov Evolution Kernels of Parton Distributions*, *Mod. Phys. Lett.* **A4** (1989) 1257.

[87] A. B. Goncharov, *Multiple polylogarithms, cyclotomy and modular complexes*, *Mathematical Research Letters* **5** (1998) 497–516 [1105.2076].

[88] A. B. Goncharov, M. Spradlin, C. Vergu and A. Volovich, *Classical Polylogarithms for Amplitudes and Wilson Loops*, *Phys. Rev. Lett.* **105** (2010) 151605 [1006.5703].

[89] J. Vollinga and S. Weinzierl, *Numerical evaluation of multiple polylogarithms*, *Comput. Phys. Commun.* **167** (2005) 177 [hep-ph/0410259].

[90] C. Duhr and F. Dulat, *PolyLogTools — polylogs for the masses*, *JHEP* **08** (2019) 135 [1904.07279].

[91] C. Duhr, *Mathematical aspects of scattering amplitudes*, in *Proceedings, Theoretical Advanced Study Institute in Elementary Particle Physics: Journeys Through the Precision Frontier: Amplitudes for Colliders (TASI 2014): Boulder, Colorado, June 2-27, 2014*, pp. 419–476, 2015, 1411.7538, DOI.

[92] E. Remiddi and J. Vermaseren, *Harmonic polylogarithms*, *Int. J. Mod. Phys. A* **15** (2000) 725 [hep-ph/9905237].

[93] F. C. Brown, *Polylogarithmes multiples uniformes en une variable*, *Compt. Rend. Math.* **338** (2004) 527.

[94] K.-T. Chen, *Iterated path integrals*, *Bull. Amer. Math. Soc.* **83** (1977) 831.

[95] F. Brown, *Iterated integrals in quantum field theory*, in *Proceedings, Geometric and Topological Methods for Quantum Field Theory : 6th Summer School: Villa de Leyva, Colombia, July 6-23, 2009*, pp. 188–240, 2013, DOI.

[96] A. V. Kotikov, *Differential equations method: New technique for massive Feynman diagrams calculation*, *Phys. Lett.* **B254** (1991) 158.

[97] A. V. Kotikov, *Differential equation method: The Calculation of N point Feynman diagrams*, *Phys. Lett.* **B267** (1991) 123.

[98] Z. Bern, L. J. Dixon and D. A. Kosower, *Dimensionally regulated pentagon integrals*, *Nucl. Phys.* **B412** (1994) 751 [hep-ph/9306240].

[99] T. Gehrmann and E. Remiddi, *Differential equations for two loop four point functions*, *Nucl. Phys.* **B580** (2000) 485 [hep-ph/9912329].

[100] J. M. Henn, *Multiloop integrals in dimensional regularization made simple*, *Phys. Rev. Lett.* **110** (2013) 251601 [1304.1806].

[101] K. G. Chetyrkin and F. V. Tkachov, *Integration by Parts: The Algorithm to Calculate beta Functions in 4 Loops*, *Nucl. Phys.* **B192** (1981) 159.

[102] S. Laporta, *High precision calculation of multiloop Feynman integrals by difference equations*, *Int. J. Mod. Phys.* **A15** (2000) 5087 [hep-ph/0102033].

[103] R. N. Lee, *LiteRed 1.4: a powerful tool for reduction of multiloop integrals*, *J. Phys. Conf. Ser.* **523** (2014) 012059 [1310.1145].

[104] A. von Manteuffel and C. Studerus, *Reduze 2 - Distributed Feynman Integral Reduction*, 1201.4330.

[105] A. V. Smirnov, *FIRE5: a C++ implementation of Feynman Integral REduction*, *Comput. Phys. Commun.* **189** (2015) 182 [1408.2372].

[106] A. von Manteuffel and R. M. Schabinger, *A novel approach to integration by parts reduction*, *Phys. Lett.* **B744** (2015) 101 [1406.4513].

[107] T. Peraro, *Scattering amplitudes over finite fields and multivariate functional reconstruction*, *JHEP* **12** (2016) 030 [1608.01902].

[108] P. Maierhoefer, J. Usovitsch and P. Uwer, *Kira - A Feynman Integral Reduction Program*, 1705.05610.

[109] A. V. Smirnov and F. S. Chuharev, *FIRE6: Feynman Integral REduction with Modular Arithmetic*, 1901.07808.

[110] J. Henn, B. Mistlberger, V. A. Smirnov and P. Wasser, *Constructing d-log integrands and computing master integrals for three-loop four-particle scattering*, *JHEP* **04** (2020) 167 [2002.09492].

[111] C. Meyer, *Transforming differential equations of multi-loop Feynman integrals into canonical form*, *JHEP* **04** (2017) 006 [1611.01087].

[112] C. Meyer, *Algorithmic transformation of multi-loop master integrals to a canonical basis with CANONICA*, 1705.06252.

[113] M. E. Peskin and D. V. Schroeder, *An Introduction to quantum field theory*. Addison-Wesley, Reading, USA, 1995.

[114] A. Mitov, G. F. Sterman and I. Sung, *The Massive Soft Anomalous Dimension Matrix at Two Loops*, *Phys. Rev.* **D79** (2009) 094015 [0903.3241].

[115] A. Ferroglia, M. Neubert, B. D. Pecjak and L. L. Yang, *Two-loop divergences of massive scattering amplitudes in non-abelian gauge theories*, *JHEP* **11** (2009) 062 [0908.3676].

[116] A. Waelkens, *Calculation of webs in non-abelian gauge theories using unitary cuts*, *Thesis* (2017) .

[117] L. Adams and S. Weinzierl, *The ε-form of the differential equations for Feynman integrals in the elliptic case*, *Phys. Lett.* **B781** (2018) 270 [1802.05020].

[118] J. Drummond, J. Foster, Ö. Gürdoğan and G. Papathanasiou, *Cluster adjacency and the four-loop NMHV heptagon*, *JHEP* **03** (2019) 087 [1812.04640].

[119] S. Caron-Huot, L. J. Dixon, F. Dulat, M. von Hippel, A. J. McLeod and G. Papathanasiou, *Six-Gluon amplitudes in planar $\mathcal{N} = 4$ super-Yang-Mills theory at six and seven loops*, *JHEP* **08** (2019) 016 [1903.10890].

[120] S. Caron-Huot, L. J. Dixon, F. Dulat, M. Von Hippel, A. J. McLeod and G. Papathanasiou, *The Cosmic Galois Group and Extended Steinmann Relations for Planar $\mathcal{N} = 4$ SYM Amplitudes*, *JHEP* **09** (2019) 061 [1906.07116].

[121] S. Abreu, J. Dormans, F. Febres Cordero, H. Ita and B. Page, *Analytic Form of Planar Two-Loop Five-Gluon Scattering Amplitudes in QCD*, *Phys. Rev. Lett.* **122** (2019) 082002 [1812.04586].

[122] G. P. Korchemsky and A. V. Radyushkin, *Infrared factorization, Wilson lines and the heavy quark limit*, *Phys. Lett.* **B279** (1992) 359 [hep-ph/9203222].

[123] W. Kilian, T. Mannel and T. Ohl, *Unimagined imaginary parts in heavy quark effective field theory*, *Phys. Lett. B* **304** (1993) 311 [hep-ph/9303224].

[124] M. Neubert, *Heavy-quark symmetry*, *Physics Reports* **245** (1994) 259 .

[125] A. Grozin, *Leading and next-to-leading large-n_f terms in the cusp anomalous dimension and quark-antiquark potential*, *PoS* **LL2016** (2016) 053 [1605.03886].

[126] A. Grozin, *Four-loop cusp anomalous dimension in QED*, *JHEP* **06** (2018) 073 [1805.05050].

[127] R. Brüser, A. Grozin, J. Henn and M. Stahlhofen, *Four-loop results for the cusp anomalous dimension*, *PoS* **LL2018** (2018) 018 [1807.05145].

[128] M. Harley, *Multiparton webs in non-abelian gauge theories at three-loops and beyond*, *Thesis* (2015) .

[129] S. Borowka, G. Heinrich, S. Jahn, S. P. Jones, M. Kerner, J. Schlenk et al., *pySecDec: a toolbox for the numerical evaluation of multi-scale integrals*, *Comput. Phys. Commun.* **222** (2018) 313 [1703.09692].

[130] T. Binoth and G. Heinrich, *An automatized algorithm to compute infrared divergent multiloop integrals*, *Nucl. Phys. B* **585** (2000) 741 [hep-ph/0004013].

[131] T. Hahn, *CUBA: A Library for multidimensional numerical integration*, *Comput. Phys. Commun.* **168** (2005) 78 [hep-ph/0404043].

[132] J. C. Collins, D. E. Soper and G. F. Sterman, *Transverse Momentum Distribution in Drell-Yan Pair and W and Z Boson Production*, *Nucl. Phys.* **B250** (1985) 199.

[133] Y. Li, D. Neill and H. X. Zhu, *An Exponential Regulator for Rapidity Divergences*, *Submitted to: Phys. Rev. D* (2016) [1604.00392].

[134] Y. Li and H. X. Zhu, *Bootstrapping Rapidity Anomalous Dimensions for Transverse-Momentum Resummation*, *Phys. Rev. Lett.* **118** (2017) 022004 [1604.01404].

[135] A. A. Vladimirov, *Correspondence between Soft and Rapidity Anomalous Dimensions*, *Phys. Rev. Lett.* **118** (2017) 062001 [1610.05791].

[136] A. V. Belitsky, *Two loop renormalization of Wilson loop for Drell-Yan production*, *Phys. Lett.* **B442** (1998) 307 [hep-ph/9808389].

[137] R. V. Harlander, *Virtual corrections to g g —¿ H to two loops in the heavy top limit*, *Phys. Lett.* **B492** (2000) 74 [hep-ph/0007289].

[138] E. G. Floratos, D. A. Ross and C. T. Sachrajda, *Higher Order Effects in Asymptotically Free Gauge Theories: The Anomalous Dimensions of Wilson Operators*, *Nucl. Phys.* **B129** (1977) 66.

[139] E. G. Floratos, D. A. Ross and C. T. Sachrajda, *Higher Order Effects in Asymptotically Free Gauge Theories. 2. Flavor Singlet Wilson Operators and Coefficient Functions*, *Nucl. Phys.* **B152** (1979) 493.

[140] A. Gonzalez-Arroyo, C. Lopez and F. J. Yndurain, *Second Order Contributions to the Structure Functions in Deep Inelastic Scattering. 1. Theoretical Calculations*, *Nucl. Phys.* **B153** (1979) 161.

[141] A. Gonzalez-Arroyo and C. Lopez, *Second Order Contributions to the Structure Functions in Deep Inelastic Scattering. 3. The Singlet Case*, *Nucl. Phys.* **B166** (1980) 429.

[142] G. Curci, W. Furmanski and R. Petronzio, *Evolution of Parton Densities Beyond Leading Order: The Nonsinglet Case*, *Nucl. Phys.* **B175** (1980) 27.

[143] W. Furmanski and R. Petronzio, *Singlet Parton Densities Beyond Leading Order*, *Phys. Lett.* **97B** (1980) 437.

[144] E. G. Floratos, C. Kounnas and R. Lacaze, *Higher Order QCD Effects in Inclusive Annihilation and Deep Inelastic Scattering*, *Nucl. Phys.* **B192** (1981) 417.

[145] S. Moch and J. A. M. Vermaseren, *Deep inelastic structure functions at two loops*, *Nucl. Phys.* **B573** (2000) 853 [hep-ph/9912355].

[146] I. Korchemskaya and G. Korchemsky, *On light-like wilson loops*, *Physics Letters B* **287** (1992) 169 .

[147] L. J. Dixon, L. Magnea and G. F. Sterman, *Universal structure of subleading infrared poles in gauge theory amplitudes*, *JHEP* **08** (2008) 022 [0805.3515].

[148] O. Erdoğan and G. Sterman, *Gauge Theory Webs and Surfaces*, *Phys. Rev.* **D91** (2015) 016003 [1112.4564].

[149] V. Del Duca, *Iterating QCD scattering amplitudes in the high-energy limit*, *JHEP* **02** (2018) 112 [1712.07030].

[150] V. S. Fadin, M. I. Kotsky and R. Fiore, *Gluon Reggeization in QCD in the next-to-leading order*, *Phys. Lett.* **B359** (1995) 181.

[151] V. S. Fadin, R. Fiore and M. I. Kotsky, *Gluon Regge trajectory in the two loop approximation*, *Phys. Lett.* **B387** (1996) 593 [hep-ph/9605357].

[152] V. S. Fadin, R. Fiore and A. Quartarolo, *Reggeization of quark quark scattering amplitude in QCD*, *Phys. Rev.* **D53** (1996) 2729 [hep-ph/9506432].

[153] J. Blumlein, V. Ravindran and W. L. van Neerven, *On the gluon Regge trajectory in O alpha-s**2*, *Phys. Rev.* **D58** (1998) 091502 [hep-ph/9806357].

[154] V. Del Duca and E. W. N. Glover, *The High-energy limit of QCD at two loops*, *JHEP* **10** (2001) 035 [hep-ph/0109028].

[155] I. A. Korchemskaya and G. P. Korchemsky, *Evolution equation for gluon Regge trajectory*, *Phys. Lett.* **B387** (1996) 346 [hep-ph/9607229].

[156] L. Magnea and G. F. Sterman, *Analytic continuation of the Sudakov form-factor in QCD*, *Phys. Rev.* **D42** (1990) 4222.

[157] V. S. Vanyashin and M. V. Terentev, *The Vacuum Polarization of a Charged Vector Field*, *Zh. Eksp. Teor. Fiz.* **48** (1965) 565.

[158] I. B. Khriplovich, *Green's functions in theories with non-abelian gauge group.*, *Sov. J. Nucl. Phys.* **10** (1969) 235.

[159] D. J. Gross and F. Wilczek, *Ultraviolet Behavior of Nonabelian Gauge Theories*, *Phys. Rev. Lett.* **30** (1973) 1343.

[160] H. D. Politzer, *Reliable Perturbative Results for Strong Interactions?*, *Phys. Rev. Lett.* **30** (1973) 1346.

[161] W. E. Caswell, *Asymptotic Behavior of Nonabelian Gauge Theories to Two Loop Order*, *Phys. Rev. Lett.* **33** (1974) 244.

[162] D. R. T. Jones, *Two Loop Diagrams in Yang-Mills Theory*, *Nucl. Phys.* **B75** (1974) 531.

[163] O. V. Tarasov and A. A. Vladimirov, *Two Loop Renormalization of the Yang-Mills Theory in an Arbitrary Gauge*, *Sov. J. Nucl. Phys.* **25** (1977) 585.

[164] E. Egorian and O. V. Tarasov, *Two Loop Renormalization of the QCD in an Arbitrary Gauge*, *Teor. Mat. Fiz.* **41** (1979) 26.

[165] O. V. Tarasov, A. A. Vladimirov and A. Yu. Zharkov, *The Gell-Mann-Low Function of QCD in the Three Loop Approximation*, *Phys. Lett.* **93B** (1980) 429.

[166] S. A. Larin and J. A. M. Vermaseren, *The Three loop QCD Beta function and anomalous dimensions*, *Phys. Lett.* **B303** (1993) 334 [hep-ph/9302208].

[167] T. O. Eynck, E. Laenen and L. Magnea, *Exponentiation of the Drell-Yan cross-section near partonic threshold in the DIS and MS-bar schemes*, *JHEP* **06** (2003) 057 [hep-ph/0305179].

[168] J. C. Collins and D. E. Soper, *Parton distribution and decay functions*, *Nuclear Physics B* **194** (1982) 445 .

[169] D. J. Gross and F. Wilczek, *Asymptotically Free Gauge Theories - I*, *Phys. Rev.* **D8** (1973) 3633.

[170] H. Georgi and H. D. Politzer, *Electroproduction scaling in an asymptotically free theory of strong interactions*, *Phys. Rev.* **D9** (1974) 416.

[171] R. Hamberg and W. L. van Neerven, *The Correct renormalization of the gluon operator in a covariant gauge*, *Nucl. Phys.* **B379** (1992) 143.

[172] A. Vogt, S. Moch and J. A. M. Vermaseren, *The Three-loop splitting functions in QCD: The Singlet case*, *Nucl. Phys.* **B691** (2004) 129 [hep-ph/0404111].

[173] G. P. Korchemsky and G. Marchesini, *Structure function for large x and renormalization of Wilson loop*, *Nucl. Phys.* **B406** (1993) 225 [hep-ph/9210281].

[174] Yu. L. Dokshitzer, G. Marchesini and G. P. Salam, *Revisiting parton evolution and the large-x limit*, *Phys. Lett.* **B634** (2006) 504 [hep-ph/0511302].

[175] A. V. Belitsky, G. P. Korchemsky and R. S. Pasechnik, *Fine structure of anomalous dimensions in N=4 super Yang-Mills theory*, *Nucl. Phys.* **B809** (2009) 244 [0806.3657].

[176] M. D. Schwartz, *Quantum Field Theory and the Standard Model*. Cambridge University Press, 2014.

[177] G. Heinrich and Z. Kunszt, *Two loop anomalous dimension in light cone gauge with Mandelstam-Leibbrandt prescription*, *Nucl. Phys.* **B519** (1998) 405 [hep-ph/9708334].

[178] A. Bassetto, G. Heinrich, Z. Kunszt and W. Vogelsang, *The Light cone gauge and the calculation of the two loop splitting functions*, *Phys. Rev.* **D58** (1998) 094020 [hep-ph/9805283].

[179] D. A. Kosower and P. Uwer, *Evolution kernels from splitting amplitudes*, *Nucl. Phys.* **B674** (2003) 365 [hep-ph/0307031].

[180] C. F. Berger, *Higher orders in A(alpha(s))/[1-x]+ of nonsinglet partonic splitting functions*, *Phys. Rev.* **D66** (2002) 116002 [hep-ph/0209107].

[181] J. C. Collins, D. E. Soper and G. F. Sterman, *Factorization of Hard Processes in QCD*, *Adv. Ser. Direct. High Energy Phys.* **5** (1989) 1 [hep-ph/0409313].

[182] E. Gardi, E. Laenen, G. Stavenga and C. D. White, *Webs in multiparton scattering using the replica trick*, *JHEP* **11** (2010) 155 [1008.0098].

[183] O. Erdoğan, *Coordinate-space singularities of massless gauge theories*, *Phys. Rev.* **D89** (2014) 085016 [1312.0058].

[184] O. Erdoğan and G. Sterman, *Ultraviolet divergences and factorization for coordinate-space amplitudes*, *Phys. Rev.* **D91** (2015) 065033 [1411.4588].

[185] J. Frenkel, J. G. M. Gatheral and J. C. Taylor, *Is quark-antiquark annihilation infrared safe at high-energy?*, *Nucl. Phys.* **B233** (1984) 307.

[186] C. F. Berger, *Soft gluon exponentiation and resummation*, Ph.D. thesis, SUNY, Stony Brook, 2003. hep-ph/0305076.

[187] J. M. Drummond, J. Henn, G. P. Korchemsky and E. Sokatchev, *On planar gluon amplitudes/Wilson loops duality*, *Nucl. Phys.* **B795** (2008) 52 [0709.2368].

[188] J. M. Drummond, J. Henn, G. P. Korchemsky and E. Sokatchev, *Conformal Ward identities for Wilson loops and a test of the duality with gluon amplitudes*, *Nucl. Phys.* **B826** (2010) 337 [0712.1223].

[189] J. M. Drummond, J. Henn, G. P. Korchemsky and E. Sokatchev, *Hexagon Wilson loop = six-gluon MHV amplitude*, *Nucl. Phys.* **B815** (2009) 142 [0803.1466].

[190] H. Elvang and Y.-t. Huang, *Scattering Amplitudes in Gauge Theory and Gravity*. Cambridge University Press, 2015, 10.1017/CBO9781107706620.003.